D_A DITMARS (25)

NATIONAL BUREAU OF STANDARDS REPORT

10 904

INTERIM REPORT
ON THE THERMODYNAMICS
OF CHEMICAL SPECIES
IMPORTANT IN AEROSPACE TECHNOLOGY
(including Special Topics in Chemical Kinetics)

(The previous reports in this series have the NBS Report Nos. 6297, 6484, 6645, 6928, 7093, 7192, 7437, 7587, 7796, 8033, 8186, 8504, 8628, 8919, 9028, 9389, 9500, 9601, 9803, 9905, 10004, 10074, 10326, and 10481.)

<NBS>

U.S. DEPARTMENT OF COMMERCE

NATIONAL BUREAU OF STANDARDS

NATIONAL BUREAU OF STANDARDS REPORT

NBS PROJECT

232–0423
316–0401
316–0403
316–0405
316–0426

1 July 1972

NBS REPORT

10 904

INTERIM REPORT
ON THE THERMODYNAMICS
OF CHEMICAL SPECIES
IMPORTANT IN AEROSPACE TECHNOLOGY
(including Selected Topics in Chemical Kinetics)

(The previous reports in this series have the NBS Report Nos. 6297, 6484, 6645, 6928, 7093, 7192, 7437, 7587, 7796, 8033, 8186, 8504, 8628, 8919, 9028, 9389, 9500, 9601, 9803, 9905, 10004, 10074, 10326, and 10481.)

<NBS>

U.S. DEPARTMENT OF COMMERCE
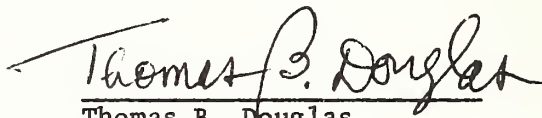## NATIONAL BUREAU OF STANDARDS

FOREWORD

Structure, propulsion, and guidance of new or improved weapons
delivery systems are dependent in crucial areas of design on the avail-
ability of accurate thermodynamic data. Data on high-temperature
materials, new rocket propellant ingredients, and combustion products
(including exhaust ions) are, in many cases, lacking or unreliable.
This broad integrated research program at the National Bureau of Standards
supplies new or more reliable thermodynamic properties essential in
several major phases of current propulsion development and application.
Measured are compounds of those several chemical elements important in
efficient propulsion fuels; those substances most affecting ion concen-
trations in such advanced propulsion concepts as ion propulsion; and the
transition and other refractory metals (and their pertinent compounds)
which may be suitable as construction materials for rocket motors, rocket
nozzles, and nose cones that will be durable under extreme conditions
of high temperature and corrosive environment. The properties determined
extend in temperature up to 6000 degrees Kelvin. The principal research
activities are experimental, and involve developing new measurement
techniques and apparatus, as well as measuring heats of reaction, of
fusion, and of vaporization; specific heats; equilibria involving gases;
several properties from fast processes at very high temperatures; spectra
of the infrared, matrix-isolation, microwave, and electronic types; and
mass spectra. Some of these techniques, by relating thermodynamic pro-
perties to molecular or crystal structures, make it possible to tabulate
reliably these properties over far wider ranges of temperature and pressure
than those actually employed in the basic investigations. Additional
research activities of the program involve the critical review of published
chemical-thermodynamic (and some chemical-kinetic) data, and the generation
of new thermochemical tables important in current chemical-laser research.

ABSTRACT

This report presents recent results of the NBS research program. The nature and scope of the subjects covered may be inferred from the detailed Table of Contents to be found on the following pages. The most significant results may be summarized as follows, under four main headings. (1) <u>Thermodynamic properties of molybdenum compounds</u>-- As a necessary preliminary to later measurement of the standard heat of formation of MoF_5, that of MoF_6 (ℓ) was determined by solution calorimetry and found to be $\triangle Hf° = -376.43 \pm 0.52$ kcal mol^{-1}. The related standard heat of formation of F^-(aq) and heat of solution of NaF(c) are discussed critically. Fifteen new transpiration measurements on $MoF_5(\ell)$ at 70°, 90°, and 110°C are reported. To enable determination of the individual partial pressures of monomer and dimer vapor species, a second vapor-pressure method was developed which reproduced known vapor pressures of iodine to within 1 to 2%. Assuming the MoF_5 molecule to have D_{3h} symmetry, a complete vibrational assignment was made on the basis of new studies (infrared spectra of the matrix-isolated vapor, using double-boiler techniques to enhance the monomer; and Raman spectra of the crystal and the liquid). The heat capacity of what is approximately Mo_2C was measured from 273 to 1475 K using two drop-type calorimeters; these results are consistent among themselves and with two published low-temperature heat-capacity sets of data, and extension of the measurements to well above a first-order transition (at about 1675 K) is planned. (2) <u>Thermophysical properties of refractory metals and alloys</u>--The subsecond-duration pulse-heating technique previously developed and applied was used to measure simultaneously the specific heat, electrical resistivity, and hemispherical total emittance of two alloys, Ta-10(weight %) W(1500-3200 K) and Nb-1(weight %) Zr (1500-2700 K), with estimated accuracies comparable to those obtained on other samples previously. The specific heats show small departures from the additive values based on the pure components. The electrical resistivity of the former alloy shows significant departure from Mattiessen's law, and that of the latter alloy is 0.5% lower than for pure Nb. The pulse-technique melting point of W was found to be 3695 K, and that of Nb, 2750 K (both IPTS-68), with estimated uncertainties of 15 K and 10 K, respectively; the electrical resistivities of both metals also were measured above their melting points, and the normal spectral emittance of Nb remained constant at 0.348 (±3%) during melting. The feasibility of a pulse-heating technique for measuring the heats of fusion of refractory metals was demonstrated by preliminary experiments on Nb; and the feasibility of another such technique for solid-solid phase transformations at high temperatures was demonstrated by the rate of surface radiance-temperature variation in the gamma-to-delta transformation of Fe, during which the electrical resistivity increased by 0.3%. (3) <u>Chemical kinetics of simple-gas reactions</u>--On the basis of a critical examination of the data (especially shock-tube), suggested thermal rate constants are tabulated for the six

dissociation and recombination reactions (a) $NH_3 \rightleftarrows NH_2 + H$ (0-100 atm, and 200-4000 K), (b) $N_2H_4 \rightleftarrows 2NH_2$ (10^{-5} -100 atm, and 200-3000 K), and (c) $N_2F_4 \rightleftarrows 2NF_2$ (10^{-5} -100 atm, and 200-1800 K). The best fit of (a) appears to require external rotation. A satisfactory data correlation of (b) was made using RRKM unimolecular rate theory, and the results are consistent with $\Delta Hf^\circ_{298} = 45.5 \pm 1.5$ kcal mol^{-1} for NH_2 (g) (incorporated in a new thermochemical table) instead of the JANAF-table value of 40.1 ± 3. The RRKM data correlation of (c) requires 18.0 kcal (0 K) for the N-N bond energy (JANAF value, 20.8 kcal). In addition, a bibliography (1934-June 1972) covers the chemical kinetics of 60 gas-phase reactions of fluorides of $C\ell$, N, and O based on 51 papers, with emphasis on the processes occurring during the thermal decompositions of these fluorides. (4) New ideal-gas thermochemical tables--Based on a critical review and correlation of the up-to-date heat-of-formation and molecular-constant data, new ideal-gas thermochemical tables and texts of the JANAF-Table format are given for 31 simple gas species containing H (or ^{1}H), D (or ^{2}H), F, $C\ell$, O, S, and/or N. Included are $(HF)_n$ with n = 1 to 7, and texts (but no tables) for F and H_2O.

Thomas B. Douglas

Charles W. Beckett

TABLE OF CONTENTS

TABLE OF CONTENTS (Continued)

TABLE OF CONTENTS (Continued)

TABLE OF CONTENTS (Continued)

TABLE OF CONTENTS (Continued)

Table I. Rate Constants for the Reaction

$$M + N_2H_4 \underset{k(COM)}{\overset{k(DEC)}{\rightleftharpoons}} 2NH_2\cdot + M$$

Chap. 13. <u>RATE CONSTANTS FOR THE REACTIONS</u>

$$\underline{(M) + N_2F_4 \underset{k_r}{\overset{k_d}{\rightleftharpoons}} 2NF_2\cdot + (M)}$$

Chapter 1
THE HEAT OF FORMATION OF $MoF_6(\ell)$
BY SOLUTION CALORIMETRY

R. L. Nuttall, K. L. Churney, M. V. Kilday

1. Introduction

This laboratory is currently engaged in a program to determine the heats of formation of the lower fluorides (and the oxy-fluorides) of molybdenum. Since it was deemed unlikely that the compound currently of interest, $MoF_5(c)$, could be formed in reasonable quantities by direct reaction of $F_2(g)$ with $Mo(c)$, two other reaction schemes are being used which involve either $MoF_6(g)$ or $MoF_6(\ell)$. The first, the method of choice, is the reaction of $MoF_5(c)$ with $F_2(g)$ to form $MoF_6(g)$. Because the available quantity of $MoF_5(c)$ and the heat of reaction[1/] were expected to be small, a second, more sensitive, scheme was deemed necessary either as a check or as an alternative route. The method selected was the heat of solution of $MoF_6(\ell)$ in base and $MoF_5(c)$ in base containing an oxidant, based on the apparent success of this method with $MoCl_5(c)$ [3], for example. Both methods require an accurate value for the heat of formation of $MoF_6(\ell)$ or $MoF_6(g)$. Unfortunately, the heat of formation of $MoF_6(g)$

[1/] -24 ± 15 kcal per mol $MoF_5(c)$ based on an estimated heat of formation of $MoF_5(c)$ [2] and the heat of formation of $MoF_6(g)$ [1].

1

derived by solution calorimetry differs from that deter-
mined by direct combination of the elements.

Settle et al [1] obtained -372.35 ± 0.22 kcal/mol
for the reaction

$$Mo(c) + 3F_2(g) = MoF_6(g) \tag{1}$$
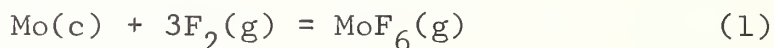
by burning molybdenum sheet suspended on a nickel rod in
14-15 atm of $F_2(g)$ in a nickel combustion bomb. Correction
for unburned molybdenum ($\leq$ 4% of initial sample weight)
could be made unambiguously and accurately. While the cor-
rections for the formation of $MoF_5(c)$ (typically 0.10 ±
0.05% of molybdenum burned), $NiF_2(c)$ formed due to corrosion,
and impurities in the original sample were somewhat uncertain,
all made relatively small contributions to the resulting
value of ΔH_f^0 [$MoF_6(g)$] (0.003%, 0.059%, and 0.087% on the
average, respectively). Recalculation of the latter two
corrections using newer selected values for heats of for-
mation (see [2,4]) yielded a value of -372.29 kcal [5] for
reaction (1).

The only other determination of the heat of formation
of $MoF_6(\ell)$ was made by Myers and Brady [6] by measuring the
heats of solution of $MoF_6(\ell)$ and $MoO_3(c)$ in 0.531 N aqueous
NaOH and of NaF(c) in 0.531 N aqueous NaOH containing molybdate.
These authors calculated their results according to the re-
action scheme given by:
$$MoF_6(\ell) + 8NaOH(soln) = Na_2MoO_4(soln) + 6NaF(c) + 4H_2O(soln)$$
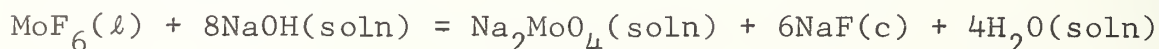
to obtain -388.6 ± 4 kcal for the heat of formation of $MoF_6(\ell)$. Recalculation of their results using newer selected values [2,4] of the heat of formation [NaOH · $515H_2O](soln)$, $MoO_3(c)$, and NaF(c) yields a value of -393.2 kcal mol^{-1}. Using the selected value of 6.66 kcal/mol for the heat of vaporization of $MoF_6(\ell)$ [5] (based on the measurements of Ruff and Ascher [7], Cady and Hargreaves [8], and Osborne et al [9]), one obtains -386.6 ± 4 kcal for reaction (1). The uncertainty in this result greatly exceeds any error due to the failure of Myers and Brady to maintain rigid stoichiometry. The result is 14.2 ± 4 kcal more negative than that obtained by Settle et al.

Because of this discrepancy and particularly because solution calorimetry involving $MoF_6(\ell)$ is also to be used to determine the heat of formation of $MoF_5(c)$, it was con-sidered necessary to repeat the measurements of Myers and Brady. We considered it more likely that the error lay in their work than in that of Settle et al.

In the following three sections an outline of the re-action scheme for the solution experiments is given, a summary of experimental method, and a summary and discussion of results.

2. Reaction Scheme of Solution Experiments

The actual reaction scheme involves the following five reactions:

$$MoF_6(\ell) + [(8+x)NaOH + yH_2O](soln) = \tag{2}$$

$$[Na_2MoO_4 + 6NaF + xNaOH + (4+y)H_2O](soln) - \Delta H_2$$

$$MoO_3(c) + [(2+x)NaOH + (3+y)H_2O](soln) = \tag{3}$$

$$[Na_2MoO_4 + xNaOH + (4+y)H_2O](soln) - \Delta H_3$$

$$6NaF(c) + [Na_2MoO_4 + xNaOH + (4+y)H_2O](soln) = \tag{4}$$

$$[Na_2MoO_4 + 6NaF + xNaOH + (4+y)H_2O](soln) - \Delta H_4$$

$$6NaF(c) = 6NaF(aq) - \Delta H_5 \tag{5}$$

$$[(2+x)NaOH + (3+y)H_2O](soln) + 6NaOH(aq) = \tag{6}$$

$$3H_2O(\ell) + [(8+x)NaOH + yH_2O](soln) - \Delta H_6$$
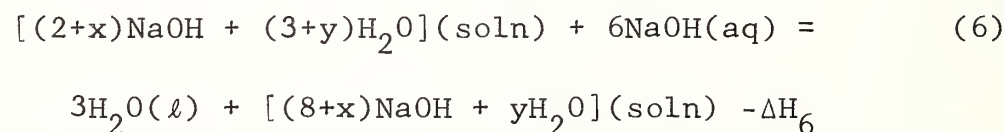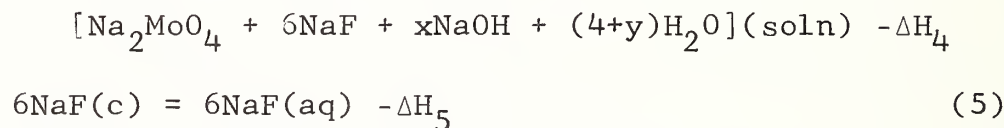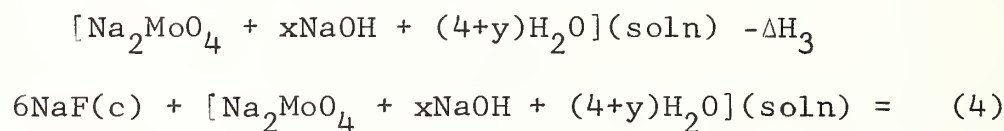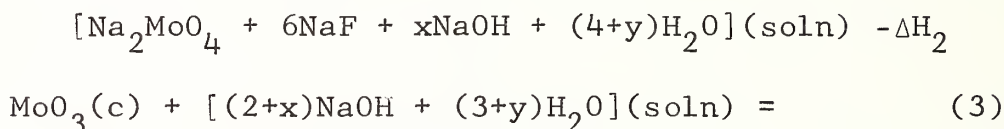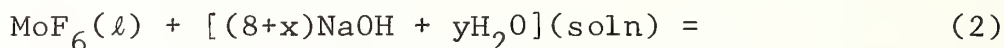
Adding reactions (2) - (3) - (4) + (5) + (6), one obtains:

$$MoF_6(\ell) + 6OH^-(aq) = MoO_3(c) + 6F^-(aq) + 3H_2O(\ell) \tag{7}$$

$$- \Delta H_7$$
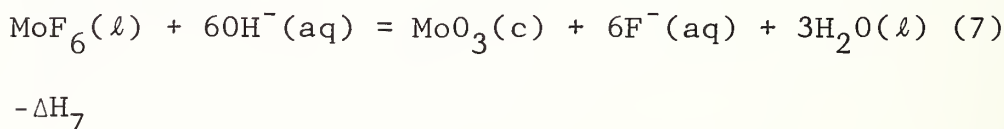
Thus, the heat of reaction (7), ΔH_7, is given by

$$\Delta H_7 = \Delta H_2 - \Delta H_3 - \Delta H_4 + \Delta H_5 + \Delta H_6$$

The heat of formation of $MoF_6(\ell)$, $\Delta H_f^o[MoF_6(\ell)]$, would then be given by the heats of formation of the other species in reaction (7) and ΔH_7:

$$\Delta H_f^o[MoF_6(\ell)] = \Delta H_f^o[MoO_3(c)] + 3\Delta H_f^o[H_2O(\ell)] + \tag{8}$$

$$6\Delta H_f^o[F^-(aq)] - 6\Delta H_f^o[OH^-(aq)] - \Delta H_7$$

Apart from experimental uncertainties, the uncertainty in the assumed value for heat of formation of $F^-(aq)$ will cause the largest systematic error in the heat of formation of $MoF_6(\ell)$.

Experimental determinations of the heat of reactions (2) through (5) were made; (4) and (5) were done to eliminate possible uncertainties due to the state and impurities of the NaF(c) sample.

3.0 Materials

MoF_6 was purchased from Ozark-Mahoning Company. It was purified by trap-to-trap distillation in an all-metal system and was then transferred by distillation into Kel-F (polychlorotrifluoroethylene) bulbs for introduction into the calorimeter. Samples of MoF_6 which had received similar treatment were analyzed by freezing point lowering by Krause [10] who found an impurity of .03 mol percent. The nature of the impurity was not determined.

The $MoO_3(c)$ was CP grade and used without further purification. It was examined spectroscopically by the Analytical Chemistry Division, NBS, for metals. The only ones detected in amounts greater than 0.001 percent were Magnesium and Silicon which were in the range 0.001 to 0.01 percent. From the weight change on drying, the percent of water was estimated to be of the order of 0.02%.

5

NaF was CP grade used without further purification and was not analyzed for impurities. From the weight change on drying, the percent of water was estimated to be of the order of 0.12%.

3.1 Sample Bulbs for $MoF_6(\ell)$

The sample bulbs for the $MoF_6(\ell)$ were made from 1/2 inch lengths of 3/8 inch I.D. tubing by sealing on end windows of 0.005 inch film and a 1/8 inch O.D. tube side-arm. The bulbs were filled through the sidearm which was then sealed off. Each bulb was tested for leakage by using a helium leak detector. The thin end windows were all permeable to the helium. A suitable maximum leak rate was chosen that corresponded to bulb leakage and bulbs were rejected if the leak rate exceeded this maximum value.

Some experiments were carried out to test the suita-bility of Kel-F capsules for containing the $MoF_6(\ell)$ in a NaOH solution as follows: (1) a bulb was weighed and then soaked in NaOH solution for nineteen hours. It was then washed, dried, and weighed. The change in weight was less than 0.1 mg; (2) a weighed bulb was filled with $MoF_6(\ell)$, sealed, and the bulb and remainder of the sidearm were weighed. This bulb was then soaked in NaOH solution for nineteen hours. It lost 5.1 mg of weight. The bulb was

then allowed to sit in the laboratory for ten days. During
this time blue (later turning yellow) material formed on
the outside of the bulb and small white crystals formed
on the inside walls of the bulb above the liquid. The
weight of the bulb increased by at least 14.6 mg over the
period of ten days. The bulb was then opened under a
solution of ammonium hydroxide, allowing the MoF_6 to react.
The washed and dried bulb had gained 12.6 mg in weight;
(3) a sample bulb was made with 1/32 inch thick end
windows (instead of the usual 0.005 inch). Leakage
through these windows could not be detected with the
helium leak detector. After a period of three weeks this
bulb also showed blue colored material on the outside of
the windows and white crystals on the inside. It appears
from the results of these experiments that Kel-F does
not react with or absorb NaOH solution at room temperature;
that it is permeable to moisture, oxygen, and/or MoF_6.
The consequences of this permeability are discussed further
in the section on experimental results.

3.2 Calorimeter

The platinum-lined calorimeter used in this work is
the precise adiabatic solution calorimeter developed by
E. J. Prosen and M. V. Kilday which has been described
previously in earlier stages of development [11,12] and in
more detail in its present state [13]. The calorimeter has

a solution capacity of 300 ± 15 cm^3 and, when filled with 300 cm^3 of H$_2$O, an energy equivalent of approximately 1700 J·K^{-1}. The stirring speed of the liquid for most of the experiments was 350 r.p.m. For the experiments involving NaF(c) and MoO$_3$(c), the regular platinum sample holder of the calorimeter was used. It has a volume of approximately 2.7 cm^3, an opening energy of 0.00 ± 0.02 J, and is described in detail in ref. [13].

For the MoF$_6$ solution experiments, the regular sample holder was replaced with a Monel frame which held a sample bulb with its end windows aligned horizontally. A Monel cutter was provided which cut out the end windows so that solution could flow freely through the bulb during the solution reaction. The energy required to open the bulbs in this way was normally about 0.44 J.

3.3 Experimental Procedures

The amount of sample introduced into the calorimeter was determined by weight. The MoO$_3$ and NaF samples were weighed as crystalline solids directly in the sample holder. The weight of MoF$_6$(ℓ) was determined by two weighing schemes, A and B. The empty bulb with its sidearm was weighed (W1). It was then filled with sample and the sidearm sealed off. The filled bulb was weighed (W2). The remaining sidearm was weighed (W3). The sample weight (WA) is then given by: WA = W2 + W3 - W1. After the calorimetric experiment was

8

complete the now empty sample bulb (with its end windows) was cleaned and weighed (W4). The sample weight (WB) is given by: WB = W2 - W4. In general, the sample weights WA and WB do not agree, WA was always found to be greater than WB. We have used as the weight of sample the average value and have weighted experimental results and assigned uncertainties based on the difference between WA and WB.

The operation of the calorimeter is discussed in detail in reference [13]. Basically the operation con-sists of measuring a temperature-time curve for four rating (drift) periods, two electrical heating (calibration) periods and the reaction period.

The energy equivalent of the initial calorimetric system is determined from the first rating period, first electrical heating period, and the second rating period, taken in that order. The solution reaction is started after the second rating period by opening the sample con-tainer. It is followed by the third rating period. A second electrical heating period is then carried out and is followed by the fourth rating period and an energy equiva-lent for the final calorimetric system is determined. The temperature rise due to the solution reaction is determined from rating periods two and three and the reaction period. It is combined with the average energy equivalent to deter-mine the enthalpy change for the solution reaction.[*]

[*]After correcting for the opening energy of the sample con-tainer and, if added, electrical energy (Eit of Table 6).

9

The experiments were carried out in six sets. Sets 1, 2, and 3 were for reaction (2) in which $MoF_6(\ell)$ was dissolved in NaOH solution. The primary division between these sets is time but they also may have some procedure changes such as a different tolerance on sample bulb leakage rate. Set 4 is for measurements on reaction (3) where $MoO_3(c)$ is dissolved in NaOH solution. Set 5 and 6 are for measurements on reactions (4) and (5) where NaF(c) is dissolved in a solution of Na_2MoO_4 and NaOH, and in water, respectively.

4. Experimental Results

4.1 Reaction (2)

The calorimetric data for reaction (2) is presented in Table 1. Columns (1) and (2) are set and experiment numbers. Column (3) is the weight of $MoF_6(\ell)$ sample introduced into the calorimeter and is the average of weights WA and WB. Column (4) is the uncertainty in the sample weight given by (WA - WB)/2. Columns (5) and (6) give the electrical energy equivalent of the initial and final calorimetric systems, EEE_i and EEE_f, respectively. Column (7) gives the temperature rise of the calorimeter due to the reaction, ΔR_c, in ohms resistance increase of the platinum thermometer. Column (8) gives $\overline{T}$, the mean temperature of the reaction. Column (9) gives the concentration of the

10

NaOH solution initially in the calorimeter. Column (10)
gives $\Delta H(\overline{T})$, the enthalpy change for the reaction at
the mean temperature, $\overline{T}$.

The experiments in set (1) are considered prelimi-
nary. They have   two possible sources of error: pre-
reaction and incomplete reaction. If the permeability
of the windows of the sample bulb is too great a signifi-
cant amount of reaction can occur before the bulb is
opened to start the solution reaction. This situation
can be detected by observing a blue color on the bulb
windows before placing the sample in the calorimeter or
by observing a larger than normal drift rate during the
first rating period. If insufficient time is allowed for
the reaction period, the reaction may not be complete
before the third rating period is started. This can be
detected by a larger than normal drift rate in the third
rating period.

Table 2 shows the drift rates and the time allowed for
the reaction period for experiments on reaction (2).
Columns (8) and (9) are comments on observations concerning
the experiment and conclusions drawn from analyses of the
drift rate differences, respectively. In the "obs" column,
P means possible prereaction; W means a weighing error;
W(A) means sample weight by method A was not possible; Sp
means that splashing of solution occurred in the calorimeter

as indicated by spots of blue around the top of the calorimeter above the solution (the sample in this experiment was much larger than in the other experiments); and St means that there were variations in stirring energy which would invalidate analysis of drift rate differences. In the "Drift" column, P means prereaction and an I means incomplete reaction. Previous experience with this calorimeter indicates that a difference in successive drift rates (D.R.) of greater than 3×10^{-6} ohm min^{-1} is significant so we have set the criteria that: P means

D.R. (1) $-$D.R. (3) $\geq 6 \times 10^{-6}$ ohm min^{-1} or

D.R. (2) $-$D.R. (3) $\geq 3 \times 10^{-6}$ ohm min^{-1}.

I means D.R. (3) $-$D.R. (4) $\geq 3 \times 10^{-6}$ ohm min^{-1}.

Based largely on our observations and these criteria, we have rejected some of the experiments and not considered them further in calculations of results. These experiments are marked with an asterisk in Tables 1 and 2.

Table 3 gives the results of calculations of the enthalpy change for reaction (2), ΔH_2. As shown in column (3), the experiments are arranged in order of concentration of base. Columns (4), (5), and (6) give the molar ratios of NaOH to MoF_6 (which equals (8+x) in eq (2); H_2O to MoF_6 (which equals y in eq (2); and H_2O to NaOH. A temperature coefficient for ΔH_2 of +0.613 kJ mol^{-1} K^{-1} was derived from experiment 584 and the mean of experiments 586 and 588.

This has been used to calculate the values of $\Delta H_2(25)$
given in columns (7) and (8). The uncertainties given
in column (9) are derived from the sample weight un-
certainties given in Table 1.

4.2 Reaction (3)

Table 4 gives the calorimetric data for reaction (3),
the solution of $MoO_3(c)$ in NaOH (soln). The column
headings have the same meaning as in Table 1.

Table 5 gives the results of calculations for ΔH_3.
A value of ΔC_p = +93.6 J mol^{-1} K^{-1} was derived from run
636 and the mean of runs 557, 561, and 634. It was used
to calculate the values of $\Delta H_3(25)$ given in columns (6)
and (7).

4.3 Reactions (4) and (5)

Table 6 gives the calorimetric data for reactions (4)
and (5), the solution of NaF(c) in a Na_2MoO_3 - NaOH solution
(set 5) and in H_2O (set 6), respectively.

Table 7 gives the results for calculation of ΔH_4. A
temperature coefficient of +0.192 kJ (6 mol NaF)$^{-1}$ K^{-1} was
derived from experiments 635 and 637.

Table 8 gives the results of calculations of ΔH_5. The
values of Φ_L used to extrapolate to infinite dilution were
taken from Parker's compilation [14]. A value of ΔC_p =
-102.37 J mol^{-1} K^{-1} was derived from runs 641-642, 647-649,
and 643-645 was used to calculate $\Delta H_5'/6$ at 298K.

13

4.3 Reaction (7)

Table 9 gives the results of calculating ΔH_7 from the data on the previous tables. The uncertainty given in column (9) is that given in Table 1 for ΔH_2. The experiments are weighted as shown in column (10) by giving a weight of 1 if the uncertainty is less than 0.3 kcal and a value of 0.2/(uncertainty) if the uncertainty is greater than 0.3 kcal. The values of ΔH_4 for experiments 628 to 633 were obtained by extrapoling data from runs 635, 637 and 565 correlated with respect to base concentration. For experiment 584 to 588 the value of ΔH_4 was the average of runs 635 and 637.

The dependence of ΔH_7 on base concentration is small and cannot be determined accurately from the data. We have therefore assumed it to be zero and have calculated a weighted mean value of $-\Delta H_7 = 153.78$ kcal mol^{-1} with a standard deviation of the mean of 0.16 kcal. Combining twice this value with our estimates of systematic errors we estimate an uncertainty of 0.50 kcal giving a value of $-\Delta H_7 = 153.78 \pm 0.50$ kcal over the concentration range of the experiments.

8.0 Discussion of Results

8.1 Enthalpy of Formation of $MoF_6(\ell)$ and $F^-(aq)$

In accordance with equation (8) the enthalpy of formation of $MoF_6(\ell)$ can be calculated from ΔH_7 and enthalpy

of formation data for the other species in reaction (7).
The needed auxiliary data are:

$$\Delta H_f^o[MoO_3(c)] = -178.08 \pm 0.08 \text{ kcal} \qquad [5]$$

$$3\Delta H_f^o[H_2O(\ell)] = -204.945 \pm 0.030 \text{ kcal} \qquad [4]$$

$$6\Delta H_f^o[F^-(aq)] = -477.0 \text{ kcal} \qquad [4]$$

$$6\Delta H_f^o[OH^-(aq)] = -329.82 \pm 0.14 \text{ kcal} \qquad [4]$$

The heat of formation of $MoO_3(c)$ is that selected by Parker
[5] of -178.08 kcal to which we assign an uncertainty of
0.08 kcal. The latter value is based on the work of
Staskiewicz et al [15] (-177.99[*] $\pm$ 0.10 kcal) and Mah [16]
(178.15[*] $\pm$ 0.11 kcal) rather than the earlier work of
Delepine [17] (-167 kcal), Mixter [18] (-185 kcal), Moose
and Parr [19] (-175.6 kcal) or Neumann et al [20] (-180.4
kcal). Combining these enthalpies of formation values
with the value of ΔH_7 we get for the enthalpy of formation
of $MoF_6(\ell)$:

$$\Delta H_f^o[MoF_6(\ell)] = -376.43 \pm 0.52 \text{ kcal mol}^{-1}$$

$$= -1574.98 \pm 2.18 \text{ kJ mol}^{-1}$$

This value can be compared to the value of -378.95 $\pm$ 0.22
kcal mol^{-1} for the enthalpy of formation of $MoF_6(\ell)$ obtained
from the recalculated value of the results of Settle et al [1].

The selected value for the heat of formation of $F^-(aq)$
[4], -79.50 kcal mol^{-1}, has been the subject of considerable
controversy. A brief summary of the problem as of 1969 is

given by Armstrong [21] and in 1971 by Vanderzee and

Rodenburg [22]. The latter determined a value of -14.72

± 0.10 kcal mol^{-1} for the reaction at 25 C.

$$HF(g,ideal) = H^+(aq) + F^-(aq) \qquad\qquad (10)$$
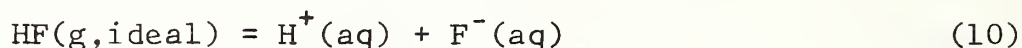
This value supports the value selected by Parker [10] of

-14.70 kcal/mol. Recently, Smith et al [23] determined

a value of -7.691 ± 0.030 kcal mol^{-1} for the reaction at

25 C

$$HF(\ell) = H^+(aq) + F^-(aq) \qquad\qquad (11)$$

Using the value of 7.231 ± 0.025 kcal mol^{-1} for the heat

of vaporization of HF(ℓ) to HF(g,ideal) in its standard

state determined by Vanderzee and Rodenburg [24], one

obtains from the previous work of Vanderzee and Rodenburg

on reaction (10) an alternative value for reaction (11)

of -7.49 ± 0.10 kcal mol^{-1}. Recently, Settle et al [25]

have completed a study of the heat of formation of HF(ℓ)

for which they obtain -72.57 ± 0.09 kcal mol^{-1}. In con-

junction with the two more recent values for the enthalpy

of reaction (11), this yields values for the enthalpy of

formation of F$^-$(aq) of -80.26 ± 0.09 kcal mol^{-1}(Smith et al)

and -80.06 ± 0.14 kcal mol^{-1} (Vanderzee and Rodenburg).

If we combine the value of enthalpy of formation of MoF$_6$(ℓ)

from the results of Settle et al [1] with our value of

ΔH_7 and the other auxiliary data given previously, we obtain

a value for the enthalpy of formation of F$^-$(aq) of -79.92

± 0.09 kcal mol^{-1}.

8.2 Heat of Solution of NaF(c)

The heat of solution of NaF(c) at infinite dilution, $\Delta H_5/6 = +0.221 \pm 0.004$ kcal mol^{-1}, confirms the value of $+0.218 \pm 0.010$ kcal mol^{-1} selected by Parker [14] (see p. 26) on the basis of very few experimental measurements. The lack of a marked trend of calculated values of $\Delta H_5/6$ with the concentration of NaF(c) supports Parker's estimates [14] (see p. 56) of ϕ_L for aqueous NaF solutions.

References

[1] Settle, J. L., Feder,M., Hubbard, W. N., J. Phys. Chem. 5, 1337 (1961).

[2] Wagman, D. D., Evans, W. H., Parker, V. B., Halow, I., Bailey, S. M., Schumm, R. H., Nat. Bur. Std. (U.S.) Tech Note 270-4 (1969).

[3] Shchukarev, S. A., Vasil'kova, I. V., Sharupin, R. N., Vestnik Leningrad Univ. 14, No. 4, Ser. Fiz. i Khim., No. 1, 73-77 (1959).

[4] Wagman, D. D., Evans, W. H., Parker, V. B., Halow, I., Bailey, S. M., Schumm, R. H., Nat. Bur. Std. (U.S.) Tech Note 270-3 (1968).

[5] Parker, V. B., Private Communication, Nat. Bur. Std. (U.S.), See Ref. [2].

[6] Myers, O. E., Brady, A. P., J. Phys. Chem. 64, 591 (1960).

[7] Ruff, O., Ascher, E., Z. Anorg. Chem. 196, 413 (1931).

[8] Cady, G. H., Hargreaves, G. B., J. Chem. Soc. 1563 (1961).

[9] Osborne, D. W., Schreiner, F., Malm, J. G., Selig, H., Rochester, L., J. Chem. Phys. 44, 2802 (1966).

[10] Krause, R. F., NBS Report 10481, Chapt. 7 (1971).

[11] Kilday, M. V., Prosen, E. J., NBS Report 8306 (1964).

[12] Kilday, M. V., Prosen, E. J., Wagman, D. D., NBS Report 10004 (1969).

[13] Prosen, E. J., Kilday, M. V., to be published in J. Res. NBS.

[14] Parker, V. P., Thermal Properties of Aqueous Uni-valent Electrolytes. National Standard Reference Data Series-NBS 2. U.S. Govt. Printing Office, Washington, D.C., 1965.

[15] Staskiewicz, B. A., Tucker, J. R., Snyder, P. E., J. Amer. Chem. Soc. 77, 2987 (1955).

[16] Mah, A. D., J. Phys. Chem. 61, 1573 (1957).

[17] Delepine, M., Bull. Soc. Chim. 29, 1166 (1903).

[18] Mixter, W. G., Amer. J. Sci. 29, 488 (1910).

[19] Moose, J. E., Parr, S. W., J. Amer. Chem. Soc. 46, 2656 (1924).

[20] Neumann, B., Kroger, C., Kunz, H., Z. anorg. und Allgem. Chem. 218, 379 (1934).

[21] Armstrong, G. T., AFOSR Scientific Report AFOSR 69-2154 TR, NBS Report 10074, July 1 (1969).

[22] Vanderzee, C. E., Rodenburg, W. W., J. Chem. Thermodynamics 3, 267 (1971).

[23] Smith, P. N., Johnson, G. K., Hubbard, W. N., Private Communication, Argonne Nat. Lab., March 1970.

[24] Vanderzee, C. E., Rodenburg, W. W., J. Chem. Thermodynamics 2, 461 (1970).

[25] Settle, J. L., Hubbard, Johnson, G. K., Greenberg, E., Private Communication, Argonne Nat. Lab., July 1970.

Table 1. Calorimetric Data for Reaction (2)

Set	Exp. No.	Sample Mass, g.	(vacuo) Uncert. g.	EEE_i -17,000 J ohm^{-1}	EEE_f -17,000 J ohm^{-1}	ΔR_c x 10^6 ohm	$\bar{T}$, React. °C	[NaOH] Moles/ liter	$\Delta H_2(\bar{T})$ -3000 Jg^{-1}
1	559*	.5060	.0005	220.67	254.26	100413	25.549	.706	419.8
do	560*	.3395	.0010	251.25	263.60	65751	24.783	.643	340.9
do	562*	.1999	.0012	252.33	256.50	39160	24.627	.643	377.9
do	563*	.2359	.0009	250.30	260.43	45603	24.666	.643	333.9
do	564*	.2536	.0033	306.81	305.73	47590	29.620	.643	245.9
2	583*	.3542	.0028	303.83	318.18	64954	35.325	.694	173.3
do	584[1]	.3698[1]	--	261.63	266.36	73648	30.155	.694	434.2
do	585*	.5530	.0009	202.19	214.38	105552	24.470	.694	283.8
do	586	.5116	.0007	179.33	218.27	102591	24.410	.694	448.0
do	587*	.8100	.0008	189.17	214.16	160735	24.363	.694	412.9
do	588	.2289	.0016	202.47	196.85	46008	23.993	.694	455.1
do	589	.2714	.0012	436.25	440.96	53369	24.905	.302	427.6
3	611	.4266	.0008	--	239.30	85551	25.169	.653	456.1
do	612	.3348	.0000	--	303.22	63301	25.076	.653	425.3
do	628	.3610	.0016	178.75	194.81	72359	24.939	.718	443.7
do	629	.3963	.0007	180.57	196.00	79788	24.961	.718	459.5
do	630	.2353	.0009	169.30	198.51	47309	24.758	.718	453.1
do	632	.4015	.0006	161.87	147.25	80670	24.930	.718	445.6
do	633	.4102	.0008	165.00	199.34	82372	24.945	.718	449.3

*Preliminary experiments

[1]Mass, Method B, the opening energy was 1.5 J rather than 0.44 J

Table 2. Drift Rate Data for Reaction (2)

| Set | Exp. No. | Drift Rate | | | | Reaction Time | Comments | |
| | | 1 | 2 | 3 | 4 | | obsv. | Drift |
		<———————$10^{-6}\Omega$ min^{-1}————>				min.		
1	559*	17.4	22.0	16.9	8.9	40	P	P,I
do	560*	19.2	21.4	10.1	8.3	40	P	P
do	562*	11.8	15.2	13.3	9.2	40	P	I ?
do	563*	17.7	20.0	11.1	9.0	40	P	P
do	564*	22.8	29.0	16.2	8.6	40	P	P,I
2	583*	67.6	74.0	22.8	19.9	60	P,W	P
do	584	24.9	26.7	26.3	23.4	55	W(A)	
do	585*	48.8	49.3	23.4	24.3	25	P	P
do	586	24.1	22.5	19.6	18.7	35		
do	587*	31.5	31.7	23.5	22.9	30	Sp	P
do	588	23.0	25.9	26.7	26.8	55		
do	589	24.9	24.3	24.0	23.0	45		
3	611	--	10.3	12.6	10.8	55		
do	612	--	8.1	6.7	5.3	35		
do	628	40.9	40.2	34.7	32.5	70	St	
do	629	36.1	35.0	34.5	32.0	85		
do	630	14.0	13.0	14.3	12.9	70		
do	632	14.6	13.9	14.3	13.1	45		
do	633	14.0	13.7	10.9	9.9	75	St	

*Preliminary experiments.

Table 3. Calculation of ΔH_2

Set	Exp. No.	[NaOH] mole/ liter	$\dfrac{[NaOH]}{[MoF_6]}$ (8+X)	$\dfrac{[H_2O]}{[MoF_6]}$ (y)	$\dfrac{[H_2O]}{[NaOH]}$	$\longleftarrow -\Delta H_2(25) \longrightarrow$		
						kJ mol^{-1}	kcal mol^{-1}	Uncert. kcal mol^{-1}
3	628	.718	126.54	9,806	77.49	722.90	172.78	0.77
do	629	.718	115.21	8,932	77.53	726.23	173.57	0.24
do	630	.718	194.05	15,044	77.53	724.65	173.20	0.33
do	632	.718	111.31	8,628	77.51	723.30	172.87	0.05
do	633	.718	107.03	8,297	77.52	724.80	173.06	0.24
2	584	.694	119.44	9,579	80.20	724.10	173.06	--
do	586	.694	86.34	6,922	80.17	723.48	172.92	0.24
do	588	.694	192.96	15,477	80.21	724.72	173.21	1.22
3	611	.653	97.58	8,318	85.24	725.64	173.43	0.31
do	612	.653	124.34	10,595	85.21	719.12	171.87	0.03
2	589	.302	72.01	13,253	184.04	719.50	171.96	0.73

Table 4. Calorimetric Data for Reaction (3)

Set	Exp. No.	Sample (vacuo) g	EEE_i -17,000 J ohm^{-1}	EEE_f -17,000 J ohm^{-1}	ΔR_{c_7} x 10^7	$\bar{T}$ (React.) °C	[NaOH] mole/ liter	$-\Delta H_3(\bar{T})$ J g^{-1}	$-\Delta H_3(\bar{T})$ kJ·mol^{-1}
4	556	.606753	101.41	119.53	192645	24.891	.706	543.26	78.196
do	557	.256518	361.08	365.63	79712	24.933	.304	539.56	77.663
do	634	.218740	117.89	122.31	68991	25.035	.694	539.97	77.722
do	636	.236135	223.61	219.18	73276	34.950	.694	534.40	76.921
do	561	.226222	139.72	147.86	71694	24.879	.643	543.32	78.205

Table 5. Calculation of ΔH_3

Exp. No.	[NaOH] moles/ liter	$\frac{[NaOH]}{[MoO_3]}$ (Z+X)	$\frac{[H_2O]}{[MoO_3]}$ (3+y)	$\frac{[H_2O]}{[NaOH]}$	$-\Delta H_3$ (25C)	
					kJ·mol^{-1}	kcal mol^{-1}
556	.706	50.77	4,000	78.80	78.182	18.687
557	.304	52.6	9,479	180.3	77.657	18.560
634	.694	138.44	11,104	80.21	77.725	18.577
636	.694	128.31	10,288	80.18	77.852	18.607
561	.643	124.26	10,757	86.57	78.194	18.689
		Mean		=	77.923	18.624
		2xSdm		=	0.226	0.054

Table 6. Calorimetric Data for ΔH_4 (Set 5) and ΔH_5 (Set 6)

Set No.	Exp. No.	Sample (vacuo)	EEE_i -17,000	EEE_F -17,000	ΔR_G x 10^7	Eit	T (React)	$+\Delta H_4(T)$
		g	Johm^{-1}	Johm^{-1}	ohm	J	°C	J g^{-1}
5	565	.386751	102.29	109.84	273441	476.26	25.022	22.00
do	635	.379646	89.75	102.23	501280	863.66	25.056	17.56
do	637	.383307	186.77	195.49	499182	861.99	34.969	10.02
do	639	.392711	337.13	332.51	493965	865.47	25.058	23.41
								$\Delta H_5'(T)$*
6	641	.383806	588.39	581.82	483354	861.23	25.047	28.436
6	642	.382450	654.37	645.02	487644	862.12	35.246	3.781
do	643	1.635741	610.02	568.69	460108	862.69	25.026	32.632
do	644	.997894	603.59	566.16	474028	863.36	25.525	29.854
do	645	1.592839	653.68	631.80	486120	871.16	35.269	8.485
do	646	1.600157	567.27	529.12	495350	872.95	25.089	33.266
do	647	1.035573	624.92	598.69	516696	863.65	35.309	5.136
do	648	.633079	557.71	545.16	509222	862.26	25.091	30.682
do	649	.797662	558.84	540.49	506911	863.70	25.100	31.070
do	650	.212321	585.81	584.69	487202	862.49	25.048	27.002

*Uncorrected for heat of dilution

**Added electrical energy

25

Table 7. Calculation of ΔH_4

Exp No.	Init. Soln.	$\dfrac{[NaOH]}{[6NaF]}$ (x)	$\dfrac{[H_2O]}{[6NaF]}$ (4+y)	$\dfrac{[MoO_3]}{[6NaF]}$	$\dfrac{[H_2O]}{[NaOH]}$	ΔH_4 kJ(6 Mol)$^{-1}$	ΔH_4(25) kcal(6 mol)$^{-1}$
565	561	124.97	10,820	1.00583	8658	5.538	1.324
635	634	139.29	11,171	1.00609	80.20	4.413	1.055
637	636	137.90	11,059	1.07495	80.20	4.438	1.061
639	638	60.91	11,138	1.12673	182.86	5.887	1.407

Table 8. Calculation of ΔH_5

Expt. No.	$\dfrac{[H_2O]}{[NaF]}$	$\dfrac{\Delta H_5' (25°C)^*}{6}$		φ_L	$\dfrac{\Delta H_5}{6}$
		$\leftarrow$ kJ mol^{-1}	$\leftarrow$ kcal mol^{-1} $\rightarrow$		
641	1898	1.1988	.2865	.066	.221
642	1904	1.2049	.2886	.066	.223
643	445	1.3728	.3281	.107	.221
644	730	1.3073	.3124	.093	.219
645	457	1.4074	.3364	.106	.230
646	419	1.4059	.3360	.109	.227
647	647	1.2709	.3038	.097	.207
648	1058	1.2942	.3093	.083	.226
649	670	1.3148	.3143	.096	.218
650	3431	1.1386	.2721	.052	.220
			Average =		.221
			2x Sdm =		.004

*Uncorrected for heat of dilution

Table 9. Calculation of ΔH_7

Exp. No.	$[H_2O]$ $[NaOH]$	$-\Delta H_2$	$-\Delta H_3$	ΔH_4	ΔH_5	ΔH_6 *	$-\Delta H_7$	Uncert.**	Weight
		←				kcal		→	
628	77.49	172.78	18.624	(0.951)	1.326	0.259	153.52	0.77	0.260
629	77.53	173.57	do	do	do	do	154.31	0.24	1
630	77.53	173.20	do	do	do	do	153.94	0.33	1
632	77.51	172.87	do	do	do	do	153.61	0.05	1
633	77.52	173.06	do	do	do	do	153.80	0.24	1
584	80.20	173.06	do	1.058	do	0.271	153.90	(1.06)	0.189
586	80.17	172.92	do	1.058	do	do	153.76	0.24	1
588	80.21	173.21	do	1.058	do	do	154.05	1.22	0.165
611	85.24	173.43	do	1.324	do	0.340	154.47	0.31	1
612	85.21	171.87	do	1.324	do	do	152.91	0.03	1
589	184.04	171.96	do	1.407	do	0.636	152.78	0.73	0.274

Mean = 153.78

2xSdm =   0.32

*$6 \cdot \bar{L}_2$ derived from φ_L values listed in ref. [14]

**Column 9, table 3

28

Chapter 2

MOLYBDENUM PENTAFLUORIDE: VAPORIZATION PROPERTIES FROM TRANSPIRATION, AND DEVELOPMENT OF AN EXPERIMENTAL METHOD TO EVALUATE THE TRUE VAPOR PRESSURES

by Thomas B. Douglas and Ralph F. Krause, Jr.

Abstract

Using $MoF_6(g)$ to suppress sample disproportionation, 15
additional precise transpiration measurements were made on
$MoF_5(\ell)$ (purity, >99.8%) at 70°, 90°, and 110°C. The remain-
ing disproportionation appears to be small (1% or less), but
will be tested in a few future measurements. Titration with
permanganate was adopted as an accurate method to analyze the
MoF_5 in the presence of the hexavalent-molybdenum contaminants.
A second method was developed to measure the small vapor pressures
directly; later application and combination with the transpi-
ration data will yield also the vapor densities of MoF_5, which
other evidence suggests will reflect considerable vapor association.
The new method is as simple as the transpiration method, but
the apparatus parameters were carefully chosen to minimize
error. Preliminary tests reproduced a known pressure of argon
(to 0.1 or 0.2%) and known vapor pressures of iodine (to 1 or
2%) and MoF_6 (to 3 or 4%).

I. Introduction

The fluoride of molybdenum most stable near room temperature is
MoF_6, and its common chemical thermodynamic properties are now known
with comparatively high accuracy. In contrast, the several known lower
fluorides of molybdenum are much less stable, and only sketchy property
data, often seriously inconsistent, have been published. A concerted
effort is being made in the present program, at the National Bureau
of Standards, to obtain reliable properties of these lower molybdenum
fluorides, beginning with MoF_5. The standard heat of formation of
$MoF_5(c)$ is being measured, and spectroscopic measurements recently
formed the basis of a frequency assignment to the monomer molecule [1][1].

---

[1] Numbers in brackets refer to literature references at the end of this
chapter.

29

The work described in this chapter and designed to measure the vaporization properties is a continuation of that reported earlier [2], which included historical background, the methods of preparation, purification, elemental sample analysis, melting point, and cryoscopic purity, as well as preliminary transpiration results.

The transpiration method is accurately applicable to a substance such as MoF_5 which has vapor pressures of a few torr in its temperature range of relative stability; but the method measures only vapor density (when the gaseous solutions are dilute) but without indicating the vapor pressure unless the effective molecular weight is unambiguous. Now MoF_5 is an "odd" molecule (in the sense of containing at least one unpaired electron), so that it would be surprising if the simple molecules showed no appreciable tendency to associate. In fact, recent rough mass-spectrometric results at the Oak Ridge National Laboratory (summarized later in this chapter) suggest that saturated molybdenum-pentafluoride vapor not only contains more dimer than monomer, but may contain appreciable proportions of trimer (and even small amounts of higher polymers). For this reason we refined and tested a simple method to measure vapor pressures directly. When applied later to molybdenum pentafluoride, the data combined with the transpiration results should yield both the true vapor pressures and vapor densities of the saturated vapor.

In principle, such methods can be extended to unsaturated vapor to yield the proportions of more than two gas species (assuming gas ideality for each species). In practice, however, it is doubtful whether the accuracy would be sufficient to be meaningful--as exemplified by the well-known difficulties encountered in trying to discriminate among the several polymers in gaseous hydrogen fluoride. A mean degree of association should, however, lead to useful thermodynamic properties.

II. Transpiration Measurements

1. Experimental Results

The sample of $MoF_5(\ell)$ used was prepared and purified as described in the earlier report [2], which presented the results of eight

preliminary transpiration experiments that clearly showed the need
to suppress disproportionation of the MoF_5, during its vaporization,
by shifting an equilibrium which may be

$$2MoF_5 = MoF_6 + MoF_4. \qquad (1)$$
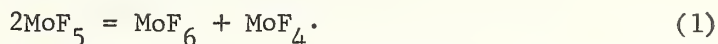
In the further transpiration experiments reported here, carefully
dried helium was passed over thrice-distilled crystalline MoF_6 in a
bath thermostated at a suitable low temperature, the approximate
partial pressures of $MoF_6(g)$ being calculated from published results
[3]. (Owing to its much greater volatility, the $MoF_6(g)$ is believed
to have dissolved in the $MoF_5(\ell)$ to less than 0.1%.) These He-MoF_6
mixtures were passed over the liquid MoF_5 sample contained in a clean-
surface monel vessel in a stirred oil bath thermostated to ±0.005°C
(see Fig. 1). The monel vessel replaced the glass vessel of the earlier
experiments [2] in order to obviate what appeared to be slight reaction
between the fluorides and the pyrex glass at the elevated temperatures.
(While there is no evidence that any slight reaction with the monel
surfaces introduced error, it was not proved that monel is better than
glass in this respect.) The combined vapors were condensed at the Dry-
Ice temperature, with subsequent evacuation at room temperature to remove
the MoF_6 and any trapped helium.

The results of the additional transpiration experiments made are
given in Table 1.

An important improvement over last year's analytical work [2] was
the adoption of titration with permanganate to determine the total amount
of MoF_5 volatilized in each experiment. (Each distillate was weighed,
then dissolved in an oxygen-free aqueous solution of $Fe_2(SO_4)_3$ and
H_2SO_4, treated with H_3PO_4, and titrated colorimetrically with a standard
solution of $KMnO_4$.) Since complete exclusion of the element oxygen
from the transpiration system was practically impossible, many of these
distillates contained condensable oxyfluorides in much greater abundance
than did the liquid sample, so that reliance on the distillate masses
would be unreliable. On the other hand, the elemental analysis for
molybdenum used previously is a more laborious and less sensitive method,
whereas permanganate oxidizes molybdenum quantitatively from valence 5
to valence 6 without reflecting any hexavalent-molybdenum contaminants.
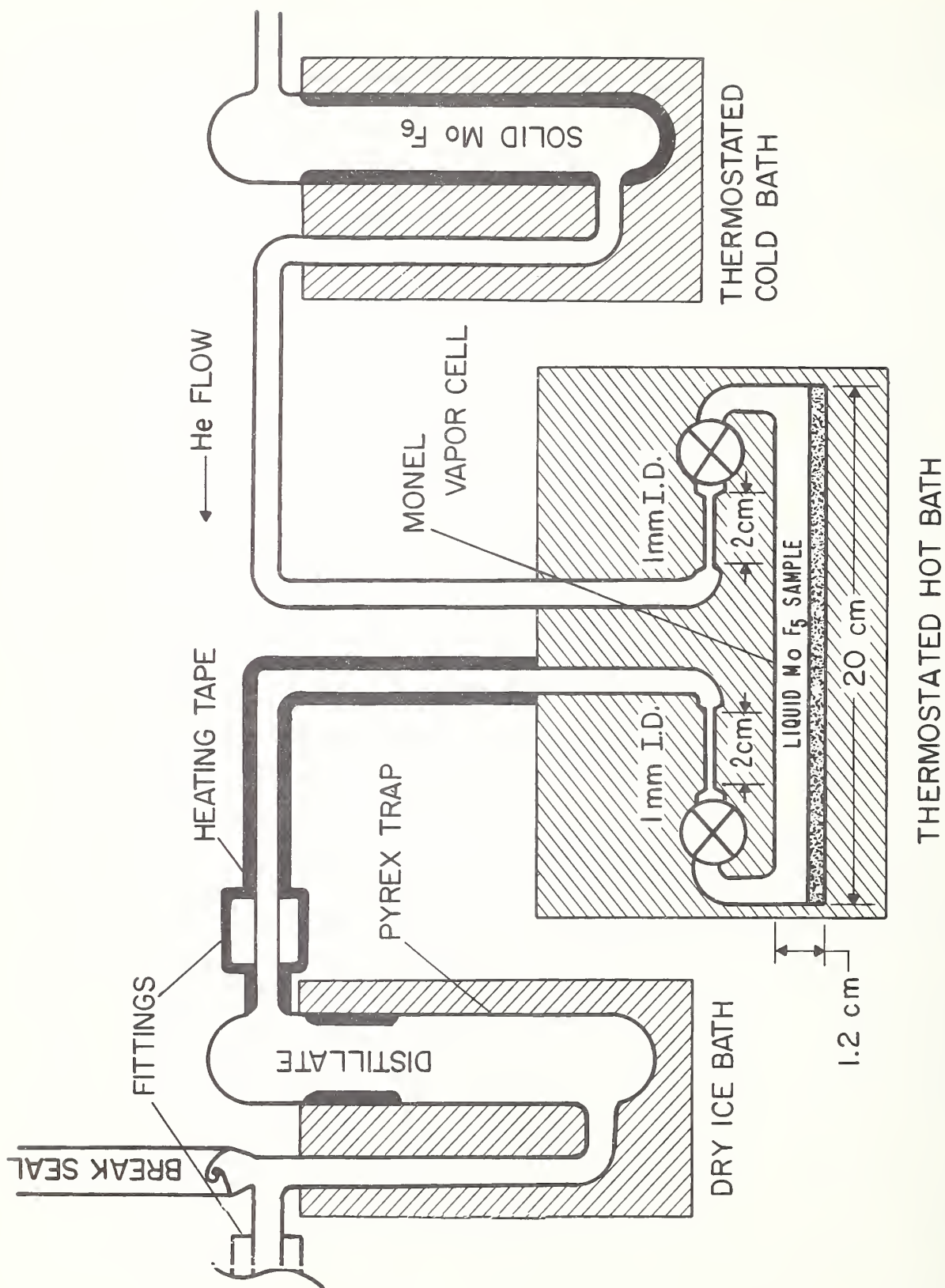
FIGURE 1. Transpiration apparatus

32

Table 1. Transpiration of $MoF_5(\ell)$ by Helium Containing $MoF_6(g)$

[The sample of $MoF_5(\ell)$ (initial mass, 11.755 g) was contained
in monel, and its vapor was condensed in pyrex glass.]

Temper-ature[a] (K)	Experi-ment No.[b]	Flow Rate ($cm^3 sec^{-1}$)	Distillate		Partial Pressure (torr)[f]		Deviation of $P(MoF_5)$ from Mean(%)
			Mass(g)[d]	% MoF_5[e]	MoF_6(added)	MoF_5(found)[g]	
362.8	9	1.26	0.6749	96.65	0.6	2.832	-1.18
	10	1.18	0.4454	96.86	0.5	2.855	-0.38
	11	0.58	0.3647	97.49	0.5	2.871	+0.18
	12	1.23	0.4402	98.22	1.0	2.909	+1.51
	13	1.30	0.4867	98.03	0.5	2.862	-0.13
					Mean:	2.866	
382.9	14	1.34	0.8657	98.71	2.1	8.265	0.00
	15	1.27	0.8791	99.13	2.1	8.249	-0.19
	16c	1.34	0.7273	99.17	2.1	8.292	+0.33
	17	0.67	0.5727	98.75	2.1	8.285	+0.24
	18	1.30	0.8424	99.02	1.0	8.234	-0.37
					Mean:	8.265	
343.2	19	1.28	0.2782	98.61	0.45	0.8999	+0.09
	20	1.36	0.2213	99.16	0.45	0.8951	-0.44
	21	1.58	0.3039	99.21	0.45	0.8979	-0.13
	22	1.75	0.2469	99.65	0.45	0.8962	-0.32
	23	1.57	0.2848	100.09	0.45	0.9063	+0.80
					Mean:	0.8991	

[a]The actual temperatures of the individual experiments differed from those listed by an
average of 0.025 kelvin, but the calculated pressures of MoF_5 (penultimate column) have
been corrected to the nominal temperatures using a temperature coefficient of 5.8%
per kelvin.

[b]This is a complete list of successive experiments in chronological order.

[c]A slight leak developed and was repaired before Experiment 16 began.

[d]Excluding the MoF_6, which, being much more volatile, was condensed further downstream.

[e]As determined by titrating the distillate with permanganate.

[f]1 torr = $(1/760)101325$ Nm^{-2}

[g]The vapor pressure of MoF_5 calculated assuming an ideal-gas vapor having a molecular
weight equal to that of the monomer (MoF_5). At each temperature the true vapor
pressure is smaller by the same factor by which the actual vapor density is greater.
See Section III of this chapter.

33

The fact that the experiments are given in Table 1 in chronological order facilitates examination of the results for chronological trends. As the mass of the liquid sample (initially 11.755 g) was successively reduced by what may be assumed to be the amounts in the fourth column, the percentage of MoF_5 found in the distillate (fifth column) steadily increased from less than 97% to approximately 100%. The simplest explanation is that a more volatile impurity was being distilled preferentially from the sample, and a "dilute solution" treatment of the first five experiments indicated a volatility ratio of greater than 5 (and so a concentration more than 5 times as great in the vapor as in the liquid). Some thin white films in the condenser in some experiments (MoF_5 is yellow) supports this explanation; the contaminant was likely $MoOF_4$, whose vapor pressures have been measured [4].

The values of vapor pressure of MoF_5 listed in the penultimate column of Table 1 for the individual experiments were calculated on the basis of the titration results by assuming gas ideality and the molecular weight of molybdenum pentafluoride monomer, MoF_5. That the last assumption, while convenient, is probably highly arbitrary is discussed in Section III.1. The last column of the table shows the percentage deviations of the calculated vapor-pressure values from the mean at each temperature.

The table may be examined further for evidence of other systematic errors. Turning to the sixth column, it is easy to realize that what could be considered an adequate partial pressure of MoF_6 will probably vary widely from one temperature to another. However, making comparisons only at the same temperature, it will be noted that deliberately doubling the MoF_6 in Experiment 12 led to the highest vapor-pressure value at 362.8 K, and deliberately halving the MoF_6 in Experiment 18 led to the lowest value at 382.9 K. We would expect the subfluoride resulting from disproportionation of the MoF_6 to be highly soluble in the liquid sample, so theoretically an infinite pressure of MoF_6 would be required to prevent disproportionation completely. (A simple calculation from these data suggested, however, less than 1% disproportionated in these experiments.) The consideration of flow rates of the transpiring (carrier) gas is similar except that one seeks a sufficiently low rate. The only

34

variation in flow rate was halving it in Experiments 11 and 17, where the effects are small and virtually within the precision (see last column). A few more transpiration experiments are planned with the aim of providing small corrections to the present results for these systematic errors.

The various detailed precautions routinely appropriate in accurate work were observed. These included calibration of the individual measuring instruments (such as thermocouples), accurate buoyancy corrections in weighing, close thermostating of temperature baths, and accurate standardization of titrating solutions and application of blank corrections in their use. Details are not given because at this stage we are unprepared to make quantitative estimates of the composite uncertainties of the experimental values obtained.

The following equation represents the "least-squares" fit of the vapor-pressure values for molybdenum pentafluoride in the penultimate column of Table 1, giving equal weight to each of the 15 values of log P. ($\underline{P}$ is in atm, $\underline{T}$ is the temperature in K, and the tolerances given are standard deviations.)

$$\log_{10}P(atm) = 6.3670(\pm 0.016) - 3189.5(\pm 6)/T \tag{2}$$

Deviations of individual values from Eq(2) are shown in Fig. 2. The limitations peculiar to molybdenum pentafluoride on deriving thermodynamic properties from this equation are discussed in the following section.

2. Concerning the Molecular Weight of Molybdenum Pentafluoride in the Vapor State

The foregoing transpiration results give practically no information as to whether MoF_5 is associated in the vapor state, but a recent mass-spectrometric study, at the Oak Ridge National Laboratory by C. F. Weaver and J. D. Redman on the various fluorides of molybdenum and niobium, does [5]. They studied molybdenum-pentafluoride vapor at a total pressure which they thought was between 0.001 and 0.1 torr, and presumably around 80°C. They reported finding under these conditions that the vapor was approximately 80% monomer (MoF_5), 20% dimer (Mo_2F_{10}),

35
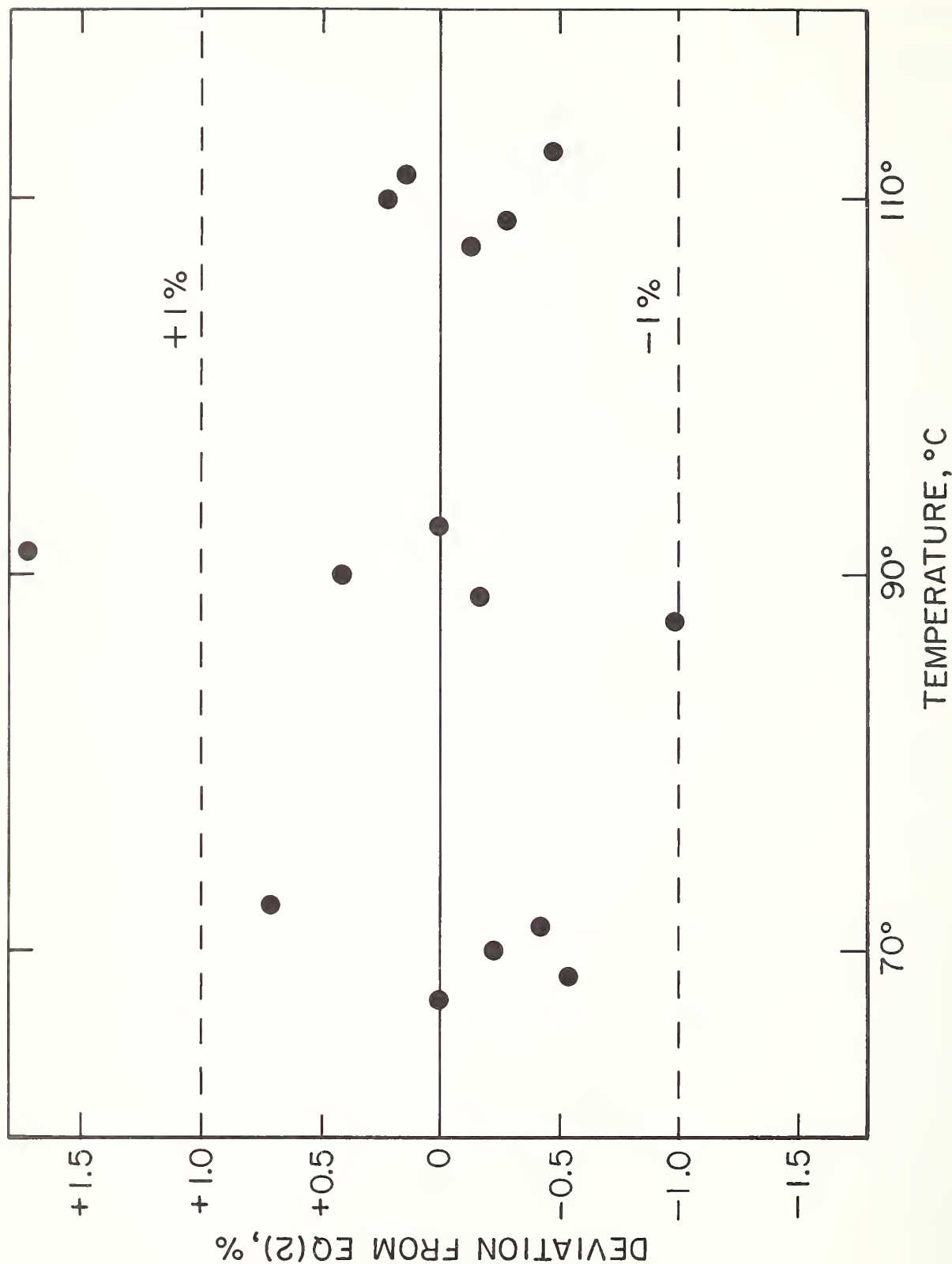
FIGURE 2. Deviations of the results of individual experiments from Equation (2) (Some of the points have been displaced horizontally to prevent overlapping.)

36

and $< 1\%$ trimer (Mo_3F_{15}). In addition, they reported standard enthalpy changes as follows:

$$Mo_2F_{10} = 2MoF_5; \quad \Delta H = 28 \text{ kcal.} \tag{3}$$

$$Mo_3F_{15} = 3MoF_5; \quad \Delta H = 34 \text{ kcal.} \tag{4}$$
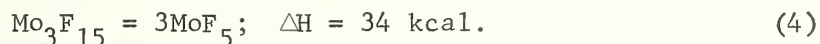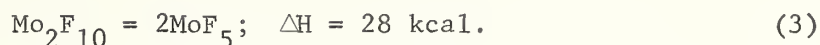
Though these data lack refinement that they hoped to achieve by improved calibration, they can easily be used to calculate for the composition of the saturated vapor at our temperatures (Table 1) considerably more dimer than monomer, as well as possibly a few percent of trimer.

Suppose for the sake of present argument we limit ourselves to monomer and dimer, and examine the consequences to transpiration results when the vapor consists of a mixture of substantial amounts of these two gas species. We can immediately dismiss gas nonideality as being small and essentially negligible at total pressures not greater than a few torr. The two (independent) vaporization reactions and the related all-gas reaction (with symbols defined for future reference) are:

$$MoF_5(\ell) = MoF_5(g): \quad \Delta H \equiv \Delta H_1, \ \Delta C_p \equiv \Delta C_1; \ p \equiv P_1 \tag{5}$$

$$2\ MoF_5(\ell) = Mo_2F_{10}(g): \ \Delta H \equiv \Delta H_2, \ \Delta C_p \equiv \Delta C_2; \ p \equiv P_2 \tag{6}$$

$$Mo_2F_{10}(g) = 2MoF_5(g): \quad \Delta H = 2\Delta H_1 - \Delta H_2 \tag{7}$$
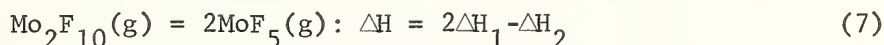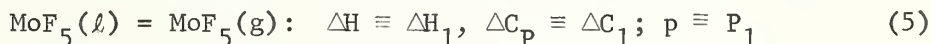
When (as in Table 1 and Eq (2)) transpiration data are treated as if the vapor is all monomer, then the calculated vapor pressure P measures the total available monomer units, so

$$P = P_1 + 2\ P_2 = (1 + r)\ P_1, \tag{8}$$

where r is defined by

$$r \equiv 2\ P_2/P_1. \tag{9}$$

Assuming ΔC_1 and ΔC_2 independent of temperature, one can combine the Clausius-Clapeyron equations for Reactions (5) and (6) with the above definitions to derive a Clausius-Clapeyron equation (and its derivative) for the transpiration process:

$$d \ln P/d(-1/RT) = (\Delta H_1 + r\Delta H_2)/(1 + r) \tag{10}$$

$$d^2 \ln P/d(-1/RT)^2 = r\ [(\Delta H_1 - \Delta H_2)/(1 + r)]^2 + (\Delta C_1 + r\ \Delta C_2)RT^2/(1 + r) \tag{11}$$

Equations (10) and (11) show two significant things worth pointing out. Firstly, the right-hand side of (10) is the "molar heat of vaporization" which one would derive from transpiration results such as Eq (2). But if the ratio r is not zero or infinity but well in between (as seems likely in the present case), the "transpiration data" heat of vaporization is neither ΔH_1 nor ΔH_2, but a function of them which is difficult to describe in simple terms (being a heat of vaporization to form an amount of vapor which is neither one actual mole nor one mole of "available" monomer). Secondly, the second term of Eq (11) cannot be negative, but the third ("heat-capacity") term ordinarily is, and in fact often overbalances the second term to give a negative curvature to a log P-vs-$1/T$ plot (first term).

Using the present transpiration results for 80°C, values of ΔH_1, ΔH_2, and r were obtained by simultaneous solution of Eqs (10), (11), and Weaver and Redman's value of Eq (3) ($2\Delta H_1 - \Delta H_2 = 28$ kcal). One of the two possible solutions is reasonable, giving $\Delta H_1 = 21$ kcal, $\Delta H_2 = 14$ kcal, $P_2/P_1 = 7$ in the saturated vapor, and Weaver and Redman's value of P_2/P_1 (= 1/4) if their total pressure were 0.008 torr, which is within their reported pressure range. Despite this rough agreement, these calculations should be considered quite uncertain, especially because the curvature of the "best" curve one could construct through the points of Fig. 2 is obviously highly uncertain. The results do suggest, however, that the saturated molybdenum pentafluoride vapor in our transpiration experiments was highly associated. Preliminary work on an attempt to measure the degree of association is described in the next section.

III. Development of a Method to Measure the True Vapor Pressures

1. Brief Description of the Method

Because of the evidence discussed in Section II. 2 that molybdenum pentafluoride is extensively but incompletely associated, yet to an ill-defined extent that leaves the thermodynamic interpretation of our precise transpiration data incomplete, we decided to adopt some additional type of measurement which, when combined with the transpiration results, will yield both the vapor density and the true vapor pressure--hopefully, with an accuracy of the order of 1%. The chemical instability and corrosiveness of MoF_5 impose serious limitations on the materials with which it can be in contact without serious error, and also dictate relatively low temperatures where the vapor pressures are only a few torr. We dismissed known vapor-density methods in favor of some method to measure the true vapor pressures, which can be combined with the transpiration data to yield the vapor densities.

Accurate pressure transducers have been developed and used which balance the vapor against a comparable known pressure of inert gas. However, because such transducer membranes, if sufficiently sensitive, are fragile and subject to calibration changes, we substituted for the membrane a valve which can be opened long enough to establish pressure equilibrium. In its simplest form the adopted method is essentially a null method, but in principle exact initial balance between vapor and gas pressures is unnecessary, since (assuming gas ideality) one can calculate the number of moles of vapor, knowing the moles of inert gas and their sum. The same type of method has been used previously--e.g., in measurements on sodium metal [6].

Obviously, pressure equilibrium must be established while the dissociable vapor is confined to a known volume. The following sections summarize the design details adopted to achieve this requirement, and preliminary measurements made on known cases to test their overall adequacy.

2. Apparatus Design and Experimental Procedure

The apparatus is diagrammed schematically (not to scale) in
Fig. 3. With the exception of two valves ($\underline{a}$ and $\underline{f}$) and their short
leads (stainless steel), all container parts were constructed of
pyrex glass. Distinguishing gas spaces by their volumes, an excess
of the condensed substance whose vapor pressure is to be measured is
placed in degassed and evacuated V_A and isolated by closed valves $\underline{a}$
and $\underline{f}$. After having evacuated the remaining gas spaces and sufficiently
degassed the manometric fluid, valve $\underline{c}$ is closed, then high-purity
argon is admitted through valve $\underline{b}$ until its pressure exceeds by a
small amount the expected vapor pressure; the argon occupies V_B at
temperature T_2, V_C at T_1 (room temperature if sufficiently constant),
and the newly created volume V_D at T_1--all at a pressure corresponding
to the manometer depression, which at this stage will be labeled x_1.
After then waiting for a sufficient time to ensure a steady state with
respect to the temperatures, the manometer displacement, and the slight
solution of argon in the manometer fluid, valve $\underline{a}$ is then opened briefly
two or more times until the new manometer depression x_2 $(x_2 < x_1)$ has
ceased to change by more than can be attributed to diffusion of vapor
through valve $\underline{a}$ and its subsequent condensation or absorption.

Assuming the ideal-gas law, the basic equation giving the vapor
pressure P $(= \Sigma_i P_i$ for all the vapor species) in terms of the data and
apparatus constants is

$$P = \rho g (1 + [d_1/d_2]^2)(x_2 - \{(x_1 - x_2)/V_A\} \{V_B + [T_2/T_1] [V_C + \pi d_1^2 (x_1 + x_2)/4]\}), \quad (12)$$

where ρ is the density of the manometric fluid and $\underline{g}$ is the gravitional
acceleration.

Di-n-butyl phthalate (vapor pressure, about 0.001 torr at room
temperature) is used as the manometric fluid; its low density and visosity
are obvious advantages. The adoption of unequal-bore manometer arms
almost doubled the sensitivity of reading the small-bore arm alone and
also almost halves the number of readings necessary, since the ratio
d_1/d_2 was carefully measured at several different manometer levels.

40
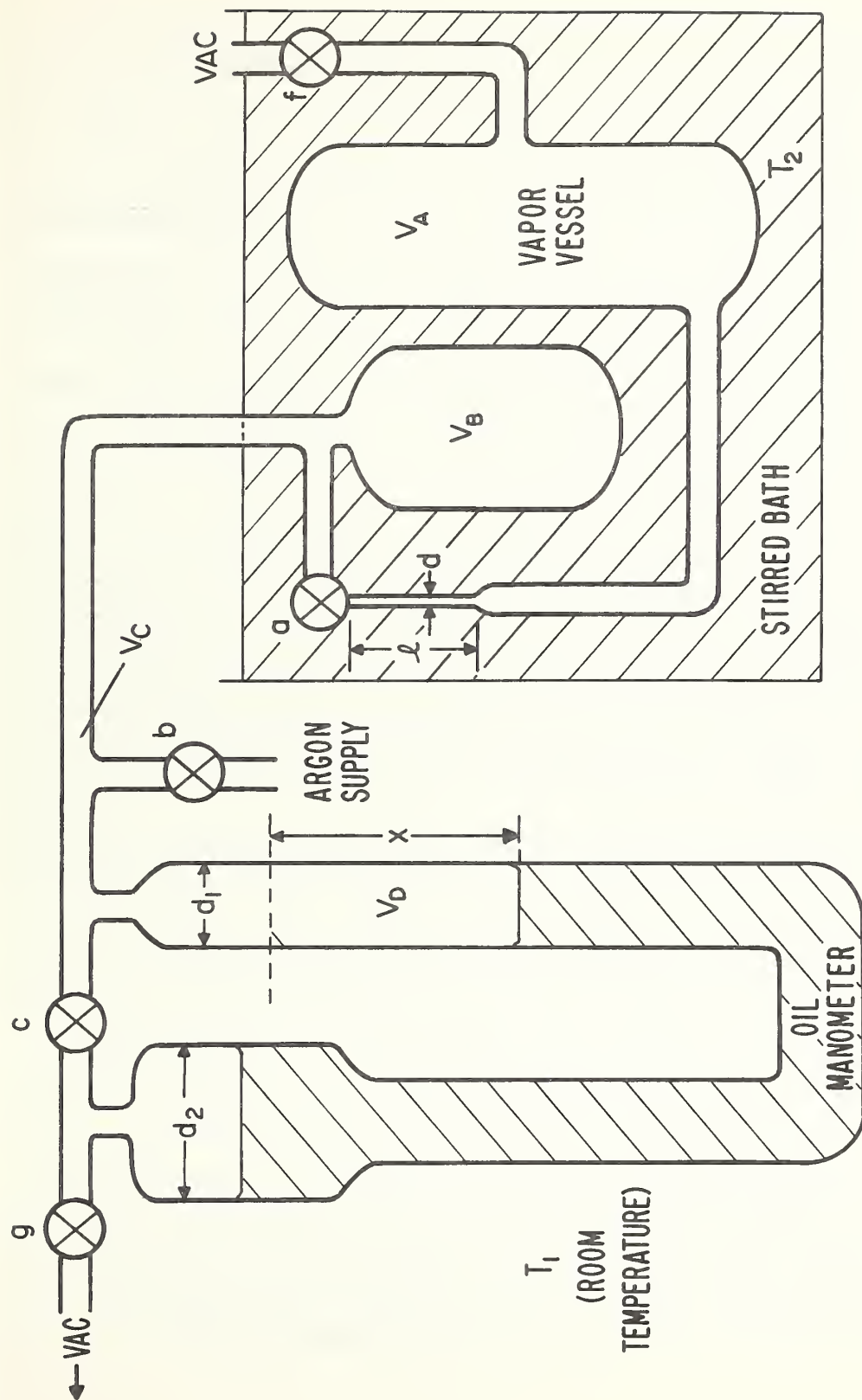
FIGURE 3. Apparatus to measure true vapor pressure (schematic)

41

The theoretical equal-pressure manometer-level inequality, 0.051 cm, was verified by observation. Precautions were taken in measuring the other apparatus constants accurately--e.g., the density of the sample of manometric fluid used was measured individually; the various volumes entering into Eq (12) were determined before assembly by filling with water and weighing; the half-meter calibrated Pt-Ir (in steel) manometer scale was read with a telescope; and the bath thermocouple was calibrated accurately. The thermomolecular pressure gradient due to the temperature difference $T_2 - T_1$ is entirely negligible for work of about 1% accuracy. Having a "ballast" volume V_B decreases the effect of uncertainty in temperature near the bath level, but too great a ratio V_B/V_A would unduly decrease the overall sensitivity.

The _rise_ in manometer level $(x_1 - x_2)$ when the valve _(a)_ to the vapor is opened must be positive and should not be too small, to prevent appreciable vapor from escaping from V_A by flow and diffusion, respectively; however, a rise which is _small_ (say, not greater than 10% of the initial manometer depression x_1) has the distinct advantages of minimizing the time required for virtual gas-pressure and manometer equilibration and of minimizing any error due to changing solubility of the argon in the manometer fluid.

The present apparatus constants are at room temperature as follows: $V_A = 70.39$ cm^3; $V_B = 38.68$ cm^3; $V_C = 19.54$ cm^3; $1 + (d_1/d_2)^2 = 1.0577$; $d_1 = 1.011$ cm; $\rho = 1.0415 \, [1 - .0007(t-25)]$ g cm^{-3} at t°C; $\ell = 5$cm; $d = 0.15$ cm. (Small corrections to these which have not been applied would change the vapor pressures calculated and listed in Section III.3 by perhaps as much as 0.2%, which is well within the overall uncertainties.)

Large erratic and systematic errors in vapor-pressure determination could occur if opening valve _a_ does not result in final pressure and vaporization equilibrium while all the vapor remains in its vessel V_A. To optimize the chance of approximating this ideal fairly closely, the length ℓ and inside diameter d of the "capillary" tube shown in Fig. 3 were selected after several kinetic-theory calculations of evaporation rate, wall adsorption, viscous flow, and gaseous interdiffusion.

42

If the rate of evaporation of the condensed vapor were comparatively slow, it is conceivable that after argon enters the vapor the vaporization equilibrium might be upset and be reestablished long after the valve (a) had been closed, producing unregistered pressure changes. A simple calculation showed that evaporation from each 1 cm^2 of solid iodine at 80°C (used for tests of the method-see Section III.3) is 99% complete in 0.05 sec if an accommodation coefficient of unity is assumed. The accommodation coefficient of the much more complexly oriented molecules in $MoF_5(\ell)$ is apparently many times smaller, requiring a correspondingly longer time; however, a subsequent opening of the valve as a test of pressure equilibrium should obviate any error from this source. Incidentally, if a little vapor were to diffuse out of the vapor vessel V_A but not be condensed or absorbed, any evaporation to replace the escaped vapor would produce a corresponding error.

Taking MoF_6 as a typical vapor, it was estimated that the adsorption of a monolayer on the inside surface of the present vapor vessel (V_A) would remove vapor equivalent to a pressure of 0.03 torr at 90°C. Adsorption should produce no systematic error if the vapor is maintained saturated by condensed phase, but obviously would (unless corrected for) if the measurements are extended to unsaturated vapor. One of the standard empirical procedures to enable correction for wall adsorption is to make measurements on an unsaturated vapor using two or more different surface-to-volume ratios. Here, some caution would be needed: it has been reported that the adsorptivity of "fire-polished" glass is increased manyfold (and unpredictably?) by a single washing with water[7].

Rapid mixing of the argon entering the vapor is needed, and this is promoted by gravitation by introducing the argon near the bottom of the (heavier) vapor, as well as having the vapor vessel (V_A) taller than its diameter (Fig. 3). Even so, it was desirable to know whether any appreciable fraction of the argon would rise to the top before time for its thorough horizontal interdiffusion with the vapor, or whether any argon reaching the top requires an undue length of time to mix by diffusing downward.

The interdiffusion of two gases in one dimension is given by

$$\partial N_i/\partial t = D(\partial^2 N_i/\partial x^2),\tag{13}$$

where N_i is the concentration of either gas, t is time, x is distance, and D is the specific interdiffusion coefficient. Although series solutions of Eq (13) are known for specified boundary conditions, dimensionless numerical integration of the equation was readily performed by computer for the initial condition of one pure gas (argon) occupying one end (10% of the volume) of a closed cylinder and the other pure gas (the vapor) occupying the other end (90% of the volume), all of course at a uniform total pressure. Using 30 steps in Δx, 1000 steps in Δt, and a constant arbitrary value $\dfrac{\Delta N_i}{\Delta t}\bigg/\dfrac{(\Delta\Delta N_i)D}{(\Delta x)^2} = 0.25$, the accuracy was checked by repetition using a coarser "grid". The interdiffusion coefficient D can be estimated [8] from

$$D = [8(1/M_1 + 1/M_2)]^{1/2}[RT/\pi]^{3/2}/3N_A P\sigma^2,\tag{14}$$

where M_1 and M_2 are the two molecular weights; R is the gas constant; T, the absolute temperature; N_A, Avogadro's number; P, the total pressure; and σ, the mean collision diameter of the two kinds of molecules. For argon and molybdenum pentafluoride at 90°C and a total pressure of 3 torr, Eq (14) gave $D = 25$ cm^2 sec^{-1}, and using this value the computer results indicated that the interdiffusion involving an original thickness of argon of 1cm would be 99.7% complete in 2 sec.

The capillary (length = ℓ and ID = d in Fig. 3) should be of such dimensions that during the time the valve (a) is open to admit argon to the vapor, only a negligible amount of vapor diffuses out (of V_A) (favoring a small d^2), yet the (viscous) flow of argon must be rapid enough to achieve virtual pressure equilibrium (favoring a large d^4). For the compromise capillary dimensions chosen, an integration of Poiseuille's equation for the volume rate of viscous flow,

$$dV/dt = \pi P d^4/128\eta\ell,\tag{15}$$

indicated 99.9% pressure equilibration in 8 sec for argon at a pressure of 3 torr. (η is the specific viscosity; and P, the average pressure, is a function of V.)

In the following section are summarized the results of four test experiments in which a known vapor pressure of iodine of about 15 torr was consistently reproduced to 1% or better without applying any hypothetical corrections. As evidence of the importance of the foregoing design considerations, it may be mentioned that an earlier version of this apparatus consistently gave values of the same vapor pressure of iodine that were in error by about 10% (but a little better if corrected for obvious vapor diffusion). The principal improvements of the present design over the earlier one are: (1) argon replaces helium (reducing vapor diffusion by a factor of about 3); (2) the capillary now abuts the valve seat (eliminating a short large-diameter dead-space whose considerable amount of vapor probably escaped quickly); (3) the length of the capillary was considerably reduced (promoting viscous flow); (4) constrictions in the manometer were eliminated, and the less viscous manometer fluid di-n-butyl phthalate was substituted (greatly hastening manometer equilibration, and thereby obviating the need to correct for compression of argon by manometer fluid after the valve (a) was closed).

3. Tests of the Apparatus in Reproducing Known Values

The apparatus and procedure in their present form (described in detail in Section III.2) were used to measure known pressures of the following three substances in the simulation of unknown vapor pressures:

1. Argon at pressures of approximately 13 to 22 torr. (This simulates a vapor except that it omits testing the features associated with vapor diffusion and condensation.)

2. Iodine at vapor pressures of approximately 15 and 8 torr. (The volatility is comparable to that of MoF_5 in the same temperature range; but iodine is completely stable, the monomer is entirely negligible at these temperatures, many observers have measured its vapor pressure, and the completeness of existing data has enabled tests of third-law consistency [9].)

3. MoF_6 at a vapor pressure of approximately 7 torr. (MoF_6 simulates MoF_5 (and its polymers) in type of molecule and chemical corrosiveness.

45

In addition, similar measurements will be needed on MoF_6 in conjunction with future measurements on MoF_5. Vapor pressures can be calculated from the Gibbs-energy functions of Osborne et al. [3], which are based on their low-temperature thermal and vapor-pressure data.)

The essential results of the measurements on the above three substances are given in Table 2. The valve between argon and the vapor cell (valve a in Fig. 3) was opened by an estimated one-half turn for 5 sec, and except in the case of Experiments 1-4 this process was repeated one or more times at intervals of 5 to 10 min each, the manometer (and temperature) readings being taken while this valve was closed. (Error in the calculated vapor pressure had been estimated to be <0.1% from diffusion during 5 sec.)

This procedure of successive openings provided an empirical test of whether equilibrium had been reached, and for each experiment one may examine the entries in the last five columns and take the last entry (or an estimated asymptotic value, particularly for Experiments 5 and 12) as the final value for that experiment. (In Experiments 1-4 no vapor was involved, so the valve was opened only once, but long enough to ensure pressure equilibrium.)

The agreement with the "accepted" values using argon (Experiments 1-4) averages 0.1%, and is entirely satisfactory, since this corresponds to the precision of reading pressures and temperatures in this apparatus. The agreement for iodine (Experiments 5-13) also is satisfactory, being essentially within the estimated uncertainty of the "accepted" value of ±1.5% (especially for the higher pressure). While no estimate was made of the uncertainty of the "accepted" (published) vapor pressure of MoF_6, this fact is irrelevant to the inferior reproducibility among different experiments (Nos. 14-16), and the need for further work on MoF_6 is indicated. The inferiority of the MoF_6 results may reflect some difficulty at that time in valve leakage, or the absence of condensed MoF_6 in the vapor cell (V_A) may be a significant factor.

So far no application of the new apparatus to molybdenum pentafluoride has been made, but such experiments are planned for the near future.

46

Table 2. Measurement of "Known" Pressures of Argon and Vapor
Pressures of Iodine and Molybdenum Hexafluoride

Substance	Experiment No.	Temperature (K)	Accepted Pressure (torr)	Deviation (%) of P_{found} from $P_{accepted}$ after Valve-Opening No.[e]				
				1	2	3	4	5
Ar	1	296.2	22.05[b]	-0.22				
	2		13.47[b]	-0.12				
	3		21.34[b]	0.00				
	4		12.75[b]	+0.06				
I$_2$	5	352.75	14.72[c]	+7.7	+3.3	+1.6		
	6			+10.4	+3.3	+0.9	-0.2	-0.3
	7	352.67	14.65[c]	+8.3	+2.3	+0.8	+1.1	
	8			+6.3	+2.0	+0.08	-0.06	
	9	342.88	8.04[c]	+10.4	+4.3	+2.0	+2.0	
	10			+12.0	+3.8	+1.1	+0.3	
	11			+6.4	+3.8	+2.9	+2.2	
	12			+2.1	+1.7			
	13			+5.1	+2.4	+1.2	+1.0	
MoF$_6$	14	231.64[a]	6.63[d]	+3.4	+3.4			
	15			+1.4	-3.4	-5.8		
	16			-2.0	-2.5			

[a] The MoF$_6$ vapor was generated from the solid at 231.64 K, but measured in the apparatus at 392.6 K.

[b] Pressures as measured by direct manometry in the apparatus.

[c] Calculated from the values of Reference [10]. The values of Reference [9] give essentially identical values for these vapor pressures.

[d] Calculated by interpolating the Gibbs-energy functions of Reference [3].

[e] The valve between argon and the vapor cell (valve a in Fig. 3) was opened by an estimated one-half turn for 5 sec , at intervals of 5 to 10 min.

IV. References

[1]   N. Acquista and S. Abramowitz, This Report, Chapter 3 .

[2]   R. F. Krause, Jr., NBS Report 10481, July 1971, p. 97.

[3]   D. W. Osborne, F. Schreiner, J. G. Malm, H. Selig, and L. Rochester, J. Chem. Phys. $\underline{44}$, 2802 (1966).

[4]   G. H. Cady and G. B. Hargreaves, J. Chem. Soc. $\underline{1961}$, 1568.

[5]   C. F. Weaver and J. D. Redman, Section 11.6.3 of ORNL Report 4449, Oak Ridge, Tenn., Feb. 1970, p. 116.

[6]   W. H. Rodebush and E. G. Walters, J. Amer. Chem. Soc. $\underline{52}$, 2654 (1930).

[7]   L. A. Guildner, National Bureau of Standards, private communication.

[8]   S. Glasstone, "Textbook of Physical Chemistry," 2nd ed., D. Van Nostrand, New York, 1946, p. 281.

[9]   JANAF Thermochemical Tables, D. R. Stull and H. Prophet, Proj. Directors, 2nd ed., NSRDS--NBS 37, U. S. Government Printing Office, Washington, D. C. June 1971 [tables for I_2 (c), I_2(g), and I(g)].

[10]   D. D. Wagman, W. H. Evans, V. B. Parker, I. Halow, S. M. Bailey, and R. H. Schumm, NBS Technical Note 270-3, U. S. Government Printing Office, Washington, D. C., January 1968, p. 36.

Chapter 3

THE VIBRATIONAL SPECTRA OF MOLYBDENUM PENTAFLUORIDE

Nicolo Acquista and Stanley Abramowitz

Introduction

The vibrational spectra of the MF_5 molecules have been
interpreted either on the basis of D_{3h} (trigonal bipyramid) or
C_{4v} structure. Recently the authors interpreted the observed in-
frared spectrum of matrix isolated NbF_5 as possibly indicative of
C_{4v} symmetry for this species[1]. The apparent observation of
three stretching modes and a feature at 513 cm^{-1} were taken as
experimental proof of the C_{4v} structure. Recently a Raman spectrum
of the vapors in equilibrium with NbF_5 (s) and NbF_5 (l) in the
stretching region has been interpreted as indicating D_{3h} structure
for the monomer.[2] The pentafluorides of arsenic[3], phosphorous[4]
and vanadium[5] have been shown to have D_{3h} symmetry while SbF_5
has C_{4v} symmetry[6]. It should be noted that the Raman spectrum of
gaseous SbF_5 has recently been observed (and in a manner similar
to NbF_5) and has been interpreted on the basis of D_{3h} symmetry for
the monomeric species[7]. Since MoF_5 is the next higher member to
NbF_5 in the transition metal series, it was thought worthwhile to
investigate its vibrational spectra.

MoF_5 has only recently been prepared[8]. Edwards et al,[9] re-
ported another method of preparation and studied the structure of
the solid using x-ray single crystal techniques. They concluded
that MoF_5 crystallize to form square tetramers in which the four
Mo atoms are joined thru fluorine bridges, and that it is iso-
structural with NbF_5 and TaF_5.

Ouellette et al,[10] have reported the Raman and infrared
spectra of liquid and polycrystaline MoF_5. A vibrational assign-
ment was proposed for molten MoF_5 on the basis of D_{3h} symmetry,
but the polycrystaline spectrum was not interpreted.

Bates[11] has remeasured the room temperature Raman spectrum of
crystalline MoF_5 observing essentially the same spectrum as Ouellette
et al[10]. Using frequencies and assignments of the bands observed
by Ouellette in molten MoF_5, he assigned the Raman spectrum by a
double correlation scheme which maps the symmetry species D_{3h} for
MoF_5 monomer into the factor group C_{2h} in the solid. The lowest
line found by Bates is at 180 cm^{-1}. The lowest frequencies of VF_5[5],
AsF_5[3] and PF_5[4] appear at 109, 138, and 179 cm^{-1} respectively. It
is therefore possible that MoF_5 crystal will have a fundamental below 180 cm^{-1}.
The Raman spectrum of polycrystalline MoF_5 was reinvestigated in this
study using both He/Ne and Ar^+ (4880 Å) excitation to within 30 cm^{-1}
of the exciting line.

A molecular beam-mass spectrometer has been designed and con-
structed by Vasile et al[12], to study reactive fluorides and similar
molecules. The pentafluorides of Nb, Ta, Mo, Re, Os, Ir, Ru, Pt,
Sb and Bi were all found to be associated in the saturated vapor
phase. Dimeric and trimeric species were dominant in the low temp-
erature vapors ($\sim$ 50°C) and tetrameters were found for MoF_5 NbF_5 and other
pentafluorides. They observed that those pentafluorides found to be
associated in the vapor phase in their study were also associated in
the solid phase as tetramers or in infinite chains. They concluded,
by implication, that the liquid is very likely associated.

Weaver et al[13] reports similar results to Vasile et al, and
finds that at 80°C the vapor is 80% MoF_5 monomer. Ouellette[10] also
reports the presence of monomer at 70°C.

There have been no reported structural studies of the vapors
of MoF_5. Infrared matrix isolation studies should be uniquely suited
for a study of the vibrational spectrum. This is particularly true
since the monomer polymer ratio in MoF_5 vapor may be expected to
be enhanced in high temperature unsaturated vapors. Therefore
a systematic study of the matrix isolated vapors of MoF_5 was initiated
using double boiler techniques. Raman spectra of polycrystalline
MoF_5 and liquid MoF_5 were also observed.

Experimental

The experimental method used to observe the infrared spectrum of matrix isolated MoF_5 monomer was essentially the same as in the NbF_5[1] study with only slight modification. An Air-Products cryotip operated at liquid hydrogen temperature, a Perkin-Elmer spectrophotometer 301 operated between 4000 to 50 cm^{-1} and a resistively heated furnace with a stainless steel tube were employed[14]. The stainless steel tube, which in the present apparatus performs as the upper crucible, is approximately 6" long. The first 3" of this tubing has 3/16" ID x 1/4" OD and is located inside of a coiled tungsten heater. The remaining 3" is 1/8" tubing with a 1 mm hole. This tubing leads to a brassplate where it is brazed to a 1/4" quick-connector. The MoF_5 sample was prepared by R. F. Krause[15] of NBS. The cryoscopic impurity was estimated to be 0.15 mol %. His vaporation data was used to set the temperature of the sample tube to the desired vapor pressure. The MoF_5 was sealed in vacuo in a pyrex sample tube and was never exposed to the atmosphere at any time during the experiments. The pyrex sample tube with teflon needle valve was connected to the stainless steel tube in the furnace. The temperature of the stainless steel tube was measured with a chromel-alumel thermocouple. It was the temperature of the stainless tube that was varied during the experiments from room temperature to $\sim 150°C$. The sample pyrex tube was maintained at room temperature, although a hot water bath could be used to change its temperature. During the course of the experiment, it was found that room temperature was adequate for developing sufficient vapor pressure in the lower-oven to obtain good intensity spectra in 3 to 4 hours.

The entire deposition system was thoroughly baked out before exposure to MoF_5 vapors; MoF_5 reacts with moisture adhering to the walls of the deposition system to form volatile oxyfluorides, which will codeposit in the matrices and give spurious bands.

MoF_5 tends to disproportionate slowly at room temperature and more rapidly at higher temperatures to involatile MoF_4 and to MoF_6 (g)[12, 15]. Therefore, when an experiment was started, the first vapors were pumped away. This procedure also served to pickle the deposition

51

system, including the stainless steel furnace. After the first few experiments it was clear that the system was seasoned because the spectra become more and more reproducible. Temperatures above 150°C were not used to form matrices because, we observed, the spectra became less reproducible probably because of increased disproportionation and decomposition.

The matrix gas used was argon. Some matrices were formed in nitrogen but yielded no new results and are not included in this report. The M/R ratios, are estimated to be in the range of 500-1000.

Atmospheric water, CO_2 and NH_3 were used to calibrate the spectra. Many of the bands were overlapped and are good to about ± 2 cm^{-1}. The solid infrared spectral bands are very broad and the measurements are not as good.

Raman spectra of the polycrystalline MoF_5 were observed with a Spex Ramalog[14] using a cooled photomultiplier. He/Ne and argon ion (4880Å) laser lines were used for excitation. Spectra were observed to within 30 cm^{-1} of the exciting line. Raman spectra of supercooled MoF_5 liquid were also observed.

<center>Experimental Results</center>

Fig 1 shows the infrared spectrum of MoF_5 vapors isolated in argon matrices at liquid hydrogen temperature. The pyrex sample tube was maintained at room temperature for all these experiments except for one, while the upper stainless steel tube was varied from room temperature to 150°C. Curve a shows the spectrum resulting when MoF_5 effuses from the double-oven when both lower and upper boilers are at room temperature. Since the saturated vapors at this temperature contains mostly dimers and trimers[12], the infrared spectrum is representative of these species. These bands appear at 768, 716, and 704 cm^{-1}. Curve b is the spectrum of vapors of MoF_5 in equilibrium with room temperature heated to 50°C. The spectrum is essentially the same as a; a weak feature appears at 735 cm^{-1} which coincides with a matrix band of MoF_6/Ar. Curve c shows the spectrum obtained when the upper crucible is at 100°C (the sample is at room

<center>52</center>

temperature). The spectrum continues to change with temperature. The polymer bands intensities have decreased, while new features are beginning to appear at 713, 695 and 683 cm^{-1}. The MoF_6 has also increased and broadened, suggesting its growth with temperature and a possible new feature at about 733 cm^{-1}.

At a temperature of 140°C, curve d, the polymeric features, at 768, 704 and 716 cm^{-1} have diminished to a greater extent. The decreased intensity of the 716 cm^{-1} feature is obscured by the growth of a new feature at 713 cm^{-1}. It is clear that the band at 683 cm^{-1} has grown considerably. The band at 695 cm^{-1} has not grown, suggesting it is not due to the same species causing the bands at 733, 713, and 683 cm^{-1}.

A final experiment was carried out, in which the lower MoF_5 sample temperature was raised to 50°C and the S.S. upper crucible was operated at 150°C. The spectrum, curve e, is a combination of polymers, and monomers; the bands are broadened. When the lower crucible is heated, above room temperature, the vapors effuse more rapidly, there is little time for equilibrium in the upper crucible, allowing more polymeric species to effuse, and possibly, also leading to poor isolation in the matrix.

To check the presence of oxyfluoride in our spectra, MoF_5 was effused at 140°C (the sample MoF_5 at room temperature) and codeposited with an Ar/H_2O,(=100) sample at liquid hydrogen temperature. The spectrum showed a decrease of all bands except the 695 cm^{-1}, which grew. Therefore this 695 cm^{-1} feature is most likely due to an oxyfluoride.

Our experiments suggest three bands that should be considered when assigning bands to MoF_5 monomer. We prefer the bands at 713 and 683 cm^{-1} as due to monomeric MoF_5. The two bands have grown most consistently together in intensity. The band at 733 cm^{-1} is weak, masked by MoF_6 and has shown some uncertain intensity variations which could be due to variable amounts of MoF_6 in the matrix. Because of these uncertainties, we feel this feature may be due to MoF_4 which, although having a low vapor pressure at the temperatures of our experiments probably is deposited in the matrix with MoF_6 and monomeric MoF_5. The solid phase Raman spectrum of MoF_4 has recently been reported by Bates[16].

Fig 2 shows the far infrared spectrum from 300 to 100 cm^{-1} when the MoF_5 vapors were heated to 140°C (the sample at room temperature), curves a, c. Three bands appear here. The bands at 261 and 112 cm^{-1} were assigned to monomers because they grew in together under conditions favorable to monomeric MoF_5. The band at 231 cm^{-1} did not appear consistently with these two bands and was considered a species other than MoF_5 monomer.

Curve "b" shows a spectrum of MoF_5 vapors in argon when the upper crucible is at 150°C and the lower at 50°C. Both the monomer feature at 261 cm^{-1} and the 231 cm^{-1} feature have grown. It is clear here that the relative intensities of these two bands are different that those in curve a.

These experiments suggest four features as due to monomeric MoF_5: 713, 683, 261 and 112 cm^{-1}. The frequencies are listed in Table I.

Fig 3 shows the infrared spectrum of solid MoF_5 at liquid hydrogen temperatures effused at 50°C from 750 to 400 cm^{-1}. The spectrum was scanned to 200 cm^{-1}. The bands shown are the only ones observed. They appear at about 725, 700, 660 and 525 cm^{-1}, are very broad and are suggestive of a polymer spectrum. The frequencies are approximate because of the uncertainty in finding the band centers. In contrast the bands in the matrices of Argon are relatively sharp. These frequencies are also in Table I.

Several diffusion experiment were performed on a MoF_5/Ar matrices. The resulting spectrum of MoF_5 residue after the argon had boiled away, was very similar to the solid spectrum of Fig 3.

The Raman spectrum of solid MoF_5 is shown in Figure 4. These results are essentially equivalent with those of Bates[11] and Ouellette et. al.[10] except in the low frequency region. The band at about 120 cm^{-1} which is also present in the liquid corresponds to the 112 cm^{-1} found in an argon matrix for monomeric MoF_5. The bands at displacements of about 90 and 60 cm^{-1} from the exciting line are only present in solid MoF_5 and may be due to vibrations of the tetrameric unit. These features were observed with both the helium-neon and argon ion lasers. The power of the argon ion laser at 4880 Å had to be kept rather low (22 milliwatts) in order to avoid melting the yellow sample.

54

Discussion

The infrared spectra of the vapors over solid MoF_5 have been
observed in argon matrices at liquid hydrogen temperatures. By
varying the temperature of the upper boiler in the double oven,
significant changes in the composition of the vapors were effected.
The low temperature spectrum of the saturated vapors produced bands
at 768, 716 704, and 231 cm^{-1} (Fig 1, curves a, andFig 2), which
were interpreted as due to polymers.[12] At high temperatures, the
unsaturated vapors are known to contain a larger proportion of monomer
relative to polymers. The spectra reflect these changes. New
bands appear at 713, 683, 261 and 112 cm^{-1} while aggregate band
intensities decrease. Our experiments suggest that these bands are
due to monomeric MoF_5.

A study of MF_5 spectra has shown these molecules to have a
D_{3h} (trigonal bipyramid or C_{4v} (tetragonal pyramid) structure. The
vibrational representation of a D_{3h} molecule is $2a_1' + 2a_2'' + 3e' +$
e'' with a_2'' and e' infrared active and the a_1', e', and e'' modes Raman
active. For a C_{4v} molecule, the vibrational representation is
$3a_1 + 2b_1 + b_2 + 3e$ ($a_1 + e$ are infrared active); a_1, b_1, b_2, and e are Raman
active.) D_{3h} requires the presence of 5 infrared ative bands while
C_{4v} requires six. Four infrared bands have been found in these
experiments. Depositions lasting longer than 6 hours have produced
no other bands.

The assignment of MoF_5 to a symmetry species is rather difficult.
The absence of a band at 500 cm^{-1} suggests that MoF_5 does not possess
C_{4v} symmetry. (although this band could be very weak). Such a band is
found in the interhalogens.[17] Tetramers of MoF_5 are associated thru
Mo-F-Mo bridge bands, a connection favored by C_{4v} monomer structure.

Bates has described the Raman spectra of the solid assuming
D_{3h} symmetry for the basic structure of MoF_5 tetramer while Ouellette
favors D_{3h} also for the structural unit in molten MoF_5.

Our spectra show only 2 bands at the high frequency region of the
infrared (ie. 713 and 683 cm^{-1}). This favors D_{3h} symmetry. Three bands
are required for C_{4v} symmetry.

Additional experimental evidence is needed before the structure of MoF_5 can be conclusively determined. We have assigned MoF_5 assuming it is a D_{3h} molecule in analogy with PF_5, AsF_5, VF_5 which are known to possess this symmetry. The assignments of all the bands found are listed in Table I with the data of Bates and Ouellette.

In polycrystaline MoF_5, the infrared band appearing at 525 cm^{-1} is not present in the matrix spectrum. This band is probably due to the Mo-F-Mo bridge that exists in the tetramer. These frequencies are also in Table 1.

References

[1]   N. Acquista, S. Abramowitz, J. Chem. Phys. J. Chem. Phys.
       $\underline{56}$, 5221 (1972).

[2]   L. E. Alexander, I. R. Beattie, P. J. Jones, J. Chem. Soc.
       (Dalton) $\underline{1972}$, 210.

[3]   a)   L. C. Hoskins, R. C. Lord, J. Chem. Phys. $\underline{46}$, 2402 (1967).
       b)   L. C. Hoskins, C. N. Perng, J. Chem. Phys. $\underline{55}$, 5063 (1971).

[4]   a)   J. E. Griffiths, R. D. Carter Jr., R. R. Holmes, J. Chem.
       Phys. $\underline{41}$, 863 (1964).
       b)   I. W. Levin, J.Mol.Spectroscopy $\underline{33}$, 61 (1970).
       c)   I. R. Beattie, R. M. S. Livingston, D. J. Reynolds, J.
       Chem. Phys. $\underline{51}$, 4269 (1969).
       d)   F. A. Miller, R. A. Capwell, Spectrochim. Acta $\underline{27A}$ 125
       (1971).

[5]   H. Selig, J. H. Holloway, J. Tyson, H. A. Claasen, J. Chem.
       Phys. $\underline{53}$, 2559 (1970).

[6]   A. L. K. Aljibury and R. L. Redington, J. Chem. Phys. $\underline{52}$,
       453 (1970).

[7]   L. E. Alexander and I. R. Beattie, J. Chem. Phys. $\underline{56}$, 5829
       (1972).

[8]   R. D. Peacock, Proc. Chem. Soc., $\underline{1957}$, 59.

[9]   A. J. Edwards, R. D. Peacock, R. W. H. Small, J. Chem. Soc.
       (A) $\underline{1962}$, 4486.

[10]   T. J. Ouellette, C. T. Ratcliffe, D. W. A. Sharp, J. Chem.
       Soc.(A) $\underline{1969}$, 2351.

[11]   J. B. Bates, Spectrochem. Acta. $\underline{27A}$, 1255 (1971).

[12]   M. J. Vasile, G. R. Jones, W. E. Falconer, International
       Journal of Mass Spectroscopy, to be published.

[13]   C. F. Weaver and J. D. Redman, ORNL Report 4449 pp. 116-119
       Oak Ridge, Tenn. February, 1970.

[14]   Certain commerical apparatus are identified to specify
         adequately the experimental procedure. In no case does
         such identification imply recommendation or endorsement by
         NBS.

[15]   R. F. Krause, Natl. Bur. Std. Report 10481 pp. 97 (1971).

[16]   J. B. Bates, Inorganic Nucl. Chem. Letters $\underline{7}$ 957 (1971).

[17]   G. M. Begun, W. H. Fletcher, and D. F. Smith, J. Chem. Phys.,
         $\underline{42}$, 2236 (1965).

Table I

Vibrational Assignment of MoF$_5$

Melt(a)		Crystal, Raman, (b)		Crystal present work		Matrix IR	Assignment
				IR	present work		
747		759	Ag			768	polymer
		738	Ag			735	MoF$_6$ (ν_3)
730	IR	747					
						733	MoF$_4$ (?)
					725		
						716	polymer
						713	MoF$_5$(E')ν_5
		706	Ag				
703		696	Ag			704	polymer
					700		
685	IR	684				683	MoF$_5$(A$_2$")ν_3
					660		
500	IR	494			525		bridge-bond
440		436					
		402					
		332					
		282					
						261	MoF$_5\nu_6$(E')
250	IR	252	Ag				
		239	Ag				
231						231	polymer
201		199					
		181					
		120	(c)			112	MoF$_5$ ν_7(E')
		90	(c)				polymer
		60	(c)				polymer

(a) Frequencies and assignments of molten MoF$_5$ were taken from reference 10. The frequencies are from the Raman spectrum except where noted otherwise.

(b) Bates assignment of solid, reference 11.

(c) Present Raman results.
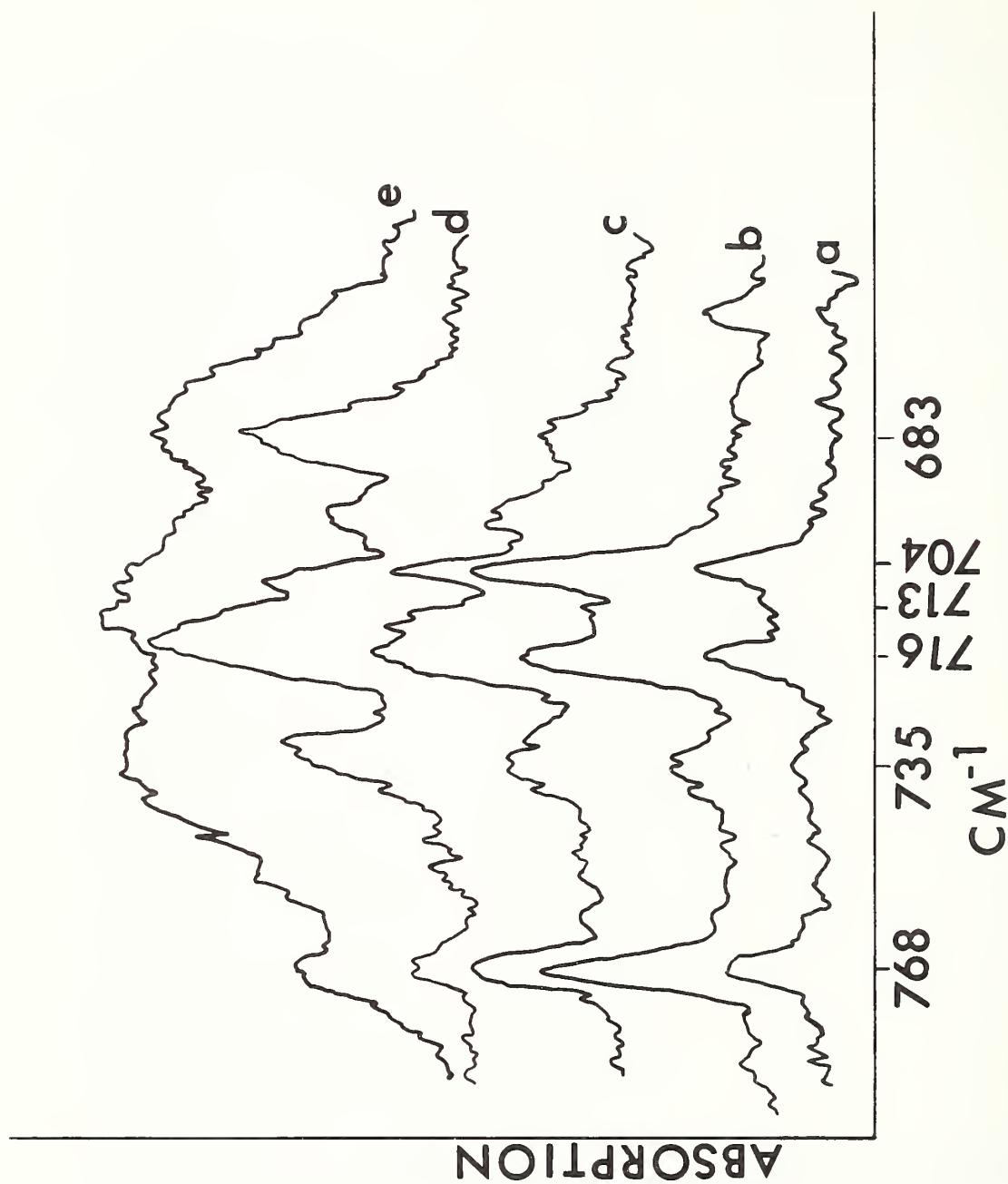
FIGURE 1. The infrared spectra of matrix isolated MoF_5 in Argon at 20° K. Double-oven Knudsen cell utilized. Curve a, both upper and lower crucible at room temperature. Curve b, upper at 50°C lower at room temperature. Curve c and d lower crucible at room temperature; upper at 100 and 140°C respectively. Curve e, lower at 50°C, upper at 150°C.
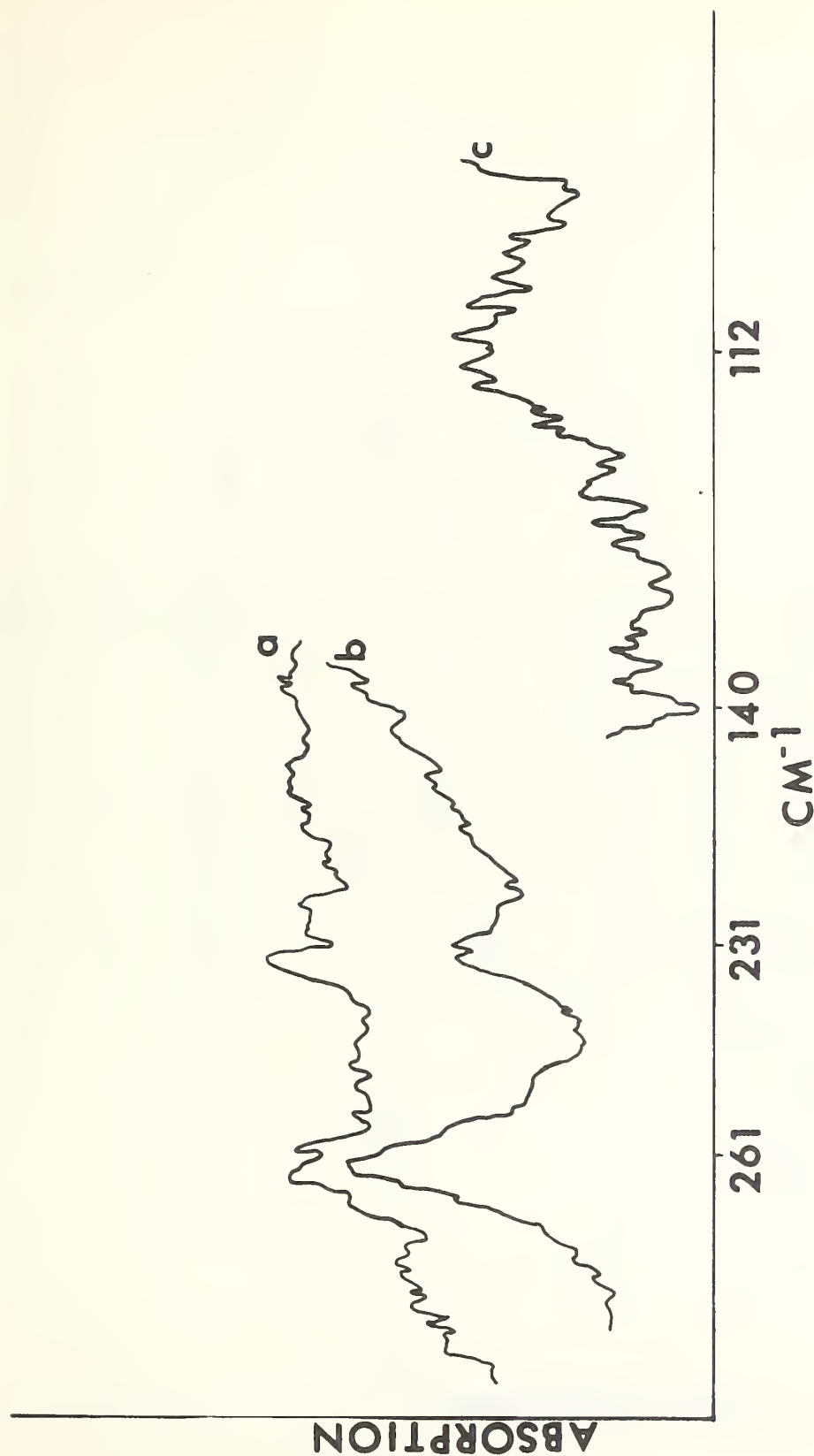
FIGURE 2. The far infrared spectrum of MoF_5 trapped in Argon matrices at liquid hydrogen temperature. Curve a and c the lower crucible at room temperature the upper at 140°C; Curve b, the lower crucible at 50°C, the upper at 150°C.
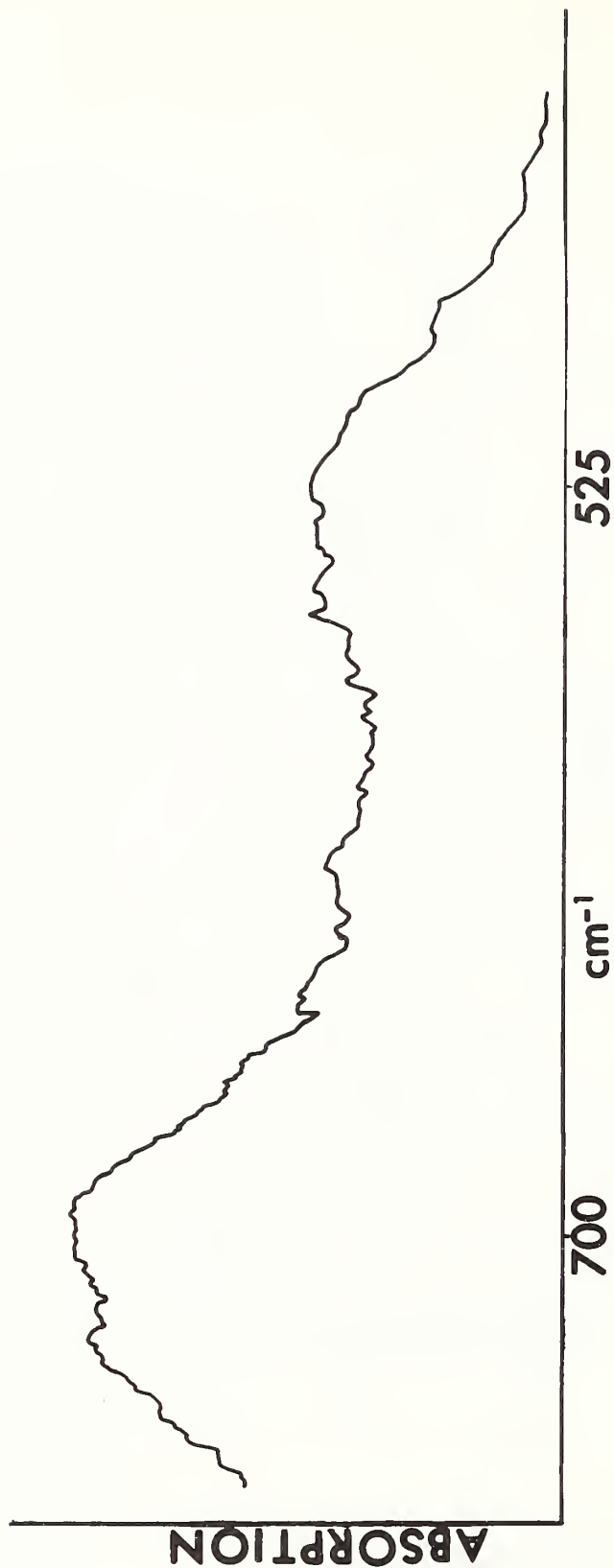
FIGURE 3. The infrared spectrum of solid MoF$_5$ at 20°K.

62
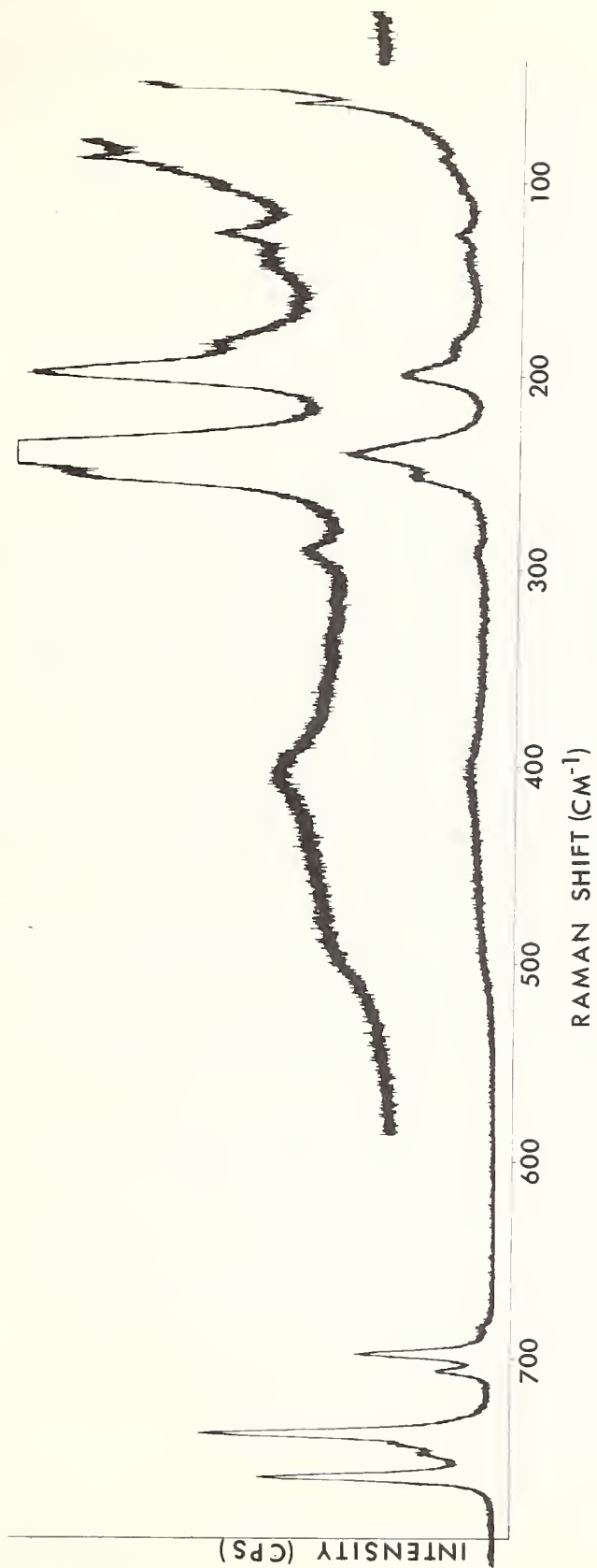
FIGURE 4. The Raman spectrum of solid MoF$_5$.

63

Chapter 4

PRELIMINARY REPORT ON THE

MEASUREMENT OF THE RELATIVE ENTHALPY OF MO_2C

FROM 273.15 TO 1475 K

D. Ditmars and S. Ishihara

1. Introduction

The molybdenum carbide Mo_2C is one of the refractory metal carbides currently being studied in a joint effort of the Los Alamos Scientific Laboratory and the NBS. The Los Alamos work, with Dr. E. K. Storms as principal investigator, has concentrated mainly on elucidating the phase behavior of this compound (and others in the Mo-C system) by DTA techniques as well as high-temperature x-ray and neutron diffraction analysis. Recently, evidence has been found for the existence of an order-disorder transition in Mo_2C in the vicinity of 1400°C [2,3][a]. The NBS contribution to this effort, a preliminary report on which follows, has been planned to eventually provide through high-temperature calorimetric measurements, additional information on this transition as well as to derive improved thermodynamic functions for $Mo_2C(s)$.

Mo_2C belongs to the class of "defect compounds", so-called because they can exist over a considerable range of composition with a high concentration of defects in the non-metal sub-lattice. Mo_2C can, for instance, exist with anywhere from 26 to 36 atomic percent carbon, depending on the temperature. Melting near 2500°C, it has

---

[a]Figures in brackets indicate literature references listed at the end of this chapter.

an attractive potential for high-temperature applications. Yet,
certain thermodynamic data on it are either lacking or seem
inadequate [1].

The complete phase diagram for the portion of the Mo-C
system of greatest interest has been given in a previous report [1].
Figure 1 of the present work, taken from reference [4], depicts
an enlarged portion of that diagram and summarizes present knowledge
on the phase relationships of compounds near to and including the one
of which this work treats.

There exist two low-temperature calorimetric studies on Mo_2C
[5,6] and two series of enthalpy measurements extending above room
temperature to 2500 K [6,7]. These investigations were carried out
with compounds with compositions differing from the one available in
the current study. This can be significant for the interpretation
of the Mo_2C enthalpy and specific heat data as it has been observed
[2,3] that the speed with which this compound completes its order-
disorder transition in cooling through 1400°C is remarkably
sensitive to the concentration of non-metal, as little as half
a weight percent difference in the carbon content considerably
retarding the process.

2. Sample

The sample of Mo_2C used in the experiments reported below was
obtained on loan from the Los Alamos Scientific Laboratory of the
University of California where it was fabricated to a specific
composition and partially anaylzed by Dr. E. K. Storms. This
composition was chosen as one which would ensure rapid completion
of the anticipated transition at 1400°C. It was achieved by taking
advantage of the fact that Mo_2C vaporizes congruently near $MoC_{.49}$ [2].
High-purity Mo and C powders in approximately this proportion were
mixed and cold-pressed into cylindrical shape with a binder which was
subsequently driven off in a vacuum. This cylinder was heated to
2400°C and held there to achieve the congruently vaporizing composition,
losing in the process approximately ten percent of its weight. It
was later annealed at 1900°C for 1/2 hour and at 1100°C for 2 hours.

Preliminary chemical analyses of portions of the sample have
indicated a carbon content of 5.75 weight percent (corresponding to
a formula of $MoC_{.4873}$) and an oxygen content of about 50. ppm. X-ray
analysis has indicated that it is single-phase α-Mo_2C.

The sample was received in the form of a cylinder approximately
3/8 in. O.D. and 1 in. long, weighing 26.6274 grams.
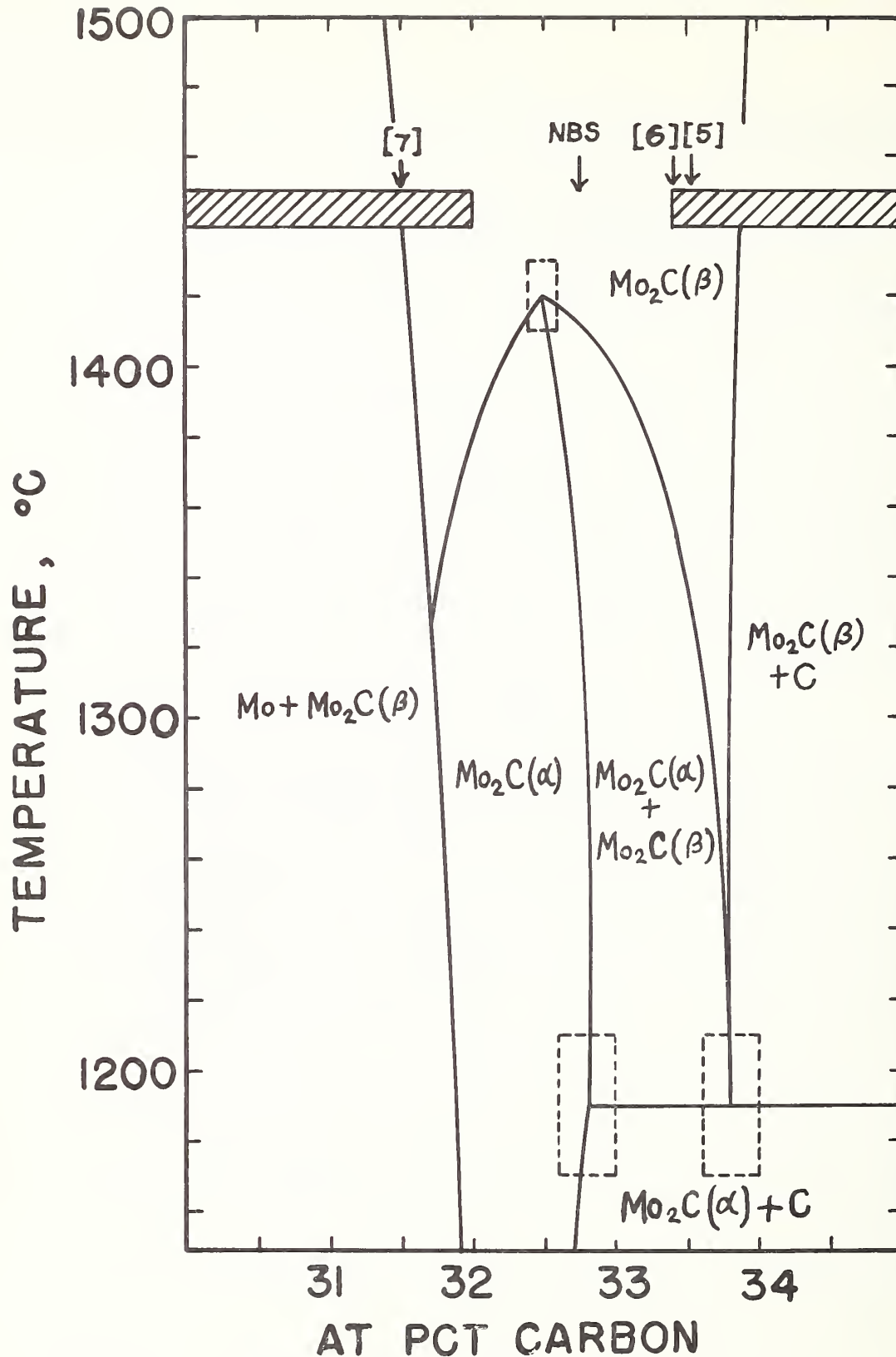
Figure 1. A portion of the Mo-C phase diagram. Shaded bars at top denote composition ranges for which order-disorder transition proceeds slowly [2,3]. Arrows indicate composition investigated by other workers and by NBS. Dashed boxes surrounding joining points indicate temperature and composition uncertainties. Diagram adapted from [4].

3. Experimental

Two different calorimeters were used to complete the enthalpy measurements over the range 273.15 K to 1475 K. The techniques used are described below with reference to the temperature range in which they were employed.

a. 273.15 K to 1173.15 K

In this temperature range, relative enthalpies were measured with a Bunsen ice calorimeter. Briefly, the procedure, more complete details of which are contained in other publications [8,9], is as follows: The sample, enclosed in a suitable container, is suspended in a resistance furnace until it attains the constant furnace temperature. It is then dropped into the ice calorimeter beneath the furnace and the heat given off is measured as the container and sample cool to 0°C. The enthalpy of the container and the heat lost during the fall into the calorimeter are accounted for by subtracting from the enthalpy of the container plus sample, that of the container alone, measured in a separate experiment. In the present study, a series of enthalpy measurements on an empty Pt10Rh container similar to the one used to contain the sample had already been made and reported [8]. The smoothing equation which was chosen to represent these previous measurements (equation 1, below) was used to calculate the empty container enthalpy values needed for the measurements on Mo_2C after making corrections for the small differences in the container masses.

$$H_t - H_{0°C} = (4.529744)10^{-8}t^3 + (8.068654)10^{-5}t^2$$

$$+ (1.901653)t - (34.94647)(\frac{t}{T}). \qquad (1)$$

H, J; T, K = t, °C + 273.15[b]

For measurements in this temperature range, the complete sample, as received from the producer, was encapsulated in a .008 in. wall Pt10Rh capsule sealed under approximately 100. torr absolute helium pressure. Prior to making the measurements on the Mo_2C sample, check measurements on a specimen of α-Al_2O_3, a calorimetric heat-capacity standard, were made which verified the correct functioning of the calorimetric system.

———————————

[b]All temperatures are to be expressed on the scale IPTS-68.

b. <u>1173.15 K to 1475 K</u>

In this temperature range, enthalpy relative to 298.15 K
for this molydenum carbide sample was measured with the
adiabatic "drop" apparatus which was comprehensively described
in a previous report [10]. This temperature interval is
sufficiently below any known transition to β phase for this
sample so a check can be made on the accuracy of the apparatus
at 1173.15 K with the results obtained from the Bunsen
calorimeter and the smoothness in fit of the relative enthalpy
and heat-capacity measurements of the two methods can be
inspected.

The principle of operation in this method is similar
to that of the Bunsen ice calorimeter. A hot capsule is
"dropped" from an RF induction furnace maintained at a
constant temperature into an adiabatic calorimeter operating
near room temperature. The heat energy added to the
calorimeter is measured by the rise in the calorimeter
temperature and a calculation of the energy equivalent
necessary for this rise. A minimum of two drop experiments,
one on an empty capsule and the other on a capsule loaded
with sample is required at each furnace temperature. The
difference in energy supplied to the calorimeter is the change
in enthalpy of the sample after a small correction is applied
to account for the difference between the final calorimeter
temperatures inherent in an adiabatic calorimeter.

For this series, three drops were made for each furnace
temperature, the first and third drops on an empty capsule
and the second drop on a capsule filled with the sample. The
agreement of the results of the first and third drops gives
a check that no serious change in the optical, physical or
chemical properties of the container had occurred and,
therefore, that the result is valid for that furnace temper-
ature.

The same brittle Mo_2C sample, described in section 2,
above, was used for this portion of the work. Only the shape
was altered by crushing part of the sample between two
1/8 in. sheets of Teflon on the jaws of a vise, so that the
"Poco" graphite capsule could accomodate the resulting
granules of Mo_2C. The Teflon sheet was sufficient in thickness
that the abrasive sample did not rupture the sheet nor
scratch the steel surface of the vise.

All high temperature measurements of the furnace were
determined using an L and N automatic optical pyrometer
focused on the bottom surface of the capsule through a
diaphragm with a 1/8 in. hole at blackbody conditions. Since
the first measurementis made at least 4 1/2 hrs. after the

68

furnace is heated, the thermal gradients along the graphite core of the furnace as well as the solid state and electronic circuitry of the temperature measuring system settle down sufficiently to give precise results. The automatic pyrometer was periodically calibrated by the NBS optical radiation laboratory.

4. Results

The NBS enthalpy measurements on Mo_2C completed to date are presented in Tables 1. and 2. In Table 1, column 1 gives the equilibrium sample temperature before dropping. Column 2 gives the total measured heat for container plus sample. Column 3 was derived by subtracting from column 2 the appropriate empty container heats derived from eq. (1), including a small correction for the difference in mass of the actual sample container and the container to which eq. (1) is applicable. The net heat so obtained was then expressed per gram formula weight of specimen, $MoC_{.4873}$. The data of column 3 were fit by eq. (2), the constants determined using the method of least squares.[c] The NBS enthalpy data above 1173.15 K was not included in this fit as measurements in this region will be extended to about 2000°C and are not yet complete.

$$H_T - H_{T_0} = A(T^3 - T_0^3) + B(T^2 - T_0^2) + C(T - T_0) + D(\frac{1}{T} - \frac{1}{T_0}) \qquad (2)$$

$A = -1.10268E{-}06$ $T_0 = 273.15$ K
$B = +6.23370E{-}03$ $H_T = J/GFW$; GFW = 101.793
$C = +3.20199E{+}01$ T, K (IPTS-68)
$D = +4.94170E{+}05$

Preliminary results of the enthalpy measurements on Mo_2C for the temperature range 1173.15 to 1475 K are listed in table 2. Although the results were not included in the least squares fit in determining eq. (2), the agreement at 1173 K is good and the remaining data points can be expected to merge smoothly by revising eq. (2). This can be best dealt with after enthalpy measurements beyond 1475 K have been completed.

---

[c] OMNITAB programming of a UNIVAC-1108 computer used.

Table 1

NBS enthalpy measurements on $MoC_{.4873}$ to 1173.15 K

Furnace Temperature[a]	Gross Measured Heat	$H_t - H_{0°C}$		Observed-Smooth
		Net Heat Observed	Net Heat Smooth[c]	
°C	J	J/GFW^b	J/GFW^b	%
100.00	989.66	3088.9	3085.2	+.12
200.00	2061.58	6470.0	6475.4	-.08
300.00	3192.24	10060.1	10056.6	+.03
400.00	4358.70	13773.8	13778.6	-.03
500.00	5563.71	17622.1	17614.0	+.04
500.00	5561.60	17614.0	17614.0	.00
600.00	6790.06	21539.0	21544.6	-.02
700.00	8047.05	25559.9	25557.2	+.01
800.00	9323.06	29638.5	29640.9	-.01
900.00	10620.50	33784.4	33786.3	-.01
900.00	10621.78	33789.3	33786.3	+.01

a   IPTS-68

b   GFW = 101.793, Specimen mass = 26.6274 g

c   Calculated from eq. (2).

Table 2

NBS enthalpy measurements on MoC$_{.4873}$ to 1476.87 K

Furnace Temperature[a]	Heat from sample to calorimeter at 298.15 K	$H_T - H_{298.15}$ (observed)	Deviation from Eq. (2)[c]
K	(J)	(J/GFW)	(obs-calc.,%)
1173.15	1520.43	33069.6	+.04
1277.72	1711.52	37503.9	+.15
1377.04	1909.32	41854.3	+.45
1476.87	2108.47	46251.4	+.67

a   IPTS-68

b   GFW = 101.793; theoretical density = 9.18 gm/cm^3. Sample mass
    was slightly different for each run since small loose particles
    which separated were not included in subsequent runs.

c   Enthalpy data in this table was not used for determining eq. (2).

5. Discussion

The present NBS enthalpy measurements up to 1173.15 K are believed to have an accuracy of 0.2 percent. They lie on the average about .5 percent above the earlier measurements of Pankratz et al [6] (see fig. 2), and show improved precision. These differences might be though to arise from frozen-in disorder in the sample of Pankratz. However, a preliminary comparison of the present NBS thermal data with the low-temperature specific heat measurements of Pankratz et al [6] and Paukov et al [5] indicates a correct merging both with respect to magnitude and to slope of the specific heat curves in their region of overlap.

The enthalpy data of Neel et al [7], which up to 1400°C consists of three points, have not been included in the comparison of fig. (2) as they differ by two or three percent from eq. (2) and could not agree with any reasonable extrapolation of the low-temperature data.

Pankratz et al [6] and Paukov et al [5] have derived from their low-temperature data, values for $S_{298.15}$ of 15.74 ± .09 and 15.74 ± .03 cal/mole, K respectively (based on the composition $Mo_2C_{1.0180}$) although Paukov's heat capacity data are one to two percent higher than the Pankratz data below 125 K. As soon as the combined low-temperature data have been re-analyzed and the complete NBS high-temperature data become available, more reliable thermodynamic functions for $Mo_2C(s)$ will be generated.

In Figure 3 a plot of the average heat capacity from a base temperature of 298.15 K is shown. The smoothness of the experimental points indicates that the sample has probably not undergone a transition in the range of measurement. The plot also indicates that the enthalpy determinations of Mo_2C with the two different calorimeters of this study are consistent with one another.

72
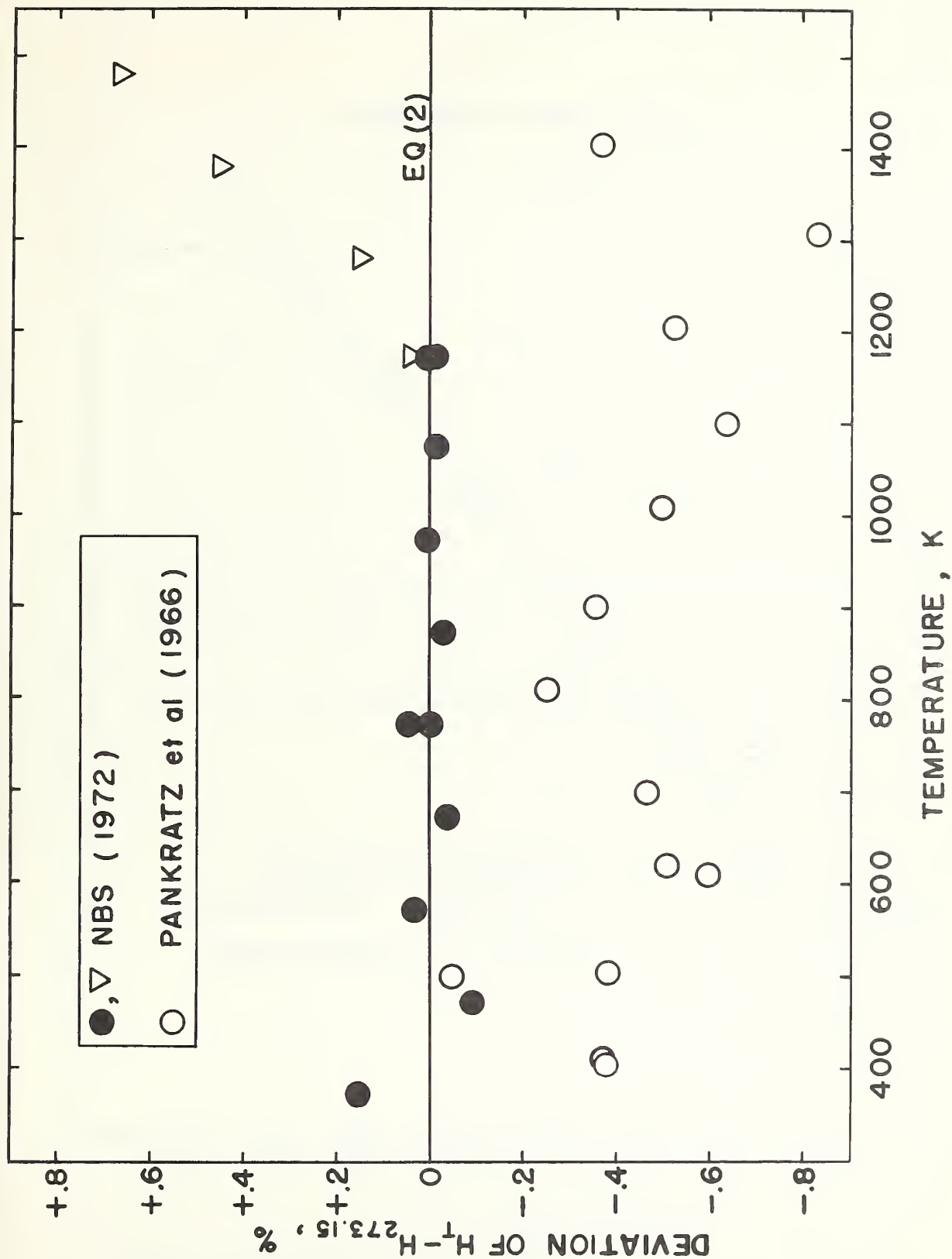
Figure 2. Deviation of Mo$_2$C enthalpy data from eq. (2). Baseline represents a fit to NBS data from 273.15 K to 1173.15 K only.
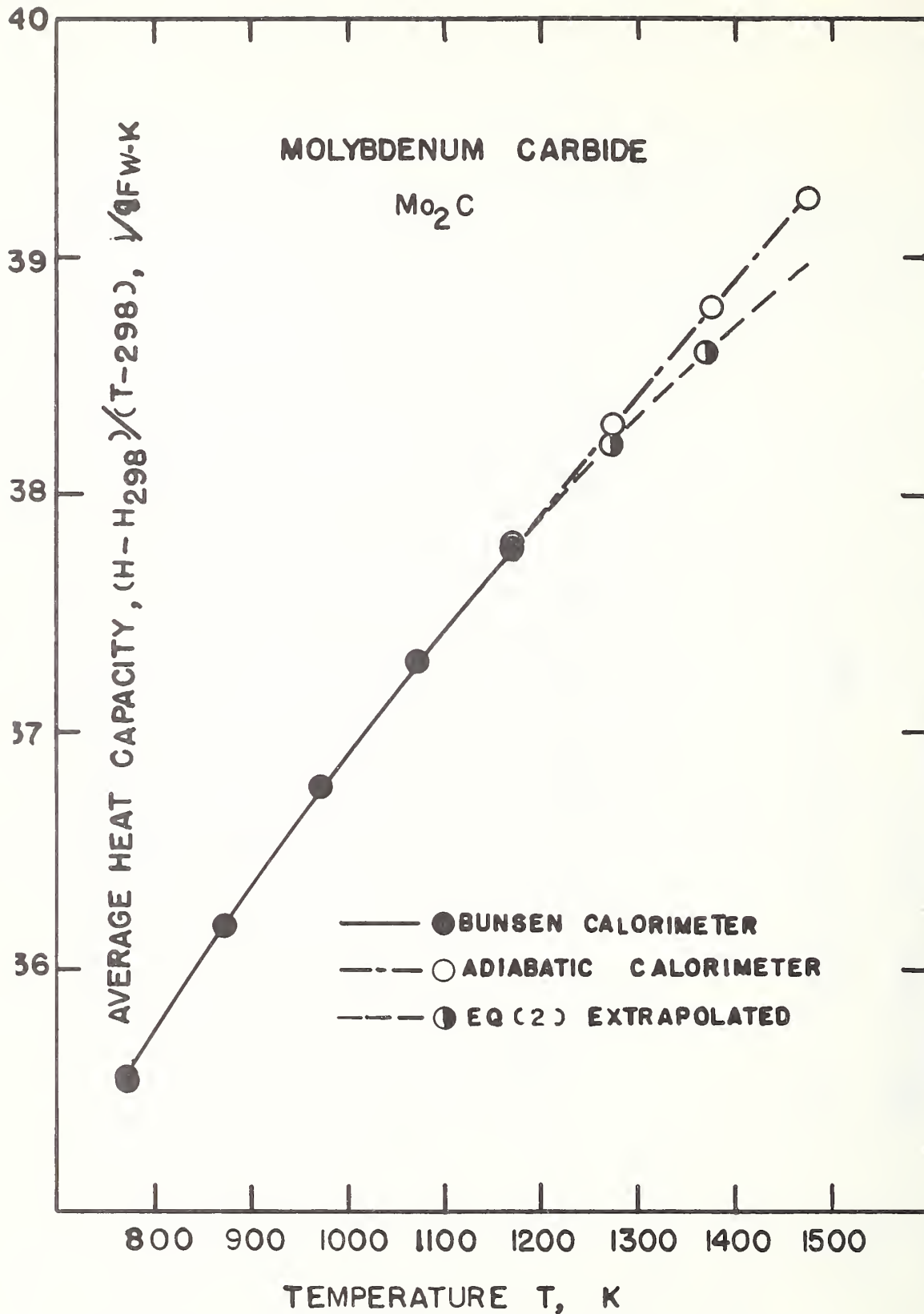
Figure 3. Comparison of the average heat capacity of Mo₂C calculated from the base temperature of 298.15 K for the two NBS calorimeters of this study.

74

References

[1] Ditmars, D. A., NBS Report 10 481, p. 120, 1 July 1971.

[2] Storms, E. K., private communication, March 1971.

[3] Rudy, E., private communication, March 1971.

[4] Rudy, E., AFML-TR-65-2, Part V, 1969.

[5] Paukov, I. E., Strelkov, P. G., and Filatkina, V. S., Russ. J. Phys. Chem. $\underline{42}$ (11), 1576 (1968).

[6] Pankratz, L. B., Weller, W. W., and King, E. G., Bureau of Mines Rept. Invest. 6861 (1966).

[7] Neel, D. S., Pears, C. D., and Oglesby, S., ASD-TDR-62-765 (1963).

[8] Ditmars, D. A., and Douglas, T. B., J. Res. Nat. Bur. Stand. (U.S.), $\underline{75A}$ (5), 401 (1971).

[9] Douglas, T. B., and King, E. G., High Temperature Drop Calorimetry, Chapter 8 in Experimental Thermodynamics V.I. (Butterworths, London, 1968).

[10] S. Ishihara and T. B. Douglas, NBS Report 10 481, U.S. Air Force OSR Agreement No. AFOSR-ISSA-70-0002, p. 59 (July, 1971).

Chapter 5

HIGH-SPEED (SUBSECOND) SIMULTANEOUS MEASUREMENT OF
SPECIFIC HEAT, ELECTRICAL RESISTIVITY, AND HEMI-
SPHERICAL TOTAL EMITTANCE OF TANTALUM - 10 (WT. %)
TUNGSTEN ALLOY IN THE RANGE 1500 to 3200 K*

Ared Cezairliyan
National Bureau of Standards
Washington, D. C. 20234

Abstract

Simultaneous measurements of specific heat, electrical resistivity,
and hemispherical total emittance of tantalum - 10 (wt. %) tungsten alloy
in the temperature range 1500 to 3200 K by a subsecond duration pulse
heating technique are described. Estimated inaccuracy of measured prop-
erties are: 3% for specific heat and hemispherical total emittance, and
0.5% for electrical resistivity. Properties of the alloy are compared
with the properties of the constituent elements. The values of measured
specific heat are approximately 2% higher than the values computed accord-
ing to   Kopp's additivity law. However, this difference is within the
combined estimated errors. The electrical resistivity results indicate
a significant departure from   Matthiessen's law. Like tantalum,
the alloy showed a negative departure from linearity in the curve
of electrical resistivity versus temperature.

76

1. Introduction

A high-speed technique was developed in this laboratory for the measurement of selected thermophysical properties of refractory metals at high temperatures. In this paper, application of this technique to the simultaneous measurements of specific heat, electrical resistivity, and hemispherical total emittance of the alloy tantalum - 10 (wt. %) tungsten in the temperature range 1500 to 3200 K is described.

The method is based on rapid resistive self-heating of the specimen from room temperature to any desired high temperature (up to its melting point) in less than one second by the passage of electrical currents through it; and on measuring, with millisecond resolution, experimental quantities such as current through the specimen, potential drop across the specimen, and specimen temperature.

Current through the specimen is determined from the measurement of the potential difference across the standard resistance placed in series with the specimen. Potential difference across the middle two thirds of the specimen is measured using spring-loaded, knife-edge probes. Specimen temperature is measured at the rate of 1200 times per second with a high-speed photoelectric pyrometer (Foley, 1970). A small hole in the wall at the middle of the tubular specimen provides an approximation to blackbody conditions. The experimental quantities are recorded with a digital data acquisition system, which has a time resolution of 0.4 ms and a full-scale signal resolution of one part in 8000. Details regarding the construction and operation of the measurement system, the methods of measuring experimental quantities, and other pertinent

77

information, such as formulation of relations for properties, etc. are given in earlier publications (Cezairliyan et al., 1970; Cezairliyan, 1971).

2. Measurements

The specimen was a tube fabricated from a tantalum - 10 (wt. %) tungsten rod[1] by removing the center portion by an electro-erosion technique. The outer surface of the specimen was polished to reduce heat loss due to thermal radiation. The nominal dimensions of the specimen were: length, 102 mm; outside diameter, 6.3 mm; and wall thickness, 0.5 mm.

Tungsten content of the specimen was 9.45% by weight. The total amount of impurities was less than 0.1%. Photomicrographs of the specimen, shown in Figure 1, indicate that considerable grain growth took place as the result of pulse heating to high temperatures.

The measurements were performed in the temperature interval 1500 to 3200 K. To optimize the operation of the pyrometer, this interval was divided into seven ranges. One experiment was performed in each range. Before the start of the experiments, the specimen was annealed by subjecting it to 30 heating pulses (up to 3000 K). All the experiments were conducted with the specimen in a vacuum environment of approximately 10^{-4} torr.

To optimize the operation of the measurement system, the heating rate of the specimens was varied depending on the desired temperature

---

[1] The specimen in rod form was furnished by the U. S. Air Force Materials Laboratory, Wright-Patterson Air Force Base, Ohio.

range by adjusting the value of a resistance in series with the specimen. Duration of current pulses in the experiment ranged from 400 to 470 ms; and the heating rate ranged from 4400 to 6700 K s^{-1}. Radiative heat loss from the specimen amounted to approximately 1% at 1500 K, 7% at 2500 K, and 20% at 3200 K of the input power.

Data on voltage, current, and temperature were used to obtain third degree polynomial functions for each quantity in terms of time, which then provided the input information for the determination of properties.

3. Experimental Results

This section presents the thermophysical properties determined from the measured quantities. All values are based on the International Practical Temperature Scale of 1968 (1969). In all computations, the geometrical quantities are based on their room temperature (298 K) dimensions. The experimental results for properties are represented by polynomial functions in temperature obtained by least squares approximation of the individual points. The final values on properties at 100 degree temperature intervals computed using the functions are presented in Table 1. Results obtained from individual experiments, by the method described previously (Cezairliyan et al., 1970), are given in the Appendix (Tables A-1 and A-2). Each number tabulated in these tables represents results from over fifty original data points.

3.1. Specific Heat

Specific heat was computed from data taken during the heating period. A correction for power loss due to thermal radiation was made using the

Table 1

Specific heat, electrical resistivity, and hemispherical total
emittance of the alloy tantalum -10 (wt.%) tungsten

Temp K	c_p $J\ g^{-1}K^{-1}$	ρ^* $10^{-8}\Omega\ m$	ϵ^*
1500	0.1662	61.60	
1600	0.1683	64.96	
1700	0.1704	68.27	0.199
1800	0.1726	71.52	0.213
1900	0.1748	74.73	0.226
2000	0.1771	77.88	0.239
2100	0.1796	80.97	0.251
2200	0.1825	84.02	0.263
2300	0.1857	87.01	0.275
2400	0.1893	89.95	0.286
2500	0.1934	92.83	0.296
2600	0.1981	95.66	0.307
2700	0.2035	98.45	0.316
2800	0.2095	101.17	0.326
2900	0.2163	103.85	0.335
3000	0.2240	106.47	0.343
3100	0.2326	109.04	
3200	0.2422	111.56	

*Based on ambient temperature (298 K) dimensions.

80

results on hemispherical total emittance. The function for specific heat (standard deviation = 1%) that represents the results in the temperature range 1500 to 3200 K is:

$$c_p = 7.769 \times 10^{-2} + 1.221 \times 10^{-4}T - 5.972 \times 10^{-8}T^2 + 1.176 \times 10^{-11}T^3 \quad (1)$$

where T is in K, and c_p is in J g^{-1}K^{-1}.

3.2. Electrical Resistivity

The electrical resistivity was determined from the same experiments that were used to calculate the specific heat. The function for electrical resistivity (standard deviation = 0.1%) that represents the results in the temperature range 1500 to 3200 K is:

$$\rho = 4.863 + 4.178 \times 10^{-2}T - 2.637 \times 10^{-6}T^2 \quad (2)$$

where T is in K, and ρ is in 10^{-8} Ω m. In the computations of the specimens cross-sectional area, that is needed for the computations of electrical resistivity, the density of the specimen was taken as 16.968×10^{3} kg m^{-3} (Taylor et al., 1971). The measurement, before the pulse experiments, of the electrical resistivity of the specimen at 293 K with a Kelvin bridge yielded a value of 17.6×10^{-8} Ω m.

3.3. Hemispherical Total Emittance

Hemispherical total emittance was computed using data taken during both heating and initial free radiative cooling periods. The function for hemispherical total emittance (standard deviation = 0.8%) that represents the results in the temperature range 1700 to 3000 K is:

$$\varepsilon = -9.765 \times 10^{-2} + 2.108 \times 10^{-4}T - 2.129 \times 10^{-8}T^2 \quad (3)$$

where T is in K.

81

4. Estimate of Errors

The details for estimating errors in measured and computed quantities in high-speed experiments using the present measurement system are given in an earlier publication (Cezairliyan et al., 1970). In this paper, the specific items in the error analysis were recomputed whenever the present conditions differed from those in the earlier publication. The results for imprecision[2] and inaccuracy[3] in the properties are: 1% and 3% for specific heat, 0.1% and 0.5% for electrical resistivity, 0.8% and 3% for hemispherical total emittance.

5. Discussion

The specific heat, electrical resistivity, and hemispherical total emittance of the tantalum - 10 tungsten alloy measured in this work are presented graphically in Figures 2, 3, and 4, respectively. For comparison purposes, similar results for tantalum and tungsten metals, measured and reported earlier (Cezairliyan et al., 1971; Cezairliyan and McClure, 1971) are also included in the figures.

A comparison of the electrical resistivity results of this work with those reported by Taylor et al. (1971) on a similar specimen up to 2400 K indicates that the present results are higher by approximately 0.3% at 1500 K, 0.6% at 2000 K, and 0.8% at 2400 K. The average absolute difference between the two results, in the temperature interval 1500 to 2400 K,

------

(2) Imprecision refers to the standard deviation of an individual point as computed from the difference between measured value and that from the smooth function obtained by the least squares method.

(3) Inaccuracy refers to the estimated total error (random and systematic).

is approximately 0.6%. However, this difference is less than the combined estimated errors. When the present measurement of electrical resistivity at 293 K is extrapolated to 300 K a value of 18.0×10^{-8} Ω m is obtained that compares favorably with the value 17.9×10^{-8} Ω m reported by Taylor et al. (1971).

A comparison of the hemispherical total emittance results of this work with those of Taylor et al. (1971) up to 2700 K indicates that the present results are higher by approximately 4% at 1700 K, and 1% at 2200 K, and are lower by approximately 2% at 2700 K. Some of this difference may be attributed to the differences in specimen surface conditions.

According to Kopp's law, specific heat of a binary alloy, c_{12} (on mass basis), may be expressed as

$$c_{12} = x_1 c_1 + x_2 c_2 \tag{4}$$

where x_1 and x_2 are mass fractions of the constituent elements 1 and 2, and c_1 and c_2 are their respective specific heats.

Departure of the measured specific heat of this work from Kopp's law was computed using the data on tantalum and tungsten reported in earlier publications (Cezairliyan et al., 1971; Cezairliyan and McClure, 1971). The results are presented graphically in Figure 5. It may be seen that in the temperature interval 2000 to 3000 K the measured values are approximately two percent higher than the computed values. Above 3000 K, the difference between measured and computed values decreases, changes sign and then increases (in the negative direction). A sharp increase in tantalum specific heat above 3000 K may account for this trend. However, one should not place too much significance to the

difference between measured and computed specific heat values since
its magnitude is less than the combined estimated errors in the measure-
ments of specific heat of the alloy and its two constituents.

According to Matthiessen's law (as presented by Gerritsen, 1956),
electrical resistivity of a binary alloy, ρ_{12}, may be expressed as

$$\rho_{12} = X_1\rho_1 + X_2\rho_2 + \rho_o \tag{5}$$

where X_1 and X_2 are atomic fractions of the constituent elements 1 and
2, and ρ_1 and ρ_2 are their respective electrical resistivities. The
quantity ρ_o is considered to be constant (temperature independent) for
a given alloy.

Rearrangement of Equation (5) yields

$$\rho_o = \rho_{12} - (X_1\rho_1 + X_2\rho_2) \tag{6}$$

Departure of the electrical resistivity of the tantalum - 10 tungsten
alloy from   Matthiessen's law is determined using Equation (6). The
measured values for the alloy are substituted for ρ_{12} and data on tantalum
and tungsten reported in earlier publications (Cezairliyan et al., 1971;
Cezairliyan and McClure, 1971) are used for ρ_1 and ρ_2. The results are
presented graphically in Figure 6 in terms of the quantity ρ_o. According
to the law, ρ_o should be constant, however computations show that it
decreases with increasing temperature and undergoes sign reversal at high
temperatures. The dashed line in Figure 6 was obtained by fitting the
high temperature points to a linear function, using the least squares
method, and forcing the function to pass through the room temperature
value. Average absolute difference of the points from the linear function
is 0.1×10^{-8} Ω m. This is considerably less than the estimated uncertainty

of the individual points (0.8×10^{-8} Ω m which is obtained from the combination of estimated errors in the electrical resistivity of the alloy and its two constituents.

Departure from   Matthiessen's law may also be determined by comparing temperature derivatives of measured and computed electrical resistivities, namely derivatives of Equations (2) and (5), respectively. The advantage of this approach is that the quantity ρ_0 is eliminated during the differentiation. The results are shown graphically in Figure 7. Difference between the two derivatives, which may be a measure of the departure from   Matthiessen's law, is approximately 4% at 2000 K and increases to approximately 6% at 3000 K.

At 293 K, electrical resistivity of the alloy (17.6×10^{-8} Ω m is higher than the resistivity of either one of its constituents (14.0×10^{-8} Ω for tantalum, and 5.45×10^{-8} Ω m for tungsten). However, at high temperatures (Figure 3) the resistivity of the alloy is lower than that of tantalum. Like tantalum, at high temperature the alloy showed a negative departure from linearity in the curve of electrical resistivity versus temperature.

<center>6. Acknowledgement</center>

<center>85</center>

Table A-1

Experimental results on specific heat and electrical resistivity
of the alloy tantalum- 10 (wt.%) tungsten

T K	c_p J $g^{-1}K^{-1}$	Δc_p^* %	ρ $10^{-8}\Omega$ m	$\Delta\rho^*$ %
1500	0.1656	-0.30	61.75	+0.25
1550	0.1683	+0.64	63.36	+0.12
1600	0.1709	+1.52	64.98	+0.03
1650	0.1671	-1.37	66.65	+0.04
1700	0.1714	+0.61	68.23	-0.05
1750	0.1690	-1.44	69.88	-0.02
1800	0.1728	+0.17	71.44	-0.11
1850	0.1760	+1.35	73.01	-0.16
1900	0.1714	-1.91	74.73	+0.01
1950	0.1742	-0.96	76.25	-0.07
2000	0.1769	-0.09	77.77	-0.12
2050	0.1796	+0.72	79.30	-0.16
2100	0.1822	+1.44	80.83	-0.17
2150	0.1785	-1.37	82.56	+0.08
2200	0.1812	-0.71	84.04	+0.04
2250	0.1838	-0.08	85.52	+0.01
2300	0.1866	+0.50	87.00	0.00
2350	0.1894	+1.04	88.47	-0.01
2400	0.1888	-0.26	90.01	+0.08
2450	0.1911	-0.07	91.44	+0.06
2500	0.1936	+0.08	92.86	+0.04
2550	0.1961	+0.22	94.28	+0.03
2600	0.1988	+0.33	95.68	+0.02
2650	0.2016	+0.44	97.07	+0.02
2700	0.2046	+0.54	98.46	+0.02
2750	0.2078	+0.66	99.83	+0.02
2800	0.2112	+0.81	101.18	+0.02
2850	0.2150	+1.02	102.53	+0.02
2900	0.2110	-2.55	103.96	+0.12
2950	0.2164	-1.70	105.23	+0.07
3000	0.2219	-0.96	106.50	+0.04
3050	0.2275	-0.31	107.77	+0.01
3100	0.2331	+0.21	109.01	-0.02
3150	0.2388	+0.61	110.22	-0.07
3200	0.2443	+0.84	111.38	-0.15

The quantities Δc_p and $\Delta\rho$ are percentage deviations of the individual results
from the smooth functions represented by Equations (1) and (2), respectively.

Experimental results on hemispherical total emittance of the
alloy tantalum -10 (wt.%) tungsten

T K	ϵ	$\Delta\epsilon$* %
1708	0.198	-0.95
1708	0.200	+0.01
1708	0.202	+0.67
1708	0.203	+1.44
1873	0.223	+0.37
1873	0.222	-0.45
1873	0.221	-0.69
1874	0.224	+0.77
2059	0.244	-0.86
2059	0.244	-1.09
2059	0.244	-0.90
2060	0.244	-1.01
2312	0.278	+0.71
2313	0.278	+0.74
2313	0.279	+1.05
2315	0.279	+1.00
2656	0.312	-0.07
2658	0.312	-0.06
2658	0.311	-0.46
2661	0.311	-0.36
2960	0.340	+0.01
2964	0.341	+0.13
2964	0.340	-0.13
2969	0.341	+0.04

*The quantity $\Delta\epsilon$ is percentage deviation of the individual results
from the smooth function represented by equation.

8. References

1. Cezairliyan, A., Morse, M. S., Berman, H. A., and Beckett, C. W.,
    1970, J. Res. Nat. Bur. Stand. (U.S.), 74A (Phys. and Chem.),
    65-92.

2. Cezairliyan, A., 1971, J. Res. Nat. Bur. Stand. (U.S.), 75C
    Eng. and Instr.), 7-18.

3. Cezairliyan, A., and McClure, J. L., 1971, J. Res. Nat. Bur.
    Stand. (U.S.), 75A (Phys. and Chem), 283-290.

4. Cezairliyan, A., McClure, J. L., and Beckett, C. W., 1971,
    J. Res. Nat. Bur. Stand. (U.S.), 75A (Phys. and Chem.), 1-13.

5. Foley, G. M., 1970, Rev. Sci. Instr., 41, 827-834.

6. Gerritsen, A. N., 1956, in Handbuch der Physik, Vol. 19 (Springer-
    Verlag, Berlin), p. 206.

7. International Practical Temperature Scale of 1968, 1969,
    Metrologia, 5, 35-44.

8. Taylor, R. E., Kimbrough, W. D., and Powell, R. W., 1971, J. Less-
    Common Metals, 24, 369-382.

0.2 mm
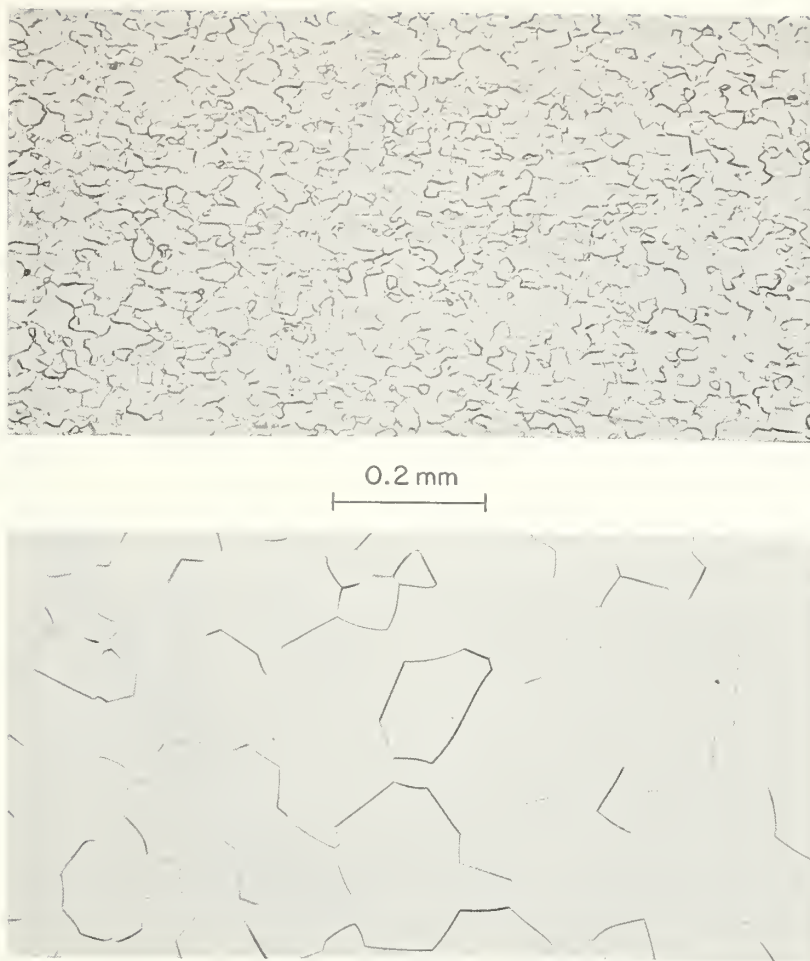
Figure 1.   Photomicrographs of the tantalum - 10 tungsten
            specimen. Upper photograph, specimen as
            received; lower photograph, specimen after the
            entire set of experiments.
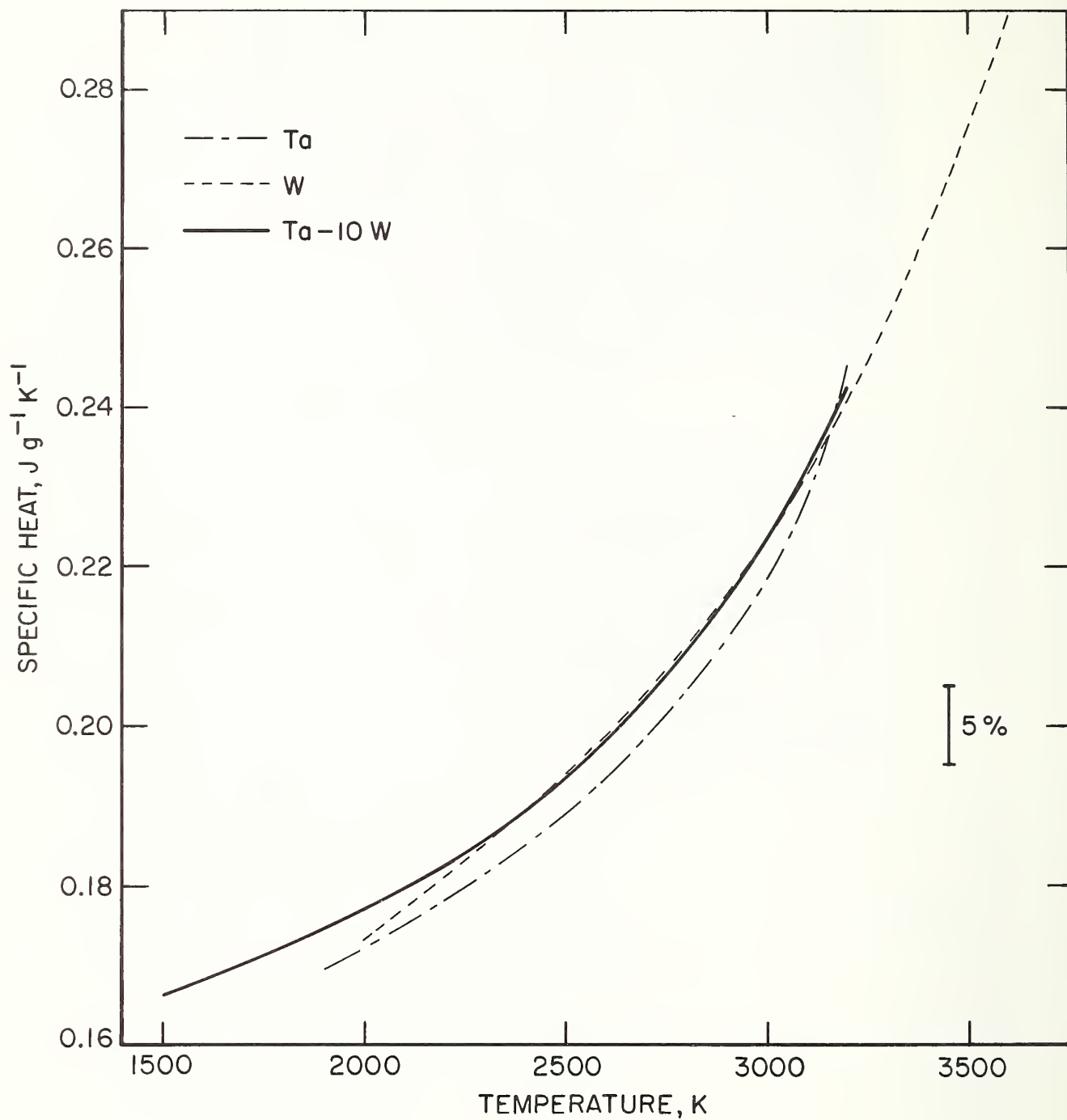
Figure 2.   Specific heat of tantalum - 10 tungsten alloy, and tantalum and tungsten metals.

90
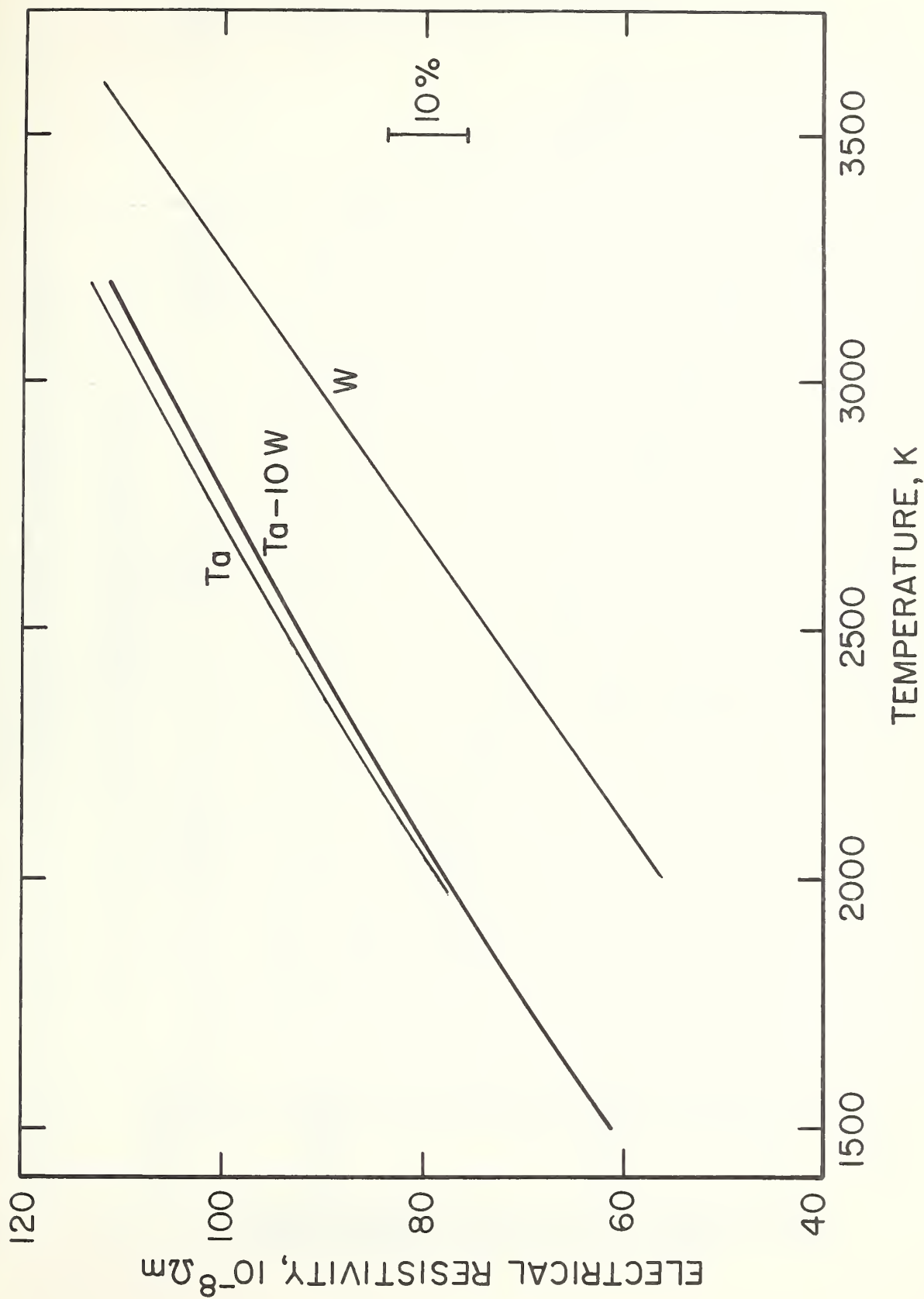
Figure 3. Electrical resistivity of tantalum - 10 tungsten alloy and tantalum and tungsten metals.
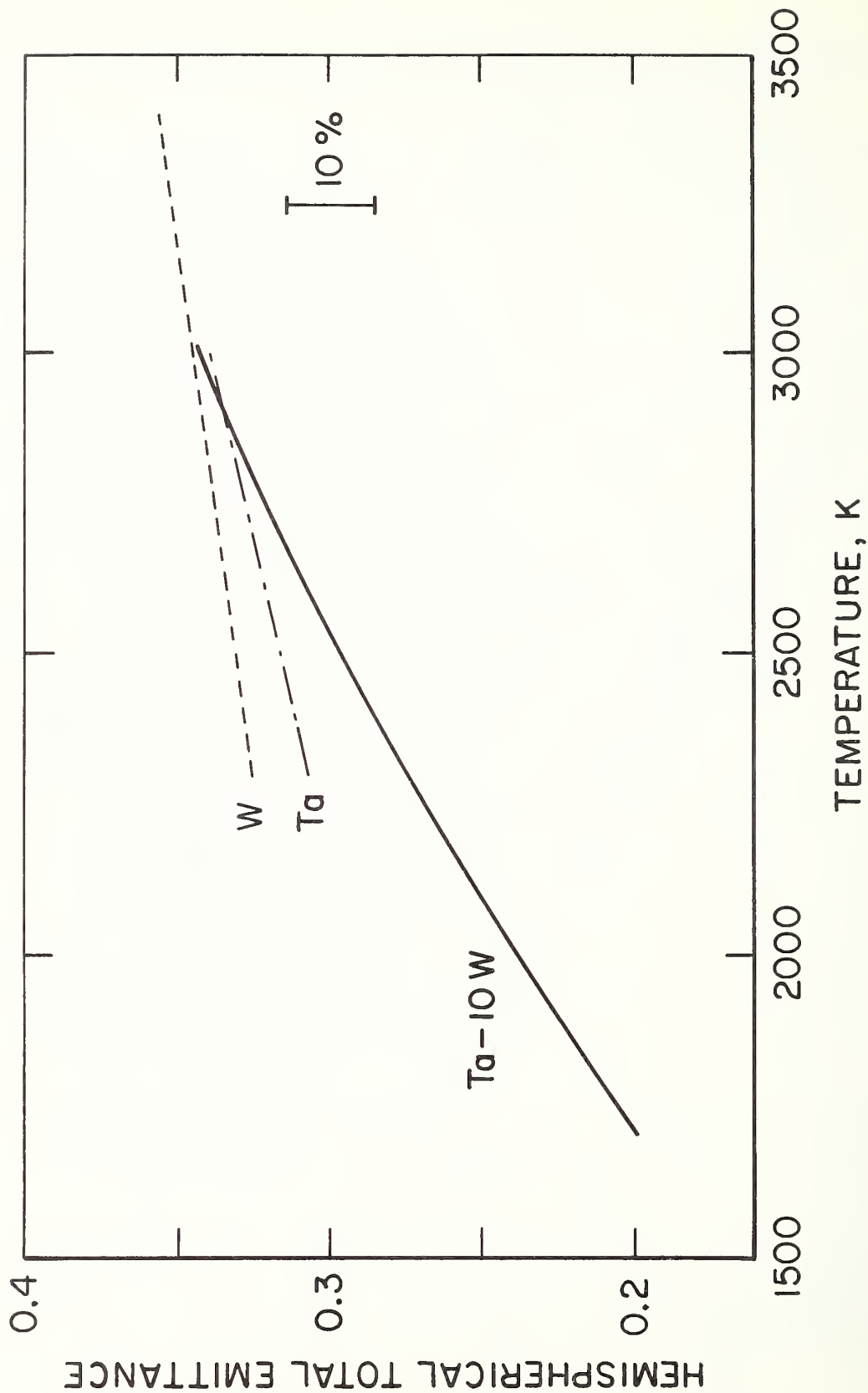
Figure 4.   Hemispherical total emittance of tantalum -
10 tungsten alloy and tantalum and tungsten
metals.

92
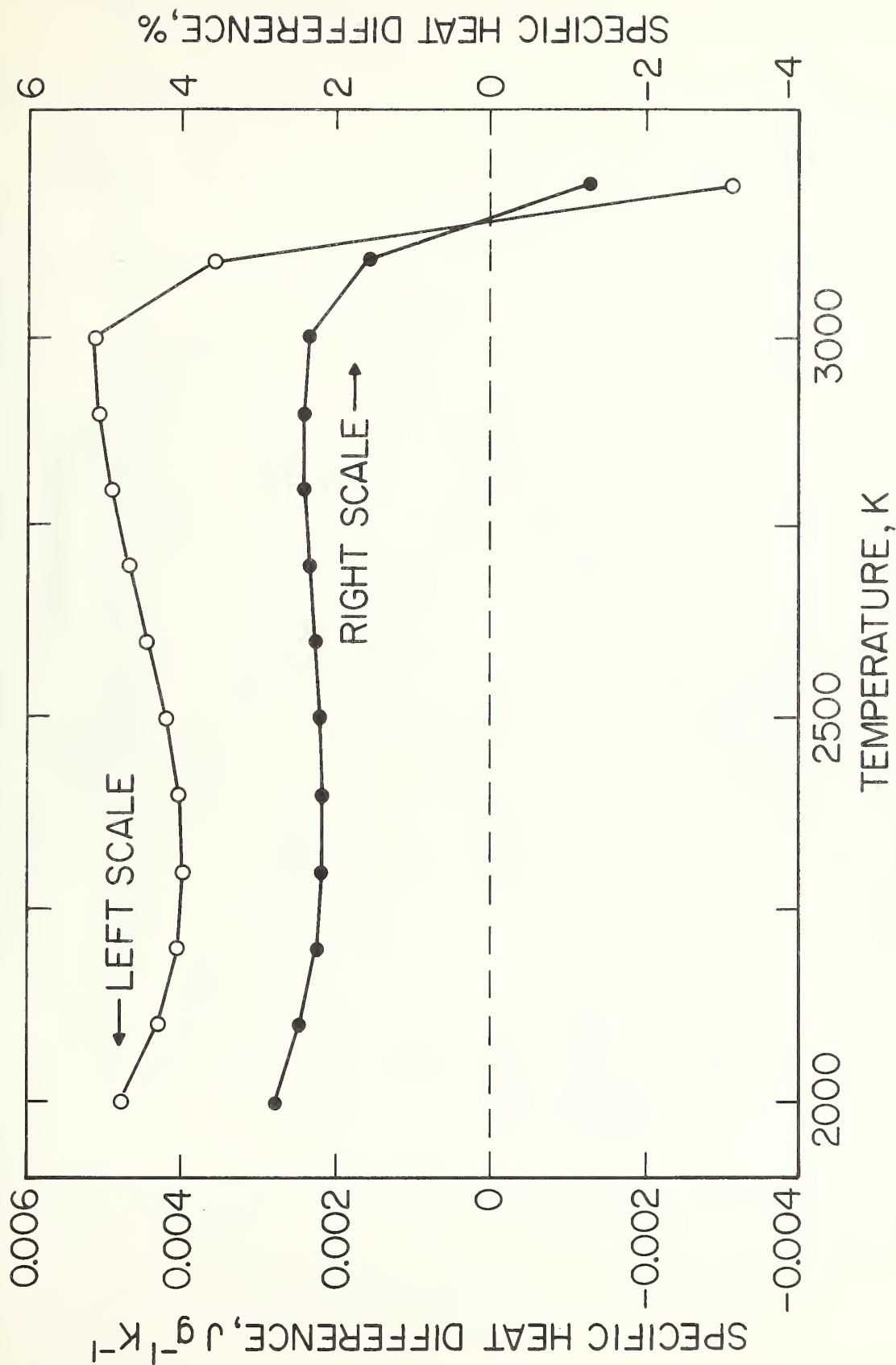
Figure 5.   Departure of the specific heat of tantalum –
10 tungsten alloy from Kopp's law. Specific
heat difference refers to measured values
minus computed values according to Equation (4).
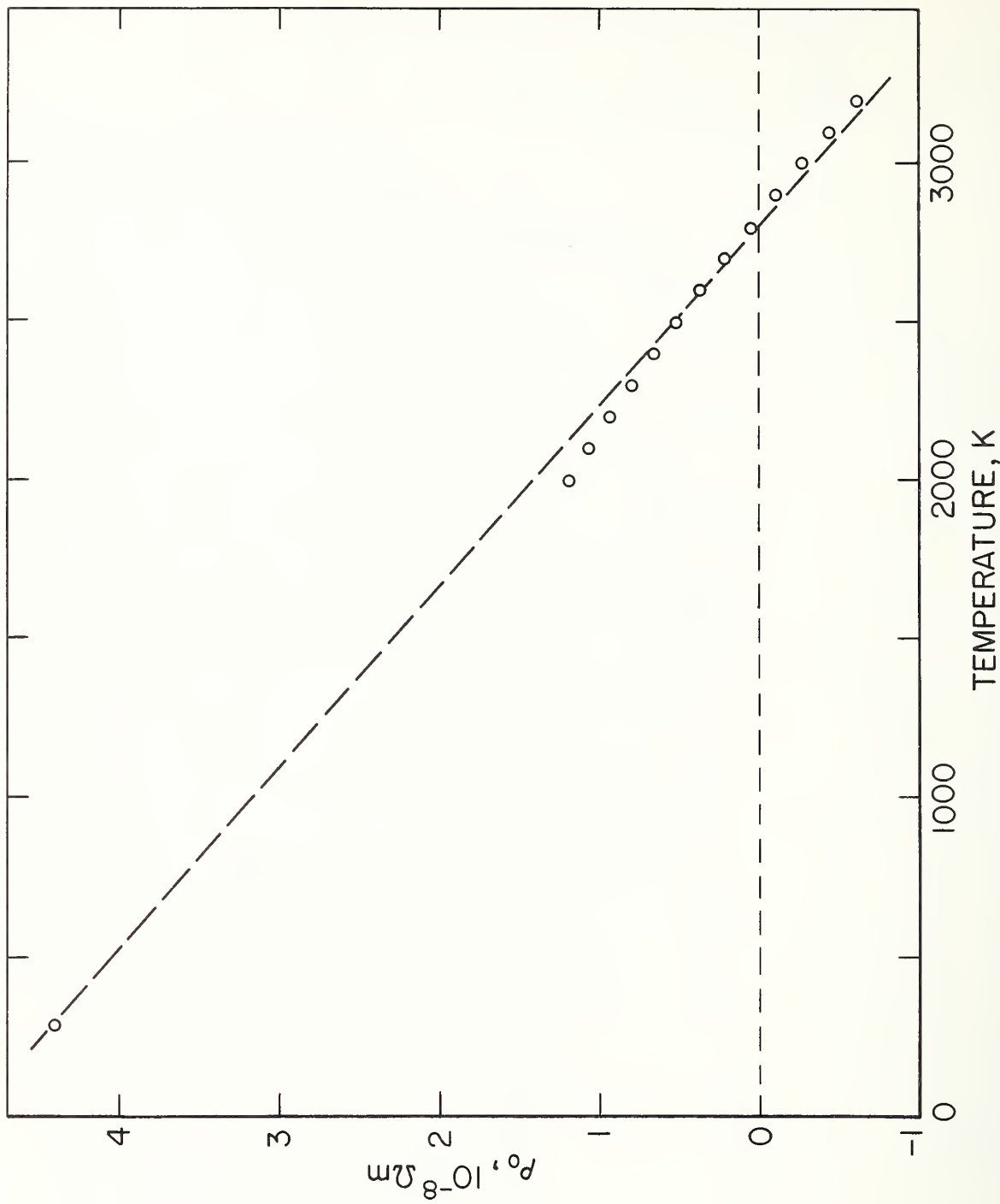
Figure 6. Variation of the quantity ρ_o, defined by Equation (6), as a function of temperature for tantalum - 10 tungsten alloy.

94
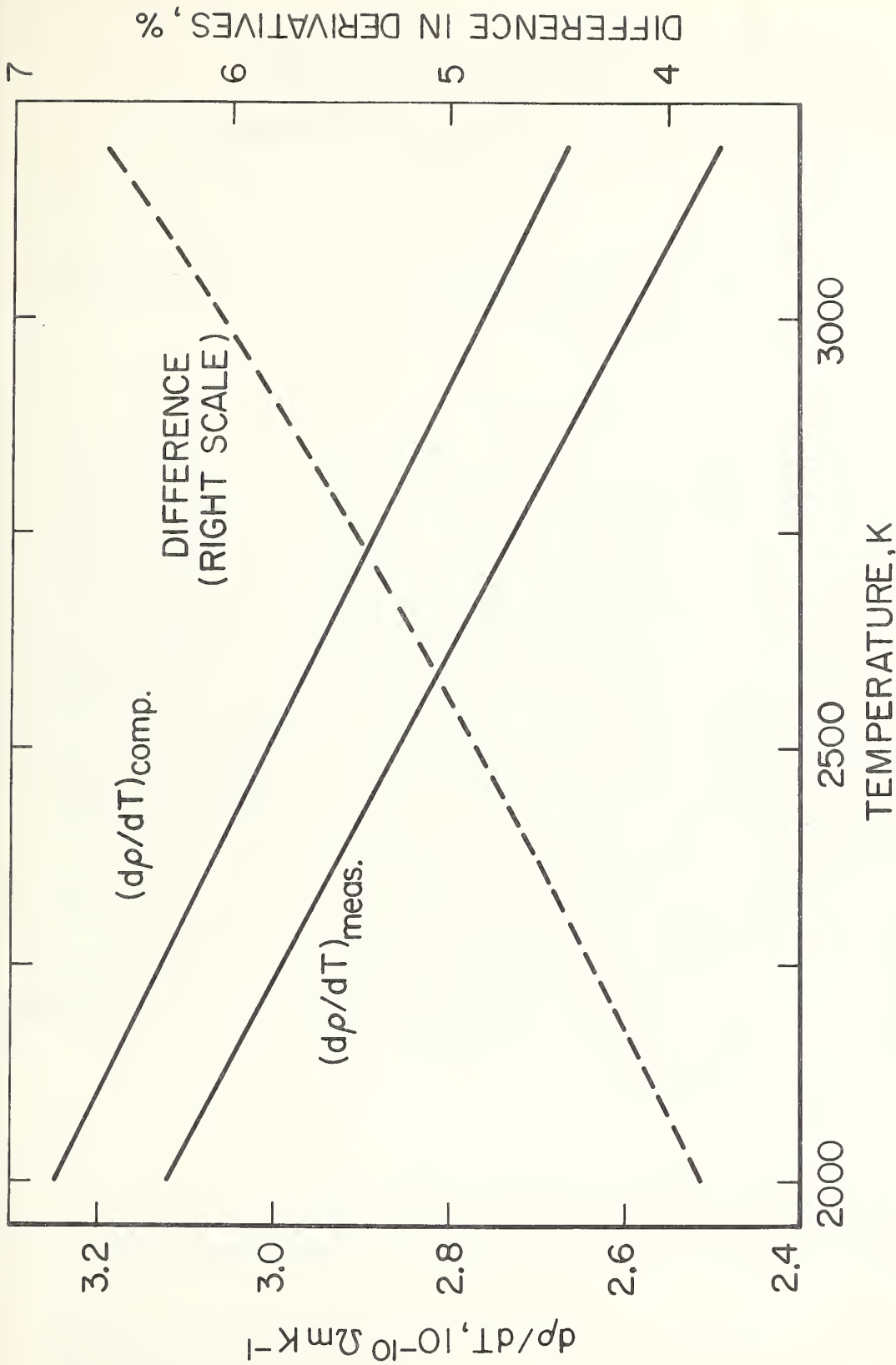
Figure 7. Temperature derivatives of the electrical resistivity (measured and computed according to Matthiessen's law) of tantalum – 10 tungsten alloy. The quantity $(d\rho/dT)_{meas.}$ is obtained from Equation (2), and $(d\rho/dT)_{comp.}$ is obtained from Equation (5). Difference in derivatives refers to computed values minus measured values.

Chapter 6
SIMULTANEOUS MEASUREMENT OF SPECIFIC HEAT, ELECTRICAL RESISTIVITY, AND HEMISPHERICAL TOTAL EMITTANCE OF NIOBIUM - 1 (WT. %) ZIRCONIUM ALLOY IN THE RANGE 1500 TO 2700 K BY A TRANSIENT (SUBSECOND) TECHNIQUE*

Ared Cezairliyan
National Bureau of Standards
Washington, D. C.   20234

Abstract

Simultaneous measurements of specific heat, electrical resistivity, and hemispherical total emittance of niobium - 1 (wt. %) zirconium alloy in the temperature range 1500 to 2700 K by a subsecond duration pulse heating technique are described. Estimated inaccuracy of measured properties are: 3% for specific heat and hemispherical total emittance, and 0.5% for electrical resistivity. Properties of the alloy are compared with the properties of pure niobium. It was found that specific heat and emittance of the alloy were approximately 0.5% and 1.5%, respectively, higher than those of pure niobium. Electrical resistivity of the alloy was 0.5% lower than that of pure niobium. Like niobium, the alloy showed a negative departure from linearity in the curve of electrical resistivity versus temperature.

---

1. Introduction

In this paper, application of a transient technique to the simultaneous measurements of specific heat, electrical resistivity, and hemispherical total emittance of the alloy niobium - 1 (wt. %) zirconium in the temperature range from 1500 to 2700 K is described.

The method is based on rapid resistive self-heating of the specimen from room temperature to any desired high temperature (up to its melting point) in less than one second by the passage of electrical currents through it; and on measuring, with millisecond resolution, experimental quantities such as current through the specimen, potential drop across the specimen, and specimen temperature. Details regarding the construction and operation of the measurement system, the methods of measuring experimental quantities, and other pertinent information, such as formulation of relations for properties, etc. are given in earlier publications [1,2][1].

2. Measurements

The specimen was a tube of the following nominal dimensions: length, 102 mm; outside diameter, 6.3 mm; and wall thickness, 0.5 mm. Zirconium content of the specimen was 1.05% by weight. The total amount of impurities was less than 0.17%; the major impurity was tantalum with 0.09%. Photomicrographs of the specimen, shown in Figure 1, indicate that considerable grain growth took place as the result of pulse heating to high temperatures.

---

[1]Figures in brackets indicate the literature references at the end of this paper.

To optimize the operation of the high-speed pyrometer, the temperature interval (1500 to 2700 K) was divided into six ranges. One experiment was performed in each range. Before the start of the experiments, the specimen was annealed by subjecting it to 30 heating pulses (up to 2500 K). The experiments were conducted with the specimen in a vacuum environment of approximately 10^{-4} torr.

To optimize the operation of the measurement system, the heating rate of the specimen was varied depending on the desired temperature range by adjusting the value of a resistance in series with the specimen. Duration of current pulses in the experiment ranged from 360 to 410 ms; and the heating rate ranged from 4500 to 6600 K s^{-1}. Radiative heat loss from the specimen amounted to approximately 1% at 1500 K, and 9% at 2700 K of the input power.

3. Experimental Results

The thermophysical properties reported in this paper are based on the International Practical Temperature Scale of 1968 [3]. In all computations, the geometrical quantities are based on their room temperature (298 K) dimensions. The experimental results for properties are represented by polynomial functions in temperature obtained by least squares approximation of the individual points. The final values on properties at 100 degree temperature intervals computed using the functions are presented in Table 1. Results obtained from individual experiments, by the method described previously [2], are given in the Appendix (Tables A-1 and A-2). Each number tabulated in these tables represents results from over fifty original data points.

Table 1

Specific heat, electrical resistivity, and hemispherical total
emittance of the alloy niobium -1 (wt.%) zirconium

Temp. K	c_{p} $J g^{-1} K^{-1}$	ρ^{*} 10^{-8} Ωm	ϵ^{*}
1500	0.3207	57.36	
1600	0.3263	60.13	
1700	0.3322	62.87	0.218
1800	0.3385	65.59	0.232
1900	0.3455	68.27	0.245
2000	0.3535	70.93	0.257
2100	0.3627	73.56	0.268
2200	0.3735	76.16	0.278
2300	0.3861	78.74	0.287
2400	0.4007	81.29	0.295
2500	0.4177	83.81	0.303
2600	0.4373	86.30	0.309
2700	0.4598	88.76	

*Based on ambient temperature (298K) dimensions.

Specific Heat. Specific heat was computed from data taken during the heating period. A correction for power loss due to thermal radiation was made using the results on hemispherical total emittance. The function for specific heat (standard deviation = 1%) that represents the results in the temperature range 1500 to 2700 K is:

$$c_p = 7.073 \times 10^{-2} + 3.783 \times 10^{-4}T - 2.091 \times 10^{-7}T^2 + 4.532 \times 10^{-11}T^3 \quad (1)$$

where T is in K, and c_p is in J g^{-1} K^{-1}.

Electrical Resistivity: The electrical resistivity was determined from the same experiments that were used to calculate the specific heat. The function for electrical resistivity (standard deviation = 0.06%) that represents the results in the temperature range 1500 to 2700 K is:

$$\rho = 12.50 + 3.199 \times 10^{-2}T - 1.387 \times 10^{-6}T^2 \quad (2)$$

where T is in K, and ρ is in 10^{-8} Ωm. The measurement, before the pulse experiments, of the electrical resistivity of the specimen at 293 K with a Kelvin bridge yielded a value of 16.2×10^{-8} Ωm.

Hemispherical Total Emittance: Hemispherical total emittance was computed using data taken during both heating and initial free radiative cooling periods. The function for hemispherical total emittance (standard deviation = 1%) that represents the results in the temperature range 1700 to 2600 K is:

$$\varepsilon = -1.647 \times 10^{-1} + 3.056 \times 10^{-4}T - 4.749 \times 10^{-8}T^2 \quad (3)$$

where T is in K.

4.   Estimate of Errors

The details for estimating errors in measured and computed quantities in transient experiments using the present measurement system are given in

100

an earlier publication [2]. In this paper, the specific items in the
error analysis were recomputed whenever the present conditions differed
from those in the earlier publication. The results for imprecision[2] and
inaccuracy[3] in the properties are: 1% and 3% for specific heat, 0.06%
and 0.5% for electrical resistivity, 1% and 3% for hemispherical total
emittance.

5. Discussion

The specific heat, electrical resistivity, and hemispherical total
emittance of the niobium-1 zirconium alloy measured in this work are
presented in Figure 2. A comparison of the present results for the alloy
with those for pure niobium [4] obtained using the same method is given
in Figure 3. It may be seen that specific heat and hemispherical total
emittance of the alloy were approximately 0.5% and 1.5%, respectively,
higher than those of pure niobium. The difference in specific heat
cannot be accounted for by the additivity law. Electrical resistivity
of the alloy was 0.5% lower than that of pure niobium. However, one
should not place too much significance to these differences since their
magnitudes are less than the combined estimated errors in the measure-
ments for the alloy and for the pure metal.

At 293 K, electrical resistivity of the alloy (16.2×10^{-8} Ωm)
is higher than the resistivity of pure niobium (15.9×10^{-8} Ωm) [4].
However, at high temperatures (Figure 3) the resistivity of the alloy

---

[2]Imprecision refers to the standard deviation of an individual point
as computed from the difference between measured value and that from
the smooth function obtained by the least squares method.

[3]Inaccuracy refers to the estimated total error (random and systematic).

is lower than that of niobium. A similar trend was also observed in the electrical resistivity of the alloy tantalum - 10 (wt. %) tungsten [5]. Like tantalum, at high temperature the alloy showed a negative departure from linearity in the curve of electrical resistivity versus temperature.

6. Acknowledgement

Table A-1

Experimental results on specific heat and electrical resistivity
of the alloy niobium-1 (wt.%) zirconium

T K	c_p $J\ g^{-1}\ K^{-1}$	Δc_p^* $\%$	ρ $10^{-8}\ \Omega m$	$\Delta\rho^*$ $\%$
1500	0.3198	-0.24	57.37	+0.01
1550	0.3206	-0.87	58.75	-0.01
1600	0.3275	+0.37	60.13	0.00
1650	0.3344	+1.57	61.53	+0.03
1700	0.3311	-0.31	62.90	+0.04
1750	0.3392	+1.19	64.27	+0.05
1800	0.3339	-1.34	65.59	+0.01
1850	0.3416	-0.06	66.92	-0.02
1900	0.3480	+0.74	68.26	-0.03
1950	0.3419	-2.14	69.58	-0.03
2000	0.3505	-0.82	70.88	-0.07
2050	0.3587	+0.26	72.19	-0.09
2100	0.3666	+1.08	73.50	-0.09
2150	0.3739	+1.62	74.81	-0.08
2200	0.3700	-0.91	76.25	+0.10
2250	0.3779	-0.42	77.51	+0.06
2300	0.3859	-0.00	78.77	+0.03
2350	0.3943	+0.33	80.03	+0.01
2400	0.4030	+0.60	81.28	-0.01
2450	0.4024	-1.59	82.68	+0.16
2500	0.4217	+0.98	83.79	-0.02
2550	0.4228	-1.01	85.11	+0.07
2600	0.4426	+1.24	86.28	-0.02
2650	0.4461	-0.43	87.52	-0.02
2700	0.4594	-0.07	88.69	-0.08

*The quantities Δc_p and $\Delta\rho$ are percentage deviations of the individual
results from the smooth functions represented by equations (1) and
(2), respectively.

Experimental results on hemispherical total emittance of the
alloy niobium-1 (wt.%) zirconium

T K	ε	$\Delta \epsilon^*$ %
1711	0.218	-0.44
1711	0.223	+1.71
1711	0.217	-1.01
1712	0.223	+1.76
1899	0.242	-1.01
1899	0.242	-0.93
1899	0.240	-1.76
1900	0.241	-1.50
2055	0.264	+0.36
2056	0.265	+0.62
2056	0.266	+1.05
2057	0.266	+1.22
2322	0.287	-0.69
2324	0.289	-0.11
2324	0.290	+0.14
2325	0.291	+0.64
2667	0.312	-0.31
2670	0.312	-0.11
2670	0.313	+0.02
2672	0.314	+0.20

*The quantity $\Delta \epsilon$ is percentage deviation of the individual results
from the smooth function represented by equation

8. References

[1] Cezairliyan, A., Design and operational characteristics of a high-speed (millisecond) system for the measurement of thermo-physical properties at high temperatures, J. Res. Nat. Bur. Stand. (U.S.), 75C (Eng. and Instr), 7 (1971).

[2] Cezairliyan, A., Morse, M. S., Berman, H. A., and Beckett, C. W., High-speed (subsecond) measurement of heat capacity, electrical resistivity, and thermal radiation properties of molybdenum in the range 1900 to 2800 K, J. Res. Nat. Bur. Stand. (U.S.), 74A (Phys. and Chem.), 65 (1970).

[3] International Practical Temperature Scale of 1968, Metrologia, 5, 35 (1969).

[4] Cezairliyan, A., High-speed (subsecond) measurement of heat capacity, electrical resistivity, and thermal radiation properties of niobium in the range 1500 to 2700 K, J. Res. Nat. Bur. Stand. (U.S.), 75A (Phys. and Chem.), 565 (1971).

[5] Cezairliyan, A., High-speed (subsecond) simultaneous measurement of specific heat, electrical resistivity, and hemispherical total emittance of tantalum-10 (wt. %) tungsten alloy in the range 1500 to 3200 K, High Temperatures-High Pressures, to be published.

0.2 mm
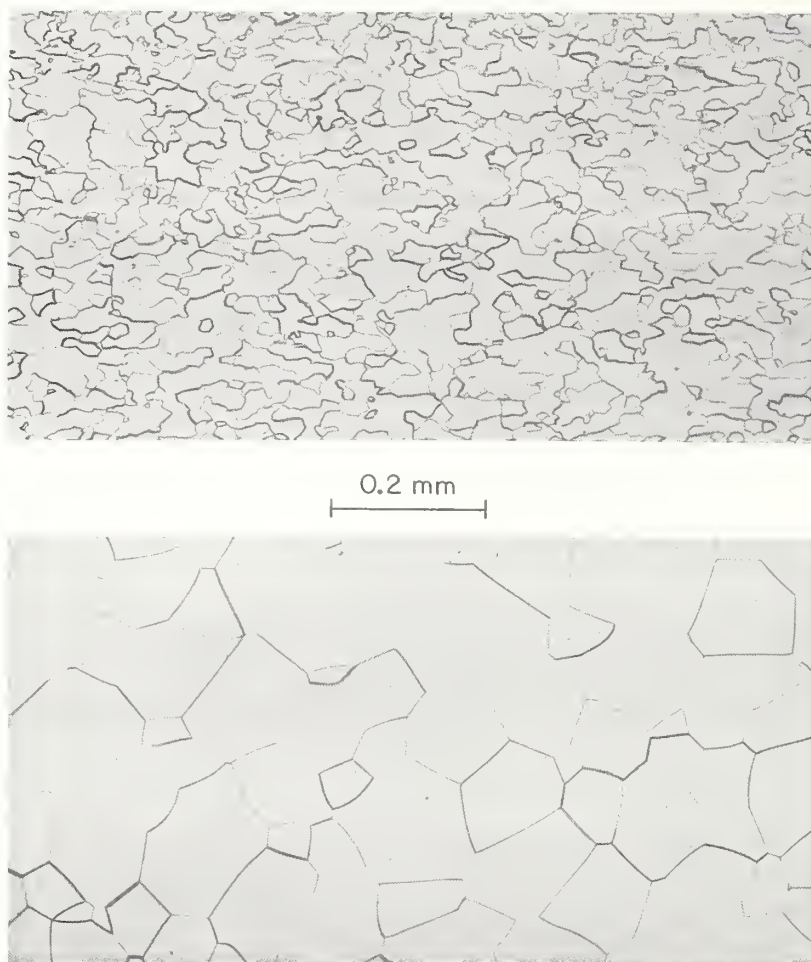
Figure 1. Photomicrographs of the niobium - 1 zirconium specimen.
Upper photograph, specimen as received; lower photograph,
specimen after the entire set of experiments.

106
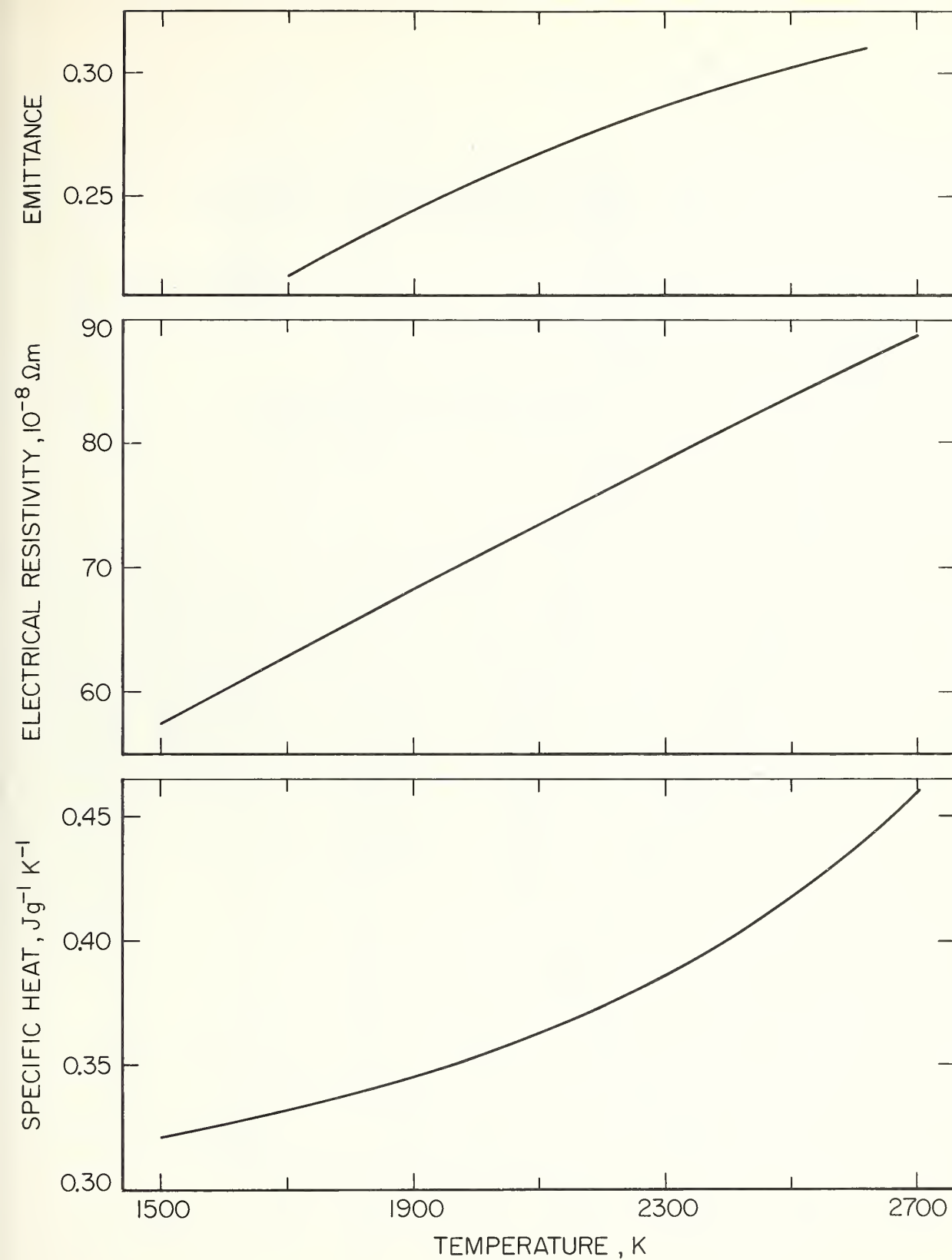
Figure 2. Specific heat, electrical resistivity, and hemispherical

total emittance of niobium - 1 zirconium alloy.
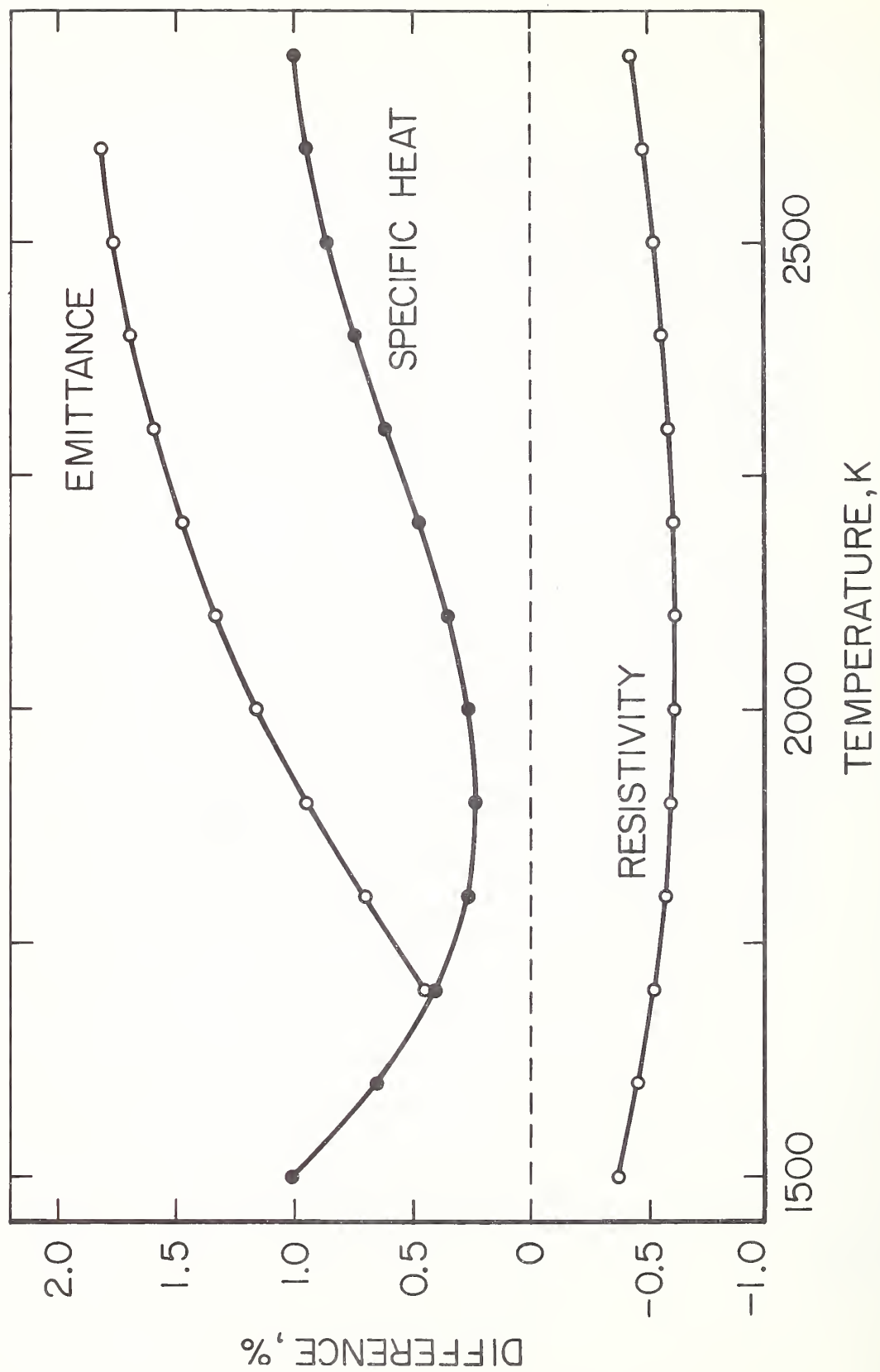
Figure 3. Differences in specific heat, electrical resistivity, and hemispherical total emittance of niobium - 1 zirconium alloy with those of pure niobium.

Chapter 7

MEASUREMENT OF MELTING POINT AND
ELECTRICAL RESISTIVITY (ABOVE 3600 K) OF
TUNGSTEN BY A PULSE HEATING METHOD*

Ared Cezairliyan
National Bureau of Standards
Washington, D. C. 20234

Abstract

A subsecond duration pulse heating method is used to measure the melting point, and electrical resistivity of tungsten above 3600 K. The results yield a value of 3695 K (on the International Practical Temperature Scale of 1968) for the melting point with an estimated inaccuracy of 15 K. Estimated inaccuracy in electrical resistivity measurements is 1 percent.

---

1. Introduction

Serious difficulties are encountered in the measurement of electrical resistivity and melting point of substances at temperatures above 2500 K by conventional steady-state and quasi steady-state methods. Most of the problems inherent in these methods are eliminated by using high-speed measurement techniques. An application of a high-speed (pulse heating) technique to the accurate measurement of the melting point and electrical resistivity (above 2940 K) of molybdenum is described in the literature [1].

In the present study, the same pulse heating technique was used for the measurement of the melting point and electrical resistivity of tungsten above 3600 K. The tubular specimen was heated in vacuum (10^{-4} torr) from room temperature to its melting point in 0.7 s by a single heavy current pulse. During the heating period, current flowing through the specimen, potential difference across the specimen, and specimen temperature were measured. Temperature was measured with a high-speed photoelectric pyrometer [2] which permits 1200 evaluations of specimen temperature per second. The pyrometer's target was a rectangular hole (1 x 0.5 mm) in the wall at the middle of the specimen. Recordings of voltage, current, and temperature were made with a high-speed digital data acquisition system [3], which is capable of recording data with a full-scale signal resolution of approximately one part in 8000 and a time resolution of 0.4 ms. Details regarding the construction and operational characteristics of the entire measurement system are given in earlier publications [3, 4].

110

2. Measurements

Measurements were performed on two specimens designated as tungsten-1 and tungsten-2. Each specimen was a tube fabricated from a tungsten rod by removing the center portion by an electro-erosion technique. The nominal dimensions of the specimens were: length 102 mm (4 in.), outside diameter, 6.3 mm (0.25 in.); and thickness, 0.5 mm (0.02 in.). The outer surface of the specimen was polished to reduce heat loss due to thermal radiation. The rods used in the fabrication of the two specimens were obtained from two different sources. They were manufactured by two different techniques: sintered (tungsten-1), and arc cast (tungsten-2). Both specimens were 99.9^+ percent pure. Spectrochemical analyses on tungsten-1 indicate the presence of the following impurities in ppm by weight: Mo, 310; Th, < 250; Fe, 60; Zr, 30; Ca, Nb, < 20 each; Cu, Ti, 10 each; Al, Cr, Si, 5 each; and B, Co, Mg, Mn, Ni, Pb, Sn, Sr, < 2 each. The residual resistivity ratio of tungsten-1 was 41. All measurements reported in this paper, unless stated otherwise, are based on the International Practical Temperature Scale of 1968 (IPTS-1968) [5].

Specimen temperature near and during the initial melting period was measured as a function of time. The plateau in temperature indicates the region of solid and liquid equilibria. By averaging temperature points on the plateau the following values were obtained for the melting point: 3692.6 K for tungsten-1, and 3696.8 K for tungsten-2, with a standard deviation (individual point) of 1.3 K and 1.1 K, respectively. The measured temperatures at the plateau for the two specimens are shown in

111

figure 1. Averaging the results of the two specimens yields a value
of 3695 K for the melting point of tungsten. To determine the trend of
measured temperatures at the plateau, temperature data were fitted to a
linear function in time using the least squares method. This procedure
indicated that the slope of the linear function was small, corresponding
to a maximum temperature difference of less than 0.5 K between the beginning
and end of the plateau for both specimens.

Electrical resistance of tungsten-1 near and at the melting point
is shown in figure 2. It may be seen that resistance behaved normally
until approximately 10 K below the melting point was reached. Electrical
resistivity was calculated using the relation $\rho = RA/L$, where R is the
resistance, A the cross-sectional area, and L the length of the specimen
between the potential probes. Dimensions were based on their room
temperature values. The cross-sectional area was determined from measure-
ments of density and weight. Measured values for the electrical resistivity
(in $10^{-8}\Omega m$) are: 112.0 at 3600 K, 113.5 at 3650 K, and 114.4 at 3680 K.

Sources and estimates of errors in experiments similar to the one
conducted in this study are given in detail in earlier publications [1, 3].
The combination of errors gives an estimate for the
inaccuracy of measured properties: 1 percent for electrical resistivity,
and 15 K for the melting point.

112
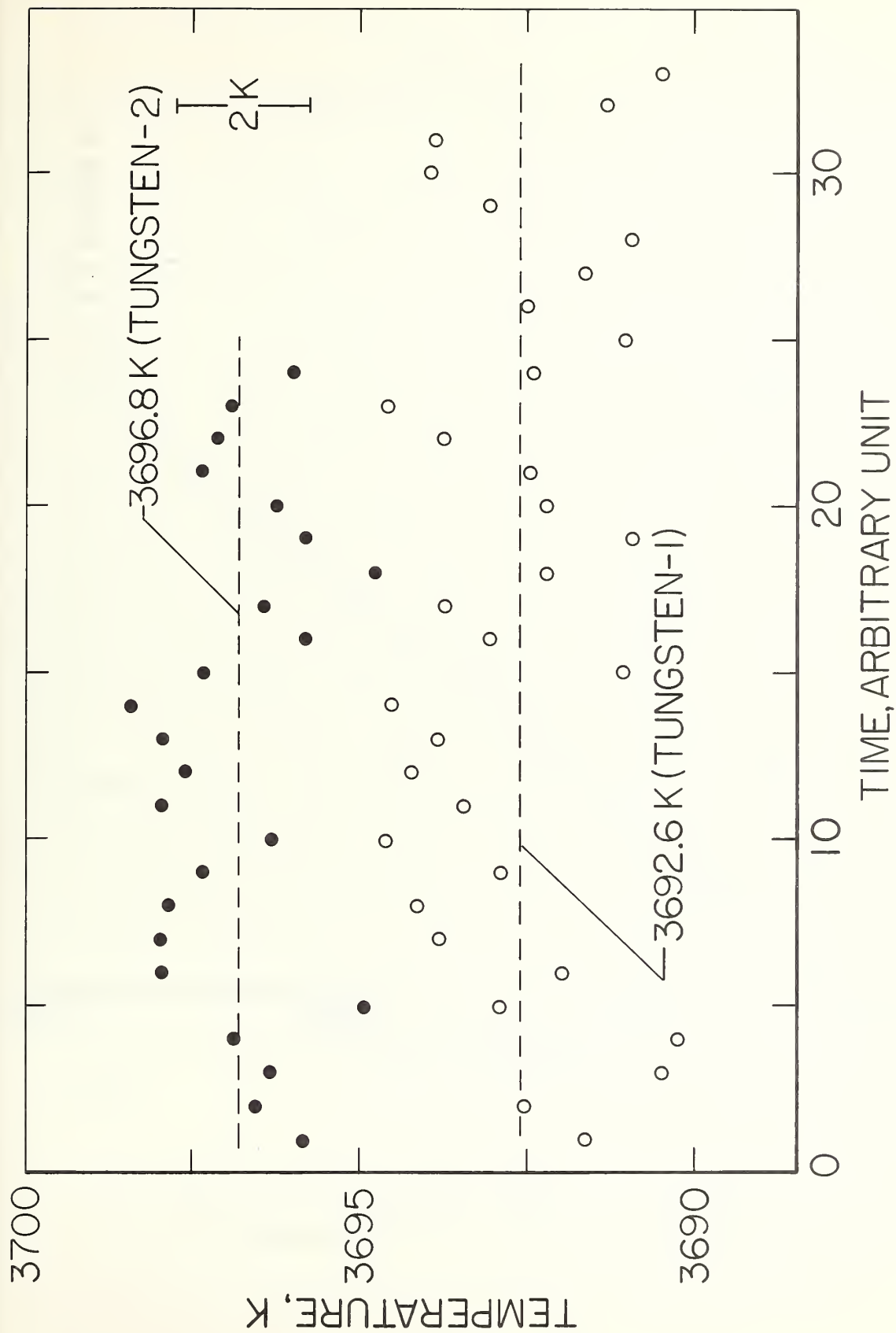
FIGURE 1. Temperature of the two tungsten specimens as a function of time at the melting point (1 time unit = 0.833 ms).
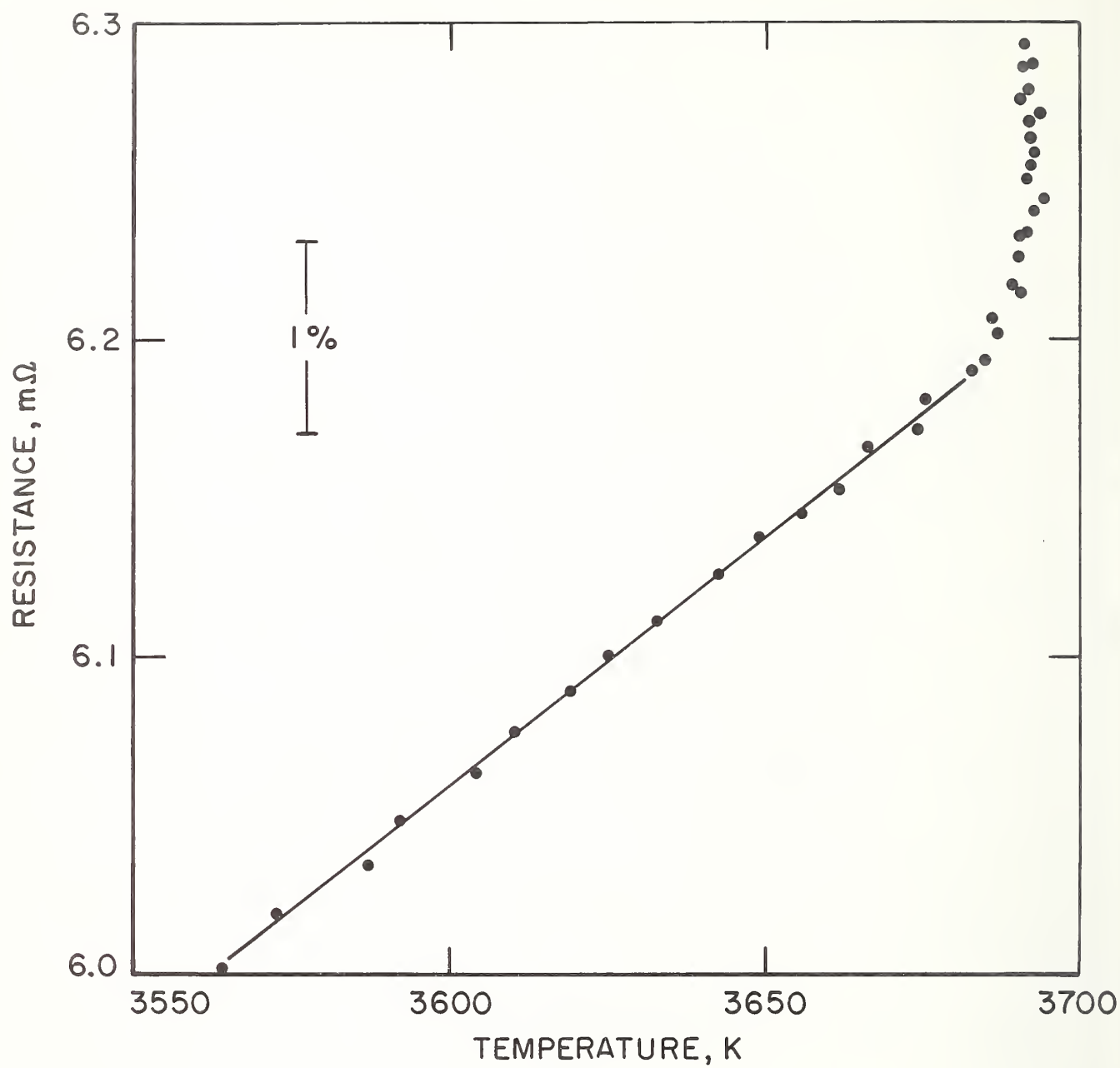
FIGURE 2. Electrical resistance of tungsten-1 as a function of temperature near and at the melting point.

114

3. Discussion

As may be seen in Table 1, considerable differences exist in the tungsten melting points reported in the literature. In order to have a common ground for comparisons, all reported values were converted to IPTS-1968. It is interesting to note that, in general, the reported values increase chronologically. The measurements were performed either before 1930 or after 1960. The melting points reported prior to 1915, as were summarized by Langmuir [6], were lower than that of Langmuir by as much as 50 to 500 K. Experimental difficulties, including pyrometry problems, encountered in high temperature quasi steady-state measurements might have been responsible for the large discrepancies. Another source of the discrepancies could have been the differences in the purity of various tungsten specimens.

Probably, the most reliable measurement performed on the melting point of tungsten before 1930 was that of Worthing [7] which is 25 K below the present value; however, this difference is within the combined uncertainties of the two results. The average value of the melting points reported by three investigators [11, 12, 14] since 1960 is 3693 K; average and maximum differences from this value being 7 K and 10 K, respectively. The melting point obtained in this study is 2 K higher than the above average.

TABLE I

Melting Point of Tungsten Reported in the Literature

| Investigator | Ref. | Year | Constants* | | Melting Point, K | |
			T_{Au} (K)	c_2 (cm K)	as reported**	on IPTS-1968
Langmuir	6	1915	1335	1.439	3540±30	3559
Worthing	7	1917	1336	1.435	3675 ± 15	3670
Henning and Heuse	8	1923	1336	1.430	3643	3616
Pirani	9	1923	1336	1.430	3660 ± 60	3633
Forsythe and Worthing	10	1925	1336	1.433	3655	3641
Zalabak	14	1961	1336.15	1.438	3680 ± 25	3687
Allen	11	1962	1336.15	1.438	3682 ± 20	3689
Rudy et al.	12	1966	1336.15	1.438	3696 ± 30	3703
IPTS-1968***	5	1968	1337.58	1.4388	3660	3660
Present Work			1337.58	1.4388	3695 ± 15	3695

*Values of T_{Au} (gold point) and c_2 (second radiation constant) used by the investigator.

**Based on T_{Au} and c_2 used by the investigator.

***Recommended as secondary reference point on IPTS-1968.

The presence of impurities in a specimen alters (in general, reduces) the melting point of the element. Based on the Raoult-Van't Hoff equation, the melting point depression for the tungsten specimen (with total amount of impurities less than 0.1 percent) is estimated to be less than 3 K. Also, under the present operating conditions, it is very unlikely that the effect of superheating, if present at all, is more than a fraction of a degree. One may conclude that the melting point of tungsten is 3695 ± 15 K.

The electrical resistivity of this work at 3600 K is approximately 2 percent lower than the value reported by Jones [13].

Measurements indicate a normal behavior of electrical resistivity until approximately 10 K below the melting point was reached. Above this temperature, a departure from normalcy is observed which may be due to: (1) premelting effects of impurities present in the specimen, and (2) increase in vacancy concentration. Small temperature gradients in the specimen also may partially account for this.

With the present system it was not possible to follow the entire melting process because the specimen collapsed and opened the main electrical circuit prior to the completion of melting.

4. <u>References</u>

[1]   Cezairliyan, A., M. S. Morse, and C. W. Beckett. Measurement of
      melting point and electrical resistivity (above 2840 K) of
      molybdenum by a pulse heating method. Rev. Int. Hautes Tempér. et
      Réfract. <u>7</u>, 382 (1970).

[2]   Foley, G. M. High-speed optical pyrometer. Rev. Sci. Instr. <u>41</u>,
      827 (1970).

[3]   Cezairliyan, A., M. S. Morse, H. A. Berman, and C. W. Beckett.
      High-speed (subsecond) measurement of heat capacity, electrical
      resistivity, and thermal radiation properties of molybdenum in the
      range 1900 to 2800 K. J. Res. Nat. Bur. Stand. (U.S.) <u>74A</u> (Phys. and
      Chem.), 65 (1970).

[4]   Cezairliyan, A. Design and operational characteristics of a high-
      speed (millisecond) system for the measurement of thermophysical
      properties at high temperatures. J. Res. Nat. Bur. Stand. (U.S.)
      <u>75C</u> (Eng. and Instr.), 7 (1971).

[5]   International Practical Temperature Scale of 1968. Metrologia <u>5</u>,
      35 (1969).

[6]   Langmuir, I. The melting point of tungsten. Phys. Rev. <u>6</u>, 138 (1915).

[7]   Worthing, A. G. The true temperature scale of tungsten and its emissive
      powers at incandescent temperatures. Phys. Rev. <u>10</u>,377 (1917).

[8]   Henning, F. and W. Heuse. Melting points of platinum and tungsten.
        Zeit. Physik 16, 63 (1923).

[9]   Pirani, M. and H. Alterthum. A method of measuring the melting
        points of metals having high melting points. Zeitschrift
        Electrochemie 29, 5 (1923).

[10]   Forsythe, W. E. and A. G. Worthing. The properties of tungsten
        and the characteristics of tungsten lamps. Astrophys. J. 61,
        146 (1925).

[11]   Allen, R. D. Techniques for melting point determination on an
        electrically heated refractory metal. Nature 193, 769 (1962).

[12]   Rudy, E., S. Windisch, and J. R. Hoffman. AFML-TR-65-2, Part
        I, Vol. VI, Air Force Materials Laboratory Research and Technology
        Division, Dayton, Ohio (1966).

[13]   Jones, H. A. A temperature scale for tungsten. Phys. Rev. 28,
        202 (1926).

[14]   Zalabak, C. F. NASA Technical Note D-761, 1961.

Chapter 8

MEASUREMENT OF MELTING POINT, NORMAL SPECTRAL EMITTANCE (AT MELTING POINT), AND ELECTRICAL RESISTIVITY (ABOVE 2650 K) OF NIOBIUM BY A PULSE HEATING METHOD*

Ared Cezairliyan

National Bureau of Standards

Washington, D. C.   20234

Abstract

A subsecond duration pulse heating method is used to measure the melting point, normal spectral emittance (at the melting point), and electrical resistivity (above 2650 K) of niobium. The results yield a value of 2750 K for the melting point on the International Practical Temperature Scale of 1968. Normal spectral emittance at the melting point is 0.348, and remained constant during melting. At 2740 K, electrical resistivity is 90.11×10^{-8} Ω m. Estimated inaccuracy is 10 K in the melting point, 3% in normal spectral emittance and 0.5% in electrical resistivity.

---

1. Introduction

A millisecond resolution pulse heating technique was developed earlier in connection with the measurement of selected thermophysical properties of electrical conductors at high temperatures (Cezairliyan et al., 1970a). This technique was also applied to the measurement of the melting point of molybdenum (Cezairliyan et al., 1970b), and the normal spectral emittance of tantalum at its melting point (Cezairliyan, 1970).

In the present study, the same technique is used for the measurements of the melting point, normal spectral emittance (at the melting point), and electrical resistivity (above 2650 K) of niobium.

The technique is based on resistive pulse heating of the specimen from room temperature to its melting point in less than one second and measuring, with millisecond resolution, current through the specimen, potential difference across the specimen, and specimen temperature. Specimen temperature was measured with a high-speed photoelectric pyrometer (Foley, 1970) which permits 1200 evaluations of specimen temperature per second. The recordings of voltage, current, and temperature were made with a high-speed digital data acquisition system (Cezairliyan et al., 1970a), which is capable of recording data with a full-scale signal resolution of approximately one part in 8000 and a time resolution of 0.4 ms. Details regarding the construction and operational characteristics of the entire measurement system is given in an earlier publication (Cezairliyan, 1971a).

121

2. Measurements

Melting point and electrical resistivity measurements were performed on two niobium specimens in the form of tubes, designated as niobium-1 and niobium-2. The nominal dimensions of the tubes were: length, 102 mm; outside diameter, 6.3 mm; thickness, 0.5 mm. A small rectangular hole (0.5 x 1 mm) fabricated in the wall at the middle of the specimen approximated blackbody conditions for temperature measurements. Normal spectral emittance measurements were performed on two niobium specimens in the form of strips, designated as niobium-3 and niobium-4. The nominal dimensions of the strips were: length, 102 mm; width, 6.3 mm; thickness, 0.25 mm. The surfaces of all specimens were polished.

The specimens were 99.9 percent pure. Spectrochemical analysis indicated the presence of the following impurities in ppm by weight: Ta, 450; W, < 100; Hf, < 50; Sb and Zn, < 10 each; Al, Mo, 5 each; As, Bi, Cd, Si, Te, Zr, < 5 each; Sn, 3; Fe, < 3; and B, Ca, Co, Cr, Cu, Mg, Mn, Ni, Pb, Ti, V, < 1 each.

Before starting the experiments, all the specimens were annealed by subjecting them to 30 heating pulses (up to 2400 K). The experiments were conducted with the specimens in a vacuum environment of approximately 10^{-4} torr. Duration of the current pulses was 500 ms for the tubes and 600 ms for the strips. This corresponds to a heating rate of approximately 4700 K s^{-1} for the tubes and 2000 K s^{-1} for the strips near the melting point. The magnitude of current pulses near the melting point was approximately 1400 A in the case of the tubes, and 250 A in the case of the strips.

122

All measurements reported in this paper, unless stated otherwise, are based on the International Practical Temperature Scale of 1968 (IPTS-68, 1969).

2.1. Melting Point

Temperature of the tubular specimens was measured near and during the initial melting period. The results on niobium-1 are shown in Figure 1. Temperature of the heating specimen increased almost linearly with time above 2650 K. A linear fit of temperature in terms of time obtained using the least squares method yielded a standard deviation (individual point) of 0.8 K. The plateau in temperature indicates the region of solid and liquid equilibria. Measured temperatures at the plateau for the two niobium specimens are shown in Figure 2. The melting point was obtained by averaging temperature points on the plateau of a given specimen.

The melting point obtained by this approach was 2750.6 K for niobium-1, and 2750.5 K for niobium-2. Standard deviation of an individual temperature point from the average for each specimen was 0.7 K. The duration of the plateau of niobium-1 was longer than that of niobium-2. This may be attributed to an early collapse of niobium-2. To determine the trend of measured temperatures at the plateau, temperatures for niobium-1 were fitted to a linear function in time using the least squares method. The slope of the linear function was 1.8 K s^{-1}, which corresponds to a maximum temperature difference of less than 0.03 K between the beginning and the end of the plateau. This procedure gave a standard deviation of 0.7 K, which is the same as that obtained by averaging the temperatures.

It may be concluded that the melting point of niobium is 2750 K.

2.2. Normal Spectral Emittance

Normal spectral emittance was determined from the measurements of
the surface radiance temperature of niobium strips and the melting point
obtained from the measurements on the tubular specimens. Based on the
Wien radiation equation, the relation between emittance and temperature is

$$\epsilon = \frac{1}{\exp\left[\frac{c_2}{\lambda}\left(\frac{1}{T_s} - \frac{1}{T_m}\right)\right]} \tag{1}$$

where ϵ is normal spectral emittance, T_m the melting point, T_s the
surface radiance temperature, c_2 the second radiation constant (1.4388
$\times 10^{-2}$ m K), and λ the effective wavelength of the optical system. The
measurements were performed at 650 nm which corresponds to the effective
wavelength of the pyrometer's interference filter. The bandwith of the
filter was 10 nm. The circular area viewed by the pyrometer was 0.2 mm
in diameter.

The experimental results of the surface radiance temperature for
niobium-3 near and at the melting point are shown in Figure 3. Each
measured temperature during melting is an average quantity representing
a combination of solid and liquid phases over the area viewed by the
pyrometer. It is interesting to note the sharp peak in the radiance
temperature, which amounts to approximately 5 K, at the start of melting.
A peak similar in shape and magnitude was also observed in the case of
niobium-4. The plateau in the surface radiance temperature corresponds
to melting of the specimen.

124

The average surface radiance temperature was computed to be 2432.5 K for niobium-3, and 2431.0 K for niobium-4 with a standard deviation of 0.7 K. To check the deviations from constancy at the plateau, temperature data for niobium-3 were fitted to a linear function in time (standard deviation = 0.7 K). The results do not indicate any significant departure from constancy. The slope of this function was approximately 0.6 K s^{-1}, which corresponds to a maximum temperature difference of 0.1 K between the beginning and the end of the plateau.

Normal spectral emittance was computed for each temperature using Equation (1). The average of the results for each specimen was 0.349 for niobium-3 and 0.347 for niobium-4 with a standard deviation of 0.3%. The results on the two specimens are in agreement within 0.6%. It may be concluded that the normal spectral emittance of niobium at its melting point is 0.348.

2.3. Electrical Resistivity

Electrical resistivity of the tubular niobium specimens was calculated using the relation ρ = RA/L, where R is the resistance, A the cross-sectional area, and L the length of the specimen between the potential probes. Dimensions were based on their room temperature values. Cross-sectional area was determined from the measurement of weight and density. The results of the electrical resistivity of niobium-1 above approximately 2650 K are shown in Figure 4. In the range 2650 to 2740 K, the electrical resistivity was fitted to a linear function in temperature with a standard deviation of 0.02% using the least squares method. The average absolute difference in the measured electrical resistivity of

125

the two niobium specimens in the range 2650 to 2740 K was approximately

0.4%. The final result for the electrical resistivity of niobium was

obtained by averaging the results of the two specimens. This yielded a

value of 87.92 x 10^{-8} Ω m at 2650 K, 89.14 x 10^{-8} Ω m at 2700 K, and 90.11

x 10^{-8} Ω m at 2740 K. As shown in Figure 4, electrical resistivity

continued to increase during melting of the specimen.

3. Estimate of Errors

Sources and estimates of errors in experiments similar to the one

conducted in this study are given in detail in earlier publications (Cez-

airliyan et al., 1970a, 1970b). Specific items in the error analysis were

recomputed whenever the present conditions differed from those in the

earlier publications. A summary of the results on imprecision and in-

accuracy of some of the measured and computed quantities are given in

Table 1.

It may be seen from Table 1 that the imprecision of blackbody temp-

erature measurements during heating of the specimen (before reaching the

melting point) was approximately the same as that during the melting

period. This indicates that in the experiment the initial melting phase

progressed normally and that there were no undesirable effects during

melting of the specimen, such as vibration of the specimen, movement of

the blackbody sighting hole in the specimen, and the instantaneous

development of hot spots or zones in the specimen. Also the imprecision

of the surface radiance temperature measurements was the same as that of

blackbody temperature measurements, which indicates that the specimen's

surface conditions did not change in a random fashion during the melting

period.

4. Discussion

Conversion of the results of the two recent measurements reported in the literature to IPTS-68 yields 2746 K (Schofield, 1956-1957) and 2745 K (Pemsler, 1961) for the melting point of niobium. These are 4 to 5 K lower than the present result, 2750 K. However, the differences are within the measurement uncertainties reported by the investigators. In addition to this, there are indications that the specimens used in the earlier measurements were less pure than those used in the present study, which may account partially for the lower melting points obtained earlier. The melting point depression due to the impurities in the present specimens is estimated to be not more than 2 K.

Normal spectral emittance of niobium at its melting point is reported to be 0.368 (Pemsler, 1961); this is approximately 4% higher than the present value of 0.348. Earlier results (Cezairliyan, 1971b) on tubular niobium specimens in the range 1700 to 2300 K showed a linear variation of normal spectral emittance with temperature. Extrapolation of these results to the melting point yields 0.348 for normal spectral emittance, which is identical to the present value.

Electrical resistivity reported by Gebhardt et al. (1966) goes only to 2500 K. Extrapolation of the results to 2700 K yields a value of 90.74 x 10^{-8} Ω m, which is 1.8% higher than the present valueof 89.14 x 10^{-8} Ω m. Electrical resistivity behaved normally until approximately 5 to 10 K below the melting point was reached (Figure 4). Above this, a departure

127

from normalcy was observed which may be due to: (1) premelting
effects of impurities present in the specimen, and (2) increase in
vacancy concentration. Small temperature gradients in the specimen
also may partially account for this.

The sharp peak in surface radiance temperature observed at the
beginning of melting (Figure 3) was reproducible, both in shape and
magnitude, for the two strips. However, no such peak was observed in
the true temperature of the tubes (Figure 1). This implies that the
peak could not have been due to superheating of the specimen. The
effect of superheating in metals (if present at all), under the present
operating conditions, is unlikely to be more than a fraction of a
degree. Also, it is not likely that the strip surface was in the liquid
phase several degrees above the melting point for a short period before
establishing the melting plateau. A possible explanation is that a sudden
change in the surface conditions took place at the start of melting. An
earlier investigation on tantalum (Cezairliyan, 1970) did not show a
sharp peak in surface radiance temperature at the start of melting. How-
ever, a uniform decrease in normal spectral emittance was observed in
tantalum as melting progressed. The results on niobium do not show any
such variation.

5. Acknowledgement

The author expresses his gratitude to Dr. C. W. Beckett for his
continued interest and encouragement of research in high-speed methods
of measuring thermophysical properties. The contribution of Mr. M. S.
Morse in connection with electronic instrumentation is also greatly
appreciated.

128

6. References

1. Cezairliyan, A., 1970, High Temp. - High Pres., **2**, 501-506.

2. Cezairliyan, A., Morse, M. S., Berman, H. A., and Beckett, C. W., 1970a, J. Res. Nat. Bur. Stand. (U. S.), **74A** (Phys. and Chem.), 65-92.

3. Cezairliyan, A., Morse, M. S., and Beckett, C. W., 1970b, Rev. Int. Hautes Tempér. et Réfract. **7**, 382-388.

4. Cezairliyan, A., 1971a, J. Res. Nat. Bur. Stand. (U. S.), **75C** (Eng. and Instr.), 7-18.

5. Cezairliyan, A., 1971b, J. Res. Nat. Bur. Stand. (U. S.), **75A** (Phys. and Chem.), 565-571.

6. Foley, G. M., 1970, Rev. Sci. Instr., **41**, 827-834.

7. Gebhardt, E., Dürrschnabel, W., and Hörz, G., 1966, J. Nuc. Materials, **18**, 119-133.

8. International Practical Temperature Scale of 1968, 1969, Metrologia, **5**, 35-44.

9. Pemsler, J. P., 1961, J. Electrochem. Soc., **108**, 744-750.

10. Schofield, T. H., 1956-1957, J. Inst. Metals, **85**, 372-374.

TABLE 1

Imprecision and inaccuracy of measured and computed quantities*

Quantity	Imprecision	Inaccuracy
Temperature-blackbody (during heating)	0.8 K	7 K
Temperature-blackbody (during melting)	0.7 K	7 K
Temperature-surface radiance (during melting)	0.7 K	7 K
Voltage	0.02%	0.05%
Current	0.02%	0.05%
Melting point	0.7 K	10 K
Normal spectral emittance	0.3%	3%
Electrical resistivity	0.02%	0.5%

*Imprecision refers to the standard deviation of an individual point as computed from the difference between measured value and that from the smooth function obtained by the least squares method. Inaccuracy refers to the estimated total error (random and systematic).
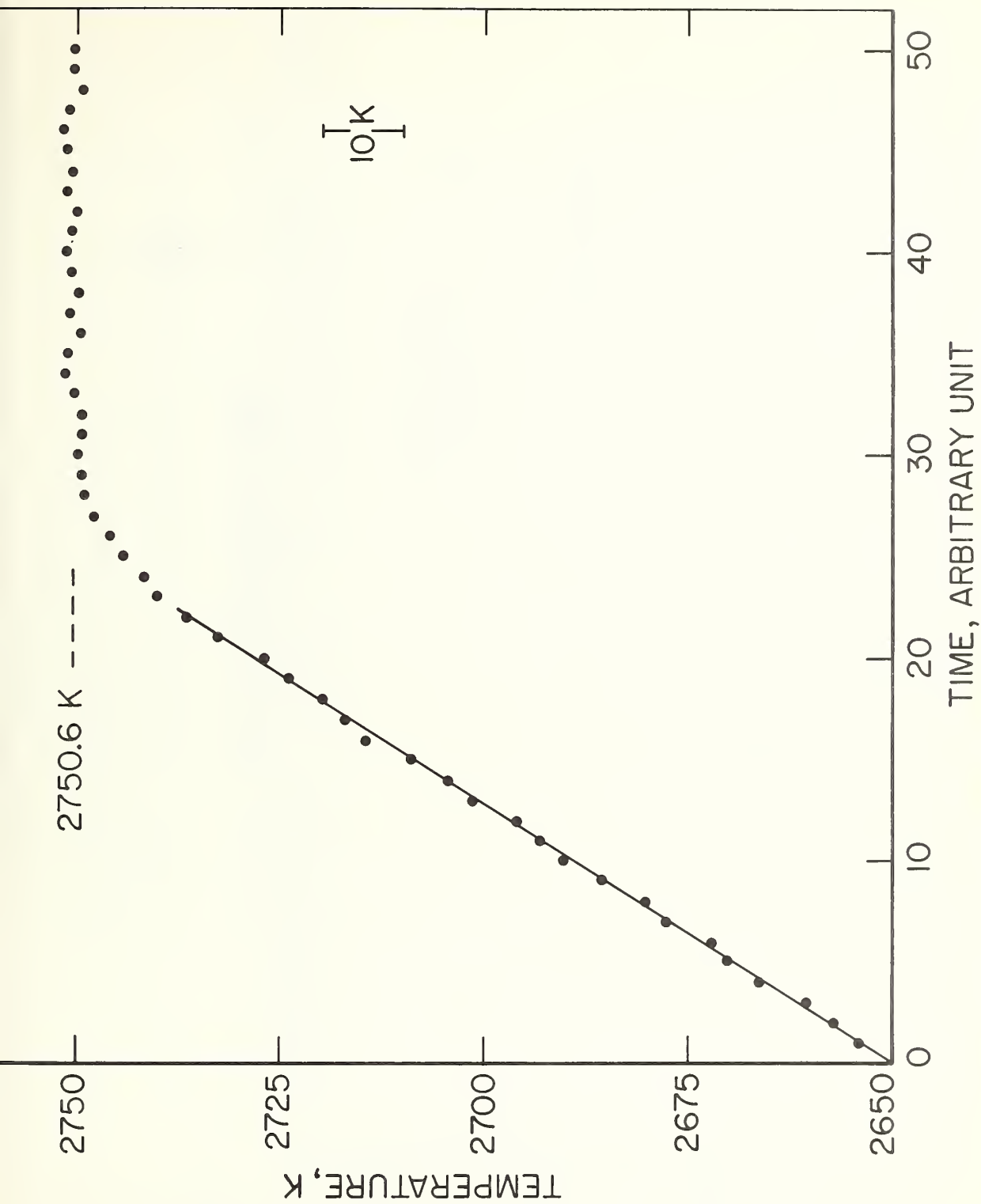
FIG. 1. Variation of temperature of niobium (niobium-1) as a function of time near and at the melting point. (1 time unit = 0.833 ms).
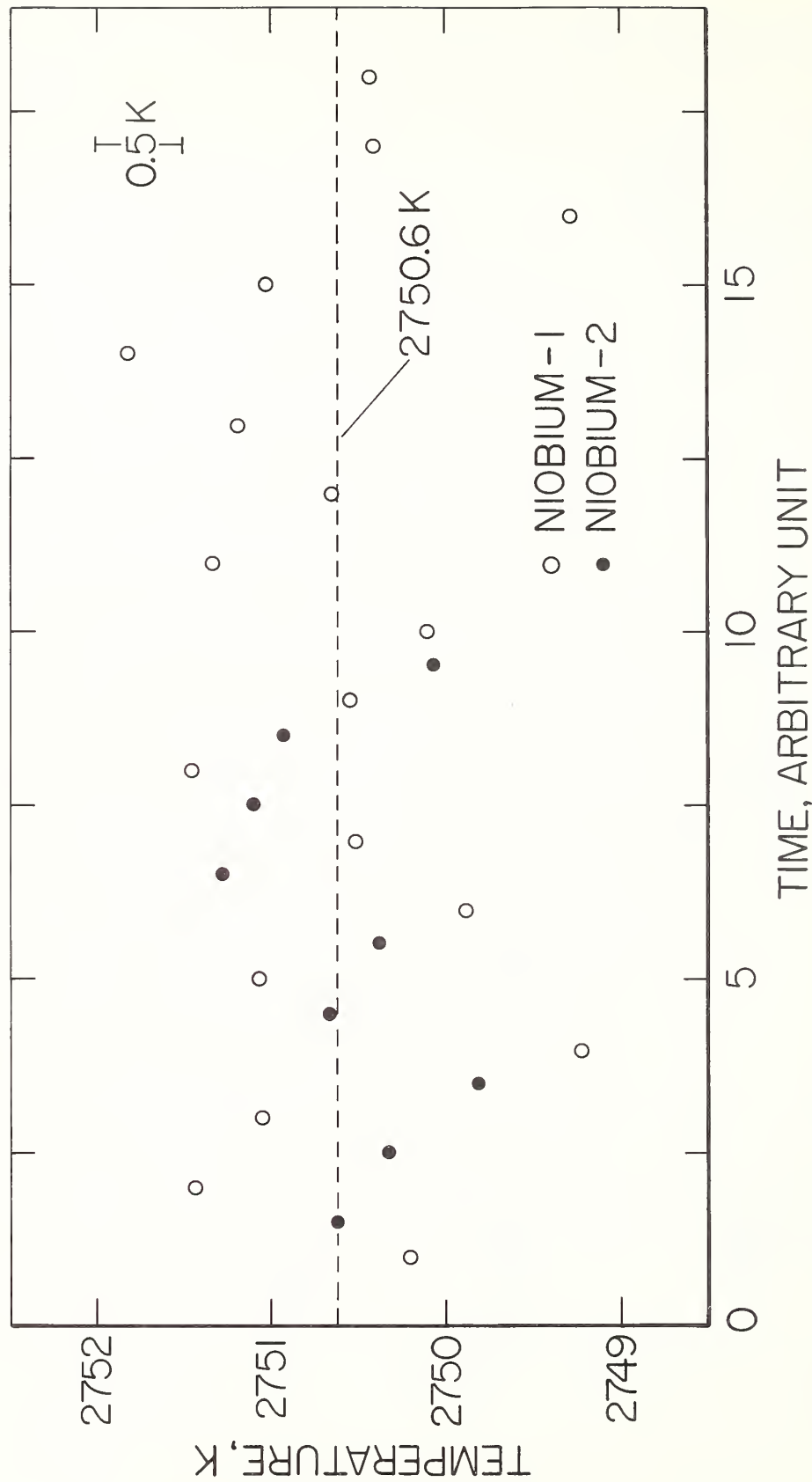
FIG. 2. Variation of temperature of niobium (niobium-1 and niobium-2) as a function of time at the melting point. (1 time unit = 0.833 ms).
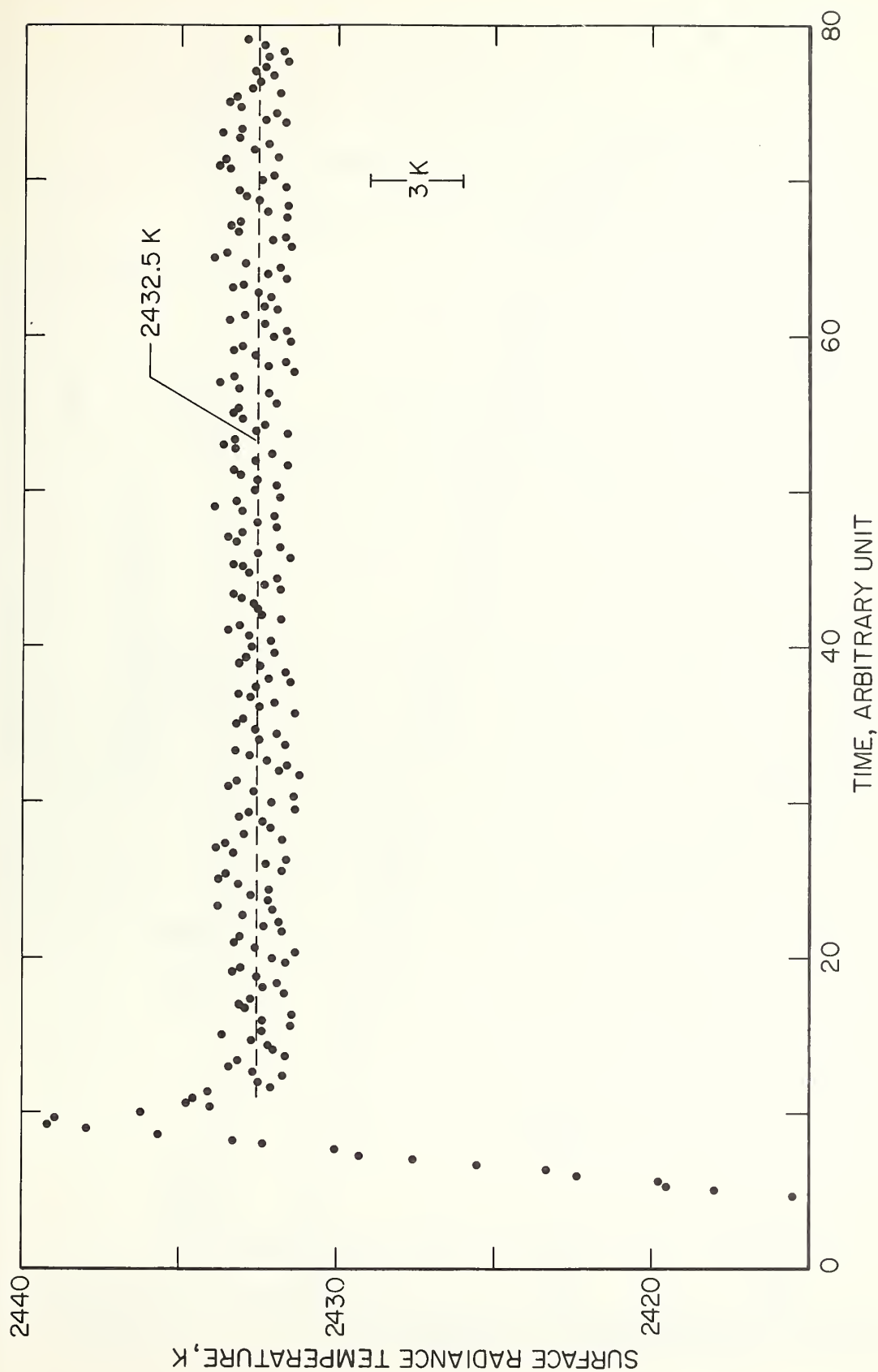
FIG. 3. Variation of surface radiance temperature of niobium (niobium-3) as a function of time near and at the melting point. (1 time unit = 2.5 ms).
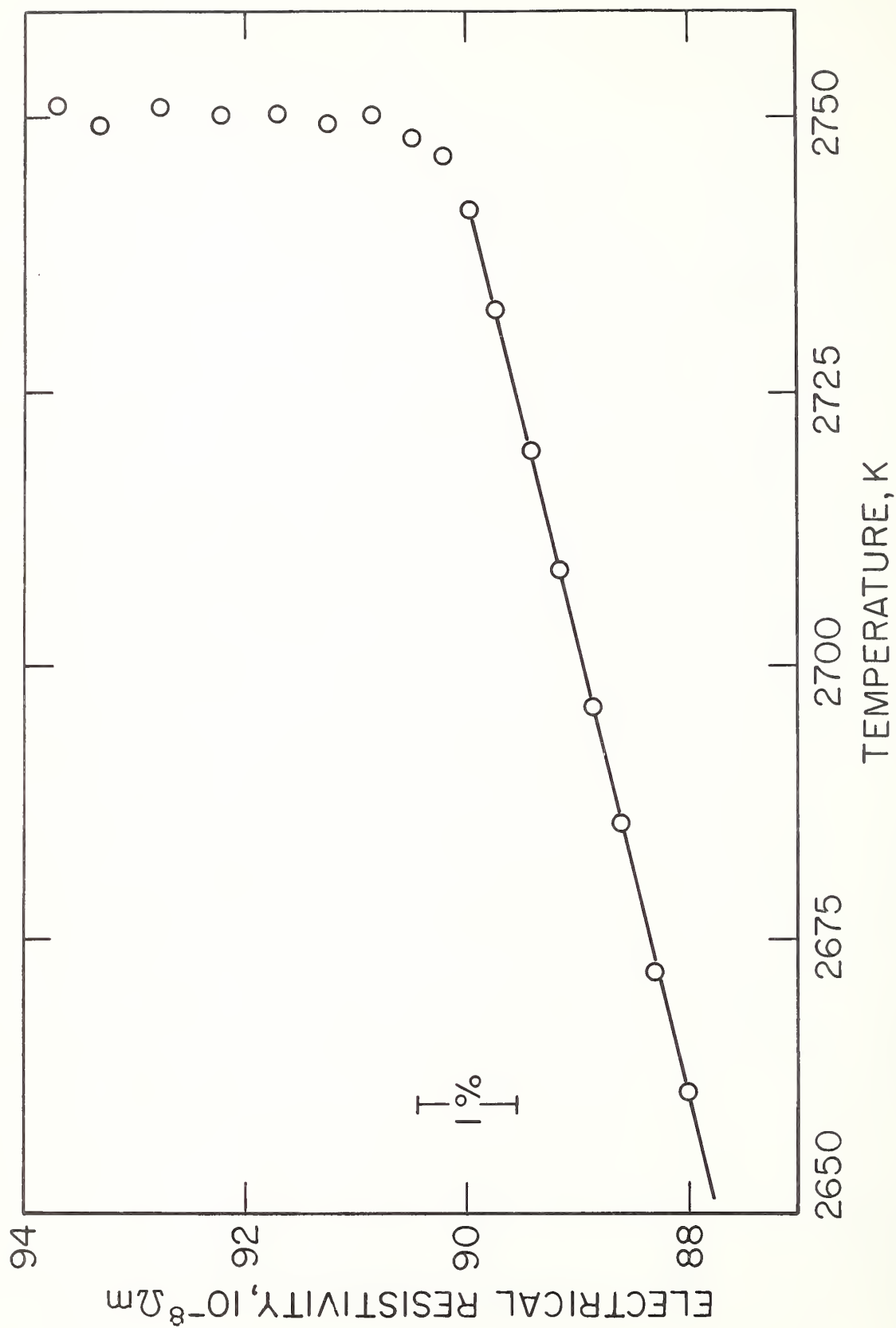
FIG. 4. Variation of electrical resistivity of niobium (niobium-1) as a function of temperature near and at the melting point.

Chapter 9

A PULSE HEATING TECHNIQUE FOR
THE MEASUREMENT OF HEAT OF FUSION OF
METALS AT HIGH TEMPERATURES*

A. Cezairliyan

National Bureau of Standards

Washington, D. C. 20234

A pulse heating technique was developed earlier for the measure-
ment of selected thermophysical properties (specific heat, electrical
resistivity, and hemispherical total emittance) of electrically con-
ducting substances at high temperatures. In this paper a preliminary
experiment (on niobium) is described which demonstrates the feasibility
of extending the technique to the measurement of heat of fusion of metals.

The method is based on rapid resistive self-heating of a composite specimen by the passage of high currents through it, and measuring the pertinent quantities as a function of time. The details of the measurement system and its operational characteristics may be found in an earlier publication [1].

The composite specimen (Figure 1) was made of three strips, each having the following nominal dimensions: length, 75 mm; width, 6.3 mm; and thickness 0.25 mm. The middle strip was niobium, and the two outer strips were tantalum. The specimen was pulse heated from room temperature to approximately 200 K above the melting point of niobium in 0.8 s. During the heating period, current through the composite specimen, potential drop across the composite specimen, and surface radiance temperature of the outer strip were measured every 0.4 ms. Potential measurements were made across the middle 25 mm portion of the specimen using spring-loaded knife-edge probes. Temperature was measured with a high-speed photoelectric pyrometer [2].

Variation of surface radiance temperature of the tantalum strip as a function of time is shown in Figure 2. The plateau corresponds to melting of the inner strip (niobium). When niobium reached a temperature approximately 200 K above its melting point, heating was stopped by automatically switching off the current. Since the melting point of tantalum is approximately 500 K higher than that of niobium, the outer strips did not melt during the entire experiment and acted as a container for niobium. At the end of the experiment (after the specimen cooled down to room temperature), it was observed that the entire specimen had retained its original geometry and weight.

136

The heat of fusion of niobium was computed using the following equation:

$$Q_f = ei \, \triangle t - Q_r - Q_s$$

where

Q_f = heat of fusion

e = potential drop across the specimen

i = current through the specimen

$\triangle t$ = duration of plateau, t_2-t_1 in Figure 2

Q_r = heat loss due to thermal radiation

Q_s = energy absorbed by two outer strips during melting of niobium

The quantity $\triangle t$ was obtained from the points of intersaction of polynomial functions (obtained by the least squares method) representing temperature versus time data in premelting, melting, and postmelting periods of niobium. Standard deviation of an individual point from the function was 0.7 K for premelting and postmelting regions, and 0.9 K for the melting region. Heat loss by thermal radiation, Q_r, was determined from data obtained during the radiative cooling period following the rapid heating period. The correction Q_s was necessitated as the result of the existing 5 K difference between the temperatures at the beginning and the end of the plateau.

137

The results of computations using the experimental data indicate that energy imparted to the specimen (ei Δt) was 145.1 J, energy radiated (Q_r) was 47.5 J, and energy absorbed by the two outer strips (Q_s) was 1.5 J. The above yield 96.1 J for energy absorbed during melting, which corresponds to a value of 26,900 J mol^{-1} for the heat of fusion of niobium. In the computations the atomic weight of niobium was taken as 92.91. If one considers that the melting point of niobium is 2750 K [3], entropy of fusion becomes 9.80 J $mol^{-1}K^{-1}$ (2.34 cal $mol^{-1}K^{-1}$).

The only other experimental results on the heat of fusion of niobium were those reported by Margrave [4], and more recently by Sheindlin et al. [5]. Both investigations utilized the lavitation calorimetry technique. A summary of the results is given in Table 1. It may be seen that the result of the present work agrees, within 2.6%, with that of Sheindlin et al. However, the value reported by Margrave is considerably higher than the value given both in the present work (by 23%) and by Sheindlin et al. (by 20%).

The present preliminary investigation has demonstrated that the millisecond resolution transient technique shows considerable promise in measuring heat of fusion of electrically conducting substances at temperatures above 2000 K where other more conventional techniques encounter serious difficulties. However, additional work, both mathematical and experimental, is required to assess the reliability and the accuracy of the technique.

138

TABLE 1

Heat of fusion of niobium reported in the literature

Investigator	Ref.	Year	Heat of Fusion		Melting Point K	Entropy of Fusion	
			cal mol^{-1}	J mol^{-1}		cal mol^{-1}K^{-1}	J mol^{-1}K^{-1}
Margrave	4	1970	7,900	33,050	2740	2.88	12.1
Sheindlin et al.	5	1972	6,600	27,600		2.41	10.1
Present work			6,430	26,900	2750	2.34	9.8

References

[1]   Cezairliyan, A., Design and operational characteristics of a
       high-speed (millisecond) system for the measurement of thermo-
       physical properties at high temperatures, J. Res. Nat. Bur.
       Stand. (U.S.), 75C (Eng. and Instr.), 7 (1971).

[2]   Foley, G. M., High-speed optical pyrometer, Rev. Sci. Instr.,
       41, 827 (1970).

[3]   Cezairliyan, A., Measurement of melting point, normal spectral
       emittance (at melting point), and electrical resistivity (above
       2650 K) of niobium by a pulse heating method, High Temperatures-
       High Pressures, to be published.

[4]   Margrave, J. L., Thermodynamic properties of liquid metals,
       High Temperatures-High Pressures, 2, 583 (1970).

[5]   Sheindlin, A. E., Berezin, B. Ya., and Chekhovskoi, V. Ya.,
       Enthalpy of niobium in solid and liquid states, High Temperatures-
       High Pressures, to be published.
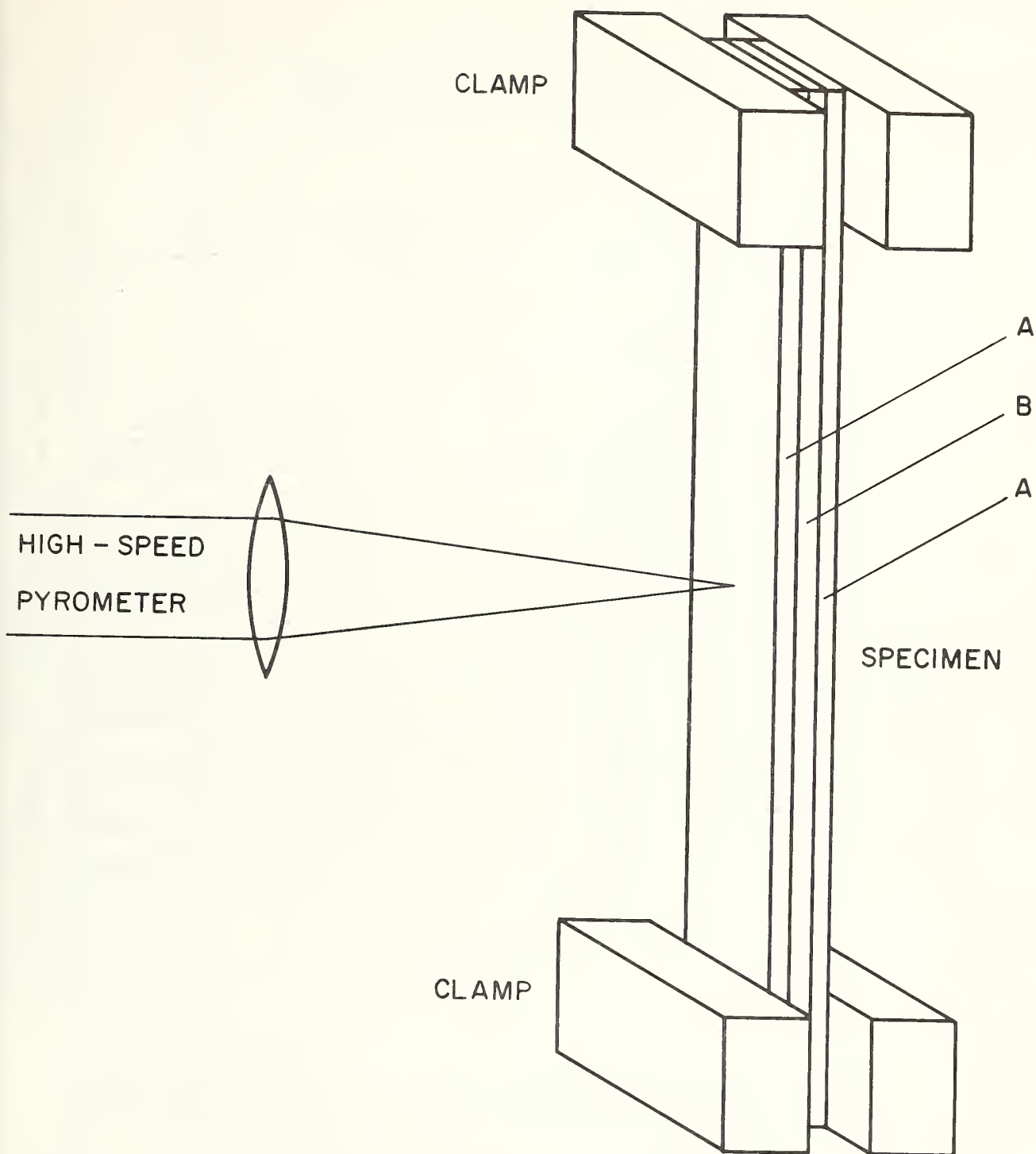
Figure 1. Schematic diagram showing the arrangement of the composite specimen, clamps, and surface radiance temperature measurement system (dimensions are not to scale). Strip of material "B" is sandwiched between two strips of material "A". The melting point of "B" is lower than that of "A".

141

Figure 2.   Variation of surface radiance temperature of a composite specimen, similar to that shown in Figure 1, as a function of time during its heating period. The inner strip is niobium and the two outer strips are tantalum. The plateau corresponds to melting of niobium. One time unit is 0.833 ms.

142

Chapter 10

APPLICATION OF A PULSE HEATING TECHNIQUE TO PRELIMINARY INVESTIGATIONS OF SOLID-SOLID PHASE TRANSFORMATIONS AT HIGH TEMPERATURES*

A. Cezairliyan and J. L. McClure
National Bureau of Standards
Washington, D. C.   20234

Abstract

Preliminary results of an experiment concerning the $\gamma \to \delta$ phase transformation in iron demonstrate the feasibility of applying a high-speed pulse heating technique to the study of high temperature solid-solid phase transformations in electrically conducting substances. The variations of surface radiance temperature as a function of time and the electrical resistivity as a function of surface radiance temperature clearly show the phase transformation. The surface radiance temperature of iron at the transformation point is 1561 K. Electrical resistivity shows an increase of approximately 0.3% during the phase transformation.

A millisecond resolution pulse heating technique was developed in connection with the measurement of selected thermophysical properties of electrical conductors at high temperatures [1]. This technique has recently been applied to measurements of the melting point and the normal spectral emittance at the melting point of selected metals [2, 3, 4].

This paper describes an experiment which was conducted to demonstrate the feasibility of applying the same technique to a study of solid-solid phase transformations. A preliminary investigation of the phase transformation ($\gamma \rightarrow \delta$) in iron, that occurs at approximately 1675 K, is reported. Approximate determinations of the transformation temperature, the normal spectral emittance at the melting point, and the electrical resistivity above 1600 K are also reported.

The high-speed technique is based on rapid resistive self-heating of the specimen from room temperature to its melting point. During an experiment, which lasts less than one second, the current through the specimen, the potential across the specimen, and the specimen temperature are measured as functions of time and recorded with a digital data acquisition system which has a full-scale signal resolution of one part in 8,000 and a time resolution of 0.4 ms. Temperature measurements are made with a high-speed photoelectric pyrometer [5]. Details regarding the construction and operation of the measurement system are given in an earlier publication [6].

Iron was chosen for this study because it has a high temperature phase transformation (approximately at 1675 K). A lower temperature

phase transformation in iron (approximately at 1185 K) could not be studied because of pyrometric limitations.

The experiment was conducted on an iron specimen of 99.9% purity. The specimen was a rod of the following nominal dimensions: length, 76 mm; and diameter, 3.2 mm. The surface was polished to reduce radiation losses. The specimen was used for only one experiment, in which it was heated from room temperature to its melting point. It was not possible to conduct a series of experiments on the same specimen in the vicinity of the transformation point, because of the distortions in the specimen resulting from volume changes that accompany the phase transformations. Using the recorded data, surface radiance temperature was plotted as a function of time and electrical resistivity was obtained as a function of surface radiance temperature.

Figure 1 shows the heating curve for the specimen. The solid-solid phase transformation is clearly evident as a temperature arrest or plateau in the heating curve (the plateau on the left). There were 22 temperature measurements during the transformation which were averaged to give a surface radiance temperature at the transformation point of 1561 K. The standard deviation of the individual points from the average is 0.7 K. The heating rate just below the plateau was approximately 1300 K s^{-1}.

The second plateau in Figure 1 (the plateau on the right) shows the melting of the iron specimen. The average surface radiance temperature at the melting point is 1667 K. The standard deviation from the average is 0.6 K.

The resistivity of the specimen was calculated using the relation $\rho = RA/L$ where R is the resistance, A the cross-sectional area, and L the length of the specimen between the potential probes. Dimensions were based on their room temperature values. The results for resistivity of iron are shown in Figure 2. The resistivity is clearly discontinuous at the transformation. During the transformation it increased by approximately 0.3%.

The melting point data was used to compute an approximate value for the normal spectral emittance of iron at the melting point. Based on the Wien radiation equation, the relation between emittance and temperature is

$$\epsilon = \frac{1}{\exp\left[\frac{c_2}{\lambda}\left(\frac{1}{T_s} - \frac{1}{T_m}\right)\right]}$$

(1)

where ϵ is the normal spectral emittance, T_m the melting point, T_s the surface radiance temperature at the melting point, c_2 the second radiation constant (1.4388 x 10^{-2} m K) and λ the effective wavelength of the optical system. The measurements were made at 650 nm, which is the effective wavelength of the interference filter of the pyrometer. The bandwidth of the filter is 10 nm.

The generally accepted melting temperature of iron is 1810 K [7]. When this value and the observed surface radiance temperature at the melting point are substituted into Equation (1), the normal spectral emittance is computed to be 0.352. If it is assumed that this value can approximate the normal spectral emittance at the transformation

146

temperature, an approximate true temperature can be obtained for the transformation point. This method yields a transformation temperature of 1685 K which is 10 K higher than the accepted value. A higher value is to be expected in this approximation since the normal spectral emittance at the melting point would have a lower value than that at the transformation point. A normal spectral emittance of 0.38 is required to correct the observed surface radiance temperature at the transformation point to the accepted value.

Using the value of 0.352 for the normal spectral emittance, the resistivities at 1500 K and 1600 K (surface radiance temperatures) were associated with approximate true specimen temperatures (1614 K and 1731 K respectively). The resistivities thus obtained are higher than those of another investigator [8] by about 1.8% at 1614 K and 0.8% at 1731 K.

The preliminary results reported in this paper demonstrate the feasibility of studying solid-solid phase transformations in electrically conducting substances at high temperatures using the high-speed pulse heating technique. The major limitation of this preliminary work was that true specimen temperature could not be obtained directly. In future investigations tubular specimens with blackbody sighting holes will be used in order to obtain true temperature directly. Such studies will yield reliable measurements of the transformation and melting temperatures. It is also possible to obtain the energy of solid-solid phase transformation if the duration of the transformation is accurately determined.

References

1. Cezairliyan, A., M. S. Morse, H. A. Berman, and C. W. Beckett, High-speed (subsecond) measurement of heat capacity, electrical resistivity, and thermal radiation properties of molybdenum in the range 1900 to 2800 K, J. Res. Nat. Bur. Stand. (U.S.) 74A (Phys. and Chem.), 65 (1970).

2. Cezairliyan, A., M. S. Morse, and C. W. Beckett, Measurement of melting point and electrical resistivity (above 2840 K) of molybdenum by a pulse heating method, Rev. Int. Hautes Temper. et Refract. 7, 382 (1970).

3. Cezairliyan, A., Measurement of the variation of normal spectral emittance of tantalum during melting by a pulse heating method, High Temperatures - High Pressures 2, 501 (1970).

4. Cezairliyan, A., Measurement of melting point, normal spectral emittance (at melting point), and electrical resistivity (above 2650 K) of niobium by a pulse heating method, High Temperatures - High Pressures, to be published.

5. Foley, G. M., High-speed optical pyrometer, Rev. Sci. Instr. 41, 827 (1970).

6. Cezairliyan, A., Design and operational characteristics of a high-speed (millisecond) system for the measurement of thermophysical properties at high temperatures, J. Res. Nat. Bur. Stand. (U.S.) 75C (Eng. and Instr.), 7 (1971).

7. Schofield, T. H., and A. E. Bacon, The melting point of titanium,
    J. Inst. Metals 82   , 167 (1953 – 1954).

8. Kollie, T. C., private communication.
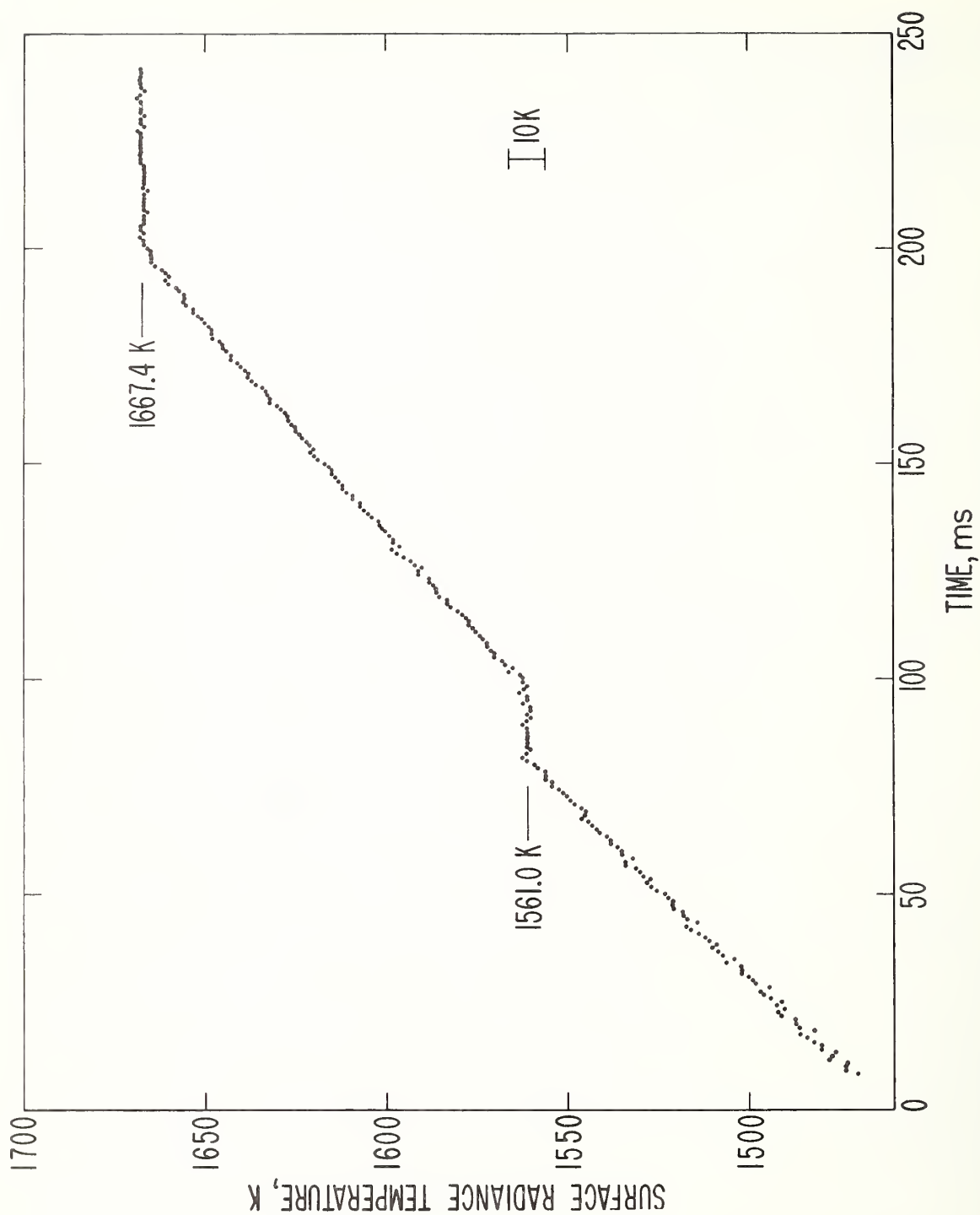
Figure 1. Heating curve showing the solid-solid phase transformation

($\gamma \rightarrow \delta$) and the melting point in iron.
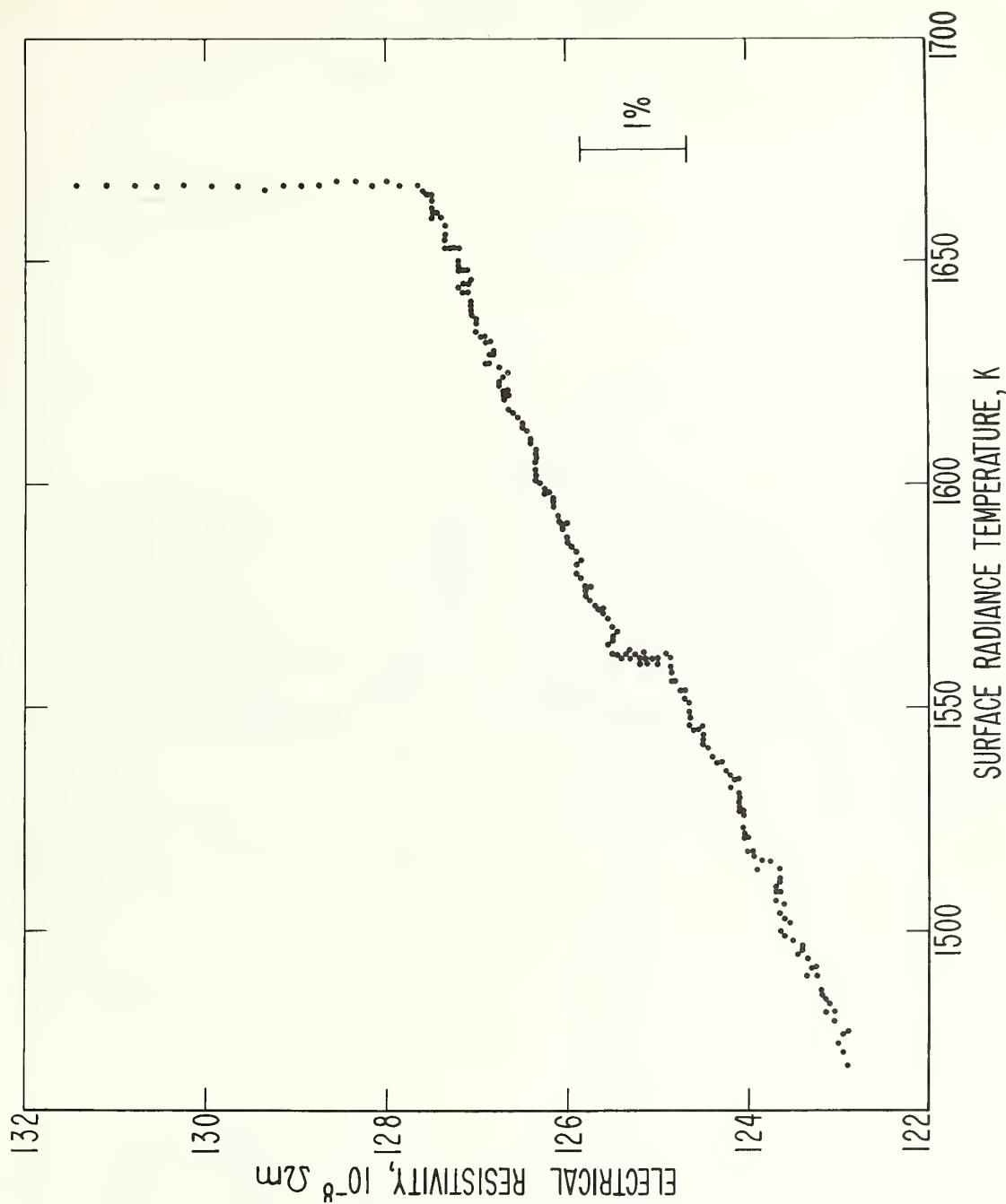
Figure 2. Variation of electrical resistivity of iron as a function
of surface radiance temperature showing the behavior at
$\gamma \rightarrow \delta$ transformation and the melting point.

Chapter 11
RATE CONSTANTS FOR THE REACTIONS
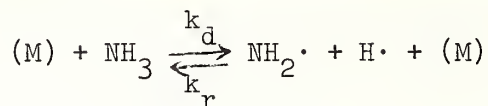
$$(M) + NH_3 \underset{k_r}{\overset{k_d}{\rightleftharpoons}} NH_2\cdot + H\cdot + (M)$$

W. Tsang

ABSTRACT

Data for the reactions $NH_3 + (M) \underset{k_r}{\overset{k_d}{\rightleftharpoons}} NH_2\cdot + H\cdot + (M)$ have been critically examined and tabulated. A best fit of the data appears to require active external rotations. Suggested rate constants of these reactions over the range $0 - 10^2$ atm and 200–4000°K are tabulated.

1. Summary of Experimental Data

$$NH_3 \overset{k_d}{\underset{k_r}{\rightleftarrows}} NH_2\cdot + H\cdot$$

(M)	NH_3	$NH_2\cdot$	$H\cdot$	(M)
$\Delta H_f(300)$	-10.98	45.5 ^{IIc}	52.1	kcals/mol
$S(300)$	46.09	46.54	27.42	cals/mol°K
$Cp(300)$	8.53	8.02	4.97	cal/°K
$Cp(1000)$	13.47	10.18	4.97	cal/°K
$Cp(3000)$	19.0	13.13	4.97	cal/°K

$\Delta H_R(300)$	108.6	kcals
$S_R(300)$	27.96	cal/°K

I. DIRECT STUDIES

RESULTS

METHOD AND CONDITION

REFERENCE

a. Ammonia decomposition occurs with 3/2 order dependence on NH_3, 1/2 order dependence on Ar concentration. On this basis

$$\frac{d(NH_3)}{dt} = k(NH_3)^{3/2}(Ar)^{1/2}$$

where

$$k = 2.5 \times 10^{13} \exp(-77,700/RT)\, 1/\text{mol sec}$$

Decomposition of 1 and 8% NH_3 in argon behind incident shock at 2000-3000°K ∿1 atm pressure. NH_3 concentration monitored by i-r emission at 2.7-3.2 μ.

T. A. Jacobs, J. Phys. Chem. <u>67</u>, 685 (1963).

b. First order rate constants are linearly dependent on argon pressure. Bimolecular rate expression for total NH_3 disappearance

$$k_d^1 = 10^{12.60} \exp(-83,000/RT)\, 1/\text{mol sec}$$

where $\dfrac{d(NH_3)}{dt} = k_d^1(NH_3)(A)$

Decomposition of 5-20% NH_3 in argon behind incident shock at 2000-3000°K. .08-.6 atm pressure. NH_3 concentration monitored by i-r emission at 3 μ.

J. N. Bradley, R. N. Butler and D. Lewis, Trans. Faraday Soc. <u>63</u>, 2962 (1967).

153

c. Assuming 1st order dependence on argon and NH_3

$k_d^1 = 10^{12.36} \exp(-71,100/RT)$ l/mol sec

Decomposition of 1% NH_3 mixture in argon behind reflected shock wave at 2500-3000°K and ~7 atm concentration monitored by u.v. absorption at 2245 A.

T. Takeyama, H. Miyama, Bull. of the Chemical Society of Japan 39, 2352 (1966).

d. 1st order rate constants are independent of NH_3 concentration and linearly dependent on total pressure. Bimolecular rate expression is

$k_d^1 = 10^{12.64} \exp(-79,500/RT)$ l/mol cc.

Decomposition of .1%-1% NH_3 in argon behind incident and reflected shocks at 2100-2900°K and 2-20 atm NH_3 concentration monitored by u.v. absorption at 2300 Å.

K. W. Michel and H. Gg Wagner, Tenth Symposium on Combustion, pg. 353, Combustion Institute, Pittsburgh, Pa. (1963).

II. INDIRECT STUDIES

RESULTS	METHOD AND CONDITION	REFERENCE
a. $k_r = 2.1 \times 10^{10}$ l/mol sec	Radiolysis of NH_3 at high does rates. From product analysis and an assumed mechanism, numerical integration of the rate expressions give the desired rate constant 20-250°C 1-5 atm NH_3	A. W. Boyd, C. Willis, O. A. Miller, Can. J. of Chemistry 49, 2283 (1971).
b. $k_r = 12 \times 10^{10}$ l/mol sec (1000 mm) $= 4.2 \times 10^{10}$ l/mol sec (500 mm) $= 2.9 \times 10^{10}$ l/mol sec (250 mm)	Pulse radiolysis of NH_3 at 250-1500 mm Hg and room temperature. Amino radical disappearance measured directly from decrease in absorption at 5976 Å.	S. Gordon, W. Mulac, and P. Nangia, J. Phys. Chem. 75, 2087 (1971).
c. $\Delta H_f(NH_2 \cdot) = 45.5$ at 300°K.	Analysis of kinetic results on hydrozene decomposition.	W. Tsang, Rate Constants for the Reaction $N_2H_4 \rightleftharpoons 2NH_2$, (earlier report).

154

2. Comments on Experimental Data

Ia) The data analysis involve a best fit of the onccentration time traces with the integrated rate expression. Unfortunately no provision has been made for reaction endothermicity. This will be especially serious for the 8% runs and a decrease in temperature of several hundred degrees during the course of the reaction must be expected. This may account for the apparent $3/2^{\text{th}}$ order dependence on NH_3 concentration. Due to the possibility of large errors in reaction temperature, the uncertainty of these results may well be as much as a factor of ten.

Ib) Reactions are carried out at very high NH_3 concentrations. Although initial rates are used, the published traces suggest that the first measurable point occurs no less than 100 μsecs after the passage of the shock wave. Thus, considerable reaction must have occurred and as in Ia the true reaction temperature is probably much lower than calculated. This will be most serious at higher temperatures (large conversions). Estimated uncertainty is about an order of magnitude.

Ic) The use of the reflected shock may cause problems in defining reaction temperature.[2] An induction period is observed at lower temperatures ($<2400°K$). Rates were determined from higher temperature experiments. The estimated uncertainty is about a factor of 5.

Id) This should be the most reliable of the direct studies. Unfortunately the authors do not present sufficient data so as to permit a more detailed analysis. The estimated uncertainty is a factor of 3.

155

IIa) This must be considered a rough estimate. The number is dependent not only on the correctness of the mechanism but also on a whole string of other rate constants whose values are uncertain.

IIb) This number may be a satisfactory upper limit, as in all such experiments the reliability is dependent on the postulated mechanism. In the present case it is assumed that equivalent amounts of NH_2 and H radicals are formed and that subsequently the important processes are

$$NH_2 \cdot + NH_2 \cdot \quad \rightarrow H_2H_4$$
$$H \cdot + H \cdot + (M) \quad \rightarrow H_2 + (M)$$

and $NH_2 \cdot + H \cdot + (M) \rightarrow NH_3 + (M)$
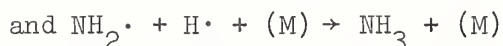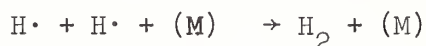
Even after accepting the mechanism the reported number is dependent to a considerable extent on the rate constants for the other two processes. A particularly disturbing fact is the detection of NH radicals. Thus, the true mechanism may be more complex. Furthermore, each NH radical suggests the presence of 2 additional H-atoms as well as serve as a sink for active specie.

3. Discussion

The data from Ia,b,c,d are plotted in Figure I. In view of the large estimated uncertainties, the agreement is very satisfactory. It appears that within the temperature range 2000-3000°K, the bimolecular rate constant for NH_3 decomposition in argon can be considered to be well established. Note that in plotting the data we have set the true bimolecular rate to be one-half the measured rate constant for NH_3 disappearance since under the reaction conditions the processes

156

$$(M) + NH_3 \xrightarrow{k_d} NH_2 \cdot + H \cdot + (M)$$

$$H \cdot + NH_3 \longrightarrow H_2 + NH_2 \cdot$$
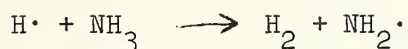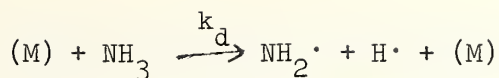
must be concurrent. We have also converted the data of Ia so that it reflects a first order order dependence in ammonia and argon.

The problem that remains is to project these numbers into other temperature ranges. Note that the experimental activation energies are all lower than the bond energy. This is expected since with increasing temperature more internal degrees of freedom become activated. Thus, linear extrapolation of the standard Arrhenius plot will lead to gross errors. Our approach is to calculate the bimolecular rate constant on the basis of the expression

$$k_d = \frac{\lambda Z}{Q} \int_{\Delta E_0^o}^{\infty} N(E) e^{-E/RT} dE \qquad (3)$$

where λ is the transmission coefficient and is usually set as 1, although for the present purposes we will use it as a temperature independent adjustable parameter; Z collision numbers (for NH_3 we use collision diameter = 4 Å); $N(E)$, the density of vibrational and rotational states at energy E; Q, the partition function for the molecule, and ΔE_0^o, the energy change for the reaction at 0°K. In this approach the vibrations and external rotations are taken as fully coupled. This is contrary to the most common practice and indeed there are angular momentum constraints against complete coupling. The present approach is purely empirical in that for other similar systems[4] agreement with regard to the shape of the log k vs 1/T plots is improved using active external rotations. For $N(E)$ we use the Laplace Transform technique. A complete discussion of this and

157

other techniques for computing the density of states and the ranges of validity can be found in a recent review[5].

The results of such a computation suing an argon efficiency of .136[6] and $\lambda = \sim.27$ (in order to obtain the best fit) can be seen in Figure I. For completeness we have also plotted the results of a computation using $\lambda = 1$ and all external rotations inactive. These are the most commonly used assumptions and it can be seen that this reproduces the data with almost equal facility. On the other hand it has a somewhat stronger temperature dependence. However, with neither model can we reproduce the experimental activation energy exactly. It is suspected that this is an experimental artifact. Jacobs (Ia) has discussed the possibility of O_2 impurities affecting the shock tube results while Takeyama et al (Ic) mentions the presence of an induction period at lower temperatures. All of these factors will tend to lower the experimental activation energy. In any case the discrepancies are all within the uncertainty limits. Note that these results are not sufficiently sensitive as to shed any light on the current controversy on the heat of formation of NH_2(IIc).

On this basis recommended bimolecular and termolecular rate constants, for ammonia dissociation and amino and H atom combination, respectively, in the temperature range 200-4000°K are summarized in Table I. The estimated uncertainty is about a factor of 5. Note that the numbers refer to NH_3 as the third body. For other third bodies data from the dissociation of NO_2Cl[7] and the isomerization of CH_3NC[6] are summarized in Table II.

The data for the bimolecular combination process are not directly related to the termolecular process since the former is dependent on

158

the structure of the transition state. It does permit an estimate
to be made of the range of validity of the data in Table I. On the
basis of RRKM calculations with external rotations inactive we are not
able to reproduce either the rate constants or the pressure dependence
derived by Gordon and coworkers (IIb). With external rotations
active (for both the transition state and normal molecule) a very
satisfactory fit can be achieved. Details may be found in Tables III
and IV. In view of our earlier analysis of the recombination results
it is difficult to draw definitive conclusions with regard to this fit.
Further experiments are needed. In any case it is clear that over
most accessible temperature and pressure ranges the data in Table I
are valid. At 1 atm or higher and at sufficiently low temperatures
deviations can be expected and recourse must be made to the numbers
of Table IV.

References

1. D. R. Stull and H. Prophet, JANAF Thermochemical Tables NSRDS-NBS 37, U. S. Government Printing Office, Washington, D. C. 20406

2. R. L. Belford and R. Strehlow, Ann. Ref. of Phys. Chem., pg. 247 Palo Alto, California 94306.

3. W. Forst, J. Phys. Chem. $\underline{76}$, 342 (1972).

4. W. Tsang, unpublished results.

5. W. Forst, Chemical Review $\underline{71}$, 339 (1971).

6. S. C. Chan, B. S. Rabinovitch, J. Bryant, L. D. Spicer, T. Fujimoto, Y. N. Lin, and S. D. Pavlou, J. Phys. Chem. $\underline{74}$, 3160 (1970).

7. H. S. Johnston, Gas Phase Reaction Rate Theory, pg. 295, Ronald Press, New York (1966).

Table I

Recommended Rate Constants for the Decomposition of
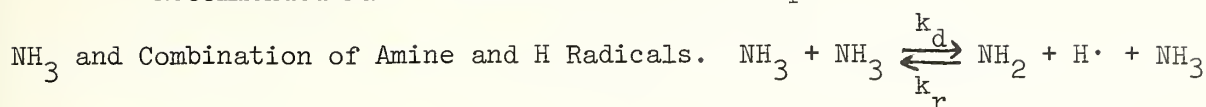
NH_3 and Combination of Amine and H Radicals. $NH_3 + NH_3 \underset{k_r}{\overset{k_d}{\rightleftarrows}} NH_2 + H\cdot + NH_3$

Temperature	Rate Constant Decomposition L/mole-sec (k_d)	Rate Constant Combination L^2/mole^2 sec (k_r)
200	5.5×10^{-102}	1.1×10^{13}
300	1.5×10^{-62}	4.6×10^{12}
400	7.6×10^{-43}	3.3×10^{12}
500	4.8×10^{-31}	2.6×10^{12}
600	3.3×10^{-23}	2.2×10^{12}
700	1.3×10^{-17}	1.9×10^{12}
800	1.8×10^{-13}	1.6×10^{12}
900	3.1×10^{-10}	1.4×10^{12}
1000	1.1×10^{-7}	1.3×10^{12}
1200	7.5×10^{-4}	1.0×10^{12}
1400	3.7×10^{-1}	8.1×10^{11}
1600	$3.7 \times 10^{+1}$	6.6×10^{11}
1800	$1.2 \times 10^{+3}$	5.4×10^{11}
2000	2.0×10^{4}	4.5×10^{11}
2200	1.8×10^{5}	3.7×10^{11}
2400	1.1×10^{6}	3.1×10^{11}
2600	5.1×10^{6}	2.6×10^{11}
2800	1.8×10^{7}	2.2×10^{11}
3000	5.4×10^{7}	1.9×10^{11}
3200	1.4×10^{8}	1.6×10^{11}

Table I (continued)

Temperature	Rate Constant Decomposition L/mole-sec (k_d)	Rate Constant Combination L^2/mole^2 sec (k_r)
3400	3.1×10^8	1.4×10^{11}
3600	6.2×10^8	1.2×10^{11}
3800	1.1×10^9	1.0×10^{11}
4000	2.0×10^9	8.9×10^{10}

Table II: Third body efficiencies from (a) decomposition of NO_2Cl[7]

(b) isomerization of CH_3NC[6]

(a)				(b)		
He	.25			He	.171	
Ne	.18			Ne	.120	
Ar	.21			Ar	.136	
Kr	.21			Kr	.115	
H_2	.34			D_2	.23	
N_2	.29			N_2	.21	
O_2	.26			SF_6	.42	
CO_2	.39			H_2	.28	
SF_6	.36			CD_4	.41	
				CH_4	.44	
				C_2H_6	.56	
				C_2H_4	.43	
				C_3H_6	.60	
				C_3H_8	.62	
				$C_6H_5CH_3$	.80	

a) Transition state is assumed to have same geometrical structure
    as molecules.

b) Collision diameter is $4\overset{\circ}{A}$.

c) Vibrational frequencies for the molecules are 3400(3),
    1620(2), 960(1).

d) Vibrational frequencies for the transition states are 3200(2)
    1500(1) 40(2)

e) All external rotations are active.

f) Transmission coefficient = .27.

Table IV

Recommended rate constants for the unimolecular decomposition of ammonia and the bimolecular combination of amino and H radicals

$$NH_3 \xrightleftharpoons[k(COM)]{k(DEC)} NH_2 + H\cdot$$
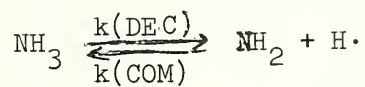
(Table is on pages 166-168.)

TEMPERATURE IS 200 K
A.R.T. A-FACTOR IS 1.99578E+14 /SEC
REACTION THRESHOLD IS 107090. CALS
EXPERIMENTAL A-FACTOR IS 2.80918E+15 /SEC(HIGH PRESSURE)
EXPERIMENTAL ACTIVATION ENERGY IS 108028. CALS
                                    (HIGH PRESSURE)
HIGH PRESSURE RATE CONSTANT IS 2.14504E-103 /SEC

PRESSURE	K(DEC)	K(COM)
(MM HG)	(/SEC)	(L/MOL-SEC)
10	4.26018E-105	8.46398E+9
100	3.56205E-104	7.07695E+10
1000	1.37881E-103	2.73937E+11
10000	2.01043E-103	3.99425E+11
100000	2.12939E-103	4.23060E+11
1.00000E+6	2.14343E-103	4.25850E+11

TEMPERATURE IS 300 K
A.R.T. A-FACTOR IS 6.08735E+14 /SEC
REACTION THRESHOLD IS 107090. CALS
EXPERIMENTAL A-FACTOR IS 9.23941E+15 /SEC(HIGH PRESSURE)
EXPERIMENTAL ACTIVATION ENERGY IS 108598. CALS
                                    (HIGH PRESSURE)
HIGH PRESSURE RATE CONSTANT IS 6.38718E-64 /SEC

PRESSURE	K(DEC)	K(COM)
(MM HG)	(/SEC)	(L/MOL-SEC)
10	7.38098E-66	2.31121E+9
100	6.44338E-65	2.01762E+10
1000	2.97327E-64	9.31021E+10
10000	5.33263E-64	1.66981E+11
100000	6.20595E-64	1.94327E+11
1.00000E+6	6.36632E-64	1.99349E+11

TEMPERATURE IS 400 K
A.R.T. A-FACTOR IS 1.34539E+15 /SEC
REACTION THRESHOLD IS 107090. CALS
EXPERIMENTAL A-FACTOR IS 2.01165E+16 /SEC(HIGH PRESSURE)
EXPERIMENTAL ACTIVATION ENERGY IS 109127. CALS
                                    (HIGH PRESSURE)
HIGH PRESSURE RATE CONSTANT IS 4.41072E-44 /SEC

PRESSURE	K(DEC)	K(COM)
(MM HG)	(/SEC)	(L/MOL-SEC)
10	2.81390E-46	1.20425E+9
100	2.52642E-45	1.08122E+10
1000	1.33267E-44	5.70336E+10
10000	2.97297E-44	1.27232E+11
100000	4.04467E-44	1.73098E+11
1.00000E+6	4.35924E-44	1.86560E+11

TEMPERATURE IS 500 K
A.R.T. A-FACTOR IS 2.46131E+15 /SEC
REACTION THRESHOLD IS 107090. CALS
EXPERIMENTAL A-FACTOR IS 3.47427E+16 /SEC(HIGH PRESSURE)
EXPERIMENTAL ACTIVATION ENERGY IS 109607. CALS
                                        (HIGH PRESSURE)
HIGH PRESSURE RATE CONSTANT IS 4.01509E-32 /SEC

PRESSURE	K(DEC)	K(COM)
(MM HG)	(/SEC)	(L/MOL-SEC)
10	1.41643E-34	7.69059E+8
100	1.29697E-33	7.04195E+9
1000	7.57384E-33	4.11226E+10
10000	2.05044E-32	1.11330E+11
100000	3.33276E-32	1.80954E+11
1.00000E+6	3.89381E-32	2.11416E+11

TEMPERATURE IS 600 K
A.R.T. A-FACTOR IS 3.97652E+15 /SEC
REACTION THRESHOLD IS 107090. CALS
EXPERIMENTAL A-FACTOR IS 5.19783E+16 /SEC(HIGH PRESSURE)
EXPERIMENTAL ACTIVATION ENERGY IS 110041. CALS
                                        (HIGH PRESSURE)
HIGH PRESSURE RATE CONSTANT IS 4.07327E-24 /SEC

PRESSURE	K(DEC)	K(COM)
(MM HG)	(/SEC)	(L/MOL-SEC)
10	8.20147E-27	5.39678E+8
100	7.61879E-26	5.01336E+9
1000	4.81209E-25	3.16648E+10
10000	1.53136E-24	1.00767E+11
100000	2.95495E-24	1.94444E+11
1.00000E+6	3.82241E-24	2.51525E+11

TEMPERATURE IS 700 K
A.R.T. A-FACTOR IS 5.88693E+15 /SEC
REACTION THRESHOLD IS 107090. CALS
EXPERIMENTAL A-FACTOR IS 7.07347E+16 /SEC(HIGH PRESSURE)
EXPERIMENTAL ACTIVATION ENERGY IS 110434. CALS
                                        (HIGH PRESSURE)
HIGH PRESSURE RATE CONSTANT IS 2.24009E-18 /SEC

PRESSURE	K(DEC)	K(COM)
(MM HG)	(/SEC)	(L/MOL-SEC)
10	2.68023E-21	4.00079E+8
100	2.51724E-20	3.75749E+9
1000	1.69098E-19	2.52413E+10
10000	6.14747E-19	9.17636E+10
100000	1.38447E-18	2.06661E+11
1.00000E+6	2.00257E-18	2.98925E+11

```
TEMPERATURE IS 800   K
A.R.T. A-FACTOR IS  8.17218E+15  /SEC
REACTION THRESHOLD IS 107090. CALS
EXPERIMENTAL A-FACTOR IS 9.01258E+16  /SEC(HIGH PRESSURE)
EXPERIMENTAL ACTIVATION ENERGY IS 110792. CALS
                                      (HIGH PRESSURE)
HIGH PRESSURE RATE CONSTANT IS 4.67917E-14  /SEC


PRESSURE           K(DEC)            K(COM)
(MM HG)            (/SEC)            (L/MOL-SEC)

  10               3.46098E-17       3.07434E+8
  100              3.27844E-16       2.91220E+9
  1000             2.31374E-15       2.05527E+10
  10000            9.38916E-15       8.34027E+10
  100000           2.42155E-14       2.15103E+11
  1.00000E+6       3.92345E-14       3.48515E+11



TEMPERATURE IS 900   K
A.R.T. A-FACTOR IS  1.08018E+16  /SEC
REACTION THRESHOLD IS 107090. CALS
EXPERIMENTAL A-FACTOR IS 1.09472E+17  /SEC(HIGH PRESSURE)
EXPERIMENTAL ACTIVATION ENERGY IS 111118. CALS
                                      (HIGH PRESSURE)
HIGH PRESSURE RATE CONSTANT IS 1.09763E-10  /SEC

PRESSURE           K(DEC)            K(COM)
(MM HG)            (/SEC)            (L/MOL-SEC)

  10               5.20131E-14       2.42257E+8
  100              4.96080E-13       2.31055E+9
  1000             3.64469E-12       1.69755E+10
  10000            1.62095E-11       7.54977E+10
  100000           4.70416E-11       2.19101E+11
  1.00000E+6       8.51002E-11       3.96364E+11



TEMPERATURE IS 1000    K
A.R.T. A-FACTOR IS  1.37397E+16  /SEC
REACTION THRESHOLD IS 107090. CALS
EXPERIMENTAL A-FACTOR IS 1.28277E+17  /SEC(HIGH PRESSURE)
EXPERIMENTAL ACTIVATION ENERGY IS 111415. CALS
                                      (HIGH PRESSURE)
HIGH PRESSURE RATE CONSTANT IS 5.54934E-8   /SEC

PRESSURE           K(DEC)            K(COM)
(MM HG)            (/SEC)            (L/MOL-SEC)

  10               1.73835E-11       1.94458E+8
  100              1.66723E-10       1.86501E+9
  1000             1.26634E-9        1.41656E+10
  10000            6.08389E-9        6.80562E+10
  100000           1.95659E-8        2.18870E+11
  1.00000E+6       3.92909E-8        4.39520E+11
```

168
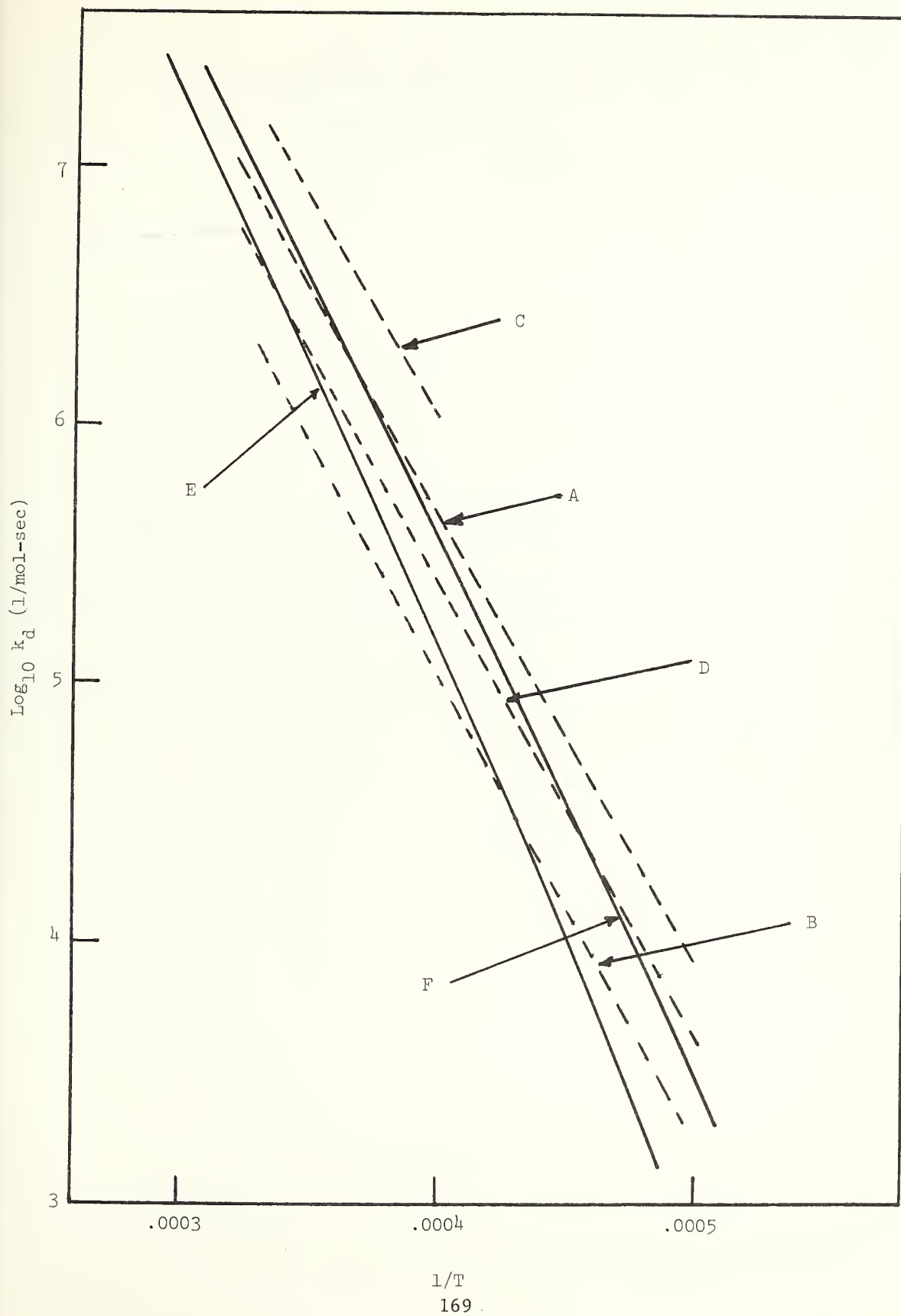
FIGURE 1: Experimental and calculated rate constants for NH_3 decomposition (in argon) (See page 170 for legend.)

Figure 1:   Experimental and calculated rate constants for NH_3
            decomposition (in argon)

Experimental results ----

        (A)   reference Ia

        (B)   reference Ib

        (C)   reference Ic

        (D)   reference Id

Calculated results ----

        (E)   no external rotations, transmission coefficient = 1
            argon efficiency = .136[6]

        (F)   all external rotations active, transmission coefficient =
            .27   argon efficiency = .136[6]

Chapter 12

RATE CONSTANTS FOR THE REACTIONS $(M) + N_2H_4 \underset{k_d}{\overset{k_r}{\rightleftarrows}} 2NH_2{}^{\cdot} + (M)$

W. Tsang

ABSTRACT

Data for the reactions $N_2H_4 + (M) \underset{k_d}{\overset{k_r}{\rightleftarrows}} 2NH_2{}^{\cdot} + M$ have been tabulated and critically examined. These span the range 0.01–200 atm and 300–1600 K. A satisfactory correlation of the data has been made using RRKM unimolecular rate theory. The results are consistent with $\Delta H_f^{300}(NH_2{}^{\cdot}) = 45.5 \pm 1.5$ kcals/mol. This is in marked contrast to the JANAF value of 40.1 kcals/mol. On this basis suggested rate constants for these reactions over the range 10^{-5}–10^2 atm and 200–3000°K are tabulated.

1) Survey of Experimental Data

$$N_2H_4 \underset{k_r}{\overset{k_d}{\rightleftarrows}} 2NH_2\cdot$$

	N_2H_4	$2NH_2\cdot$		
$\Delta H_f(300)$	22.8	40.1 (46)	kcals	(1)
S (300)	57.1	46.5	cals/mol°K	
C_p (300)	12.2	8.0		
C_p (700)	18.9	9.1		
C_p (1000)	23.0	10.2		
C_p (2000)	28.3	12.4		

$$\Delta H_R(300) = 57.4 \ (69.2) \quad \text{kcals}$$
$$\Delta S_R(300) = 35.9 \quad \text{cals/mol°K}$$

I. Direct Studies

Results

a. Assuming first order kinetics, the rate expression for unimolecular decomposition is

$$k_d = 10^{12.6} \exp(-60,000/RT) \text{ sec}^{-1} .$$

A small pressure dependence has been observed but is ignored in data treatment. See analysis of Gilbert (IIa).

Method and Condition

Toluene carrier
Temperature: 894–1057°K
Heating time: .26–1.1 sec.
Composition: .05–.78 mm N_2H_4 in 5–15 mm toluene.

Reference

M. Szwarc, P. R. S. A198, 267 (1949)

172

Results	Method and Condition	Reference

b. A linear dependence between pressure and unimolecular rate constant is observed. Apparent 1st order rate expression is

$$k_d = 10^{11.70} \exp(-54,150/RT) \, sec^{-1}$$

Toluene carrier
Temperature: 887–1034°K
Heating time: ~.5 sec.
Composition: 6–30 mm toluene

J. A. Kerr, R. C. Sekhar, and A. R. Trotman-Dickenson, J. Chem. Soc., 3217 (1963).

c. Under these conditions reaction is in the bimolecular region. The best rate expression for a second order reaction $N_2H_4 + M \rightarrow M + 2NH_2$ is

$$k_d(0) \cong 10^{12.6} \exp(-19,400/RT) \, cc/mol \, sec.$$

Reactions are carried out behind reflected shock wave with T.O.F. mass spectrometer for in situ determination of reactants.
Temperature: 1200–2500°K
Composition: 0.1 to 1% N_2H_4 in .04 to .25 atm Argon.

R. W. Diesen, J. Chem. Phys. 39, 2121 (1963).

d. The rate expression for the unimolecular disappearance of hydrazine is

$$k(N_2H_4) = 10^{12.4} \exp(-50,600/RT) \, sec^{-1}$$

On the basis of the assumed mechanism $k_d = k(N_2H_4)/2$. From the observed half-order pressure dependence

$$k_d(\infty) = 10^{13.0} \exp(-54,000/RT) \, sec^{-1}.$$

Single pulse shock tube
Temperature: 970–1120°K
Heating time: 1–4 msec.
Composition: 1% N_2H_4 in 2.3 to 8.6 atm argon.

E. T. McHale, B. E. Knox, and H. B. Palmer, Tenth Symposium on Combustion (International) pg. 341, The Combustion Institute Pittsburgh, Pa. (1965).

e. The first order rate constant for hydrazine decomposition is given by the expressions

$$k_d \sim 10^{12.8} \exp(-52,000/RT) \, sec^{-1} \quad (10 \, atm)$$
$$k_d \sim 10^{12.0} \exp(-48,000/RT) \, sec^{-1} \quad (3 \, atm)$$

Reactions are carried out behind reflected shock wave. Rate of hydrazine pyrolysis followed by decrease of absorption at 2300 Å.
Temperature: 1100–1600°K
Composition: .03–5% N_2H_4 in 3–10 atm argon.

K. W. Michel, and H. Gg. Wagner, Tenth Symposium on Combustion (International) pg. 353, The Combustion Institute, Pittsburgh, Pa. (1965).

173

Results

f. At low pressures the bimolecular rate for hydrazine decomposition is
$k_d(o) = 10^{15.6} \exp(-41,000/RT)$ cc/mol-sec (1280-1580°K).

At high pressures unimolecular rate is
$k_d(\infty) = 10^{13.9} \exp(-55,000/RT)$ sec^{-1}
RRK calculation has been carried out using rate expression for $k_d(\infty)$ and all the data can be fitted with reasonable accuracy.

II. Indirect Studies

a. Hydrazine flame data and Szwarc's (Ia) toluene carrier results are all compatible with a bimolecular rate expression for hydrazine decomposition of

$$k_d(\text{low pressure}) \cong 10^{19} \exp(-60,000/RT) \text{ cc/mol sec}$$

b. The two limiting models yield
$$k_d(\infty) = 10^{17.8} \exp(-61,200/RT) \text{ sec}^{-1}$$
(1200°K)
$$k_d(\infty) = 10^{16.5} \exp(-60,500/RT) \text{ sec}^{-1}$$
(1200°K)

On this basis all published results are well into the fall-off region.

c. $k_d(\infty) = 10^{16.5} \exp(-70,800/RT)$
$\Delta H_f(300)$ for $NH_2 = 46$ kcals.

Method and Condition

Reactions at low pressures are carried out behind incident shocks while those at high pressures are from reflected shocks N_2H_4 concentration monitored by N_2H_4 absorption at 2300 Å. Temperature: 1110°K-1580°K Composition: .001%–.5% N_2H_4 in .2-300 atm argon.

Analysis of hydrazine flame data and the fluid dynamic properties of the toluene carrier system.

ART calculation assuming transition state structure for hydrazine decomposition 47, 2593 (1969). are similar. Critical energy for decomposition is taken to be 56.8 kcals.

It is assumed that combination rates of nitrogen and carbon radicals are similar and that the extrapolated (to high pressures) rate constants of McHale et. al. (Id) are correct

Reference

E. Meyer, H. A. Olscheusik, J. Troe, and H. Gg. Wagner, Eleventh Symposium on Combustion (International) 345, The Combustion Institute, Pittsburgh, Pa. (1967).

M. Gilbert, Combustion and Flame $\underline{2}$, 137, 149 (1958).

D. W. Setser and W. C. Richardson, Can. J. Chem. 47, 2593 (1969).

S. W. Bensen, H. E. O'Neal, Kinetics Data on Gas Phase Unimolecular Reaction, pg. 34 NSRDS-NBS 21 U. S. Government Printing Office Washington, DC 20402 (1970).

174

Results

Method and Condition

Reference

d. $D(NH_2-H) = 106 \pm 3$ kcals
$\Delta H_f(300)$ for $NH_2 = 43 \pm 3$
Based on appearance potential of NH_2^+ from NH_2 and NH_3.

Electron impact study on the products formed from an electrodeless discharge in hydrazine in a fast flow system.

S. N. Foner and R. L. Hudson, J. Chem. Phys. _29_, 442 (1958).

e. $k_r = 2.33 \times 10^{12}$ cc/mole sec. no pressure dependence.

Photometric determination of NH_2 absorption at 16725.40 Å as a function of time following rf discharge through NH_3. Pressure .425–.850 μ NH_3

M. H. Hanes and E. J. Bair, J. Chem. Phys. _39_, 672 (1963).

f. $k_r = 2.5 \times 10^{12}$ cc/mole sec (limiting high pressure result)

Same as above except 5–10 (mm Hg) NH_3

J. D. Saltzman and E. J. Bair, J. Chem. Phys. _41_, 3654 (1964).

g. $k_r = 6.2 \times 10^{13}$ cc/mole sec

Pulse radiolysis of NH_3 with 2MV electrons at 250–1520 mm. Rate of NH_2 disappearance followed by measurement of decrease in absorption at 5976 Å.

S. Gordon, W. Mulac, and P. Nangia, J. Phys. Chem. _75_, 2087 (1971).

h. Data is compatible with rate expression for benzyl amine decomposition of $k_\infty(\phi CH_2NH_2 \rightarrow \phi CH_2\cdot + NH_2\cdot) = 10^{15.2} \exp(-71,900/RT)$ sec^{-1}. Thus $\Delta H_f(300)$ for $NH = 47.2$ kcal. Predicts $k_d(\infty) = 10^{17.82} \exp(-74,000/RT)$ sec^{-1}.

Very low pressure pyrolysis of benzyl amine.

D. M. Golden, R. K. Solly, N. A. Gac, and S. W. Benson, J. Amer. Chem. Soc. _94_, 363 (1972).

Results	Method and Condition	Reference
i. $k(\phi CH_2NH_2 \to \phi CH_2\cdot + NH_2\cdot) = 10^{13.0}$ $\exp(-59,000/RT)$ sec^{-1}. Using $\Delta H_f^{300}(\phi CH_2\cdot) = 45$ kcals and $\Delta H_f^{300}(\phi CH_2NH_2) = 21.0$ kcals this yields $\Delta H_f^{300}(NH_2) = 36$ kcals	Toluene carrier Thermal decomposition of ben- zyl amine.	J. A. Kerr, R. C. Sekhar, and A. F. Trotman-Dickensen, J. Chem. Soc. 3217, (1963).
j. $k(\phi CH_2NH_2 \to \phi CH_2\cdot + NH_2\cdot) = 10^{12.8}$ $\exp(-59,000/RT)$ sec^{-1}. Using $\Delta H_f^{300}(\phi CH_2\cdot) = 45$ kcals and $\Delta H_f^{300}(\phi CH_2NH_2) = 21$ kcals This yields $\Delta H_f^{300}(NH_2) = 35$ kcals	Toluene carrier Thermal decomposition of ben- zyl amine.	M. Szwarc, Proc. Roy. Soc. A198, 285 (1949).

2) Comments on Individual Studies

Ia. The main decomposition reaction is heterogeneous. Contributions from the homogeneous reaction are deduced from the presence of dibenzyl. Overall mechanism is _assumed_ to be

$$3N_2H_4 \rightarrow N_2 + 4NH_3$$

$$2N_2H_4 \rightarrow H_2 + N_2 + 2NH_3 \qquad \text{heterogeneous}$$

$$N_2H_4 \rightarrow 2NH_2\cdot$$

$$NH_2 + \phi CH_3 \rightarrow NH_3 + \phi CH_2\cdot$$
$$2\ \phi CH_2\cdot \rightarrow (\phi CH_2\cdot)_2 \qquad \text{homogeneous}$$
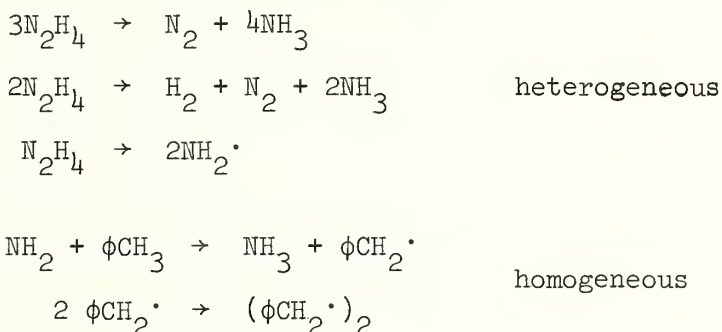
and is supported by stoichiometric checks. Rate constants are determined _assuming_ heterogeneous and homogeneous processes proceed by 1st order kinetics.

Although the measured rate constants are probably accurate to a factor of 2 or 3, it should be noted that practically every set of rate parameters determined by Szwarc (IIc) using this method has turned out to be much lower than the currently accepted number. The causes for such errors are unknown. Furthermore, the small size of the molecule and the low pressures and high temperatures all lead to the conclusion that the reaction is in the 2nd order region. Gilbert (IIa) has demonstrated that this is the case if the fluid dynamics of reactor is taken into account.

Thus, these results are strongly indicative of a N-N bond energy far in _excess_ of 60 kcals.

Ib. Similar experiments as in Ia, except that homogeneous con-
tribution is determined from the production of ammonia, after taking
into account the heterogeneous contribution. The mechanism of Szwarc
(Ia) is assumed. The data treatment involves the subtraction of two
large numbers. Uncertainties are at least as large as for (Ia). Rate
constants and parameters are in excellent agreement with (Ia).

Ic. The use of this technique for quantitative work must be ser-
iously questioned. Reaction conditions are very poorly defined. Rate
constants for hydrazine disappearance are probably no better than
order of magnitude estimates. Rate parameters are only compatible
with extremely low N-N bond energies.

Id. The experimental rate constants are based on the <u>assumed</u>
mechanism.

$$N_2H_4 \xrightarrow{k_d} 2NH_2$$

$$NH_2 + N_2H_4 \rightarrow NH_3 + N_2H_3\cdot$$

$$N_2H_3\cdot + NH_2 \rightarrow NH_3 + N_2 + H_2$$
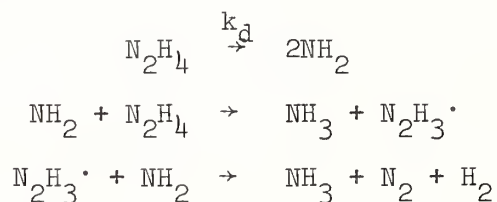
For steady state in $N_2H_3\cdot$ and $NH_2\cdot$ concentrations

$$d(N_2H_4)/dt = -2k_d(N_2H_4)$$

An important omission is the neglect of the reverse reaction $2NH_2\cdot \xrightarrow{k_r}$
N_2H_4. All direct measurements (Ie,f,g) give very high values. If this
reaction is of importance calculated rate constants and the activation
energy will be smaller than the true values.

Considerable effort has been devoted to purification of the hydra-
zine. The authors claim that with hydrazine dried over CaH_2, a lower
activation energy and slightly higher rate constants (at low temperatures)

178

can be obtained. Their sample has been dried over molecular sieve.

Questions regarding the purity of the hydrazine used are fundamental

to all the decomposition studies. Although rigorous purification is

the most direct procedure, it is probably only in the toluene carrier

studies and the shock tube experiments with extremely low concentrations

of hydrazine that one can assume the relative unimportance of homo-

geneous catalytic effects.

Belford and Strehlow[2] have questioned the used of the single

pulse shock tube for quantitative kinetic studies. Ignoring mechan-

istic problems, (which may be very serious) the uncertainty in rate

constants is probably no less than a factor of 3.

Ie. Details of the hydrazine decomposition process are followed

with time resolution of ∿1 μsec. The oscilloscopic traces show under

varying conditions, induction periods and deviation from first order

behavior. Thus the processes which are represented by the calculated

first order rate constants are uncertain.

Induction periods occurred only in the low temperature runs 1100-

1200°K. They have been ignored in the data analysis. However, this is

just at the high temperature end of the results of McHale et. al. (If)

and calls into question their mechanism. Palmer[3] maintains that

they represent artifacts arising from non-ideal shock behavior.

Commercial liquid hydrazine is used without special attempts at

purification. Hydrazine is absorbed on the shock tube walls. In

order to maintain concentration a continuous flow system is used. The

substitution of helium for argon as the inert diluent showed no striking

179

effects.   This is also the case with added traces of oxygen.

The reported rate expressions are in excellent agreement with that of McHale et. al. (Id). The estimated uncertainty is probably a factor of 3.

If. This represents a continuation of (Ie). Reactions are now carried out under more extreme conditions. Problems encountered earlier appear to have been surmounted through the proper choice of reaction variables. RRK theory is used to fit all the existing data. High pressure limiting rates are achieved at 200-300 atm.

It is claimed that the rate expression for the unimolecular high pressure decomposition of hydrazine is compatible with the recombination number of Bair (II,e,f). This is incorrect. See (IIb,c).

Uncertainty is probably a factor of 3.

IIb. From the subsequent discussion it can be seen that if these rate expressions are correct, all the measured numbers are in error.

IId.. Electron impact studies of this type are no longer considered satisfactory means of determining bond energies.[4] However, in the present case there may have been a fortuitous cancellation of errors.

IIe,f. The derivation of the necessary calibration factors depend on assumptions regarding the nature of the processes occurring during and after the rf discharge. Thus, large errors may be introduced. It should be noted that the reported number represents the rate of the 2nd order disappearance of $NH_2 \cdot$. It must be regarded as a maximum rate for the recombination of amino radicals.

180

There also appears to be a discrepancy between these two studies. In (IIe) k_r is reported to be pressure independent in the sub mm Hg range. This is in contrast to the situation in (IIf) where high pressure behavior is not reached till 10 mm Hg pressure. The possibility that the number reported in (IIe) is due to the reaction $NH_2 + NH_2 \rightarrow NH + NH_3$ would seem to be ruled out by the fact that the rate for this reaction as reported in (IIf) is $.46 \times 10^{12}$ cc/mol sec.

IIg. Similar comments as for (IIe,f). However, the initial excitation is orders of magnitude shorter. Furthermore, the radiolytic behavior of NH_3 is probably better understood. On this basis Ausloos[5] suggests an uncertainty of no more than a factor of 2 for the rate of the 2nd order disappearance of NH_2.

IIh. Although the data are compatible with the published numbers, it is not clear that other sets of rate parameters may not produce equally satisfactory agreement.

II(i,j). See comments (Ia,b).

3) Discussion

The main discrepancy in the data is between the <u>rate parameters</u> for decomposition and the <u>recombination rates</u>. These are related by the equilibrium constant $K_E = k_d/k_r$. If it is assumed that the latter has little or no temperature dependence, then $A_d/A_r \sim A_d/k_r \sim \dfrac{e^{\Delta S/R}}{eRT}$ (where A is the temperature independent factor). Thus, for $k_r \sim 10^{13.8}$ cc/mol-sec, at 300°K, A_d is approximately 10^{17} sec^{-1}. This is three or more orders of magnitude higher than any of the published numbers and is in accord with the surmises of Setser and Richardson (IIb) and

181

Benson and O'Neal (IIc). The possibility that the A-factor for recombination is in fact 3 orders of magnitude lower due to a negative activation of about 4 kcals can be ruled out since it implies a "tight" transition state. This is physically implausible and is also unrealizable since the lowest frequencies for hydrazine are 875, 780, and 378 cm^{-1}. Thus, at 300°K it is not possible to raise these numbers so as to give the required temperature dependence. The remaining possibility is that the published rate parameters are in gross error, but that hopefully the rate constants are (within the estimated uncertain limit) correct. There is ample precedence in gas kinetics for such occurrences, since small errors in rate constants can result in catastrophically large mistakes in the rate parameters. Furthermore, the methods used in deriving the hydrazine decomposition data are well known for this sort of error.

The present approach to the problem of deriving k_d and k_r for any arbitrary reaction condition is to make RRKM calculations of the fall-off behavior assuming an A-factor (and a transition state) consistent with the pulse radiolysis experiments (IIg) and with a variety of bond energies. This is dictated by the current controversy over the N-N bond energy in hydrazine. Furthermore, the small size of hydrazine makes it probable that most, if not all, of the published data are in the fall-off region. The results of such calculations may be found in Figure I. The transition state model (I) involve the frequencies 3300 (4), 1300 (2), 1000 (2), 20 (3). It is assumed that the molecular structure remain unchanged. The collision diameter is assumed to be

5 Å. With regard to third bodies the results of Rabinovitch and co-workers[6] are the best available. In the present analysis we have used Ar = .136 and toluene = (N_2H_4 = T). The density of states of the activated molecule is calculated using the Laplace transform method.[7] For the transition state a direct count is employed up to an energy where it gives comparable ($\sim$10% deviation) answers as the Laplace transform method. After which, the latter is used.

Except for the data of Diesen (Ic) which is derived from shock tube studies using _in situ_ mass spectroscopic detection an unambiguous choice of an optimum bond energy can be made. With regard to the former, it is suspected that an important cause for the discrepancy is due to sampling from the cold boundary layer; thus, making the calculated temperatures meaningless. This data will not be considered further. From the other experiments, the best bond energies are 65, 64.5, 64, 65.5, 67.5, 64.5, and 69 kcals. The mean value is 66 kcals. With this number all except the data of Diesen can be accomodated with a maximum deviation of a factor of 3. This is within the esti-mated error limits. It should be noted that in no case is it possible to fit the data with ΔE_O^O of 57 kcals. This itself is 1.5 kcals higher than the value that can be deduced from the JANAF Tables[1] with $\Delta H_f^{300}(NH_2)$ = 40.1 $\pm$ 3 kcals. The present number gives $\Delta H_f^{300}(NH_2)$ = 45.5 kcals with an estimated uncertainty of $\pm$ 1.5 kcals. That this analysis leads to a substantially different $\Delta H_f^{300}(NH_2)$ should not be surprising. The older estimate was based on a more limited set of rate data (Ia and Ib). Both studies were at pressures far below the

high pressure limit. Their activation energies did not reflect the bond strength. Indeed, from Figure Ia and Ib it can be seen that the experimental and calculated temperature dependences are in good agreement. There remains important differences between the shock tube and calculated temperature dependences.

The calculated rates constants for the decomposition of hydrazine and the combination of amino radicals over a range of 10^{-2}-10^5 mm $Hg(N_2H_4)$ and 200-3000°K are summarized in Table I. With regard to other third bodies some of the results of Rabinovitch and coworkers[6] can be found in Table II.

Although there is considerable arbitrariness in the definition of the transition state, it is generally agreed[8] that for a given A-factor the fall-off characteristics will be relatively unchanged in spite of variations in the pattern of the assumed frequencies. In the current investigation this has been verified by carrying out fall-off calculations with (model II) 3330 (4), 1300 (2), 200 (3), 40 (2) and (model III); and 3300 (4), 1300 (2), 80 (2), 60 (3) complexes. They give numbers close to the desired A-factor and have rates of decomposition which are never more than a factor of 3 or those in Table I (usually less, especially at higher temperatures). Characteristic results can be seen in Figures IIa,b. It is also necessary to consider the consequences of error in the pulse radiolysis experiments. Accordingly, experiments have been carried out with a (model IV) 3300 (4), 1300 (2), 1000 (2), 40 (3), complex. This gives an A-factor and recombination rate at 300°K of about a factor of 8 lower. Fitting

this data in the same manner as before we obtain the results in Figures III. This results in a best N-N bond energy of about 64.5. The key points are: (a) This is still 9 kcals higher than the JANAF number and (b) for the decomposition studies there is probably a range of rate parameters which will fit the data. Thus, it is not surprising that Meyer, et. al., (If) should also be able to fit the existing decomposition data with their much lower rate parameters. It is only after the combination rates are considered (in essence extending the range of rate constants tremendously k_d^{300} (1000 mm) $\sim 10^{-32.5}$ sec^{-1}) that definite distinction can be made. Finally, it is gratifying to note that the data in Table I also demonstrate that the difference between the r-f discharge and pulse radiolytic determinations of amino radical recombinations is due to the latter being considerably further into the fall-off region. Indeed at 10 mm pressure (NH_3, efficiency $\sim .76^6$) the calculated number is 3.0×10^{12} cc/mol sec while the experimental number at this pressure is 2.5×10^{12} cc/mol sec.

References

1. D. R. Stull and H. Prophet, JANAF Thermochemical Tables NSRDS-NBS-37, U. S. Government Printing Office, Washington, DC 20402

2. R. L. Belford and R. Strehlow, Ann. Rev. of Phys. Chem., pg. 247, Palo Alto, California, 94306

3. H. Palmer, Tenth Combustion Symposium (International), pg. 364, The Combustion Institute, Pittsburgh, Pennsylvania (1965).

4. H. Rosenstock, personal communication.

5. P. Ausloos, personal communication.

6. S. C. Chan, B. S. Rabinovitch, J. Bryant, L. D. Spicer, T. Fujimoto, Y. N. Len, and S. P. Pavlou, J. Phys. Chem. $\underline{74}$, 3160 (1970).

7. W. Forst, Chemical Review $\underline{71}$, 339 (1971).

8. W. Forst, J. Phys. Chem $\underline{76}$, 342 (1972).

Table I. Rate Constants for the reaction

$$M + N_2H_4 \underset{k(COM)}{\overset{k(DEC)}{\rightleftarrows}} 2NH_2\cdot + M$$
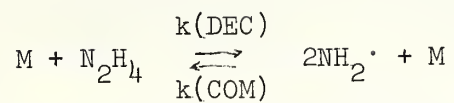
in the temperature range 200–3000°K and pressure range

.01– 100,000 mm Hg (N_2H_4).

(The table is on pages 188-195.)

TEMPERATURE IS 200 K
A.R.T. A-FACTOR IS 1.60715E+15 /SEC
REACTION THRESHOLD IS 66000. CALS
EXPERIMENTAL A-FACTOR IS 5.19307E+16 /SEC(HIGH PRESSURE)
EXPERIMENTAL ACTIVATION ENERGY IS 67311.4 CALS
                              (HIGH PRESSURE)
HIGH PRESSURE RATE CONSTANT IS 1.31156E-57 /SEC

PRESSURE	K(DEC)	K(COM)
(MM HG)	(/SEC)	(L/MOL-SEC)
.01	5.09590E-61	2.75486E+7
.1	4.50187E-60	2.43373E+8
1	3.26970E-59	1.76761E+9
10	1.74707E-58	9.44471E+9
100	5.79699E-58	3.13387E+10
1000	1.06909E-57	5.77952E+10
10000	1.27321E-57	6.88300E+10
100000	1.30736E-57	7.06762E+10

TEMPERATURE IS 300 K
A.R.T. A-FACTOR IS 6.49981E+15 /SEC
REACTION THRESHOLD IS 66000. CALS
EXPERIMENTAL A-FACTOR IS 1.68812E+17 /SEC(HIGH PRESSURE)
EXPERIMENTAL ACTIVATION ENERGY IS 67871.5 CALS
                              (HIGH PRESSURE)
HIGH PRESSURE RATE CONSTANT IS 5.67615E-33 /SEC

PRESSURE	K(DEC)	K(COM)
(MM HG)	(/SEC)	(L/MOL-SEC)
.01	5.82289E-37	6.98691E+6
.1	5.40080E-36	6.48044E+7
1	4.39414E-35	5.27254E+8
10	2.88105E-34	3.45698E+9
100	1.30728E-33	1.56861E+10
1000	3.43774E-33	4.12495E+10
10000	5.12106E-33	6.14478E+10
100000	5.60084E-33	6.72046E+10

TEMPERATURE IS 400 K
A.R.T. A-FACTOR IS 1.60736E+16 /SEC
REACTION THRESHOLD IS 66000. CALS
EXPERIMENTAL A-FACTOR IS 3.09771E+17 /SEC(HIGH PRESSURE)
EXPERIMENTAL ACTIVATION ENERGY IS 68281.3 CALS
                              (HIGH PRESSURE)
HIGH PRESSURE RATE CONSTANT IS 1.45204E-20 /SEC

PRESSURE	K(DEC)	K(COM)
(MM HG)	(/SEC)	(L/MOL-SEC)
.01	5.50753E-25	3.38946E+6
.1	5.22957E-24	3.21839E+7
1	4.50894E-23	2.77490E+8
10	3.30168E-22	2.03193E+9
100	1.80335E-21	1.10982E+10
1000	6.11101E-21	3.76085E+10
10000	1.14565E-20	7.05151E+10
100000	1.39555E-20	8.58874E+10

188

```
TEMPERATURE IS 500   K
A.R.T. A-FACTOR IS   3.02444E+16   /SEC
REACTION THRESHOLD IS 66000.   CALS
EXPERIMENTAL A-FACTOR IS 4.35202E+17   /SEC(HIGH PRESSURE)
EXPERIMENTAL ACTIVATION ENERGY IS 68578.8 CALS
                                  (HIGH PRESSURE)
HIGH PRESSURE RATE CONSTANT IS 4.41914E-13   /SEC
```

PRESSURE (MM HG)	K(DEC) (/SEC)	K(COM) (L/MOL-SEC)
.01	7.37608E-18	2.01819E+6
.1	7.09902E-17	1.94238E+7
1	6.33785E-16	1.73412E+8
10	4.97086E-15	1.36009E+9
100	3.06602E-14	8.38902E+9
1000	1.24931E-13	3.41826E+10
10000	2.88194E-13	7.88535E+10
100000	4.03256E-13	1.10336E+11

```
TEMPERATURE IS 600   K
A.R.T. A-FACTOR IS   4.81273E+16   /SEC
REACTION THRESHOLD IS 66000.   CALS
EXPERIMENTAL A-FACTOR IS 5.34254E+17   /SEC(HIGH PRESSURE)
EXPERIMENTAL ACTIVATION ENERGY IS 68799.2 CALS
                                  (HIGH PRESSURE)
HIGH PRESSURE RATE CONSTANT IS 4.49747E-8    /SEC
```

PRESSURE (MM HG)	K(DEC) (/SEC)	K(COM) (L/MOL-SEC)
.01	3.67623E-13	1.30544E+6
.1	3.56885E-12	1.26730E+7
1	3.26056E-11	1.15783E+8
10	2.67928E-10	9.51415E+8
100	1.80011E-9	6.39221E+9
1000	8.42450E-9	2.99155E+10
10000	2.32159E-8	8.24400E+10
100000	3.77921E-8	1.34200E+11

```
TEMPERATURE IS 700   K
A.R.T. A-FACTOR IS   6.86275E+16   /SEC
REACTION THRESHOLD IS 66000.   CALS
EXPERIMENTAL A-FACTOR IS 6.09422E+17   /SEC(HIGH PRESSURE)
EXPERIMENTAL ACTIVATION ENERGY IS 68966.9 CALS
                                  (HIGH PRESSURE)
HIGH PRESSURE RATE CONSTANT IS 1.73720E-4    /SEC
```

PRESSURE (MM HG)	K(DEC) (/SEC)	K(COM) (L/MOL-SEC)
.01	7.48935E-10	880290.
.1	7.31382E-9	8.59658E+6
1	6.79187E-8	7.98309E+7
10	5.77144E-7	6.78369E+8
100	4.13076E-6	4.85525E+9
1000	2.15215E-5	2.52961E+10
10000	6.89285E-5	8.10178E+10
100000	1.30392E-4	1.53261E+11

TEMPERATURE IS 800 K
A.R.T. A-FACTOR IS 9.07513E+16 /SEC
REACTION THRESHOLD IS 66000. CALS
EXPERIMENTAL A-FACTOR IS 6.66103E+17 /SEC(HIGH PRESSURE)
EXPERIMENTAL ACTIVATION ENERGY IS 69098. CALS
                                (HIGH PRESSURE)
HIGH PRESSURE RATE CONSTANT IS 8.62552E-2 /SEC

PRESSURE (MM HG)	K(DEC) (/SEC)	K(COM) (L/MOL-SEC)
.01	2.06872E-7	607487.
.1	2.02891E-6	5.95795E+6
1	1.90700E-5	5.59997E+7
10	1.66187E-4	4.88015E+8
100	1.24861E-3	3.66659E+9
1000	7.08451E-3	2.08039E+10
10000	2.57625E-2	7.56524E+10
100000	5.61664E-2	1.64935E+11

TEMPERATURE IS 900 K
A.R.T. A-FACTOR IS 1.13707E+17 /SEC
REACTION THRESHOLD IS 66000. CALS
EXPERIMENTAL A-FACTOR IS 7.09164E+17 /SEC(HIGH PRESSURE)
EXPERIMENTAL ACTIVATION ENERGY IS 69202.8 CALS
                                (HIGH PRESSURE)
HIGH PRESSURE RATE CONSTANT IS 10.8685 /SEC

PRESSURE (MM HG)	K(DEC) (/SEC)	K(COM) (L/MOL-SEC)
.01	1.51643E-5	427226.
.1	1.49203E-4	4.20352E+6
1	1.41543E-3	3.98771E+7
10	1.25789E-2	3.54388E+8
100	9.82048E-2	2.76674E+9
1000	.597165	1.68240E+10
10000	2.41877	6.81444E+10
100000	6.00693	1.69234E+11

TEMPERATURE IS 1000   K
A.R.T. A-FACTOR IS 1.36906E+17 /SEC
REACTION THRESHOLD IS 66000. CALS
EXPERIMENTAL A-FACTOR IS 7.42300E+17 /SEC(HIGH PRESSURE)
EXPERIMENTAL ACTIVATION ENERGY IS 69288.2 CALS
                                (HIGH PRESSURE)
HIGH PRESSURE RATE CONSTANT IS 523.32 /SEC

PRESSURE (MM HG)	K(DEC) (/SEC)	K(COM) (L/MOL-SEC)
.01	4.40113E-4	304675.
.1	4.34108E-3	3.00518E+6
1	4.14839E-2	2.87178E+7
10	.374468	2.59231E+8
100	3.0156	2.08759E+9
1000	19.4178	1.34422E+10
10000	86.2466	5.97055E+10
100000	241.029	1.66856E+11

```
TEMPERATURE IS 1100    K
A.R.T. A-FACTOR IS  1.59933E+17  /SEC
REACTION THRESHOLD IS 66000.  CALS
EXPERIMENTAL A-FACTOR IS 7.68170E+17  /SEC(HIGH PRESSURE)
EXPERIMENTAL ACTIVATION ENERGY IS 69359.2 CALS
                                (HIGH PRESSURE)
HIGH PRESSURE RATE CONSTANT IS 12502.  /SEC

PRESSURE          K(DEC)           K(COM)
(MM HG)           (/SEC)           (L/MOL-SEC)

 .01             6.52903E-3        219866.
 .1              6.45261E-2        2.17293E+6
 1                .62026           2.08874E+7
 10              5.67056           1.90957E+8
 100             46.8467           1.57757E+9
 1000            316.495           1.06580E+10
 10000           1522.03           5.12547E+10
 100000          4730.8            1.59311E+11


TEMPERATURE IS 1200    K
A.R.T. A-FACTOR IS  1.82505E+17  /SEC
REACTION THRESHOLD IS 66000.  CALS
EXPERIMENTAL A-FACTOR IS 7.88662E+17  /SEC(HIGH PRESSURE)
EXPERIMENTAL ACTIVATION ENERGY IS 69418.9 CALS
                                (HIGH PRESSURE)
HIGH PRESSURE RATE CONSTANT IS 176426. /SEC

PRESSURE          K(DEC)           K(COM)
(MM HG)           (/SEC)           (L/MOL-SEC)

 .01             5.86957E-2        160353.
 .1               .581008          1.58728E+6
 1               5.61202           1.53317E+7
 10              51.8486           1.41647E+8
 100             437.592           1.19547E+9
 1000            3079.53           8.41307E+9
 10000           15867.9           4.33501E+10
 100000          54269.7           1.48261E+11


TEMPERATURE IS 1300    K
A.R.T. A-FACTOR IS  2.04438E+17  /SEC
REACTION THRESHOLD IS 66000.  CALS
EXPERIMENTAL A-FACTOR IS 8.05118E+17  /SEC(HIGH PRESSURE)
EXPERIMENTAL ACTIVATION ENERGY IS 69469.9 CALS
                                (HIGH PRESSURE)
HIGH PRESSURE RATE CONSTANT IS 1.65981E+6   /SEC

PRESSURE          K(DEC)           K(COM)
(MM HG)           (/SEC)           (L/MOL-SEC)

 .01              .359759          118100.
 .1              3.56576           1.17055E+6
 1               34.581            1.13521E+7
 10              322.321           1.05811E+8
 100             2770.02           9.09332E+8
 1000            20189.5           6.62772E+9
 10000           110507.           3.62767E+10
 100000          411890.           1.35214E+11
```

```
TEMPERATURE IS 1400    K
A.R.T. A-FACTOR IS  2.25617E+17  /SEC
REACTION THRESHOLD IS 66000.  CALS
EXPERIMENTAL A-FACTOR IS 8.18502E+17  /SEC(HIGH PRESSURE)
EXPERIMENTAL ACTIVATION ENERGY IS 69513.9 CALS
                                   (HIGH PRESSURE)
HIGH PRESSURE RATE CONSTANT IS 1.13514E+7   /SEC


PRESSURE          K(DEC)          K(COM)
(MM HG)           (/SEC)          (L/MOL-SEC)

  .01             1.6354          87797.5
  .1              16.2268         871149.
  1               157.905         8.47722E+6
  10              1482.87         7.96090E+7
  100             12942.9         6.94849E+8
  1000            97246.9         5.22077E+9
  10000           561358.         3.01369E+10
  100000          2.26097E+6      1.21382E+11



TEMPERATURE IS 1500    K
A.R.T. A-FACTOR IS  2.45981E+17  /SEC
REACTION THRESHOLD IS 66000.  CALS
EXPERIMENTAL A-FACTOR IS 8.29515E+17  /SEC(HIGH PRESSURE)
EXPERIMENTAL ACTIVATION ENERGY IS 69552.2 CALS
                                   (HIGH PRESSURE)
HIGH PRESSURE RATE CONSTANT IS 6.01357E+7   /SEC


PRESSURE          K(DEC)          K(COM)
(MM HG)           (/SEC)          (L/MOL-SEC)

  .01             5.8653          65870.1
  .1              58.2499         654175.
  1               568.481         6.38432E+6
  10              5373.05         6.03419E+7
  100             47530.6         5.33791E+8
  1000            366738.         4.11865E+9
  10000           2.21916E+6      2.49223E+10
  100000          9.58631E+6      1.07659E+11



TEMPERATURE IS 1600    K
A.R.T. A-FACTOR IS  2.65501E+17  /SEC
REACTION THRESHOLD IS 66000.  CALS
EXPERIMENTAL A-FACTOR IS 8.38676E+17  /SEC(HIGH PRESSURE)
EXPERIMENTAL ACTIVATION ENERGY IS 69585.9 CALS
                                   (HIGH PRESSURE)
HIGH PRESSURE RATE CONSTANT IS 2.58840E+8   /SEC


PRESSURE          K(DEC)          K(COM)
(MM HG)           (/SEC)          (L/MOL-SEC)

  .01             17.3866         49876.4
  .1              172.804         495720.
  1               1690.67         4.85000E+6
  10              16068.9         4.60965E+7
  100             143819.         4.12571E+8
  1000            1.13595E+6      3.25866E+9
  10000           7.16848E+6      2.05640E+10
  100000          3.29937E+7      9.46482E+10
```

```
TEMPERATURE IS 1700     K
A.R.T. A-FACTOR IS  2.84172E+17  /SEC
REACTION THRESHOLD IS 66000.  CALS
EXPERIMENTAL A-FACTOR IS 8.46369E+17  /SEC(HIGH PRESSURE)
EXPERIMENTAL ACTIVATION ENERGY IS 69615.7 CALS
                                    (HIGH PRESSURE)
HIGH PRESSURE RATE CONSTANT IS 9.38877E+8    /SEC

PRESSURE            K(DEC)              K(COM)
(MM HG)             (/SEC)              (L/MOL-SEC)

 .01            44.1496             38125.9
 .1             439.092             379183.
 1              4305.29             3.71789E+6
 10             41119.              3.55089E+7
 100            371820.             3.21089E+8
 1000           2.99826E+6          2.58919E+9
 10000          1.96457E+7          1.69653E+10
 100000         9.57824E+7          8.27141E+10


TEMPERATURE IS 1800     K
A.R.T. A-FACTOR IS  3.02008E+17  /SEC
REACTION THRESHOLD IS 66000.  CALS
EXPERIMENTAL A-FACTOR IS 8.52888E+17  /SEC(HIGH PRESSURE)
EXPERIMENTAL ACTIVATION ENERGY IS 69642.3 CALS
                                    (HIGH PRESSURE)
HIGH PRESSURE RATE CONSTANT IS 2.95264E+9    /SEC

PRESSURE            K(DEC)              K(COM)
(MM HG)             (/SEC)              (L/MOL-SEC)

 .01            98.7624             29434.
 .1             982.81              292905.
 1              9654.73             2.87739E+6
 10             92605.8             2.75992E+7
 100            845021.             2.51840E+8
 1000           6.94093E+6          2.06860E+9
 10000          4.70437E+7          1.40204E+10
 100000         2.41713E+8          7.20374E+10


TEMPERATURE IS 1900     K
A.R.T. A-FACTOR IS  3.19030E+17  /SEC
REACTION THRESHOLD IS 66000.  CALS
EXPERIMENTAL A-FACTOR IS 8.58456E+17  /SEC(HIGH PRESSURE)
EXPERIMENTAL ACTIVATION ENERGY IS 69666.1 CALS
                                    (HIGH PRESSURE)
HIGH PRESSURE RATE CONSTANT IS 8.23366E+9    /SEC

PRESSURE            K(DEC)              K(COM)
(MM HG)             (/SEC)              (L/MOL-SEC)

 .01            199.01              22961.7
 .1             1981.39             228612.
 1              19496.9             2.24954E+6
 10             187718.             2.16588E+7
 100            1.72677E+6          1.99234E+8
 1000           1.44197E+7          1.66374E+9
 10000          1.00762E+8          1.16259E+10
 100000         5.43122E+8          6.26651E+10
```

```
TEMPERATURE IS 2000    K
A.R.T. A-FACTOR IS  3.35270E+17 /SEC
REACTION THRESHOLD IS 66000. CALS
EXPERIMENTAL A-FACTOR IS 8.63248E+17 /SEC(HIGH PRESSURE)
EXPERIMENTAL ACTIVATION ENERGY IS 69687.6 CALS
                                     (HIGH PRESSURE)
HIGH PRESSURE RATE CONSTANT IS 2.07285E+10  /SEC
```

PRESSURE (MM HG)	K(DEC) (/SEC)	K(COM) (L/MOL-SEC)
.01	370.896	18264.4
.1	3694.33	181924.
1	36406.	1.79278E+6
10	351700.	1.73192E+7
100	3.25857E+6	1.60465E+8
1000	2.76179E+7	1.36002E+9
10000	1.98402E+8	9.77016E+9
100000	1.11733E+9	5.50220E+10

```
TEMPERATURE IS 2200    K
A.R.T. A-FACTOR IS  3.65535E+17 /SEC
REACTION THRESHOLD IS 66000. CALS
EXPERIMENTAL A-FACTOR IS 8.71020E+17 /SEC(HIGH PRESSURE)
EXPERIMENTAL ACTIVATION ENERGY IS 69724.8 CALS
                                     (HIGH PRESSURE)
HIGH PRESSURE RATE CONSTANT IS 1.02200E+11  /SEC
```

PRESSURE (MM HG)	K(DEC) (/SEC)	K(COM) (L/MOL-SEC)
.01	991.875	11298.7
.1	9886.78	112623.
1	97672.3	1.11261E+6
10	948948.	1.08097E+7
100	8.90057E+6	1.01388E+8
1000	7.73845E+7	8.81505E+8
10000	5.83280E+8	6.64428E+9
100000	3.54823E+9	4.04187E+10

```
TEMPERATURE IS 2400    K
A.R.T. A-FACTOR IS  3.93087E+17 /SEC
REACTION THRESHOLD IS 66000. CALS
EXPERIMENTAL A-FACTOR IS 8.76991E+17 /SEC(HIGH PRESSURE)
EXPERIMENTAL ACTIVATION ENERGY IS 69755.9 CALS
                                     (HIGH PRESSURE)
HIGH PRESSURE RATE CONSTANT IS 3.86485E+11  /SEC
```

PRESSURE (MM HG)	K(DEC) (/SEC)	K(COM) (L/MOL-SEC)
.01	2118.24	7178.27
.1	21126.1	71592.1
1	209124.	708677.
10	2.04114E+6	6.91698E+6
100	1.93367E+7	6.55279E+7
1000	1.71684E+8	5.81802E+8
10000	1.34696E+9	4.56458E+9
100000	8.74690E+9	2.96414E+10

```
TEMPERATURE IS 2600      K
A.R.T. A-FACTOR IS  4.18209E+17  /SEC
REACTION THRESHOLD IS 66000.  CALS
EXPERIMENTAL A-FACTOR IS 8.81675E+17  /SEC(HIGH PRESSURE)
EXPERIMENTAL ACTIVATION ENERGY IS 69782.2 CALS
                                  (HIGH PRESSURE)
HIGH PRESSURE RATE CONSTANT IS 1.19163E+12  /SEC

PRESSURE          K(DEC)          K(COM)
(MM HG)           (/SEC)          (L/MOL-SEC)

 .01           3823.61          4675.03
 .1            38151.9          46647.3
 1             378271.          462502.
 10            3.70600E+6       4.53122E+6
 100           3.53981E+7       4.32804E+7
 1000          3.19813E+8       3.91027E+8
 10000         2.59501E+9       3.17285E+9
 100000        1.78143E+10      2.17811E+10


TEMPERATURE IS 2800      K
A.R.T. A-FACTOR IS  4.41166E+17  /SEC
REACTION THRESHOLD IS 66000.  CALS
EXPERIMENTAL A-FACTOR IS 8.85415E+17  /SEC(HIGH PRESSURE)
EXPERIMENTAL ACTIVATION ENERGY IS 69804.8 CALS
                                  (HIGH PRESSURE)
HIGH PRESSURE RATE CONSTANT IS 3.12925E+12  /SEC

PRESSURE          K(DEC)          K(COM)
(MM HG)           (/SEC)          (L/MOL-SEC)

 .01           6071.37          3115.29
 .1            60602.2          31095.7
 1             601661.          308719.
 10            5.91290E+6       3.03398E+6
 100           5.68632E+7       2.91772E+7
 1000          5.21277E+8       2.67474E+8
 10000         4.35160E+9       2.23286E+9
 100000        3.13239E+10      1.60727E+10


TEMPERATURE IS 3000      K
A.R.T. A-FACTOR IS  4.62195E+17  /SEC
REACTION THRESHOLD IS 66000.  CALS
EXPERIMENTAL A-FACTOR IS 8.88447E+17  /SEC(HIGH PRESSURE)
EXPERIMENTAL ACTIVATION ENERGY IS 69824.5 CALS
                                  (HIGH PRESSURE)
HIGH PRESSURE RATE CONSTANT IS 7.22671E+12  /SEC

PRESSURE          K(DEC)          K(COM)
(MM HG)           (/SEC)          (L/MOL-SEC)

 .01           8727.06          2119.98
 .1            87136.2          21167.2
 1             866039.          210378.
 10            8.53302E+6       2.07284E+6
 100           8.25267E+7       2.00474E+7
 1000          7.65835E+8       1.86037E+8
 10000         6.54878E+9       1.59083E+9
 100000        4.90910E+10      1.19252E+10
```

Table II. Collisional Efficiencies of Bath Gases[*]

1.	N_2H_4	(1.00)
2.	He	.171
3.	Ne	.120
4.	Ar	.136
5.	Kr	.115
6.	D_2	.23
7.	N_2	.21
8.	SF_6	.42
9.	H_2	.28
10.	NH_3	.76
11.	CD_4	.41
12.	CH_4	.44
13.	C_2H_6	.56
14.	C_2H_4	.43
15.	C_3H_6	.60
16.	C_3H_8	.62
17.	iC_4H_{10}	.73
18.	$C_6H_5CH_3$	.80

[*]From results of ref. 6 on CH_3NC isomerization.

<u>Figure I.</u> Comparison of calculated —— and experimental - - - rate constants for hydrazine decomposition at constant pressure. Transition state model (I) for hydrazine 3300, (4), 1300 (2), 1000 (2), 20 (3). Collision diameter 5Å, Argon efficiency[6] .136, Toluene efficiency[6] .8. The numbers are assumed bond energies in kcals.

  (a) reference Ia   (7mm Hg toluene)

  (b) reference Ib   (15 mm Hg toluene)

  (c) reference Ic   (100 mm Hg argon)

  (d) reference Id   (3000 mm Hg argon)

  (e1) reference Ie   (2000 mm Hg argon)

  (e2) reference Ie   (5500 mm Hg argon)

  (f1) reference If   (150 mm Hg argon)

  (f2) reference If   (200,000 mm Hg argon)

<u>Figure II.</u> Comparison of the results of RRKM calculations with varying frequency patterns for the transition state, but essentially invariant high pressure rate parameters˙

  a. $k(I)/k(II)$; 300°K $k_\infty(I) = 10^{17.2} \exp(-67,871/RT)$

                   $k_\infty(II) = 10^{17.2} \exp(-68,397/RT)$

         900°K $k_\infty(I) = 10^{17.8} \exp(-69,203/RT)$

                   $k_\infty(II) = 10^{18.2} \exp(-70,659/RT)$

       1500°K $k_\infty(I) = 10^{17.9} \exp(-69,552/RT)$

                   $k_\infty(II) = 10^{18.4} \exp(-71,279/RT)$

b. $k(I)/k(III)$; 300°K k (III) = $10^{17.3}$ exp(-68,585/RT)

900°K k (III) = $10^{18.5}$ exp(-70,893/RT)

1500°K k (III) = $10^{18.6}$ exp(-71,552/RT)

Figure III: Comparison of calculated —— and experimental – – – rate constants for hydrazine decomposition at constant pressure. Transition state model (IV) for hydrazine 3300 (4), 1300 (2), 1000 (2), 40 (3). Collision diameter 5 Å, Argon efficiency[6] .136 Toluene efficiency[6] .8. The numbers are assumed bond energies in kcals.

(a) reference Ia (7 mm Hg toluene)

(b) reference Ib (15 mm Hg toluene)

(c) reference Ic (100 mm Hg argon)

(d) reference Id (3000 mm Hg argon)

(e1) reference Ie (2000 mm Hg argon)

(e2) reference Ie (5500 mm Hg argon)

(f1) reference If (150 mm Hg argon)

(f2) reference If (200,000 mm Hg argon)

Figure 2

200

Figure 3

201
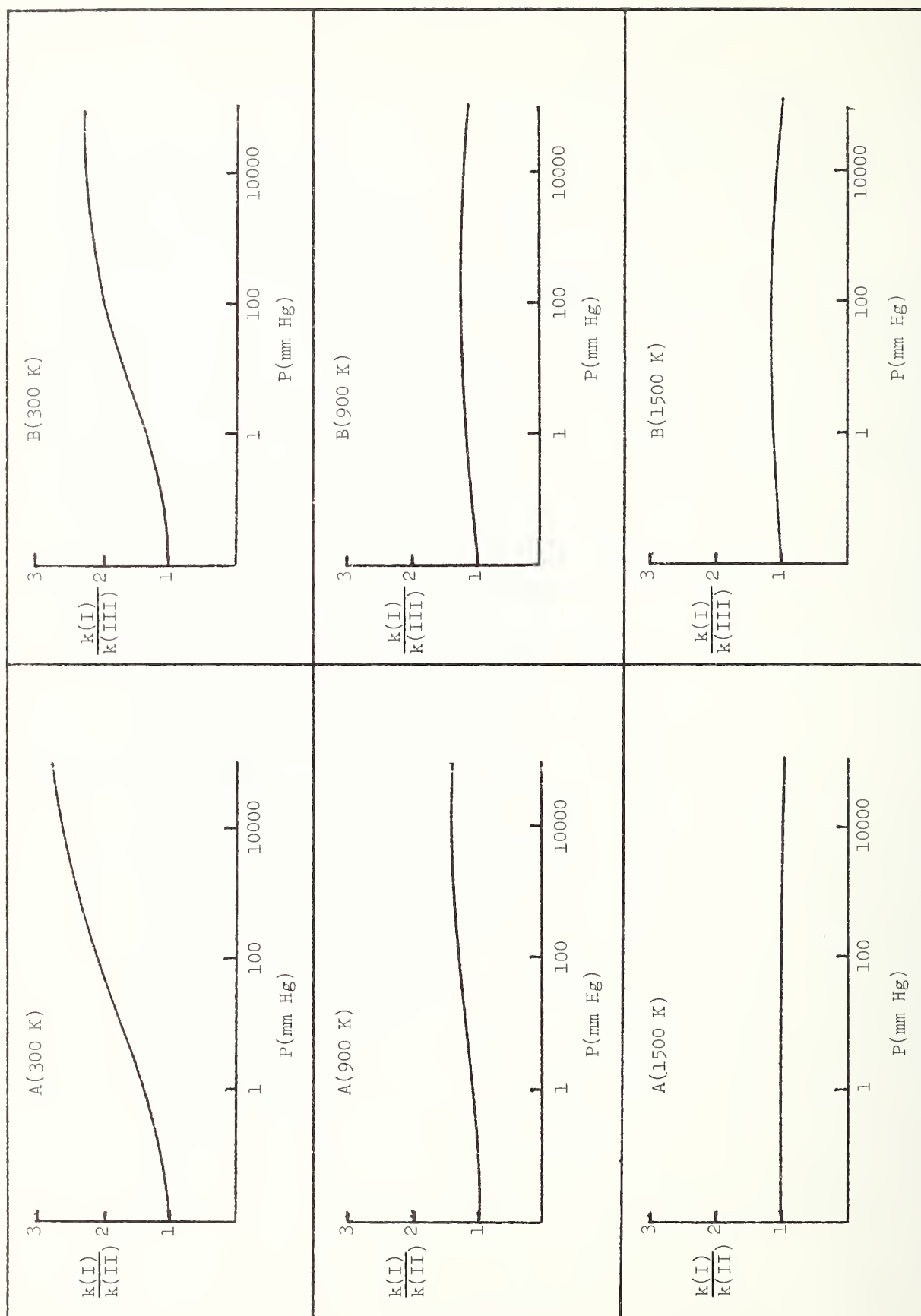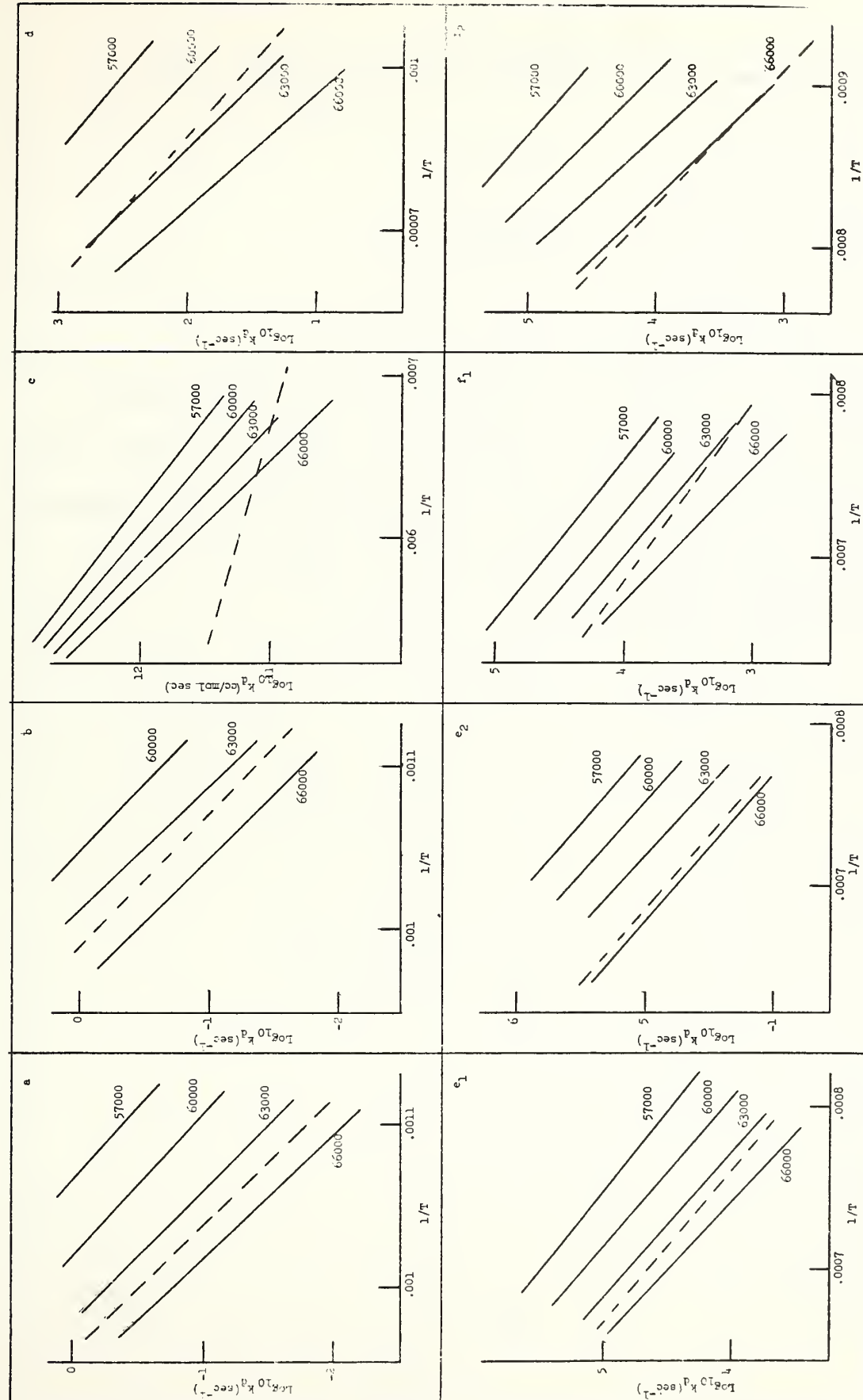
Chapter 13
RATE CONSTANTS FOR THE REACTIONS $(M) + N_2F_4 \underset{k_d}{\overset{k_r}{\rightleftarrows}} 2NF_2 \cdot + (M)$

W. Tsang

ABSTRACT

Data for the reactions $N_2F_4 + M \underset{k_d}{\overset{k_r}{\rightleftarrows}} 2NF_2 \cdot + M$ have been critically examined and tabulated. A correlation of the data on the basis of RRKM calculations require a N-N bond energy of $\Delta E_o^\circ = 18.0$ kcals. This is somewhat lower than the JANAF value of $\Delta E_o^\circ = 20.8$ kcals. Suggested rate constants for these reactions over the ranges $10^{-5} - 10^2$ atm and 200-1800 °K are tabulated.

1. Survey of Experimental Data

$$N_2F_4 \underset{k_d}{\overset{k_r}{\rightleftarrows}} 2NF_2$$

$\Delta H_f(300)$	=	-2.01 ± 2.5 10.1 ± 2 kcals
$S(300)$	=	72.08 59.8 cals/mol °K
$Cp(300)$	=	19.00 9.82
$Cp(700)$	=	27.87 12.54
$Cp(1000)$	=	29.72 13.18
$\Delta H_R(300)$	=	22.2 kcals
$\Delta S_R(300)$	=	47.5 cals/mol °K

*

I. Direct Studies

Results	Method and Condition	Reference
a. $k_d(N_2) = 10^{14.98} \exp(-19,400 \pm 700/RT)$ sec^{-1} (2 atm).	Shock tube at 344-410°K with .6 to 6 atm Ar or N_2 (1% N_2F_4)	L. Brown and B. Darwent, J. Chem. Phys., 279, 42 (1965).
$k_d(Ar) = 10^{13.47} \exp(-17,100 \pm 700/RT)$ sec^{-1} (2 atm).	Spectrophotometric detection of NF_2 at 2602 Å (4 A bandpass) (incident shock).	
Reactions appear close to high pressure limit at 6 atm N_2.		

I. Direct Studies (Continued)

Results	Method and Condition	Reference

b. Reaction order is close to bimolecular $k_d(Ar) = 1.5 \times 10^{12}$ $T^{.5}$ $\exp(-15,200/RT)$ l/mol sec with respect of 3rd bodies $k_d(He)/k_d(Ar) = 1.2 \pm .1$

$k_d(SF_6)/k_d(Ar) = 1.7 \pm .1$

$k_d(N_2F_4)/k_d(Ar) = 1.8 \pm .2$

Shock tube at $350-450°K$ and argon helium and SF_6 at $.58-2.7$ atm ($.5-16\%$ N_2F_4). Spectrophotometric detection of NF_2 at 2600 Å (300 Å bandpass) (incident shock).

A. P. Modica and D. F. Hornig, J. Chem. Phys., $\underline{1317}$, 49 (1968).

II. Indirect Studies

a. $\Delta H_R(300) = 22.2$ kcals
$\Delta S_R(300) = 47.5$ cals/mol °K
(as given above)

Review and recalculation of existing data for the equilibrium

$$N_2F_4 \underset{\rightarrow}{\overset{K_E}{\leftarrow}} 2NF_2 .$$

JANAF Thermochemical Tables NSRDS-NBS 37, U. S. Government Printing Office, Washington, DC 20402

*All data from Ref. IIa.

204

III. Comments:

Ia,b. The results are derived from very straight forward shock tube
experiments. Since reactions are carried out behind incident shock waves,
at low temperatures and for the most part dilute mixtures of N_2F_4, mech-
anistic complications as well as non-ideal shock tube behavior are pro-
bably absent. Measured rates are probably reliable. Absolute uncertainties
in rate constants should be less than a factor of 2. A direct comparison
of runs under similar condition can be found in Fig. I. Agreement is
satisfactory.

There may be discrepancies in the reported pressure dependence.
Modica and Hornig (Ib) publish data which indicate a linear dependence
of unimolecular rate constant with pressure. This means that under these
conditions (.58-2.7 atm) reaction is in the bimolecular region. Brown
and Darwent (Ia) find at 6 atm N_2 pressure they are close to the high
pressure limit. These results are not compatible since this suggests an
unacceptably sharp fall-off curve. The collisional efficiency of argon
as reported by Modica and Hornig (Ib) is rather high. This may be an indi-
cation that they are not as far into the fall-off region as they believe.

There is a disagreement of about 2 kcals in activation energy for
decomposition in the presence of argon. Although this may not be consid-
ered large at first sight note that the process in question has an extremely
low activation energy. The percentage deviation is more of the order of
12%. This is fairly large even in the context of shock tube experiments.

IIa. The numbers given here is based on the measured equilibrium
constants and calculated entropies of reaction. The reported 2nd law

205

determinations give numbers of 19.8, 21.7, 19.3, 19.8, and 21.5 kcals (see ref. in IIa). The source of this discrepancy is unknown. Ordinarily, one would favor the 3rd law determination. It should be noted all the entropies are based on spectroscopic data. A direct measurement of the entropy of N_2F_4 will increase our confidence in the validity of the 3rd law determinations.

2. Discussion

The two studies are in substantial agreement with regard to measured rates of $NF_2 \cdot$ formation. The unimolecular rate constants have a pressure dependence but it would seem that the extent of this dependence is uncertain. The activation energy is also uncertain.

Assuming the correctness of the measured rate constants, a series of RRKM calculations will permit (in essence) a best two parameter fit of the data. The results of such calculations for a range of A-factors (details regarding transition state models and other parameters used in RRKM calculation can be found in Table I) and N-N bond energies confirm the experimental observation that results are in the "fall-off" region. For reactions at 2 atmospheres argon comparisons between calculation and experiments can be found in Figures Ia,b,c. For each A-factor two rates have been determined. One involves the use of an argon efficiency of .5 as determined by Modica and Hornig (Ib) while the other uses .136 from the work of Rabinovitch and coworkers.[1] This should cover the possible range of argon efficiencies. The key factors to be noted are: 1) For $\Delta E_o^o = 20.8$ kcals reaction is so far into the fall-off region such that

there is no transition state model which will fit the data; 2) with $\Delta E_O^O =$ 19.6 kcals, if one considers the uncertainty limits in the experiments (factor of 2) and calculation (factor of 3) then a tenuous fit may be possible; c) Finally for $\Delta E_O^O = 18$ kcals one obtains a comfortable fit with A-factors which are commonly observed for other bond dissociation reactions. With this bond energy a transition state compatible with an A-factor of $10^{17.3}$ sec^{-1} and an argon efficiency of .136 and N_2 efficiency of .21 the accumulated data on the pressure dependence of the unimolecular rate constant and the results of shocks in N_2 at 2.5 atm can be accomodated. This can be seen in Figure IIa,b,c. In addition from the present results we can compute the apparent third body efficiencies of SF_6, He and A (since reaction is not completely in the bimolecular region) using the numbers given by Rabinovitch and coworkers.[1] The values are $k_d(SF_6)/k_d(Ar) = 1.6$, $k_d(N_2F_4)/k_d(Ar) = 3.5$, and $k_d(He)/k_d(Ar) = 1.0$. These numbers are in reasonable accord with the values given by Modica and Hornig (Ib).

The N-N bond energy that is recommended in the JANAF Tables (Ia) is 22.2 kcals (298°K). This corresponds to $\Delta E_O^O = 20.8$ kcals. As we have noted it is not possible to fit the data on this basis. Thus if this number is correct than the only proper conclusion is that the experimental results are in error and the satisfactory fits that have been obtained with $\Delta E_O^O = 18.0$ kcals mere coincidences. Although the former is always possible (for example, presence of NF_2 producing impurities) the gross discrepancies make it unlikely. Furthermore, we are not convinced that N-N bond energy has been settled. The value of $\Delta E_O^O = 18.0$

kcals corresponds to a ΔH_{298} = 19.4 kcals which is in agreement with the 2nd law determinations.

Pending the settlement of this question we summarize in Table II rate constants for N_2F_4 decomposition and NF_2 combination over the range .01-100,000 mm Hg(N_2F_4) and 200-1800°K using ΔE_O^O = 18.0 and a transition state which yields an A-factor of $\sim 10^{17.3}$ sec^{-1}. Assuming the correctness of the experimental data these numbers should have an uncertainty of about a factor of 3. If the JANAF N-N bond energy should be confirmed we summarize in Table III results with the same transition state and ΔE_O^O = 20.8. These are however no better than order of magnitude estimates since there will no longer be any experimental tie-points. Finally, there is also the possibility that this discrepancy is due to defects in the calculational procedure. Thus, if the high bond energy and the rate data should both proved to be correct, then the data in Table II may still be valid (it runs through the experimental numbers) but it will indicate that the computational technique is not sufficiently sensitive to this small change in bond energy. Obviously further experimental work should be carried out.

References

1. S. C. Chen, B. S. Rabinovitch, J. Bryant, L. D. Spicer, T. Fryimoto,
    Y. N. Lin, and S. P. Pavlou, J. Phys. Chem. $\underline{74}$, 3160 (1970).

TABLE I: Data Used in Fall-off Calculations.

a) Transition state is assumed to have some geometrical structure as molecule.

b) Collision diameter is 6 $\overset{\circ}{A}$.

c) Vibrational frequencies for the molecule are 950(5), 740(1), 520(5), 120(1).

d) Vibrational frequencies for transition states are

1.   950(4), 570(2), 300(2), 60(3)   giving $A_{exp}^{400}(\infty) = 10^{15.7}$ sec^{-1}

2.   950(4), 570(2), 150(2), 30(3)   giving $A_{exp}^{400}(\infty) = 10^{17.3}$ sec^{-1}

3.   950(4), 570(2), 50(2), 20(3)   giving $A_{exp}^{400}(\infty) = 10^{18.7}$ sec^{-1}

4.   950(4), 570(2), 10(5)   giving $A_{exp}^{400}(\infty) = 10^{21}$ sec^{-1}

e) Since fall-off behavior is independent of pattern of vibrational frequencies but is sensitive to exact value of $A(\infty)$, it is assumed that the above covers all possible transition state models within this range of A-factors.

TABLE II

Recommended rate constants for the reactions $N_2F_4 \underset{k(COM)}{\overset{k(DEC)}{\underset{\leftarrow}{\rightarrow}}} 2NF_2 \cdot$ over the pressure range .01-100,000 mm Hg (N_2F_4) and 200-1800°K. $A(\infty) \sim 10^{17.3}$ sec^{-1} $\Delta E_o^o = 18000$ cals. Note that k(DEC)/k(COM) = equilibrium constant with $\Delta E_o^o = 18000$ cals.

TEMPERATURE IS 200 K
A.R.T. A-FACTOR IS 6.88975E+14 /SEC
REACTION THRESHOLD IS 18000. CALS
EXPERIMENTAL A-FACTOR IS 2.86886E+16 /SEC (HIGH PRESSURE)
EXPERIMENTAL ACTIVATION ENERGY IS 19462.4 CALS
                                   (HIGH PRESSURE)
HIGH PRESSURE RATE CONSTANT IS 1.50580E-5   /SEC

PRESSURE (MM HG)	K(DEC) (/SEC)	K(COM) (L/MOL-SEC)
.01	3.11337E-10	18764.6
.1	3.07811E-9	185520.
1	2.82798E-8	1.70445E+6
10	2.10627E-7	1.26947E+7
100	1.15621E-6	6.96861E+7
1000	4.24485E-6	2.55841E+8
10000	9.57262E-6	5.76950E+8
100000	1.35960E-5	8.19442E+8

TEMPERATURE IS 300 K
A.R.T. A-FACTOR IS 3.08483E+15 /SEC
REACTION THRESHOLD IS 18000. CALS
EXPERIMENTAL A-FACTOR IS 9.99696E+16 /SEC (HIGH PRESSURE)
EXPERIMENTAL ACTIVATION ENERGY IS 20053.6 CALS
                                   (HIGH PRESSURE)
HIGH PRESSURE RATE CONSTANT IS 241.142 /SEC

PRESSURE (MM HG)	K(DEC) (/SEC)	K(COM) (L/MOL-SEC)
.01	7.72187E-4	4327.03
.1	7.67468E-3	43005.8
1	.073189	410122.
10	.612868	3.43427E+6
100	4.19646	2.35153E+7
1000	21.6034	1.21057E+8
10000	74.8421	4.19385E+8
100000	159.594	8.94300E+8

TEMPERATURE IS 400 K
A.R.T. A-FACTOR IS 8.05521E+15 /SEC
REACTION THRESHOLD IS 18000. CALS
EXPERIMENTAL A-FACTOR IS 1.81544E+17 /SEC (HIGH PRESSURE)
EXPERIMENTAL ACTIVATION ENERGY IS 20455.9 CALS
                                   (HIGH PRESSURE)
HIGH PRESSURE RATE CONSTANT IS 1.19085E+6   /SEC

PRESSURE (MM HG)	K(DEC) (/SEC)	K(COM) (L/MOL-SEC)
.01	.850684	1582.37
.1	8.47479	15764.1
1	82.2422	152980.
10	730.705	1.35920E+6
100	5630.92	1.04742E+7
1000	35179.	6.54370E+7
10000	161028.	2.99531E+8
100000	481210.	8.95107E+8

```
TEMPERATURE IS   500   K
A.R.T. A-FACTOR IS 1.56054E+16  /SEC
REACTION THRESHOLD IS 18000.  CALS
EXPERIMENTAL A-FACTOR IS 2.50174E+17  /SEC (HIGH PRESSURE)
EXPERIMENTAL ACTIVATION ENERGY IS  20736.3 CALS
                                    (HIGH PRESSURE)
HIGH PRESSURE RATE CONSTANT IS 2.13354E+8   /SEC
```

PRESSURE (MM HG)	K(DEC) (/SEC)	K(COM) (L/MOL-SEC)
.01	42.3612	677.796
.1	422.553	6761.01
1	4140.65	66252.
10	38097.7	609578.
100	315642.	5.05039E+6
1000	2.23104E+6	3.56975E+7
10000	1.23392E+7	1.97432E+8
100000	4.76811E+7	7.62916E+8

```
TEMPERATURE IS   600   K
A.R.T. A-FACTOR IS 2.52449E+16  /SEC
REACTION THRESHOLD IS 18000.  CALS
EXPERIMENTAL A-FACTOR IS 3.02202E+17  /SEC (HIGH PRESSURE)
EXPERIMENTAL ACTIVATION ENERGY IS  20939.3 CALS
                                    (HIGH PRESSURE)
HIGH PRESSURE RATE CONSTANT IS 7.05820E+9   /SEC
```

PRESSURE (MM HG)	K(DEC) (/SEC)	K(COM) (L/MOL-SEC)
.01	456.144	316.86
.1	4553.52	3163.09
1	44888.9	31182.
10	422463.	293463.
100	3.67313E+6	2.55154E+6
1000	2.82531E+7	1.96260E+7
10000	1.78803E+8	1.24205E+8
100000	8.39921E+8	5.83450E+8

```
TEMPERATURE IS   700   K
A.R.T. A-FACTOR IS 3.63523E+16  /SEC
REACTION THRESHOLD IS 18000.  CALS
EXPERIMENTAL A-FACTOR IS 3.40590E+17  /SEC (HIGH PRESSURE)
EXPERIMENTAL ACTIVATION ENERGY IS  21091.6 CALS
                                    (HIGH PRESSURE)
HIGH PRESSURE RATE CONSTANT IS 8.77533E+10  /SEC
```

PRESSURE (MM HG)	K(DEC) (/SEC)	K(COM) (L/MOL-SEC)
.01	2094.26	158.513
.1	20916.6	1583.16
1	207014.	15668.8
10	1.97874E+6	149770.
100	1.77980E+7	1.34712E+6
1000	1.45475E+8	1.10110E+7
10000	1.01713E+9	7.69859E+7
100000	5.55428E+9	4.20401E+8

```
TEMPERATURE IS  800  K
A.R.T. A-FACTOR IS 4.83636E+16  /SEC
REACTION THRESHOLD IS 18000.  CALS
EXPERIMENTAL A-FACTOR IS 3.68975E+17  /SEC (HIGH PRESSURE)
EXPERIMENTAL ACTIVATION ENERGY IS  21209.6 CALS
                                     (HIGH PRESSURE)
HIGH PRESSURE RATE CONSTANT IS 5.88043E+11  /SEC
```

PRESSURE (MM HG)	K(DEC) (/SEC)	K(COM) (L/MOL-SEC)
.01	6225.65	90.982
.1	62200.1	908.997
1	617284.	9021.03
10	5.96606E+6	87188.4
100	5.50076E+7	803885.
1000	4.70378E+8	6.87414E+6
10000	3.54745E+9	5.18426E+7
100000	2.17975E+10	3.18551E+8

```
TEMPERATURE IS  1000   K
A.R.T. A-FACTOR IS 7.34293E+16  /SEC
REACTION THRESHOLD IS 18000.  CALS
EXPERIMENTAL A-FACTOR IS 4.06437E+17  /SEC (HIGH PRESSURE)
EXPERIMENTAL ACTIVATION ENERGY IS  21379.4 CALS
                                     (HIGH PRESSURE)
HIGH PRESSURE RATE CONSTANT IS 8.58582E+12  /SEC
```

PRESSURE (MM HG)	K(DEC) (/SEC)	K(COM) (L/MOL-SEC)
.01	19513.1	29.5697
.1	195034.	295.55
1	1.94206E+6	2942.96
10	1.90390E+7	28851.3
100	1.81362E+8	274832.
1000	1.64803E+9	2.49740E+6
10000	1.37999E+10	2.09120E+7
100000	1.00376E+11	1.52108E+8

```
TEMPERATURE IS  1200   K
A.R.T. A-FACTOR IS 9.81603E+16  /SEC
REACTION THRESHOLD IS 18000.  CALS
EXPERIMENTAL A-FACTOR IS 4.28868E+17  /SEC (HIGH PRESSURE)
EXPERIMENTAL ACTIVATION ENERGY IS  21495.3 CALS
                                     (HIGH PRESSURE)
HIGH PRESSURE RATE CONSTANT IS 5.19035E+13  /SEC
```

PRESSURE (MM HG)	K(DEC) (/SEC)	K(COM) (L/MOL-SEC)
.01	33218.4	11.4897
.1	332091.	114.865
1	3.31284E+6	1145.86
10	3.27418E+7	11324.8
100	3.17931E+8	109967.
1000	2.99684E+9	1.03655E+6
10000	2.67799E+10	9.26273E+6
100000	2.17216E+11	7.51312E+7

TEMPERATURE IS   1400   K
A.R.T. A-FACTOR IS 1.21497E+17 /SEC
REACTION THRESHOLD IS 18000. CALS
EXPERIMENTAL A-FACTOR IS 4.43168E+17 /SEC (HIGH PRESSURE)
EXPERIMENTAL ACTIVATION ENERGY IS 21579.2 CALS
                                      (HIGH PRESSURE)
HIGH PRESSURE RATE CONSTANT IS 1.88769E+14 /SEC

PRESSURE	K(DEC)	K(COM)
(MM HG)	(/SEC)	(L/MOL-SEC)
.01	41717.2	5.14461
.1	417104.	51.4378
1	4.16513E+6	513.649
10	4.13592E+7	5100.46
100	4.06213E+8	50094.8
1000	3.91520E+9	482827.
10000	3.64351E+10	4.49322E+6
100000	3.17073E+11	3.91019E+7

TEMPERATURE IS   1600   K
A.R.T. A-FACTOR IS 1.43042E+17 /SEC
REACTION THRESHOLD IS 18000. CALS
EXPERIMENTAL A-FACTOR IS 4.52778E+17 /SEC (HIGH PRESSURE)
EXPERIMENTAL ACTIVATION ENERGY IS 21642.6 CALS
                                      (HIGH PRESSURE)
HIGH PRESSURE RATE CONSTANT IS 4.98781E+14 /SEC

PRESSURE	K(DEC)	K(COM)
(MM HG)	(/SEC)	(L/MOL-SEC)
.01	44139.4	2.55698
.1	441351.	25.5674
1	4.40977E+6	255.457
10	4.39077E+7	2543.56
100	4.34165E+8	25151.1
1000	4.24118E+9	245690.
10000	4.04712E+10	2.34449E+6
100000	3.68402E+11	2.13414E+7

TEMPERATURE IS   1800   K
A.R.T. A-FACTOR IS 1.62728E+17 /SEC
REACTION THRESHOLD IS 18000. CALS
EXPERIMENTAL A-FACTOR IS 4.59519E+17 /SEC (HIGH PRESSURE)
EXPERIMENTAL ACTIVATION ENERGY IS 21692.2 CALS
                                      (HIGH PRESSURE)
HIGH PRESSURE RATE CONSTANT IS 1.06407E+15 /SEC

PRESSURE	K(DEC)	K(COM)
(MM HG)	(/SEC)	(L/MOL-SEC)
.01	41871.	1.36661
.1	418686.	13.6653
1	4.18465E+6	136.581
10	4.17321E+7	1362.08
100	4.14306E+8	13522.4
1000	4.08004E+9	133167.
10000	3.95404E+10	1.29055E+6
100000	3.70402E+11	1.20894E+7

TABLE III

Estimated rate constants for the reaction $N_2F_4 \overset{k(DEC)}{\underset{k(COM)}{\rightleftarrows}} 2NF_2 \cdot$ over the pressure range .01–100,000 mm Hg (N_2F_4) and 200–1800°K. $A(\infty) \sim 10^{17.3}$ sec^{-1} $\Delta E_O^O = 20800$ cals. Note that $k(DEC)/k(COM)$ = equilibrium constant with $\Delta E_O^O = 20800$ cals.

(The table is on pages 217–220.)

TEMPERATURE IS   200   K
A.R.T. A-FACTOR IS 6.88975E+14 /SEC
REACTION THRESHOLD IS 20800. CALS
EXPERIMENTAL A-FACTOR IS 2.86886E+16 /SEC (HIGH PRESSURE)
EXPERIMENTAL ACTIVATION ENERGY IS 22259.4 CALS
                                   (HIGH PRESSURE)
HIGH PRESSURE RATE CONSTANT IS 1.31667E-8   /SEC

PRESSURE (MM HG)	K(DEC) (/SEC)	K(COM) (L/MOL-SEC)
.01	8.29910E-13	685.715
.1	8.05125E-12	6652.36
1	6.81524E-11	56311.1
10	4.46225E-10	368694.
100	2.06155E-9	1.70336E+6
1000	6.13405E-9	5.06827E+6
10000	1.11596E-8	9.22066E+6
100000	1.37881E-8	1.13925E+7

TEMPERATURE IS   300   K
A.R.T. A-FACTOR IS 3.08483E+15 /SEC
REACTION THRESHOLD IS 20800. CALS
EXPERIMENTAL A-FACTOR IS 9.99696E+16 /SEC (HIGH PRESSURE)
EXPERIMENTAL ACTIVATION ENERGY IS 22850.7 CALS
                                   (HIGH PRESSURE)
HIGH PRESSURE RATE CONSTANT IS 2.20502 /SEC

PRESSURE (MM HG)	K(DEC) (/SEC)	K(COM) (L/MOL-SEC)
.01	2.14135E-5	287.181
.1	2.10600E-4	2824.4
1	1.91034E-3	25620.
10	1.46796E-2	196871.
100	8.89234E-2	1.19257E+6
1000	.387585	5.19799E+6
10000	1.09046	1.46244E+7
100000	1.90563	2.55568E+7

TEMPERATURE IS   400   K
A.R.T. A-FACTOR IS 8.05521E+15 /SEC
REACTION THRESHOLD IS 20800. CALS
EXPERIMENTAL A-FACTOR IS 1.81544E+17 /SEC (HIGH PRESSURE)
EXPERIMENTAL ACTIVATION ENERGY IS 23252.9 CALS
                                   (HIGH PRESSURE)
HIGH PRESSURE RATE CONSTANT IS 35213.8 /SEC

PRESSURE (MM HG)	K(DEC) (/SEC)	K(COM) (L/MOL-SEC)
.01	7.54666E-2	140.377
.1	.746834	1389.2
1	7.00635	13032.6
10	58.5077	108831.
100	411.259	764988.
1000	2251.75	4.18852E+6
10000	8609.94	1.60155E+7
100000	21008.3	3.90778E+7

TEMPERATURE IS 500 K
A.R.T. A-FACTOR IS 1.56054E+16 /SEC
REACTION THRESHOLD IS 20800. CALS
EXPERIMENTAL A-FACTOR IS 2.50174E+17 /SEC (HIGH PRESSURE)
EXPERIMENTAL ACTIVATION ENERGY IS 23533.4 CALS
                                      (HIGH PRESSURE)
HIGH PRESSURE RATE CONSTANT IS 1.27580E+7   /SEC

PRESSURE (MM HG)	K(DEC) (/SEC)	K(COM) (L/MOL-SEC)
.01	7.48175	70.9141
.1	74.2928	704.167
1	710.571	6734.98
10	6238.66	59131.8
100	48115.7	456054.
1000	305727.	2.89776E+6
10000	1.45135E+6	1.37563E+7
100000	4.64923E+6	4.40667E+7

TEMPERATURE IS 600 K
A.R.T. A-FACTOR IS 2.52449E+16 /SEC
REACTION THRESHOLD IS 20800. CALS
EXPERIMENTAL A-FACTOR IS 3.02202E+17 /SEC (HIGH PRESSURE)
EXPERIMENTAL ACTIVATION ENERGY IS 23736.4 CALS
                                      (HIGH PRESSURE)
HIGH PRESSURE RATE CONSTANT IS 6.74938E+8   /SEC

PRESSURE (MM HG)	K(DEC) (/SEC)	K(COM) (L/MOL-SEC)
.01	126.519	36.7215
.1	1258.92	365.394
1	12189.2	3537.85
10	110610.	32104.
100	908277.	263622.
1000	6.40139E+6	1.85797E+6
10000	3.55795E+7	1.03267E+7
100000	1.41239E+8	4.09938E+7

TEMPERATURE IS 700 K
A.R.T. A-FACTOR IS 3.63523E+16 /SEC
REACTION THRESHOLD IS 20800. CALS
EXPERIMENTAL A-FACTOR IS 3.40590E+17 /SEC (HIGH PRESSURE)
EXPERIMENTAL ACTIVATION ENERGY IS 23888.7 CALS
                                      (HIGH PRESSURE)
HIGH PRESSURE RATE CONSTANT IS 1.17345E+10 /SEC

PRESSURE (MM HG)	K(DEC) (/SEC)	K(COM) (L/MOL-SEC)
.01	795.5	19.606
.1	7926.27	195.351
1	77381.6	1907.15
10	718575.	17710.1
100	6.17027E+6	152073.
1000	4.69000E+7	1.15590E+6
10000	2.93501E+8	7.23365E+6
100000	1.38001E+9	3.40119E+7

218

TEMPERATURE IS 800 K
A.R.T. A-FACTOR IS 4.83636E+16 /SEC
REACTION THRESHOLD IS 20800. CALS
EXPERIMENTAL A-FACTOR IS 3.68975E+17 /SEC (HIGH PRESSURE)
EXPERIMENTAL ACTIVATION ENERGY IS 24006.7 CALS
                                        (HIGH PRESSURE)
HIGH PRESSURE RATE CONSTANT IS 1.01120E+11 /SEC

PRESSURE (MM HG)	K(DEC) (/SEC)	K(COM) (L/MOL-SEC)
.01	2747.28	10.8436
.1	27399.1	108.144
1	269055.	1061.96
10	2.54074E+6	10028.3
100	2.25504E+7	89006.8
1000	1.81445E+8	716165.
10000	1.24427E+9	4.91115E+6
100000	6.69621E+9	2.64300E+7

TEMPERATURE IS 1000   K
A.R.T. A-FACTOR IS 7.34293E+16 /SEC
REACTION THRESHOLD IS 20800. CALS
EXPERIMENTAL A-FACTOR IS 4.06437E+17 /SEC (HIGH PRESSURE)
EXPERIMENTAL ACTIVATION ENERGY IS 24176.5 CALS
                                        (HIGH PRESSURE)
HIGH PRESSURE RATE CONSTANT IS 2.09954E+12 /SEC

PRESSURE (MM HG)	K(DEC) (/SEC)	K(COM) (L/MOL-SEC)
.01	11780.6	3.71096
.1	117625.	37.0524
1	1.16367E+6	366.564
10	1.12348E+7	3539.01
100	1.04259E+8	32842.
1000	9.07228E+8	285782.
10000	7.07979E+9	2.23017E+6
100000	4.64203E+10	1.46227E+7

TEMPERATURE IS 1200   K
A.R.T. A-FACTOR IS 9.81603E+16 /SEC
REACTION THRESHOLD IS 20800. CALS
EXPERIMENTAL A-FACTOR IS 4.28868E+17 /SEC (HIGH PRESSURE)
EXPERIMENTAL ACTIVATION ENERGY IS 24292.4 CALS
                                        (HIGH PRESSURE)
HIGH PRESSURE RATE CONSTANT IS 1.60502E+13 /SEC

PRESSURE (MM HG)	K(DEC) (/SEC)	K(COM) (L/MOL-SEC)
.01	24289.4	1.46671
.1	242673.	14.6537
1	2.41099E+6	145.587
10	2.35862E+7	1424.24
100	2.24917E+8	13581.5
1000	2.05540E+9	124114.
10000	1.74321E+10	1.05263E+6
100000	1.30415E+11	7.87507E+6

TEMPERATURE IS 1400 K
A.R.T. A-FACTOR IS 1.21497E+17 /SEC
REACTION THRESHOLD IS 20800. CALS
EXPERIMENTAL A-FACTOR IS 4.43168E+17 /SEC (HIGH PRESSURE)
EXPERIMENTAL ACTIVATION ENERGY IS 24376.3 CALS
                              (HIGH PRESSURE)
HIGH PRESSURE RATE CONSTANT IS 6.90291E+13 /SEC

PRESSURE (MM HG)	K(DEC) (/SEC)	K(COM) (L/MOL-SEC)
.01	34526.6	.656215
.1	345076.	6.55853
1	3.43696E+6	65.323
10	3.38952E+7	644.213
100	3.28752E+8	6248.27
1000	3.09933E+9	58905.9
10000	2.77513E+10	527442.
100000	2.26855E+11	4.31162E+6

TEMPERATURE IS 1600 K
A.R.T. A-FACTOR IS 1.43042E+17 /SEC
REACTION THRESHOLD IS 20800. CALS
EXPERIMENTAL A-FACTOR IS 4.52778E+17 /SEC (HIGH PRESSURE)
EXPERIMENTAL ACTIVATION ENERGY IS 24439.7 CALS
                              (HIGH PRESSURE)
HIGH PRESSURE RATE CONSTANT IS 2.06835E+14 /SEC

PRESSURE (MM HG)	K(DEC) (/SEC)	K(COM) (L/MOL-SEC)
.01	39794.5	.323572
.1	397810.	3.23462
1	3.96808E+6	32.2647
10	3.93269E+7	319.77
100	3.85489E+8	3134.44
1000	3.70675E+9	30139.9
10000	3.43802E+10	279548.
100000	2.98192E+11	2.42462E+6

TEMPERATURE IS 1800 K
A.R.T. A-FACTOR IS 1.62728E+17 /SEC
REACTION THRESHOLD IS 20800. CALS
EXPERIMENTAL A-FACTOR IS 4.59519E+17 /SEC (HIGH PRESSURE)
EXPERIMENTAL ACTIVATION ENERGY IS 24489.3 CALS
                              (HIGH PRESSURE)
HIGH PRESSURE RATE CONSTANT IS 4.86586E+14 /SEC

PRESSURE (MM HG)	K(DEC) (/SEC)	K(COM) (L/MOL-SEC)
.01	40230.6	.171377
.1	402219.	1.71339
1	4.01563E+6	17.106
10	3.99190E+7	170.049
100	3.93880E+8	1677.87
1000	3.83512E+9	16337.1
10000	3.63915E+10	155022.
100000	3.28356E+11	1.39875E+6

TABLE IV. Collisional Efficiencies of Bath Gases[1]

1.	N_2F_4	(1.00)
2.	He	.171
3.	Ne	.120
4.	Ar	.136
5.	Kr	.115
6.	D_2	.23
7.	N_2	.21
8.	SF_6	.42
9.	H_2	.28
10.	NH_3	.76
11.	CD_4	.41
12.	CH_4	.44
13.	C_2H_6	.56
14.	C_2H_4	.43
15.	C_3H_6	.60
16.	C_3H_8	.62
17.	iC_4H_{10}	.73
18.	$C_6H_5CH_3$	.80

Figure I. Comparison of experimental ——(Ref. Ia); +(Ref. Ib) and calculated —— —— —— and ---- rates of decomposition for various ΔE_O^O and $A_d(\infty)$. The upper of the two dotted lines refer to argon efficiency of .5. The lower efficiency is .136. Pressure $\sim$.05 mol/liter argon.

   a) ΔE_O^O = 20800 cal.; —— —— —— $A_d(\infty) \sim 10^{21}$ sec^{-1} and ---- $A_d(\infty) \sim 10^{17.3}$ sec^{-1}.

   b) ΔE_O^O = 19600 cal.; —— —— —— $A_d(\infty) \sim 10^{18.7}$ sec^{-1} and ---- $A_d(\infty) \sim 10^{17.3}$.

   c) ΔE_O^O = 18000 cal.; —— —— —— $A_d(\infty) \sim 10^{17.3}$ sec^{-1} and ---- $A_d(\infty) \sim 10^{15.8}$ sec^{-1}.

Figure II. a) Comparison of calculated (——)$A_d(\infty) \sim 10^{17.3}$ ΔE_O^O = 18,000 cals N_2 efficiency = .21 and experimental (+) rates of decomposition of N_2F_4 in N_2 at 400°K (Ref. Ia).

   b) Comparison of calculated (——) $A_d(\infty) \sim 10^{17.3}$ ΔE_O^O = 18000 cals A efficiency = .136 and experimental (+) rates of decomposition of N_2F_4 in argon at 360°K (Ref. Ib).

   c) Comparison of calculated (— — —) $A_d(\infty) \sim 10^{17.3}$ ΔE_O^O = 18000 cals N_2 efficiency = .21 and experimental (——) rates of decomposition of N_2F_4 at .07 mols/liter N_2 as a function of temperature.

FIGURE 1

223

FIGURE II

224
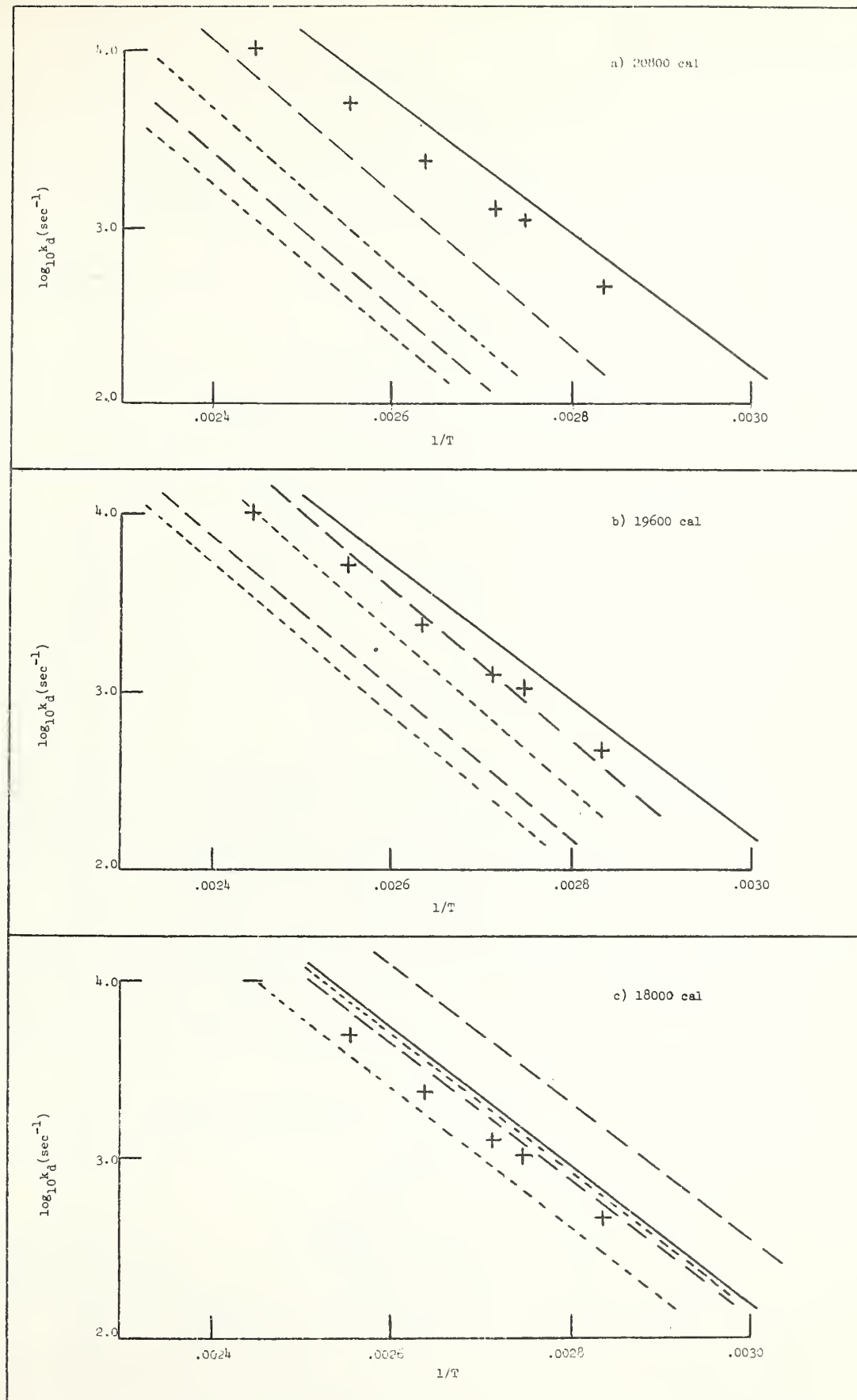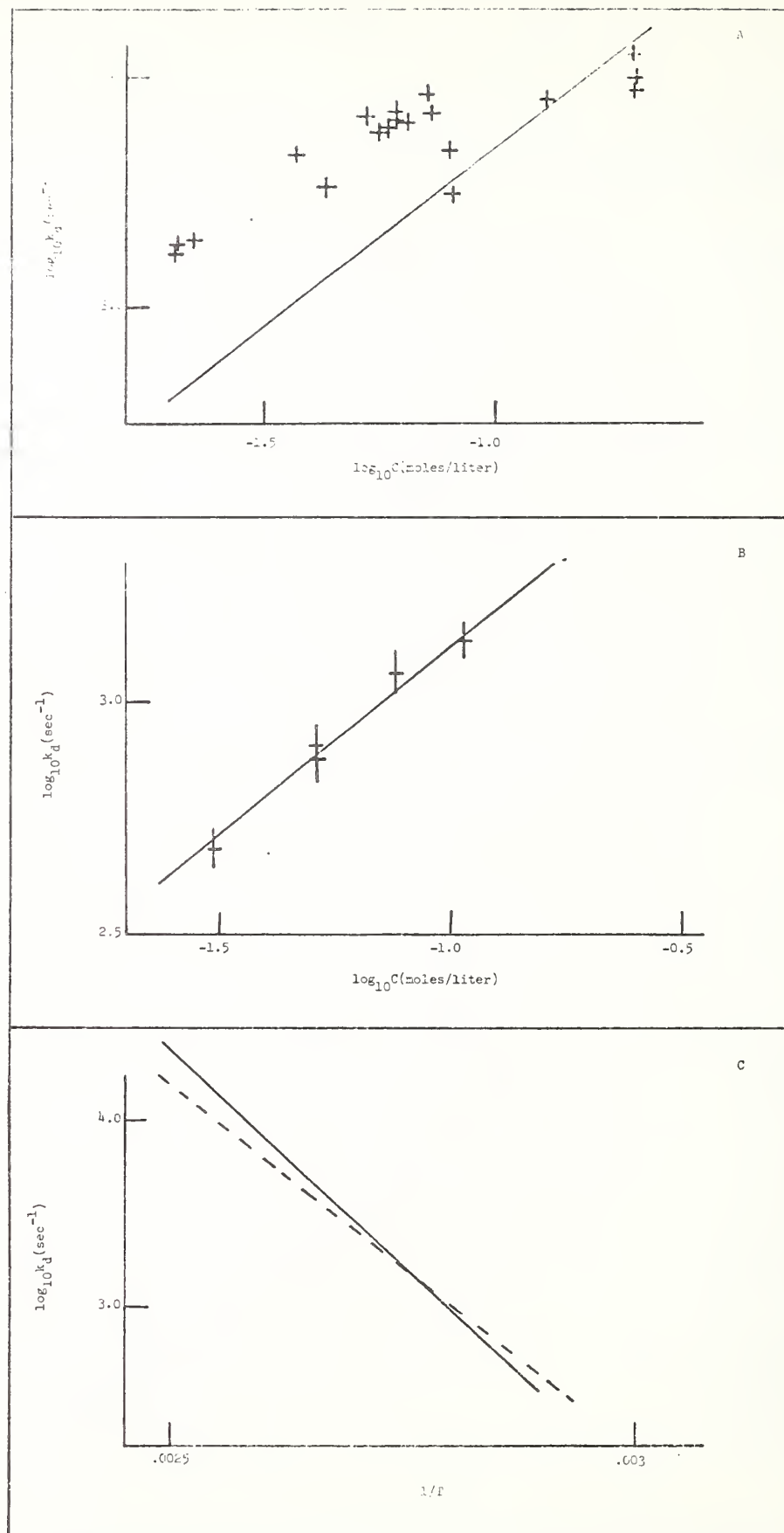
CHEMICAL KINETICS OF REACTIONS OF CHLORINE,
NITROGEN AND OXYGEN FLUORIDES IN GAS PHASE:
A BIBLIOGRAPHY - 1934 THROUGH JUNE 1972

by Francis Westley

Table of Contents

Introduction

This bibliography lists research papers on the
kinetics of gas phase reactions of the chlorine, nitrogen
and oxygen fluorides, with emphasis on the processes occuring
during their thermal decompositions.

The material is arranged by chemical reaction in three
separate lists - chlorine fluorides, nitrogen fluorides, and
oxygen fluorides. After each reaction are listed references
to papers that either report rate data or discuss the
mechanism of reaction. If it is the latter a note is
appended to the reference citations. There are sixty
reactions in the lists, based on work in 51 papers.

The references under each reaction list the author(s)
and the sources, in the following form:

Author(s)	Source-Year-Volume-Page	Number of Author(s)
Diesen, R. W.	JCPSA-1964-41-3256	1
Lin and Bauer	JACSA-1969-91-7737	2
Blauer, et al.	JPCHA-1971-75-3939	3 or more

The sources are indicated by their ASTM CODEN
abbreviation. A guide to these codes follows the introduction.

225

Part IV is a list of references, alphabetically by author, in which full citations are given for the brief citations in the reaction listings in parts I-III.

The bibliography is based on the files of the Chemical Kinetics Information Center and an examination of Chemical Abstracts 1934-1972. Most of the papers listed were published since 1962.

ACSRA   Abstracts of Papers.   American Chemical Society (Washington)

BBPCA   Berichte Der Bunsengesellschaft Fuer Physikalische Chemie (Weinheim, Germany)

BOOKA   Book

CHPLB   Chemical Physics Letters (Amsterdam)

CHREA   Chemical Reviews (Washington)

CMEAA   Commissarial A L'Energie Atomique, France, Rapport (Gif-sur-yvette, France)

DABBB   Dissertation Abstracts International B. The Sciences and Engineering

DIASA   Dissertation Abstracts

JACSA   Journal of the American Chemical Society (Washington)

JCPSA   Journal of Chemical Physics (New York)

JPCHA   Journal of Physical Chemistry (Washington/Ithaca, New York)

NSRDA   United States National Bureau of Standards, National Standard Reference Data Series (Washington)

RCRVA   Russian Chemical Reviews (London)

RJICA   Russian Journal of Inorganic Chemistry (London)

XCCIA   United States Department of Commerce, Clearinghouse for Scientific and Technical Information, A.D.

ZEELA   Zeitschrift Fuer Elektrochemie (Weinheim/Halle, Germany)

ZPCBA   Zeitschrift Fuer Physikalische Chemie, Abteilung   B. Chemie Der Elementarprozesse, Aufbau Der Materie (Leipzig)

ZPCFA   Zeitschrift Fuer Physikalische Chemie (Frankfurt am Main)

12WSA   Congreso Internacional De Quimica Pura Y Aplicada, 9 0 Congress, Madrid, April, 1934

$Cl + ClF \rightarrow Cl_2 + \dot{F}$
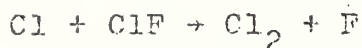
McIntyre and Diesen   XCCIA-1971-AD713938 (estimate)
McIntyre and Diesen   JPCHA-1971-75-1765 (estimate)

$Cl + F + M \rightarrow ClF + M$

Fletcher and Dahneke   JACSA-1969-91-1603 (estimate)

$Cl + F_2 \rightarrow ClF + F$

San Roman and Schumacher ZPCFA-1970-71-153 (mechanism)

$Cl_2 + F \rightarrow Cl + ClF$

McIntyre and Diesen   JPCHA-1971-75-1765 (estimate)

$Cl_2 + F_2 \rightarrow ClF + ClF$ (overall)

Fletcher and Dahneke   JACSA-1969-91-1603

$ClF + ClF_3 \rightarrow ClF_2 + ClF_2$

Blauer, et al.   JPCHA-1969-73-2683 (mechanism)
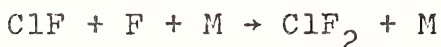
$ClF + F + M \rightarrow ClF_2 + M$

San Roman and Schumacher ZPCFA-1970-71-153 (mechanism)

$ClF + h\nu \rightarrow Cl + F$

San Roman and Schumacher ZPCFA-1970-71-153

$ClF + M \rightarrow Cl + F + M$
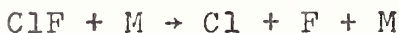
Blauer, et al.   JPCHA-1971-75-3939
McIntyre and Diesen   XCCIA-1971-AD713938 (mechanism)
McIntyre and Diesen   JPCHA-1971-75-1765 (mechanism)
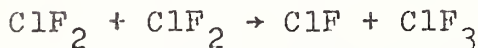
$ClF_2 + ClF_2 \rightarrow ClF + ClF_3$

San Roman and Schumacher ZPCFA-1970-71-153
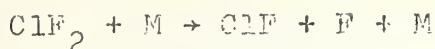
$ClF_2 + F \rightarrow ClF + F_2$

Blauer, et al.   XCCIA-1969-AD692493
Blauer, et al.   JPCHA-1969-73-2683

228

$ClF_2 + F + M \rightarrow ClF_3 + M$

San Roman and Schumacher ZPCFA-1970-71-153

$ClF_2 + M \rightarrow ClF + F + M$

Blauer, et al.   XCCIA-1969-AD692493
Blauer, et al.   JPCHA-1969-73-2683

$ClF_3 \rightarrow ClF + F_2$

Bernstein and Katz   JPCHA-1952-56-885

$ClF_3 + ClF_5^* \rightarrow ClF_4 + ClF_4$

Krieger, et al.   ZPCFA-1966-51-240

$ClF_3 + F \rightarrow ClF_2 + F_2$

Blauer, et al.   JPCHA-1969-73-2683

$ClF_3 + M \rightarrow ClF_2 + F + M$

Blauer, et al.   XCCIA-1969-AD692493
Blauer, et al.   JPCHA-1969-73-2683

$ClF_4 + F \rightarrow ClF_3 + F_2$

Krieger, et al.   ZPCFA-1966-51-240

$ClF_4 + F \rightarrow ClF_5^*$

Krieger, et al.   ZPCFA-1966-51-240

$ClF_5^* \rightarrow ClF_4 + F$

Krieger, et al.   ZPCFA-1966-51-240

$ClF_5 + M \rightarrow ClF_3 + F_2 + M$ (overall)
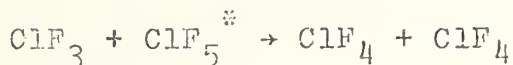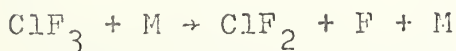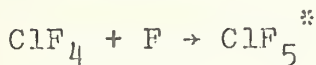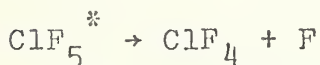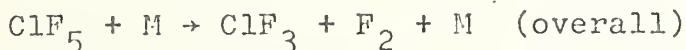
Axworthy and Sullivan   JPCHA-1970-74-949
Sullivan and Axworthy   ACSRA-1968-155-J-25
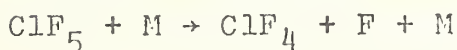
$ClF_5 + M \rightarrow ClF_4 + F + M$

Blauer, et al.   XCCIA-1969-AD692493
Blauer, et al.   JPCHA-1970-74-1183

$ClF_5^* + M \rightarrow ClF_5 + M$
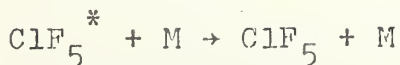
Krieger, et al.   ZPCFA-1966-51-240

Bougon, R.   CMEAA-1970-54

II(a).   REACTIONS OF NITROGEN FLUORIDES
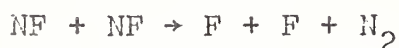
$NF^* \rightarrow NF + h\nu$

   Clyne and White   CHPLB-1970-6-465

$NF^* + M \rightarrow NF + M$

   Clyne and White   CHPLB-1970-6-465

$NF + NF \rightarrow F + F + N_2$

   Diesen, R. W.   JCPSA-1964-41-3256
   Diesen, R. W.   JCPSA-1966-45-759 (review)

$NF + NF_2 \rightarrow F_2 + N_2F$

   Diesen, R. W.   JCPSA-1966-45-759 (review)

$6NF_2 \rightarrow 4NF_3 + N_2$

   Cherednikov, et al.   RJICA-1969-14-454

$NF_2 + F + M \rightarrow NF_3 + M$

   Levy and Copeland   JPCHA-1965-69-3700

$NF_2 + F_2 \rightarrow F + NF_3$
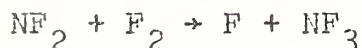
   Diesen, R. W.   JCPSA-1966-45-759 (review)
   Levy and Copeland   JPCHA-1965-69-3700
   Modica and Hornig   JCPSA-1966-45-760
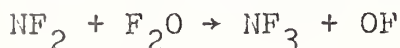
$4NF_2 + F_2O \rightarrow 3NF_3 + NOF$

   Rubinstein, et al.   ZPCFA-1964-43-51 (overall)

$NF_2 + F_2O \rightarrow NF_3 + OF$

   Rubinstein, et al.   ZPCFA-1964-43-51

$NF_2 + M \rightarrow F + NF + M$
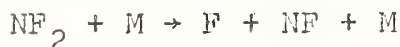
   Diesen, R. W.   JCPSA-1964-41-3256
   Diesen, R. W.   JCPSA-1966-45-759 (review)
   Modica and Hornig   JCPSA-1965-43-2739

$$NF_3 + M \rightarrow F + NF_2 + M$$

    Diesen, R. W.   JCPSA-1966-45-759 (review)

$$NF_2 + M \rightarrow NF_2^* + M$$

    Modica and Hornig   JCPSA-1966-45-760 (mechanism)

$$NF_2^* + NF_2^* \rightarrow F_2 + N_2F_2^*$$

    Modica and Hornig   JCPSA-1966-45-760 (mechanism)

$$NF_2 + N_2F \rightarrow NF_3 + N_2$$

    Diesen, R. W.   JCPSA-1966-45-759 (review)

$$N_2F_2^* \rightarrow N_2F_2 + h\nu$$

    Modica and Hornig   JCPSA-1966-45-760 (mechanism)

$$3N_2F_4 \rightarrow 4NF_3 + N_2 \text{ (overall)}$$

    Cherednikov, et al.   RJICA-1969-14-454

$$N_2F_4 + F \rightarrow NF_2 + NF_3$$

    Levy and Copeland   JPCHA-1965-69-3700

$$N_2F_4 + F_2 \rightarrow NF_3 + NF_3 \text{ (overall)}$$

    Cherednikov and Il'in   RJICA-1968-13-1750

$$2N_2F_4 + F_2O \rightarrow 3NF_3 + NOF \text{ (overall)}$$

    Rubinstein, et al.   ZPCFA-1964-43-51

$$N_2F_4 + M \rightarrow NF_2 + NF_2 + M$$

    Brown, L. M.   DIASA-1964-25-2774
    Brown and Darwent   JCPSA-1965-42-2158
    Levy and Copeland   JPCHA-1965-69-3700 (review)
    Modica, A. P.   DIASA-1964-24-4427
    Modica and Hornig   XCCIA-1963-AD425108
    Modica and Hornig   JCPSA-1968-49-629

II(b). REVIEWS

Kondratiev, V. N.   BOOKA-1970-207 (NF, and NF_2;
                                    general tables)

Troe and Wagner   BBPCA-1967-71-937 (Difluoroamino-
                                    free-radical)
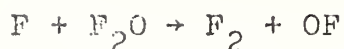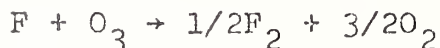
$F + F_2O \rightarrow F_2 + OF$

    Gatti, et al.   ZPCFA-1962-35-343

$F + O_3 \rightarrow 1/2F_2 + 3/2O_2$

    Staricco, et al.   ZPCFA-1962-31-385

$F + O_3 \rightarrow OF + O_2$

    Staricco, et al.   ZPCFA-1962-31-385

$F_2 + O \rightarrow F + OF$

    Lin and Bauer   JACSA-1969-91-7737 (review)

$F_2 + OF \rightarrow F + F_2O$

    Lin and Bauer   JACSA-1969-91-7737 (review)

$F_2O + h\nu \rightarrow F_2 + 1/2O_2$ (overall)

    Gatti, et al.   ZPCFA-1962-35-343

$F_2O + M \rightarrow F + OF + M$
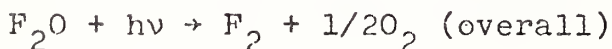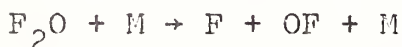
    Blauer and Solomon   JPCHA-1968-72-2307
    Henrici, et al.   JCPSA-1970-52-5834
    Lin and Bauer   JACSA-1969-91-7737
    Solomon, et al.   JPCHA-1968-72-2311

$F_2O + M \rightarrow F_2 + 1/2O_2 + M$ (overall)
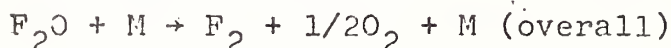
    Asmus, T. W.   DABBB-1971-31-4606
    Dauerman, et al.   JPCHA-1967-71-3999
    Dauerman, et al.   JPCHA-1969-73-1621
    Koblitz and Schumacher ZPCBA-1934-25-283
    Lin and Bauer   JACSA-1969-91-7737
    Schumacher, H.-J.   12WSA-1935-2-485
    Solomon, et al.   JPCHA-1968-72-2311
    Troe, et al.   ZPCFA-1967-56-238
    Wieder and Marcus   JCPSA-1962-37-1835 (calculation)
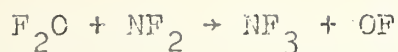
$F_2O + 4NF_2 \rightarrow 3NF_3 + NOF$

    Rubinstein, et al.   ZPCFA-1964-43-51 (overall)

$F_2O + NF_2 \rightarrow NF_3 + OF$

    Rubinstein, et al.   ZPCFA-1964-43-51

$F_2O + 2N_2F_4 \rightarrow 3NF_3 + NOF$ (overall)

    Rubinstein, et al.   ZPCFA-1964-43-51

$F_2O + O \rightarrow OF + OF$.

    Lin and Bauer   JACSA-1969-91-7737 (review)

$F_2O_2 + M \rightarrow F_2 + O_2 + M$ (overall)
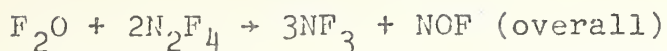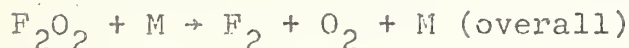
    Benson and O'Neal   NSRDA-1970-21-559 (review)
    Frisch and Schumacher   ZEELA-1937-43-807
    Frisch and Schumacher   ZPCBA-1936-34-322
    Frisch and Schumacher   ZPCBA-1937-37-18
    Schumacher, H.-J.   ZEELA-1941-47-673 (review)
    Schumacher and Frische ZPCBA-1937-37-1
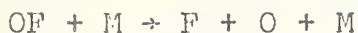
$OF + M \rightarrow F + O + M$

    Lin and Bauer   JACSA-1969-91-7737 (review)

$OF + OF \rightarrow F + F + O_2$

    Lin and Bauer   JACSA-1969-91-7737

$OF + OF \rightarrow F_2 + O_2$
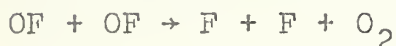
    Gatti, et al.   ZPCFA-1962-35-343 (mechanism)

$OF + O_3 \rightarrow F + O_2 + O_2$

    Staricco, et al.   ZPCFA-1962-31-385 (mechanism)

III(b). <u>REVIEWS</u>

Nikitin and Rosolovskii   RCRVA-1971-40-889 (Oxygen
                                           Fluorides)
Streng, A. G.   CHREA-1963-63-607 (Oxygen
                                           Fluorides)
Troe and Wagner   BBPCA-1967-71-937 (Oxygen
                                         Difluoride)

IV. REFERENCES

Asmus, T. W., "The Kinetics and Mechanism of the Pyrolysis
of Oxygen Difluoride and of the Reaction of Hydrogen
with Oxygen Difluoride," Dissertation Abstr. Intern.
B 31, 4606 (1971)

Axworthy, A. E., and Sullivan, J. M., "Kinetics of the Gas
Phase Pyrolysis of Chlorine Pentafluoride," J. Phys.
Chem. 74, 949 (1970)

Benson, S. W., and O'Neal, H. E., "Kinetic Data on Gas
Phase Unimolecular Reactions," Natl. Std. Ref. Data
Series NSRDS NBS 21, pg. 559 (1970)

Bernstein, R. B., and Katz, J. J., "Isotope Exchange Reactions
of Fluorine with Halogen Fluorides," J. Phys. Chem. 56,
885 (1952)

Blauer, J. A., McMath, H. G., and Jaye, F. C., "The Thermal
Dissociation of Chlorine Trifluoride behind Incident
Shock Waves," J. Phys. Chem. 73, 2683 (1969)

Blauer, J. A., McMath, H. G., Jaye, F. C., and Engleman, V. S.,
"Decomposition Kinetics of Chlorine Trifluoride and
Chlorine Pentafluoride," AF Rocket Propul. Lab., Edwards
AFB, Calif. AFRPL-TR-69-144; AD692493

Blauer, J. A., McMath, H. G., Jaye, F. C., and Engleman, V. S.,
"The Kinetics of Dissociation of Chlorine Pentafluoride,"
J. Phys. Chem. 74, 1183 (1970)

Blauer, J. A., and Solomon, W. C., "The Thermal Dissociation
of Oxygen Difluoride. I. Incident Shock Waves,"
J. Phys. Chem. 72, 2307 (1968)

Blauer, J. A., Solomon, W. C., and Engleman, V. S., "The
Kinetics of Chlorine Fluoride at High Temperatures,"
J. Phys. Chem. 75, 3939 (1971)

Bougon, R., "Chlorine Pentafluoride," Commis. Energ. At. (Fr.),
Rapp. 1970 CEA-R-3924; Chem. Abstr. 73:83318r (1970)

Brown, L. M., "Spectrophotometric Determination of the Rate
of Dissociation of Tetrafluorohydrazine behind a Shock
Wave," Dissertation Abstr. 25, 2774 (1964)

Brown, L. M., and Darwent, B. deB., "Spectrophotometric
Determination of the Rate of Dissociation of
Tetrafluorohydrazine Behind a Shock Wave," J. Chem.
Phys. 42, 2158 (1965)

234

Cherednikov, V. N., and Il'in, E. K., "Kinetics of the
    Reaction of Tetrafluorohydrazine with Fluorine,"
    Russ. J. Inorg. Chem. <u>13</u>, 1750 (1968)

Cherednikov, V. N., Pereverzev, V. S., and Ryabov, V. P.,
    "Kinetics of the Thermal Decomposition of
    Tetrafluorohydrazine," Russ. J. Inorg. Chem. <u>14</u>, 454
    (1969)

Clyne, M. A. A., and White, I. F., "Electronic Energy
    Transfer Processes in Fluorine-Containing Radicals:
    Singlet NF," Chem. Phys. Ltrs. <u>6</u>, 465 (1970)

Dauerman, L., Salser, G. E., and Tajima, Y. A., "The
    Thermal Decomposition of Oxygen Difluoride in a Flow
    System," J. Phys. Chem. <u>71</u>, 3999 (1967)

Dauerman, L., Salser, G. E., and Tajima, Y. A., "Comment on
    'The Thermal Dissociation of Oxygen Difluoride. I.
    Incident Shock Waves,'" J. Phys. Chem. <u>73</u>, 1621 (1969)

Diesen, R. W., "Observation and Kinetic Investigation of the
    NF and NF_2 Radicals," J. Chem. Phys. <u>41</u>, 3256 (1964)

Diesen, R. W., "Comment on NF_2 Decomposition behind Shock
    Waves," J. Chem. Phys. <u>45</u>, 759 (1966)

Fletcher, E. A., and Dahneke, B. E., "Kinetics of the
    Chlorine Fluoride Reaction," J. Am. Chem. Soc. <u>91</u>, 1603
    (1969)

Frisch, P., and Schumacher, H. J., "Das Thermische
    Verhalten des F_2O_2. Die Kinetik des Zerfalls und seine
    Beeinflussung Durch Fremdgase," Z. Elektrochem. <u>43</u>, 807
    (1937)

Frisch, P., and Schumacher, H.-J., "Der thermische Zerfall
    des Fluoroxyds F_2O_2," Z. Physik. Chem. B <u>34</u>, 322 (1936)

Frisch, P., and Schumacher, H.-J., "Der Einfluss der
    Zusatzgase O_2, F_2, N_2, Ar, He, CO_2, auf die
    Zerfallsgeschwindigkeit des F_2O_2," Z. Physik. Chem. <u>37</u>,
    18 (1937)

Gatti, R., Staricco, E., Sicre, J. E., and Schumacher, H.-J.,
    "Der photochemische Zerfall des F_2O," Z. Physik. Chem.
    [NF] (Frankfurt) <u>35</u>, 343 (1962)

Henrici, H., Lin, M. C., and Bauer, S. H., "Reactions of
    F_2O in Shock Waves. II. Kinetics and Mechanisms of the
    F_2O-CO Reaction," J. Chem. Phys. 52, 5834 (1970)

Koblitz, W., and Schumacher, H.-J., "Der thermische Zerfall
    des F_2O," Z. Physik. Chem. B 25, 283 (1934)

Kondratiev, V. N., "Konstanty Skorosti Gazofaznykh Reaktsij
    Spravochnik," (Handbook of Kinetic Constants of Gaseous
    Reactions) Izdatel'stvo "Nauka", Moscow (1970); also
    issued as "Rate Constants of Gas Phase Reactions,"
    Reference Book, Ed. R. M. Fristrom, translated by
    L. J. Holtschlag, NSRDS COM-72-10014 (1972)

Krieger, R. L., Gatti, R., and Schumacher, H.-J., "Die
    Kinetik der photochemischen Bildung von Chlorpentafluorid,
    ClF_5, aus Chlortrifluorid und Fluor," Z. Physik. Chem.
    [NF] (Frankfurt) 51, 240 (1966)

Levy, J. B., and Copeland, B. K. W., "The Kinetics of the
    Tetrafluorohydrazine-Fluorine Reaction," J. Phys. Chem.
    69, 3700 (1965)

Lin, M. C., and Bauer, S. H., "Reactions of Oxygen
    Fluoride in Shock Waves. I. Kinetics and Mechanism
    of Oxygen Fluoride Decomposition," J. Am. Chem. Soc. 91,
    7737 (1969)

McIntyre, J. A., and Diesen, R. W., "Mass Spectral Study of
    the Decomposition of Chlorine Fluoride Behind Shock
    Waves," Chem. Phys. Res. Lab., Dow Chem. CO., Midland,
    Mich. AD713938

McIntyre, J. A., and Diesen, R. W., "Mass Spectral Study of
    the Decomposition of Chlorine Fluoride behind Shock
    Waves," J. Phys. Chem. 75, 1765 (1971)

Modica, A. P., "Kinetics of the Thermal Dissociation of
    N_2F_4 in Shock Waves, Dissertation Abstr. 24, 4427 (1964)

Modica, A. P., and Hornig, D. F., "Kinetics of the Thermal
    Dissociation of N_2F_4 in Shock Waves," Frick Chem. Lab.,
    Princeton, N.J.; AD425108

Modica, A. P., and Hornig, D. F., "NF_2 Decomposition Behind
    Shock Waves," J. Chem. Phys. 43, 2739 (1965)

236

Modica, A. P., and Hornig, D. F., "Comment on NF_2 Decomposition behind Shock Waves," J. Chem. Phys. 45, 760 (1966)

Modica, A. P., and Hornig, D. F., "Kinetics of the Thermal Dissociation of N_2F_4 in Shock Waves," J. Chem. Phys. 49, 629 (1968)

Nikitin, I. V., and Rosolovskii, V. Ya., "Oxygen Fluorides and Dioxygenyl Compounds," Russ. Chem. Rev. 40, 889 (1971)

Rubinstein, M., Sicre, J. E., and Schumacher, H. J., "Die Kinetik der thermischen Reaktion zwischen Tetrafluorhydrazin und Fluormonoxid," Z. Physik. Chem. [NF] (Frankfurt) 43, 51 (1964)

San Roman, E. A., and Schumacher, H. J., "Die Kinetik der photochemischen Bildung von Chlortrifluorid im System Fluor-Chlormonofluorid," Z. Physik. Chem. [NF] (Frankfurt) 71, 153 (1970)

Schumacher, H. J., "Die Kinetik Chemischer Gasreaktionen," Z. Elektrochem. 47, 673 (1941)

Schumacher, H.-J., "Der thermische Zerfall des Fluoroxyds Ein Beitrag zur Theorie monomolekularer Reaktionen," Congr. Intern. Quim. Pura Apl., 9^0, Madrid, April 1934, 2, 485 (1935)

Schumacher, H.-J., and Frisch, P., "Die Kinetik des F_2O_2-Zerfalls," Z. Physik. Chem. 37, 1 (1937)

Solomon, W. C., Blauer, J. A., and Jaye, F. C., "The Thermal Dissociation of Oxygen Difluoride. II. Static Reactor," J. Phys. Chem. 72, 2311 (1968)

Staricco, E. H., Sicre, J. E., and Schumacher, H.-J., "Die photochemische Reaktion zwischen Fluor und Ozon," Z. Physik. Chem. [NF] (Frankfurt) 31, 385 (1962)

Streng, A. G., "The Oxygen Fluorides," Chem. Rev. 63, 607 (1963)

Sullivan, J. M., and Axworthy, A. E., "Kinetics of the Thermal Decomposition of Chlorinepentafluoride," Am. Chem. Soc., Abst. of Papers 155, J25 (1968)

Troe, J., and Wagner, H. Gg., "Unimolekulare Reaktionen in thermischen Systemen," Ber. Bunsenges. Physik. Chem. 71, 937 (1967)

Troe, J., Wagner, H. Gg., and Weden, G., "Zum unimolekularen Zerfall von F_2O," Z. Physik. Chem. [NF] (Frankfurt) 56, 238 (1967)

Wieder, G. M., and Marcus, R. A., "Dissociation and Isomerization of Vibrationally Excited Species. II. Unimolecular Reaction Rate Theory and Its Application," J. Chem. Phys. 37, 1835 (1962)

Wieder, G. M., "Unimolecular Reaction Rate Theory and Applications," Dissertation Abstr. 22, 104 (1961)

Zupnik, T. F., Nilson, E. N., and Sarli, V. J., "Investigation of Nonequilibrium Flow Effects in High Expansion Ratio Nozzles," United Aircraft Corp., East Hartford, Connecticut, NASA-CR-54042; N64-31452

NEW IDEAL-GAS THERMOCHEMICAL TABLES

S. Abramowitz, G. T. Armstrong, C. W. Beckett, K. L. Churney,

V. H. Dibeler, T. B. Douglas, J. T. Herron, R. F. Krause, Jr.,

K. E. McCulloh, M. L. Reilly, H. M. Rosenstock, and W. Tsang

Introduction

In the following pages of this report are collected together 31 new "JANAF-type" ideal-gas thermochemical tables recently generated in this program. The immediate purpose was to provide such tables for those gas species which are important in current chemical laser research, but for which present JANAF tables do not exist or are inconsistent with later, more accurate data. An updating literature survey (April to June, 1972) was carried out in an effort to base the new tables on as accurate and complete data as now exist. Even so, some of these tables are based on thermodynamic parameters which are not only of inferior accuracy but which may remain so for some time to come; whereas for several other gas species, tables of a higher order of accuracy could have been generated, but this has not been done because time was insufficient to review critically new data reported for them. Details may be found in the "JANAF-type" texts preceding the individual tables.

The tables and accompanying texts follow closely the format and conventions of the JANAF tables (JANAF Thermochemical Tables, 2nd Edition, NSRDS-NBS 37, June 1971, and subsequent looseleaf JANAF tables), which may be consulted for these details. Thus, for example, the temperature "298" in the tables really refers to 298.15K; the unit "gibbs" is 1 calorie per degree Kelvin; and the tables are in order of their alphabetical finding formulas, which appear in the upper-right-hand corners of the tables.

Certain differences from the JANAF tables need explanation. One major difference is the inclusion of tables for a number of chemical species containing deuterium (designated by D instead of by ^{2}H) as well as the analogous species containing the "light-hydrogen" isotope (designated by H instead of by ^{1}H). In this connection it is to be noted that the tables (but not the table texts) for the light-hydrogen species are equally applicable to the natural isotopic mixture (approximately 99.98% H and 0.02% D), since the molar thermodynamic properties of the different pure-isotope varieties differ by only a few percent at the temperatures here tabulated. For hydrogen-containing species the gram-formula-masses (GFW) and molecular constants given with these tables are to be understood as specific for the particular hydrogen isotope(s) in the chemical formula, but averaged (by adjustment of reported values when necessary) for the natural-isotopic mixture of the other elements such as chlorine, unless otherwise stated.

It is important to identify unambiguously the particular chemical-element reference-state tables on which the computation of the present tables (last three columns) is based. For four elements these are the presently latest JANAF reference-state tables, which are not reproduced here: Cl_2, O_2, and N_2 (each dated Sept. 30, 1965) and S (dated Dec. 31, 1965). But for the three remaining elements-- fluorine, hydrogen (i.e., ^{1}H), and deuterium--the reference-state tables used are not JANAF tables but those included here. (As ex- plained in the table texts for H_2 and D_2, these two tables are for the ortho-para "equilibrium" varieties at all temperatures; as tabulated, the values differ from those for the more commonly encountered "normal" varieties only at 0 K, 100 K, and 200 K, but interpolation over 100-degree intervals below 298.15 K would be inaccurate anyhow.)

The practical approximations used in computing the ideal-gas thermodynamic functions from the available molecular constants follow, in general, those used for the JANAF tables. In particular, the functions for the diatomic species account for anharmonicity, stretch- ing, and vibration-rotation interaction by the use of the same closed- bracket approximation formulas, whereas the polyatomic-species functions

/are based on the harmonic-oscillator rigid-rotor approximation. But, as in the JANAF tables, there are exceptions here too: the tables for H_2, HDO, D_2O, H_2S, and NH_3 were taken (with minor interpolation and extrapolation) directly from authors who used direct-summation methods, and these tables were used to adjust the tables for HD, D_2, D_2S, and ND_3 to a somewhat comparable degree of refinement, as described in the respective table texts for the last four species. In certain other cases (see the tables for OH, OD, SH, and SD) this refinement of the tables was not carried out for lack of time; the types of errors are indicated in the discussions of heat capacity and entropy.

For each of several molecules, substantially different molecular constants have been reported for the ground and some of the excited electronic states. In this case the partition function cannot be factored rigorously into electronic and molecular contributions, but a simple approximation was used which is satisfactorily accurate in many cases. Using respectively subscripts t, v, r, and e for translational, vibrational, rotational, and electronic, and superscripts i=0 and i for the ground and an excited electronic state, the total molecular partition function Q can be expressed exactly by

$$Q = Q_t Q_v^{i=0} Q_r^{i=0} [Q_e^{i=0} + \Sigma_i (Q_v^i Q_r^i / Q_v^{i=0} Q_r^{i=0}) Q_e^i]. \tag{1}$$

The parenthesized factor in Eq (1) was approximated as follows. For vibrational mode v we have in the harmonic approximation

$$Q_v^i \sim k T/hc\omega^i \tag{2}$$

if $(kT/hc\omega^i) \gg 1$. Using Eq (2) and the usual rigid-rotor high-temperature expressions for Q_r^i, it can be readily shown that for a linear molecule

$$(Q_v^i Q_r^i / Q_v^{i=0} Q_r^{i=0}) \sim (I^i / I^{i=0}) \Pi_v (\omega_v^{i=0} / \omega_v^i)^g =$$

$$(B^{i=0}/B^i) \Pi_v (\omega_v^{i=0}/\omega_v^i)^g, \tag{3}$$

and for a non-linear molecule

$$Q_v^i Q_r^i / Q_v^{i=0} Q_r^{i=0} \simeq (I_A^i I_B^i I_C^i / I_A^{i=0} I_B^{i=0} I_C^{i=0})^{1/2} \Pi_v (\omega_v^{i=0}/\omega_v^i)^g =$$

$$(B_A^{i=0} B_B^{i=0} B_C^{i=0}) / B_A^i B_B^i B_C^i)^{1/2} \Pi_v (\omega_v^{i=0}/\omega_v^i)^g, \tag{4}$$

where the various moments of inertia are represented by I, and the degeneracy of vibrational state v by g. (The electronic degeneracies are included in Q_e as defined. The rigid-rotor harmonic-oscillator approximation is not used for the $Q_v^{i=0}$ and $Q_r^{i=0}$ outside the brackets in Eq (1) when the necessary molecular constants are available.)

The errors resulting from using Eq (3) or (4) may be illustrated by the contributions of the ν_2 vibrational mode, the doublet ground state ($\omega = 1497$ cm^{-1}), and a doublet excited (10249 cm^{-1}) state ($\omega = 633$ cm^{-1}) of NH_2. These errors were calculated to be, at 6000 K (and in cal mole^{-1} deg K^{-1}): C_P^o, -0.018; S^o, + 0.068; $-(G^o-H_0^o)/T$, + 0.032. These errors are several times smaller than would result from the simpler approximation (commonly used) of taking 1497 cm^{-1} for both fundamentals. At lower temperatures the poorer approximation involved in Eq (2) is overshadowed by the exponentially decreasing value of the factor Q_e^i in Eq (1).

Several species of current interest in laser research may be listed together with the reasons why no ideal-gas thermochemical tables for them were generated at the present time: (a) H_2O, F (atomic), and HCl (no basis of improvement over the existing JANAF tables--however, for the first two of these, revisions of the JANAF discussions of the heats of formation seemed warranted, and these are given following the present 31 tables); (b) NCl, ClO, OF, OF_2, NF, NF_2, and N_2F_2 (cis and trans) (insufficient review of the heat-of-formation data); (c) N_2F_4 (trans and gauche), N_2H_4, and N_2D_4 (unsatisfactory means available to account accurately for the contributions of restricted internal rotation--however, JANAF tables do exist for the first two); (d) radicals such as N_2H, and peroxides such as SOO (no data found).

Finally, it is appropriate to point out here some generalities with regard to six of the present "JANAF-type" table texts. In the first place, as stated in the discussions of the heats of formation of HD, DF, and DCl, these three data reviews are to be regarded as incomplete because they omit analyses of experimental or theoretical work which was found too late to be considered. In the second place, three revisions over existing JANAF tables were made (thermodynamic functions of F_2, and the heats of formation of $C\ell F$ and atomic F) which, it appears, may warrant the revision of existing JANAF tables for many other species which properly depend on them; however, these propagated consequences were not examined in detail.

$S^°_{298.15}$ = 46.04 cal $K^{-1}mol^{-1}$ $\Delta Hf^°_{298.15}$ = -22.31 ± 0.05 kcal mol^{-1}

Electronic States and Molecular Constants

State	ϵ, cm^{-1}	g	ω_e, cm^{-1}	$\chi_e\omega_e$, cm^{-1}	B_e, cm^{-1}	α_e, cm^{-1}	r_e, Å
$X^1\Sigma^+$	0	1	2144.0	26.90	5.4444	0.1121	1.2746
$B^1\Pi$	75160	2	2199.0	[26.9]	5.1793	[0.1121]	
$V^1\Sigma^+$	76520	1	684.6	[26.9]	1.555	[0.1121]	2 43
$C^1\Pi$	77525	2	2114.1	[26.9]	4.9605	[0.1121]	

σ = 1

Heat of Formation (Provisional-evaluation incomplete)

The heat of formation was calculated from the selected value of $\Delta Hf^°_{298}$ of HCl(g) given by JANAF (1), the appropriate thermal functions (see H_2, D_2, DCl tables, and HCl (1)) and zero point energies. The zero point energies of H_2(g), D_2(g) are taken from Herzberg and Monfils (2). The zero point energies of HCl(g) and DCl(g), including the Dunham correction, were calculated from the molecular constants taken from Rosen (3).

Heat Capacity and Entropy

The vibrational and rotational constants at the respective electronic levels were taken from Rosen (3) and were adjusted to Cl^{35} = 75.4% and Cl^{37} = 24.6%.

References

1. JANAF Thermochemical Tables, 2nd Edition, NSRDS-NBS 37, June, 1971 (U. S. Govt. Printing Office, Washington, D. C., 20402).
2. G. Herzberg and A. Monfils, J. Molec. Spectroscopy 5, 482 (1960).
3. B. Rosen, Spectroscopic Data Relative to Diatomic Molecules (Pergamon Press, Oxford, 1970).

(IDEAL GAS)   GFW = 37.4671

T, °K	Cp°	S°	$-(G°-H°_{298})/T$	$H°-H°_{298}$	$\Delta Hf°$	$\Delta Gf°$	Log Kp
		gibbs/mol			kcal/mol		
0	.000	.000	INFINITE	-2.070	-22.259	-22.259	INFINITE
100	6.958	38.435	52.230	-1.379	-22.245	-22.484	49.140
200	6.961	43.259	46.676	-.684	-22.265	-22.718	24.825
298	6.972	46.039	46.039	.000	-22.310	-22.931	16.809
300	6.972	46.082	46.039	.013	-22.311	-22.935	16.708
400	7.026	48.094	46.313	.712	-22.375	-23.134	12.640
500	7.149	49.674	46.833	1.421	-22.444	-23.315	10.191
600	7.316	50.992	47.419	2.144	-22.508	-23.484	8.554
700	7.501	52.134	48.013	2.884	-22.563	-23.642	7.381
800	7.682	53.147	48.593	3.644	-22.607	-23.793	6.500
900	7.849	54.062	49.150	4.420	-22.644	-23.939	5.813
1000	7.999	54.897	49.684	5.213	-22.673	-24.082	5.263
1100	8.130	55.665	50.193	6.020	-22.696	-24.221	4.812
1200	8.244	56.378	50.679	6.838	-22.716	-24.359	4.436
1300	8.342	57.042	51.143	7.668	-22.730	-24.496	4.118
1400	8.429	57.663	51.587	8.506	-22.744	-24.631	3.845
1500	8.504	58.247	52.012	9.353	-22.755	-24.765	3.608
1600	8.570	58.798	52.419	10.207	-22.768	-24.899	3.401
1700	8.628	59.319	52.810	11.067	-22.779	-25.031	3.218
1800	8.680	59.814	53.185	11.932	-22.789	-25.164	3.055
1900	8.726	60.285	53.546	12.803	-22.799	-25.295	2.910
2000	8.768	60.733	53.895	13.677	-22.809	-25.426	2.778
2100	8.806	61.162	54.231	14.556	-22.821	-25.558	2.660
2200	8.840	61.573	54.555	15.439	-22.832	-25.687	2.552
2300	8.872	61.966	54.869	16.324	-22.844	-25.816	2.453
2400	8.901	62.344	55.172	17.213	-22.857	-25.945	2.363
2500	8.928	62.708	55.467	18.104	-22.870	-26.073	2.279
2600	8.953	63.059	55.752	18.998	-22.886	-26.201	2.202
2700	8.976	63.397	56.029	19.895	-22.901	-26.328	2.131
2800	8.998	63.724	56.298	20.794	-22.918	-26.454	2.065
2900	9.019	64.040	56.560	21.694	-22.939	-26.581	2.003
3000	9.039	64.346	56.814	22.597	-22.958	-26.706	1.946
3100	9.057	64.643	57.062	23.502	-22.982	-26.831	1.892
3200	9.075	64.931	57.303	24.409	-23.003	-26.955	1.841
3300	9.092	65.211	57.539	25.317	-23.028	-27.079	1.793
3400	9.109	65.482	57.768	26.227	-23.053	-27.200	1.748
3500	9.124	65.745	57.992	27.139	-23.083	-27.323	1.706
3600	9.140	66.004	58.211	28.052	-23.111	-27.441	1.666
3700	9.154	66.254	58.425	28.967	-23.145	-27.562	1.628
3800	9.169	66.499	58.635	29.883	-23.179	-27.683	1.592
3900	9.183	66.737	58.839	30.801	-23.216	-27.800	1.558
4000	9.196	66.970	59.040	31.719	-23.253	-27.918	1.525
4100	9.209	67.197	59.236	32.640	-23.292	-28.035	1.494
4200	9.222	67.419	59.428	33.561	-23.332	-28.149	1.465
4300	9.235	67.636	59.617	34.484	-23.372	-28.264	1.437
4400	9.247	67.849	59.801	35.408	-23.415	-28.374	1.409
4500	9.259	68.056	59.982	36.334	-23.462	-28.491	1.384
4600	9.271	68.260	60.160	37.260	-23.507	-28.600	1.359
4700	9.283	68.460	60.335	38.188	-23.553	-28.709	1.335
4800	9.294	68.655	60.506	39.117	-23.599	-28.817	1.312
4900	9.306	68.847	60.674	40.047	-23.648	-28.925	1.290
5000	9.317	69.035	60.840	40.978	-23.699	-29.035	1.269
5100	9.328	69.220	61.002	41.910	-23.750	-29.139	1.249
5200	9.339	69.401	61.162	42.843	-23.801	-29.245	1.229
5300	9.350	69.579	61.319	43.778	-23.853	-29.351	1.210
5400	9.360	69.754	61.474	44.713	-23.905	-29.452	1.192
5500	9.371	69.926	61.626	45.650	-23.959	-29.556	1.174
5600	9.381	70.095	61.775	46.587	-24.012	-29.657	1.157
5700	9.392	70.261	61.923	47.526	-24.067	-29.759	1.141
5800	9.402	70.424	62.068	48.466	-24.122	-29.856	1.125
5900	9.412	70.585	62.211	49.406	-24.178	-29.957	1.110
6000	9.423	70.743	62.352	50.348	-24.234	-30.053	1.095

July 31, 1972

$S^°_{298.15}$ = 52.157 cal K^{-1}mol^{-1} $\Delta Hf^°_{298.15}$ = -12.02 ± 0.1 kcal mol^{-1}

Electronic States and Molecular Constants

State	ε, cm^{-1}	g	ω_e, cm^{-1}	$\chi_e\omega_e$, cm^{-1}	B_e, cm^{-1}	α_e, cm^{-1}	r_e, Å
$X^1\Sigma^+$	0	1	784.49	6.201	0.51409	0.04329	1.6281
$A^3\Pi_0$	18721	6	312.74	2.207	0.37026	0.01390	1.92

σ = 1

Heat of Formation

The selected value, $\Delta Hf^°_{298}$ (ClF) = -12.0 ± 0.1 kcal mol^{-1}, is based on spectroscopy. Three studies of the visible absorption bands of ClF, by A. L. Wahrhaftig, J. Chem. Phys. 10, 248 (1942), by H. Schmitz and H. J. Schumacher, Z. Naturforsch. 29, 359 (1947), and by W. Stricker, Deutsche Luft-und Raumfahrt Forschungsbericht 66-04 (1966) agree in indicating a band convergence limit at 21,514 ± 10 cm^{-1}. Assignment of this limit to Cl($^2P_{1/2}$) + F($^2P_{3/2}$) is supported by the dissociative ionization threshold for ClF reported by V. H. Dibeler, J. A. Walker, and K. E. McCulloh, J. Chem. Phys. 53, 4414 (1970), whose ion-pair threshold, when reassigned to a hot band, corroborates this choice. From this assignment it follows that $D^°_0$(ClF) = 58.98 ± 0.02 kcal mol^{-1}.

Combining this value with $D^°_0$(F_2) = 36.7 ± 0.2 kcal mol^{-1}, reported by J. Berkowitz, W. A. Chupka, P. M. Guyon, J. H. Holloway, and R. Spohr, J. Chem. Phys. 54, 5165 (1971), and with $D^°_0$(Cl_2) = 57.177 ± 0.006 kcal mol^{-1}, given by A. E. Douglas, C. K. Möller, and B. P. Stoicheff, Can. J. Phys. 41, 1174 (1963), one obtains $\Delta Hf^°_0$(ClF) = -12.0 ± 0.1 kcal mol^{-1}.

Calorimetric values for $\Delta Hf^°_{298}$, which bracket the selected value, are as follows: -11.6 kcal mol^{-1}, E. Wicke, Nachr. Akad. Wiss. Göttingen Math-Phys. Klasse p. 89 (1946); -11.7 kcal mol^{-1}, E. Wicke and H. Friz, Z. Elektrochem. 57, 9 (1953); -14.34 and -15.0 kcal mol^{-1}, H. Schmitz and H. J. Schumacher, Z. Naturforsch 29, 362 (1947); and -14.4 ± 0.8 kcal mol^{-1}, R. L. Nuttall and G. T. Armstrong, NBS Report 10326, Chapter 1, July 1, 1970.

Heat Capacity and Entropy

The vibrational and rotational constants of the respective electronic levels were taken from B. Rosen, Spectroscopic Data Relative to Diatomic Molecules, Pergamon Press, Oxford, 1970, and were adjusted to Cl^{35} = 75.4% and Cl^{37} = 24.6%.

CHLORINE MONOFLUORIDE (ClF)

(IDEAL GAS)   GFW = 54.4514

T, °K	Cp°	S°	--(G°−H°₂₉₈)/T	H°−H°₂₉₈	ΔHf°	ΔGf°	Log Kp
		gibbs/mol			kcal/mol		
0	.000	.000	INFINITE	−2.133	−12.002	−12.002	INFINITE
100	6.961	44.303	58.685	−1.438	−12.002	−12.140	26.533
200	7.219	49.181	52.846	−.733	−12.010	−12.276	13.415
298	7.723	52.156	52.156	.000	−12.020	−12.405	9.093
300	7.732	52.204	52.157	.014	−12.020	−12.407	9.039
400	8.160	54.491	52.465	.810	−12.024	−12.536	6.849
500	8.459	56.345	53.062	1.642	−12.021	−12.663	5.535
600	8.670	57.907	53.743	2.499	−12.013	−12.793	4.660
700	8.824	59.256	54.436	3.374	−12.001	−12.924	4.035
800	8.943	60.442	55.114	4.263	−11.986	−13.057	3.567
900	9.039	61.501	55.766	5.162	−11.968	−13.191	3.203
1000	9.120	62.458	56.388	6.070	−11.947	−13.329	2.913
1100	9.190	63.331	56.980	6.985	−11.922	−13.468	2.676
1200	9.254	64.133	57.543	7.908	−11.896	−13.610	2.479
1300	9.311	64.876	58.079	8.836	−11.866	−13.754	2.312
1400	9.365	65.568	58.590	9.770	−11.834	−13.901	2.170
1500	9.416	66.216	59.077	10.709	−11.799	−14.049	2.047
1600	9.465	66.825	59.542	11.653	−11.762	−14.200	1.940
1700	9.512	67.400	59.988	12.602	−11.722	−14.353	1.845
1800	9.559	67.945	60.415	13.555	−11.680	−14.509	1.762
1900	9.606	68.464	60.825	14.514	−11.634	−14.667	1.687
2000	9.654	68.957	61.219	15.477	−11.587	−14.828	1.620
2100	9.704	69.430	61.599	16.444	−11.536	−14.992	1.560
2200	9.757	69.882	61.965	17.417	−11.482	−15.158	1.506
2300	9.814	70.317	62.319	18.396	−11.424	−15.326	1.456
2400	9.878	70.736	62.661	19.380	−11.363	−15.497	1.411
2500	9.945	71.141	62.992	20.372	−11.296	−15.671	1.370
2600	10.028	71.533	63.313	21.370	−11.224	−15.847	1.332
2700	10.117	71.913	63.625	22.378	−11.146	−16.027	1.297
2800	10.218	72.282	63.927	23.394	−11.061	−16.208	1.265
2900	10.331	72.643	64.222	24.422	−10.966	−16.394	1.235
3000	10.455	72.995	64.508	25.461	−10.863	−16.583	1.208
3100	10.599	73.340	64.788	26.514	−10.748	−16.776	1.183
3200	10.755	73.679	65.060	27.581	−10.621	−16.972	1.159
3300	10.926	74.013	65.326	28.665	−10.479	−17.173	1.137
3400	11.112	74.342	65.587	29.767	−10.322	−17.378	1.117
3500	11.313	74.667	65.842	30.888	−10.148	−17.588	1.098
3600	11.529	74.988	66.091	32.030	−9.955	−17.803	1.081
3700	11.758	75.307	66.336	33.194	−9.742	−18.023	1.065
3800	12.000	75.624	66.576	34.382	−9.508	−18.251	1.050
3900	12.253	75.939	66.812	35.595	−9.251	−18.485	1.036
4000	12.517	76.253	67.044	36.833	−8.970	−18.725	1.023
4100	12.789	76.565	67.273	38.098	−8.664	−18.972	1.011
4200	13.068	76.877	67.498	39.391	−8.332	−19.228	1.001
4300	13.351	77.187	67.719	40.712	−7.975	−19.492	.991
4400	13.638	77.498	67.938	42.061	−7.590	−19.763	.982
4500	13.926	77.807	68.154	43.440	−7.177	−20.044	.973
4600	14.213	78.117	68.367	44.947	−6.737	−20.335	.966
4700	14.496	78.425	68.578	46.292	−6.271	−20.635	.960
4800	14.778	78.733	68.786	47.746	−5.777	−20.947	.954
4900	15.048	79.041	68.993	49.237	−5.258	−21.268	.949
5000	15.313	79.349	69.197	50.755	−4.711	−21.602	.944
5100	15.565	79.653	69.399	52.299	−4.140	−21.943	.940
5200	15.812	79.958	69.599	53.868	−3.545	−22.296	.937
5300	16.044	80.261	69.797	55.461	−2.928	−22.665	.935
5400	16.262	80.563	69.994	57.077	−2.289	−23.043	.933
5500	16.467	80.864	70.189	58.713	−1.629	−23.432	.931
5600	16.656	81.162	70.382	60.369	−.951	−23.835	.930
5700	16.831	81.459	70.574	62.044	−.255	−24.252	.930
5800	16.990	81.753	70.764	63.735	.457	−24.678	.930
5900	17.134	82.044	70.952	65.441	1.182	−25.118	.930
6000	17.262	82.333	71.140	67.161	1.921	−25.570	.931

July 31, 1972

$S^\circ_{298.15}$ = 42.923 cal K^{-1}mol^{-1} $\Delta Hf^\circ_{298.15}$ = -65.85 ± 0.2 kcal mol^{-1}

Electronic States and Molecular Constants

State	ϵ, cm^{-1}	g	ω_e, cm^{-1}	$\chi_e\omega_e$, cm^{-1}	B_e, cm^{-1}	α_e, cm^{-1}	r_e, Å
$X^1\Sigma^+$	0	1	2998.19	45.76	11.000	0.2907	0.9187
$V^1\Sigma^+$	83755	1	839.4	8.90	2.121	0.00712	2.088

$\sigma = 1$

Heat of Formation

The heat of formation was calculated from ΔHf°_{298} of HF(g), -65.14 ± 0.2 kcal mol^{-1}, given in JANAF Thermochemical Tables 2nd Edition, NSRDS—NBS 37, June (1971), the appropriate thermal functions (see tables for H_2, D_2, DF and HF (JANAF loc. cit.)) and the estimated zero point energies. The energies for H_2(g), D_2(g) are those given by G. Herzberg and A. Monfils, J. Molec. Spectroscopy 5, 482 (1960). The energies for HF(g) and DF(g) include the Dunham correction and were calculated from the data given by D. E. Mann, B. A. Thrush, D. R. Lide, Jr., J. J. Ball, and N. Acquista, J. Chem. Phys. 34, 420 (1961) and R. N. Spanbauer, K. N. Rao and L. H. Jones, J. Molec. Spectroscopy 16, 100 (1965).

Heat Capacity and Entropy

The vibrational and rotational constants of the respective electronic levels were taken from B. Rosen, Spectroscopic Data Relative to Diatomic Molecules, Pergamon Press, Oxford, 1970.

Deuterium Fluoride (DF)

(Ideal Gas)   GFW = 21.0125

T, °K	Cp°	S°	−(G°−H°₂₉₈)/T	H°−H°₂₉₈	ΔHf°	ΔGf°	Log Kp
		gibbs/mol			kcal/mol		
0	.000	.000	INFINITE	−2.065	−65.836	−65.836	INFINITE
100	6.959	35.319	49.112	−1.379	−65.827	−65.977	144.193
200	6.961	40.143	43.560	−.683	−65.834	−66.125	72.258
298	6.964	42.923	42.923	.000	−65.850	−66.265	48.573
300	6.964	42.966	42.923	.013	−65.851	−66.267	48.276
400	6.973	44.970	43.196	.710	−65.887	−66.401	36.280
500	7.002	46.529	43.713	1.408	−65.941	−66.524	29.077
600	7.065	47.811	44.292	2.111	−66.005	−66.635	24.272
700	7.151	48.907	44.875	2.822	−66.075	−66.734	20.835
800	7.251	49.870	45.440	3.544	−66.144	−66.823	18.255
900	7.413	50.735	45.981	4.279	−66.214	−66.904	16.246
1000	7.548	51.523	46.497	5.027	−66.281	−66.978	14.638
1100	7.681	52.249	46.987	5.788	−66.343	−67.043	13.320
1200	7.806	52.923	47.454	6.563	−66.403	−67.105	12.222
1300	7.922	53.552	47.899	7.349	−66.457	−67.161	11.291
1400	8.029	54.143	48.324	8.147	−66.509	−67.214	10.493
1500	8.126	54.701	48.731	8.955	−66.558	−67.262	9.800
1600	8.215	55.228	49.121	9.772	−66.606	−67.307	9.194
1700	8.295	55.729	49.495	10.597	−66.651	−67.350	8.658
1800	8.367	56.205	49.854	11.431	−66.693	−67.390	8.182
1900	8.433	56.659	50.201	12.271	−66.735	−67.428	7.756
2000	8.493	57.093	50.535	13.117	−66.774	−67.462	7.372
2100	8.547	57.509	50.857	13.969	−66.815	−67.497	7.024
2200	8.597	57.908	51.168	14.926	−66.852	−67.527	6.708
2300	8.643	58.291	51.470	15.688	−66.889	−67.557	6.419
2400	8.685	58.659	51.762	16.555	−66.926	−67.586	6.155
2500	8.724	59.015	52.045	17.425	−66.961	−67.613	5.911
2600	8.760	59.358	52.319	18.299	−66.998	−67.638	5.685
2700	8.793	59.689	52.586	19.177	−67.033	−67.662	5.477
2800	8.825	60.009	52.846	20.058	−67.069	−67.684	5.283
2900	8.854	60.319	53.098	20.942	−67.106	−67.705	5.102
3000	8.881	60.620	53.344	21.829	−67.141	−67.725	4.934
3100	8.907	60.912	53.583	22.718	−67.179	−67.744	4.776
3200	8.932	61.195	53.817	23.610	−67.214	−67.762	4.628
3300	8.955	61.470	54.044	24.505	−67.250	−67.780	4.489
3400	8.977	61.738	54.267	25.401	−67.286	−67.795	4.358
3500	8.998	61.998	54.484	26.300	−67.325	−67.809	4.234
3600	9.018	62.252	54.696	27.201	−67.362	−67.822	4.117
3700	9.037	62.499	54.904	28.103	−67.403	−67.834	4.007
3800	9.055	62.741	55.107	29.008	−67.444	−67.845	3.902
3900	9.073	62.976	55.306	29.914	−67.487	−67.857	3.803
4000	9.090	63.206	55.500	30.823	−67.528	−67.866	3.708
4100	9.106	63.431	55.691	31.732	−67.572	−67.874	3.618
4200	9.122	63.650	55.878	32.644	−67.615	−67.879	3.532
4300	9.136	63.865	56.061	33.557	−67.659	−67.885	3.450
4400	9.152	64.075	56.241	34.471	−67.705	−67.889	3.372
4500	9.167	64.281	56.417	35.387	−67.754	−67.895	3.297
4600	9.181	64.483	56.591	36.305	−67.802	−67.896	3.226
4700	9.195	64.680	56.761	37.224	−67.851	−67.898	3.157
4800	9.208	64.874	56.928	38.144	−67.900	−67.896	3.091
4900	9.222	65.064	57.092	39.065	−67.952	−67.896	3.028
5000	9.234	65.251	57.253	39.988	−68.007	−67.897	2.968
5100	9.247	65.434	57.412	40.912	−68.061	−67.893	2.909
5200	9.259	65.613	57.568	41.837	−68.116	−67.889	2.853
5300	9.272	65.790	57.721	42.764	−68.173	−67.885	2.799
5400	9.283	65.963	57.872	43.692	−68.230	−67.878	2.747
5500	9.295	66.134	58.021	44.621	−68.289	−67.972	2.697
5600	9.307	66.301	58.167	45.551	−68.349	−67.863	2.648
5700	9.318	66.466	58.311	46.482	−68.410	−67.855	2.602
5800	9.329	66.628	58.453	47.414	−68.473	−67.845	2.556
5900	9.341	66.788	58.593	48.348	−68.537	−67.833	2.513
6000	9.351	66.945	58.731	49.282	−68.601	−67.920	2.470

July 31, 1972

DEUTERIUM HYDRIDE (HD, or $^1H^2H$) (IDEAL GAS) GFW = 3.0221

$D_0^\circ = 104.089 \pm 0.002$ kcal mol^{-1} $\Delta Hf_0^\circ = 0.078 \pm .002$ kcal mol^{-1}

$S_{298.15}^\circ = 34.345 \pm 0.01$ cal deg^{-1}mol^{-1} $\Delta Hf_{298.15}^\circ = 0.076 \pm .002$ kcal mol^{-1}

Ground State Configuration $^1\Sigma_g^+$

$\omega_e = 3817.09$ cm^{-1} $\omega_e x_e = 94.958$ cm^{-1} $D_e = 0.02614$ cm^{-1} $\sigma = 1$

$B_e = 45.655$ cm^{-1} $\alpha_e = 1.9927$ cm^{-1} $r_e = 0.7414$ Å

Heat of Formation (Provisional-evaluation incomplete)

The heat of formation of HD ($^1H^2H$) was calculated using zero point energies of H_2, D_2 and HD using the Dunham formulation as given by G. Herzberg and A. Monfils (1). The value obtained is consistent with the D_0° values given by G. Herzberg (2) in a later publication. The estimated uncertainty is based on the uncertainties assigned to the zero point energies (1).

Heat Capacity and Entropy

The thermodynamic functions were generated similarly as those in the table for D_2 (q.v.). To the current table for H_2 (which is based on reference 3) was added to the table for HD from reference 4, and the table for "equilibrium" H_2 from reference 3 was subtracted.

References

1. G. Herzberg and A. Monfils, J. Mol. Spectroscopy 5, 482 (1960).
2. G. Herzberg, J. Mol. Spectroscopy 33, 147 (1970).
3. H. W. Woolley, R. B. Scott, and F. G. Brickwedde, J. Research Nat. Bur. Standards 41, 379 (1948).
4. L. Haar, A. S. Friedman, and C. W. Beckett, Nat. Bur. Standards Monograph 20, U. S. Government Printing Office, Washington, D. C., 1961.

(IDEAL GAS)   GFW = 3.0221

| T, °K | gibbs/mol | | | H°−H°₂₉₈ | kcal/mol | | Log Kp |
	Cp°	S°	−(G°−H°₂₉₈)/T		ΔHf°	ΔGf°	
0	.000	.000	INFINITE	-2.034	.078	.078	INFINITE
100	6.982	26.723	40.547	-1.382	.042	-.081	.176
200	6.974	31.559	34.983	-.685	.065	-.212	.231
298	6.978	34.345	34.345	.000	.076	-.350	.257
300	6.978	34.388	34.345	.013	.076	-.353	.257
400	6.985	36.395	34.619	.710	.078	-.496	.271
500	6.997	37.955	35.136	1.410	.078	-.640	.279
600	7.024	39.232	35.714	2.111	.076	-.783	.285
700	7.072	40.319	36.296	2.816	.073	-.926	.289
800	7.150	41.268	36.860	3.526	.069	-1.069	.292
900	7.240	42.116	37.397	4.247	.064	-1.211	.294
1000	7.338	42.881	37.908	4.973	.058	-1.352	.296
1100	7.443	43.587	38.393	5.713	.053	-1.493	.297
1200	7.551	44.240	38.853	6.464	.049	-1.633	.297
1300	7.665	44.848	39.291	7.224	.045	-1.773	.298
1400	7.785	45.420	39.709	7.995	.040	-1.913	.298
1500	7.910	45.962	40.108	8.781	.036	-2.052	.299
1600	8.015	46.476	40.490	9.578	.033	-2.192	.299
1700	8.113	46.965	40.856	10.385	.030	-2.330	.300
1800	8.206	47.431	41.208	11.201	.027	-2.468	.300
1900	8.294	47.877	41.548	12.025	.024	-2.609	.300
2000	8.377	48.305	41.875	12.860	.022	-2.746	.300
2100	8.455	48.716	42.191	13.702	.020	-2.885	.300
2200	8.529	49.111	42.497	14.551	.019	-3.023	.301
2300	8.599	49.491	42.793	15.405	.017	-3.161	.301
2400	8.664	49.859	43.080	16.270	.016	-3.300	.301
2500	8.727	50.213	43.358	17.138	.015	-3.438	.301
2600	8.785	50.557	43.628	18.015	.014	-3.574	.301
2700	8.841	50.890	43.891	18.897	.013	-3.713	.301
2800	8.892	51.212	44.147	19.782	.012	-3.851	.301
2900	8.939	51.525	44.396	20.674	.012	-3.988	.301
3000	8.983	51.829	44.638	21.573	.011	-4.126	.301
3100	9.030	52.123	44.875	22.469	.008	-4.264	.301
3200	9.076	52.411	45.106	23.376	.009	-4.402	.301
3300	9.122	52.692	45.332	24.288	.010	-4.542	.301
3400	9.166	52.964	45.552	25.201	.010	-4.677	.301
3500	9.211	53.231	45.768	26.120	.010	-4.817	.300
3600	9.255	53.491	45.979	27.043	.009	-4.953	.300
3700	9.299	53.745	46.186	27.968	.008	-5.095	.300
3800	9.342	53.994	46.388	28.903	.008	-5.233	.300
3900	9.384	54.237	46.586	29.839	.008	-5.370	.300
4000	9.426	54.475	46.780	30.780	.008	-5.508	.300
4100	9.467	54.708	46.970	31.726	.009	-5.644	.300
4200	9.507	54.937	47.157	32.676	.010	-5.781	.300
4300	9.547	55.161	47.341	33.624	.009	-5.920	.300
4400	9.586	55.381	47.522	34.580	.008	-6.060	.301
4500	9.625	55.596	47.698	35.541	.008	-6.197	.301
4600	9.663	55.809	47.872	36.510	.009	-6.332	.301
4700	9.700	56.017	48.044	37.473	.010	-6.473	.301
4800	9.736	56.222	48.212	38.448	.012	-6.608	.301
4900	9.772	56.423	48.377	39.425	.013	-6.745	.301
5000	9.808	56.620	48.540	40.400	.012	-6.884	.301
5100	9.843	56.815	48.701	41.383	.010	-7.021	.301
5200	9.878	57.006	48.858	42.369	.010	-7.160	.301
5300	9.913	57.195	49.014	43.358	.010	-7.291	.301
5400	9.948	57.380	49.167	44.351	.011	-7.435	.301
5500	9.981	57.563	49.318	45.347	.011	-7.574	.301
5600	10.015	57.743	49.467	46.346	.011	-7.714	.301
5700	10.048	57.920	49.613	47.349	.012	-7.853	.301
5800	10.081	58.096	49.759	48.356	.012	-7.986	.301
5900	10.113	58.268	49.901	49.365	.012	-8.125	.301
6000	10.144	58.438	50.042	50.378	.013	-8.264	.301

July 31, 1972

Point Group C_h $\Delta Hf_0^\circ = -57.943 \pm 0.015$ kcal mol^{-1}

$S_{298.15}^\circ = 47.658$ cal deg^{-1} mol^{-1} $\Delta Hf_{298.15}^\circ = -58.645 \pm 0.015$ kcal mol^{-1}

Ground State Quantum Weight = 1

Vibrational Levels and Multiplicities

ω, cm^{-1}

2723.66 (1)
1402.80 (1)
3707.47 (1)

Bond Lengths and Angle: O-H Distance = 0.9584Å $\sigma = 1$
                          O-D Distance = 0.9584Å
                          H-O-D Angle = 104.45°
Product of Moments of Inertia: $I_A I_B I_C = 15.827 \times 10^{-120}$ g^3 cm^6

Heat of Formation

Third and second law (where possible) analyses of the more recent determinations (1-5) of the experimental equilibrium constants, Keq, were made for the reactions: (A) $H_2O(g) + HD(g) = HDO(g) + H_2(g)$, and (B)= $H_2O(g) + D_2O(g) = 2HDO(g)$. Spectroscopic values for the heats of reaction, ΔH_{R298}°, of (A) and (B) were based on the zero point energies of H_2O, D_2O, and HDO given by Hulston (6) and Wolfsberg (7) and H_2, HD given by Herzberg and Monfils (8). The earlier work on (A) cited by Kirshenbaum (9) is in poor agreement except for that of Herrick, Kirshenbaum, Brown and Herrick, Crist, Davis ($\Delta H_{R298}^\circ = 928 \pm 30$, 921 cal; respectively). ΔH_{R298}° for the reaction (C) $H_2O(\ell) + D_2O(\ell) = 2HDO(\ell)$ has been determined to be -32 ± 1 cal. (10-12) assuming ideal solutions (see (13)) and Keq(C) ~ 3.8. (We calculate Keq(C) = 3.76 ± 0.04 from Keq(B) = 3.76 ± 0.02, $P^\circ(H_2O)/P^\circ(D_2O) = 1.151 \pm 0.006$ (14) at 298K, and $P^\circ(H_2O)/P^\circ(HDO) = 1.073 \pm 0.004$ (15) at 298K.) ΔH_{R298}° of (B) was calculated from the difference in heats of vaporization at 298K of $D_2O(\ell) - H_2O(\ell) = 331 \pm 8$ cal (see D_2O table), and HDO(ℓ) - $H_2O(\ell) = 183 \pm 20$ cal. (14). Values selected for ΔH_{298}° based on non-spectroscopic and spectroscopic work for (A) and (B), underlined in the table, were used to calculate values of ΔHf_{298}° of HDO(g) - H_2O (g) of -845 ± 6, -852 ± 10, -852 ± 12, and -851 ± 10 cal, respectively (see D_2O and HD tables). An average value of -850 ± 10 cal was added to ΔHf_{298}° of $H_2O(g)$ to obtain ΔHf_{298}° HDO(g).

Reaction	Source	Temperature, K	ΔH_{R298}°, cal.	Drift, e.u.	
A	Cerrai et al (1954)	324 – 1015	-915 ± 20	0.04 ± 0.10	(-864±30, 0.12±0.07)[a]
A	Suess (1949)	353 – 473	<u>-921 ± 6</u>	0.05 ± 0.05	(-955±29, 0.09±0.09)[a]
A	Hulston (1969)	Spectroscopic	<u>-928 ± 10</u>		
A	Wolfsberg (1969)	Spectroscopic	-937 ± 10		
B	Pyper, Newbury, and Barton (1967)	273.15 297.95	56 ± 11 63 ± 11		(3.75±0.08)[b] (3.74±0.04)[b]
B	Friedman and Shiner (1966)	273.15 298.15 358.15	58 ± 3 <u>60 ± 3</u> 62 ± 7		(3.74±0.02)[b] (3.76±0.02)[b] (3.80±0.04)[b]
B	Kresge, Chiang(1968)	298.15	46 ± 5		(3.85±0.03)[b]
B	Reaction C, see text	298.15	57 ± 22		
B	Hulston (1969)	Spectroscopic	<u>65 ± 10</u>		
B	Wolfsberg (1969)	Spectroscopic	70 ± 10		

[a]Second law: H_{R298}°, S_{298}° (obsv.-calc.); [b]Keq at temperature cited.

Heat Capacity and Entropy

The thermodynamic functions of this table are analogous to those in the JANAF table for $H_2O(g)$ (dated March 31, 1961): both tables are taken from A. S. Friedman and L. Haar, J. Chem. Phys. 22, 2051 (1954). Friedman and Haar applied their non-rigid-rotor, anharmonic-oscillator treatment (with vibrational-rotational coupling terms and low-temperature rotational corrections) to the infrared-spectra analyses of W. S. Benedict, N. Gailar, and E. K. Plyler, J. Chem. Phys. 21, 1301 (1953) and of W. S. Benedict, H. H. Claasen and J. H.Shaw, J. Research Nat. Bur. Standards 49, 91 (1952). In the present table for HDO, the values of C_p° of Friedman and Haar between 4000 and 5000 K were extrapolated linearly (except with a term in T^{-2}) from 5000 to 6000 K. $I_e^A = 1.211 \times 10^{-40}$, $I_e^B = 3.060 \times 10^{-40}$ $I_e^C = 4.271 \times 10^{-40}$ gm cm^2 from Friedman and Haar.

References

1. E. Cerrai, C. Marchetti, R. Renzoni, L. Roseo, M. Silvestri, and S. Villani, Chem. Eng. Prog. Symp Ser. 50 (11), 271 (1954).
2. H. Suess, Z. Naturforschung 4a, 328 (1949).
3. J. W. Pyper, R. S. Newbury, and G. W. Barton, Jr., J. Chem. Phys. 46, 2253 (1967).
4. L. Friedman and V. J. Shiner, Jr., J. Chem. Phys. 44, 4639 (1966).
5. A. J. Kresge and Y. Chiang,J. Chem. Phys. 49, 1439 (1968).
6. J. R. Hulston, J. Chem. Phys. 50, 1483 (1969).
7. M. Wolfsberg, J. Chem. Phys. 50, 1484 (1969).
8. G. Herzberg and A. Monfils, J. Molec. Spectroscopy 5, 482 (1960).
9. I. Kirshenbaum, Physical Properties and Analysis of Heavy Water (McGraw-Hill, N. Y., 1951).
10. E. Doehlemann, F. Lange, Z. Physik. Chem. 173A, 295 (1935).

11. V. P. Skripov, I. V. Povyshev, Russ. J. Phys. Chem. 36,(2), 162 (1962).
12. W. C. Duer, G. L. Bertrand, J. Chem. Phys. 53, 3020 (1970).
13. W. A. Van Hook, J. Phys. Chem. 72, 1234 (1968).
14. W. M. Jones, J. Chem. Phys. 48, 207 (1968) [see C. Liu, W. T. Lindsay, Jr., J. Chem. Eng. Data 15, 510 (1970)].
15. A. Narten, J. Chem. Phys. 41, 1318 (1964).

MONODEUTERO-WATER (HDO)

DHO

(IDEAL GAS) GFW = 19.021

T, °K	Cp°	S°	−(G°−H°₂₉₈)/T	H°−H°₂₉₈	ΔHf°	ΔGf°	Log Kp
		gibbs/mol			kcal/mol		
0	.000	.000	INFINITE	-2.372	-57.943	-57.943	INFINITE
100	7.959	38.940	54.769	-1.583	-58.188	-57.464	125.587
200	7.974	44.459	48.392	-.787	-58.415	-56.650	61.904
298	8.075	47.658	47.658	.000	-58.645	-55.735	40.855
300	8.078	47.707	47.658	.015	-58.650	-55.717	40.590
400	8.311	50.061	47.977	.834	-58.882	-54.704	29.889
500	8.615	51.947	48.588	1.679	-59.102	-53.634	23.444
600	8.951	53.547	49.285	2.558	-59.303	-52.522	19.131
700	9.302	54.953	49.996	3.470	-59.487	-51.377	16.041
800	9.657	56.218	50.696	4.418	-59.652	-50.207	13.716
900	10.008	57.376	51.375	5.401	-59.801	-49.017	11.903
1000	10.345	58.448	52.029	6.419	-59.930	-47.812	10.449
1100	10.665	59.450	52.659	7.470	-60.043	-46.594	9.257
1200	10.964	60.391	53.264	8.551	-60.141	-45.367	8.263
1300	11.240	61.279	53.847	9.662	-60.224	-44.133	7.419
1400	11.493	62.122	54.408	10.799	-60.296	-42.892	6.696
1500	11.724	62.922	54.949	11.960	-60.359	-41.646	6.068
1600	11.935	63.686	55.472	13.143	-60.415	-40.398	5.518
1700	12.126	64.415	55.977	14.346	-60.463	-39.145	5.032
1800	12.300	65.113	56.465	15.567	-60.505	-37.890	4.601
1900	12.458	65.783	56.938	16.806	-60.542	-36.633	4.214
2000	12.603	66.425	57.396	18.059	-60.573	-35.373	3.865
2100	12.734	67.044	57.841	19.325	-60.605	-34.113	3.550
2200	12.855	67.639	58.273	20.605	-60.631	-32.850	3.263
2300	12.965	68.213	58.693	21.896	-60.656	-31.587	3.001
2400	13.066	68.767	59.101	23.198	-60.680	-30.321	2.761
2500	13.160	69.302	59.498	24.509	-60.702	-29.058	2.540
2600	13.246	69.820	59.885	25.830	-60.725	-27.790	2.336
2700	13.325	70.321	60.263	27.158	-60.747	-26.524	2.147
2800	13.399	70.807	60.631	28.494	-60.769	-25.256	1.971
2900	13.468	71.279	60.990	29.838	-60.793	-23.985	1.808
3000	13.532	71.736	61.340	31.188	-60.816	-22.717	1.655
3100	13.592	72.181	61.683	32.545	-60.841	-21.446	1.512
3200	13.648	72.613	62.018	33.906	-60.865	-20.176	1.378
3300	13.701	73.034	62.345	35.274	-60.890	-18.904	1.252
3400	13.750	73.444	62.666	36.646	-60.916	-17.632	1.133
3500	13.797	73.843	62.979	38.024	-60.946	-16.358	1.021
3600	13.841	74.233	63.287	39.406	-60.975	-15.082	.916
3700	13.883	74.612	63.587	40.792	-61.010	-13.808	.816
3800	13.922	74.983	63.883	42.182	-61.044	-12.532	.721
3900	13.960	75.345	64.172	43.576	-61.082	-11.256	.631
4000	13.996	75.699	64.456	44.973	-61.121	-9.979	.545
4100	14.030	76.045	64.734	46.375	-61.161	-8.699	.464
4200	14.062	76.383	65.007	47.780	-61.203	-7.418	.386
4300	14.093	76.715	65.276	49.187	-61.246	-6.137	.312
4400	14.123	77.039	65.540	50.598	-61.293	-4.855	.241
4500	14.151	77.357	65.799	52.012	-61.344	-3.575	.174
4600	14.178	77.668	66.053	53.428	-61.395	-2.286	.109
4700	14.204	77.973	66.307	54.833	-61.463	-1.016	.047
4800	14.230	78.273	66.550	56.269	-61.501	.288	-.013
4900	14.254	78.567	66.792	57.693	-61.559	1.573	-.070
5000	14.278	78.854	67.030	59.120	-61.620	2.860	-.125
5100	14.300	79.137	67.265	60.549	-61.682	4.155	-.178
5200	14.322	79.415	67.496	61.981	-61.745	5.443	-.229
5300	14.344	79.688	67.724	63.414	-61.810	6.738	-.278
5400	14.364	79.957	67.948	64.848	-61.879	8.029	-.325
5500	14.385	80.220	68.168	66.287	-61.947	9.325	-.371
5600	14.405	80.480	68.386	67.726	-62.018	10.620	-.414
5700	14.424	80.735	68.600	69.167	-62.092	11.917	-.457
5800	14.443	80.986	68.812	70.610	-62.168	13.217	-.498
5900	14.461	81.233	69.020	72.056	-62.244	14.519	-.538
6000	14.479	81.476	69.226	73.502	-62.323	15.820	-.576

July 31, 1972

$S^{\circ}_{298.15}$ = 44.723 cal $K^{-1}mol^{-1}$ $\Delta Hf^{\circ}_{298.15}$ = 89.7 ± 5 kcal mol^{-1}

Electronic States and Molecular Constants

State	ε, cm^{-1}	g	ω_e, cm^{-1}	$\chi_e\omega_e$, cm^{-1}	B_e, cm^{-1}	α_e, cm^{-1}	r_e, $\overset{\circ}{A}$
$X^3\Sigma^-$	0	3	2422	50.6	8.8993	0.252	1.040

σ = 1

Heat of Formation

ΔHf°_{298} of ND(g) minus NH(g) was calculated from the JANAF thermal functions and the zero point energies of $H_2(g)$, $D_2(g)$ [given by G. Herzberg and A. Monfils, J. Molec. Spectroscopy $\underline{5}$, 482 (1960)], NH(g), and ND(g) [given by L. Haar, A. S. Friedman, and C. W. Beckett, NBS Monograph 20 (1961)]. ΔHf°_{298} of ND(g) was calculated from this value and the JANAF selection for ΔHf°_{298} of NH(g).

Heat Capacity and Entropy

The molecular constants which are given for NH in the JANAF Thermochemical Tables, 2nd Edition, D. R. Stull and H. Prophet, Project Directors, NSRDS-NBS 37, Washington, D. C., June 1971, were adjusted for the isotope effect.

(IDEAL GAS)   GFW = 16.0208

T, °K	gibbs/mol			kcal/mol			
	Cp°	S°	−(G°−H°₂₉₈)/T	H°−H°₂₉₈	ΔHf°	ΔGf°	Log Kp
0	.000	.000	INFINITE	−2.067	89.693	89.693	INFINITE
100	6.959	37.118	50.914	−1.380	89.249	89.249	−195.053
200	6.962	41.942	45.360	−.684	89.700	88.795	−97.030
298	6.969	44.723	44.723	.000	89.700	88.350	−64.762
300	6.969	44.766	44.723	.013	89.700	88.342	−64.357
400	7.005	46.775	44.997	.711	89.701	87.889	−48.020
500	7.086	48.345	45.515	1.415	89.703	87.436	−38.218
600	7.221	49.649	46.098	2.130	89.710	86.982	−31.683
700	7.383	50.774	46.688	2.860	89.719	86.526	−27.015
800	7.553	51.771	47.262	3.607	89.734	86.069	−23.513
900	7.719	52.670	47.814	4.371	89.749	85.610	−20.789
1000	7.474	53.492	48.341	5.151	89.768	85.149	−18.609
1100	8.013	54.249	48.844	5.945	89.787	84.687	−16.826
1200	8.136	54.951	49.324	6.753	89.806	84.222	−15.339
1300	8.249	55.607	49.782	7.572	89.827	83.755	−14.081
1400	8.347	56.222	50.221	8.402	89.845	83.287	−13.002
1500	8.434	56.801	50.640	9.241	89.865	82.819	−12.067
1600	8.512	57.348	51.043	10.089	89.883	82.348	−11.248
1700	8.581	57.866	51.429	10.943	89.899	81.877	−10.526
1800	8.644	58.359	51.800	11.805	89.916	81.404	−9.884
1900	8.700	58.827	52.158	12.672	89.932	80.931	−9.309
2000	8.751	59.275	52.503	13.545	89.949	80.458	−8.792
2100	8.797	59.703	52.835	14.422	89.962	79.981	−8.324
2200	8.840	60.113	53.157	15.304	89.976	79.507	−7.898
2300	8.879	60.507	53.458	16.190	89.990	79.030	−7.510
2400	8.916	60.886	53.769	17.080	90.003	78.554	−7.153
2500	8.950	61.251	54.061	17.973	90.017	78.076	−6.825
2600	8.981	61.602	54.345	18.870	90.027	77.599	−6.523
2700	9.011	61.942	54.620	19.769	90.039	77.121	−6.242
2800	9.039	62.270	54.887	20.672	90.051	76.642	−5.982
2900	9.066	62.588	55.147	21.577	90.061	76.164	−5.740
3000	9.091	62.895	55.400	22.485	90.071	75.684	−5.514
3100	9.115	63.194	55.647	23.395	90.080	75.203	−5.302
3200	9.138	63.484	55.887	24.308	90.091	74.723	−5.103
3300	9.160	63.765	56.122	25.223	90.100	74.242	−4.917
3400	9.182	64.039	56.351	26.140	90.112	73.763	−4.741
3500	9.202	64.305	56.574	27.059	90.119	73.281	−4.576
3600	9.222	64.565	56.793	27.980	90.127	72.801	−4.420
3700	9.242	64.818	57.006	28.904	90.133	72.318	−4.272
3800	9.260	65.065	57.215	29.829	90.139	71.836	−4.132
3900	9.278	65.305	57.419	30.756	90.144	71.355	−3.999
4000	9.296	65.540	57.619	31.684	90.150	70.872	−3.872
4100	9.314	65.770	57.815	32.615	90.154	70.389	−3.752
4200	9.331	65.995	58.007	33.547	90.159	69.909	−3.638
4300	9.347	66.215	58.196	34.481	90.165	69.427	−3.529
4400	9.364	66.430	58.380	35.417	90.167	68.945	−3.425
4500	9.380	66.640	58.562	36.354	90.167	68.460	−3.325
4600	9.395	66.847	58.740	37.293	90.170	67.981	−3.230
4700	9.411	67.049	58.914	38.233	90.172	67.497	−3.139
4800	9.427	67.247	59.086	39.175	90.174	67.018	−3.051
4900	9.442	67.442	59.254	40.118	90.174	66.533	−2.967
5000	9.457	67.633	59.420	41.063	90.171	66.051	−2.887
5100	9.471	67.820	59.583	42.010	90.170	65.567	−2.810
5200	9.486	68.004	59.743	42.957	90.168	65.085	−2.735
5300	9.501	68.185	59.901	43.907	90.165	64.601	−2.664
5400	9.515	68.363	60.056	44.958	90.163	64.120	−2.595
5500	9.529	68.537	60.208	45.810	90.158	63.638	−2.529
5600	9.543	68.709	60.359	46.763	90.154	63.156	−2.465
5700	9.557	68.878	60.507	47.718	90.149	62.674	−2.403
5800	9.571	69.045	60.652	48.675	90.143	62.193	−2.343
5900	9.585	69.208	60.796	49.633	90.137	61.709	−2.286
6000	9.598	69.369	60.938	50.592	90.130	61.228	−2.230

July 31, 1972

$S^\circ_{298.15} = 45.307$ cal K^{-1} mol $^{-1}$[*]

$\Delta Hf^\circ_0 = 8.65_9$ kcal mol $^{-1}$[‡]

$\Delta Hf^\circ_{298.5} = 8.74_8 \pm 0.29$ kcal mol $^{-1}$

Electronic States and Molecular Constants

State	ε, cm^{-1}	g	ω_e, cm^{-1}	$\chi_e\omega_e$, cm^{-1}	B_e, cm^{-1}	α_e, cm^{-1}	r_e, Å
$X^2\Pi_i$	0	2	2720.9	44.2	10.02	0.29	0.970
	139.7	2					
$A^2\Sigma^+$	35474	2	2322.6	55.4	9.198	0.322	1.012
$B^2\Sigma^+$	68769	2	684.3	55.6	2.91	0.25	1.80

$\sigma = 1$

Heat of Formation

The heat of formation was calculated from the selected value for ΔHf°_{298} of OH(g), -9.27 ± 0.3 kcal mol $^{-1}$ (see OH table), the appropriate thermal functions, and zero point energies of H_2(g), D_2(g), OH(g), and OD(g). The zero point energies of H_2(g) and D_2(g) were taken from G. Herzberg and A. Monfils, J. Molec. Spectroscopy $\underline{5}$, 482 (1960). The zero point energies of OH and OD include the Dunham correction (see G. Herzberg and A. Monfils, loc. cit.). The molecular constants are those given by B. Rosen, Spectroscopic Data Relative to Diatomic Molecules (Pergamon Press, Oxford, 1970) with the exception of the coupling constants taken from G. Herzberg, Spectra of Diatomic Molecules, D. Van Nostrand Company, Inc., New York (1950) pp. 232, 561.

[*]Heat Capacity and Entropy

The vibrational and rotational constants of the respective electronic levels were taken from B. Rosen, Spectroscopic Data Relative to Diatomic Molecules, Pergamon Press, Oxford, 1970. Comparison of the results with those from a more exact treatment given by L. Haar, A. S. Friedman, and C. W. Beckett, NBS Monograph 20, May 29, 1961 (U. S. Govt. Printing Office, Washington, D. C., 20402) indicates errors in the tables above 400 K are negligible. Below this, they may be appreciable. In particular, it is recommended that $H^\circ_0 - H^\circ_{298}$, S°_{298}, and $C^\circ_{p\ 298}$ be taken as -2.151 kcal mol $^{-1}$, 45.307 gibbs mol $^{-1}$, and 7.156 cal deg $^{-1}$ mol $^{-1}$, respectively. These errors result from dealing with the ground state ($X^2\Pi_i$) as two different electronic states separated by 139.7 cm^{-1}.

(IDEAL GAS)   GFW = 18.0135

T, °K	Cp°	S°	$-(G°-H°_{298})/T$	$H°-H°_{298}$	$\Delta Hf°$	$\Delta Gf°$	Log Kp
		gibbs/mol			kcal/mol		
0	.000	.000	INFINITE	-2.200	8.609	8.609	INFINITE
100	7.796	37.148	51.818	-1.467	8.667	8.369	-18.289
200	7.355	42.405	45.961	-.711	8.722	8.046	-8.792
298	7.167	45.301	45.301	.000	8.748	7.708	-5.650
300	7.165	45.345	45.301	.013	8.748	7.702	-5.611
400	7.100	47.395	45.581	.726	8.757	7.351	-4.017
500	7.106	48.979	46.108	1.436	8.751	7.000	-3.060
600	7.176	50.281	46.698	2.149	8.734	6.651	-2.423
700	7.287	51.395	47.291	2.872	8.712	6.305	-1.969
800	7.423	52.376	47.867	3.608	8.687	5.963	-1.629
900	7.566	53.259	48.418	4.357	8.661	5.625	-1.366
1000	7.708	54.064	48.943	5.121	8.637	5.289	-1.156
1100	7.843	54.805	49.442	5.898	8.614	4.955	-.985
1200	7.967	55.492	49.918	6.689	8.592	4.623	-.842
1300	8.080	56.135	50.372	7.492	8.573	4.293	-.722
1400	8.183	56.737	50.805	8.305	8.554	3.965	-.619
1500	8.275	57.305	51.220	9.128	8.536	3.638	-.530
1600	8.357	57.842	51.617	9.959	8.517	3.311	-.452
1700	8.432	58.351	51.998	10.799	8.499	2.987	-.384
1800	8.499	58.835	52.365	11.646	8.482	2.663	-.323
1900	8.559	59.296	52.718	12.498	8.462	2.340	-.269
2000	8.614	59.736	53.058	13.357	8.444	2.018	-.221
2100	8.664	60.158	53.386	14.221	8.422	1.697	-.177
2200	8.710	60.562	53.703	15.090	8.400	1.378	-.137
2300	8.752	60.950	54.009	15.963	8.378	1.059	-.101
2400	8.791	61.323	54.307	16.840	8.352	.742	-.068
2500	8.827	61.683	54.594	17.721	8.327	.425	-.037
2600	8.860	62.030	54.874	18.606	8.298	.110	-.009
2700	8.891	62.365	55.145	19.493	8.269	-.205	.017
2800	8.920	62.689	55.409	20.384	8.237	-.517	.040
2900	8.948	63.002	55.665	21.277	8.202	-.829	.062
3000	8.974	63.306	55.915	22.173	8.167	-1.140	.083
3100	8.998	63.601	56.158	23.072	8.128	-1.449	.102
3200	9.021	63.887	56.395	23.973	8.091	-1.759	.120
3300	9.043	64.164	56.626	24.876	8.050	-2.067	.137
3400	9.064	64.435	56.852	25.791	8.009	-2.372	.152
3500	9.085	64.698	57.072	26.699	7.964	-2.677	.167
3600	9.104	64.954	57.288	27.598	7.919	-2.979	.181
3700	9.123	65.204	57.498	28.510	7.869	-3.282	.194
3800	9.141	65.447	57.704	29.423	7.818	-3.583	.206
3900	9.159	65.685	57.906	30.338	7.765	-3.884	.218
4000	9.176	65.917	58.103	31.255	7.712	-4.182	.228
4100	9.192	66.144	58.297	32.173	7.656	-4.479	.239
4200	9.208	66.366	58.486	33.093	7.600	-4.773	.248
4300	9.224	66.582	58.672	34.015	7.544	-5.066	.257
4400	9.239	66.795	58.854	34.938	7.483	-5.359	.266
4500	9.255	67.002	59.033	35.862	7.420	-5.652	.275
4600	9.270	67.206	59.208	36.789	7.358	-5.939	.282
4700	9.284	67.405	59.381	37.716	7.294	-6.227	.290
4800	9.299	67.601	59.550	38.646	7.231	-6.512	.296
4900	9.313	67.793	59.716	39.576	7.165	-6.800	.303
5000	9.327	67.981	59.880	40.508	7.095	-7.086	.310
5100	9.341	68.166	60.040	41.442	7.026	-7.367	.316
5200	9.355	68.348	60.198	42.376	6.956	-7.651	.322
5300	9.369	68.526	60.354	43.313	6.886	-7.930	.327
5400	9.383	68.701	60.507	44.250	6.815	-8.209	.332
5500	9.397	68.874	60.657	45.189	6.743	-8.487	.337
5600	9.411	69.043	60.806	46.130	6.670	-8.764	.342
5700	9.424	69.210	60.952	47.071	6.596	-9.040	.347
5800	9.438	69.374	61.095	48.014	6.521	-9.311	.351
5900	9.452	69.535	61.237	48.959	6.446	-9.585	.355
6000	9.465	69.694	61.377	49.905	6.370	-9.854	.359

July 31, 1972

$$S^\circ_{298.15} = 48.138 \text{ cal}^{-1} \text{ K}^{-1} \text{ mol}^{-1\ddagger}$$

$$\Delta Hf^\circ_{298.15} = 33.1 \pm 1.2 \text{ kcal mol}^{-1}$$

Electronic States and Molecular Constants

State	ε, cm^{-1}	g	ω_e, cm^{-1}	$\chi_e\omega_e$, cm^{-1}	B_e, cm^{-1}	α_e, cm^{-1}	r_e, Å
$X^2\Pi_i$	0	2	1930.4	23.44	4.949	0.101	1.345
	376.8	2					
$A^2\Sigma^+$	30769	2	1417	48.85	4.392	0.172	1.423
$B^2\Sigma$	59566	2	1917.7	29.3	4.532	0.105	1.405
$C^2\Delta$	63872	4					
$D^2\Delta$	71205	4					
$E^2\Sigma$	71328	2	[1930.4]	[23.44]	[4.949]	[0.101]	
$F^2\Delta$	76717	4					
$G^2\Delta$	79320	4					
$H^2\Delta$	80858	4					

$\sigma = 1$

Heat of Formation

The heat of formation was calculated from the appropriate thermal functions (see tables for HS, DS, H_2, D_2), the selected value for ΔHf°_{298} of HS(g) (33.3 ± 1.2 kcal mol^{-1}, see table for HS), and the zero point energies of H_2(g) (1), D_2(g) (1), HS(g) (2), and DS(g) (2). The Dunham corrections were made in ref. (1) for H_2(g) and D_2(g). Spectroscopic constants tabulated in ref. (2) were used to calculate the zero point energies of HS and DS including Dunham corrections.

$\ddagger$Heat Capacity and Entropy

The vibrational and rotational constants of the respective electronic levels were taken from B. Rosen, _Spectroscopic Data Relative to Diatomic Molecules_, Pergamon Press, Oxford, 1970. From an examination of the approximations in this calculation with more exact methods (see SH tables) it is concluded that the errors are negligible above 400 K. Below this, they may be appreciable. In particular, it is recommended that $H^\circ_0 - H^\circ_{298}$, S°_{298}, and $C^\circ_{p\ 298}$ be taken as -2.171 kcal mol^{-1}, 48.138 gibbs mol^{-1}, and 7.760 cal deg^{-1}mol^{-1}, respectively.

References

1. G. Herzberg and A. Monfils, J. Molec. Spectroscopy **5**, 482 (1960).
2. B. Rosen, "Spectroscopic Data Relative to Diatomic Molecules", Pergamon Press, New York (1970). For coupling constants, see L. Haar, A. S. Friedman, and C. W. Beckett, NBS Monograph 20, May 29, 1961 (U. S. Govt. Printing Office, Washington, D. C., 20402). For the cause of these errors, see the text (page 256) of the table for Deutero-hydroxyl (0 D).

(IDEAL GAS)   GFW = 34.0781

T, °K	Cp°	S°	−(G°−H°₂₉₈)/T	H°−H°₂₉₈	ΔHf°	ΔGf°	Log Kp
		gibbs/mol			kcal/mol		
0	.000	.000	INFINITE	−2.221	32.956	32.956	INFINITE
100	7.214	39.776	55.032	−1.526	33.159	30.924	−67.367
200	7.815	45.007	48.844	−.767	33.171	28.478	−31.119
298	7.772	48.129	48.129	.000	33.100	26.187	−19.195
300	7.770	48.177	48.129	.014	33.098	26.144	−19.046
400	7.669	50.396	48.433	.786	32.422	23.867	−13.040
500	7.678	52.107	49.003	1.552	31.899	21.789	−9.524
600	7.770	53.514	49.641	2.324	31.462	19.809	−7.215
700	7.898	54.721	50.282	3.107	31.089	17.921	−5.595
800	8.034	55.784	50.905	3.904	17.699	14.795	−4.042
900	8.162	56.738	51.501	4.714	17.703	14.432	−3.505
1000	8.277	57.604	52.068	5.536	17.709	14.069	−3.075
1100	8.378	58.398	52.608	6.369	17.718	13.703	−2.723
1200	8.467	59.131	53.122	7.211	17.728	13.338	−2.429
1300	8.544	59.812	53.610	8.061	17.740	12.973	−2.181
1400	8.611	60.447	54.076	8.919	17.751	12.605	−1.968
1500	8.670	61.043	54.521	9.783	17.762	12.236	−1.783
1600	8.722	61.605	54.946	10.653	17.772	11.868	−1.621
1700	8.768	62.135	55.354	11.528	17.781	11.499	−1.478
1800	8.810	62.637	55.745	12.406	17.789	11.128	−1.351
1900	8.847	63.114	56.120	13.289	17.797	10.759	−1.238
2000	8.881	63.569	56.481	14.176	17.806	10.389	−1.135
2100	8.911	64.003	56.829	15.065	17.810	10.015	−1.042
2200	8.940	64.418	57.165	15.958	17.816	9.647	−.958
2300	8.966	64.816	57.489	16.853	17.821	9.274	−.881
2400	8.990	65.198	57.802	17.751	17.824	8.903	−.811
2500	9.013	65.566	58.105	18.651	17.829	8.532	−.746
2600	9.035	65.920	58.399	19.554	17.830	8.160	−.686
2700	9.055	66.261	58.684	20.458	17.833	7.787	−.630
2800	9.074	66.591	58.961	21.365	17.834	7.414	−.579
2900	9.093	66.910	59.229	22.273	17.833	7.043	−.531
3000	9.110	67.218	59.490	23.183	17.832	6.672	−.486
3100	9.127	67.517	59.745	24.095	17.830	6.299	−.444
3200	9.143	67.807	59.992	25.009	17.830	5.926	−.405
3300	9.159	68.089	60.233	25.924	17.828	5.552	−.368
3400	9.174	68.362	60.468	26.840	17.826	5.184	−.333
3500	9.189	68.629	60.698	27.758	17.820	4.809	−.300
3600	9.204	68.888	60.922	28.678	17.818	4.439	−.270
3700	9.218	69.140	61.140	29.599	17.809	4.067	−.240
3800	9.232	69.386	61.354	30.522	17.803	3.695	−.213
3900	9.246	69.626	61.563	31.446	17.794	3.322	−.186
4000	9.260	69.860	61.768	32.371	17.786	2.955	−.161
4100	9.273	70.089	61.968	33.297	17.777	2.582	−.138
4200	9.287	70.313	62.164	34.225	17.767	2.213	−.115
4300	9.300	70.531	62.356	35.155	17.758	1.842	−.094
4400	9.313	70.745	62.544	36.085	17.746	1.473	−.073
4500	9.327	70.955	62.729	37.017	17.731	1.103	−.054
4600	9.340	71.160	62.910	37.951	17.719	.734	−.035
4700	9.354	71.361	63.087	38.886	17.707	.364	−.017
4800	9.367	71.558	63.262	39.822	17.694	−.004	.000
4900	9.381	71.751	63.433	40.759	17.679	−.370	.016
5000	9.395	71.941	63.601	41.698	17.660	−.742	.032
5100	9.409	72.127	63.767	42.638	17.644	−1.107	.047
5200	9.423	72.310	63.929	43.580	17.627	−1.476	.062
5300	9.437	72.490	64.089	44.523	17.610	−1.845	.076
5400	9.452	72.666	64.246	45.467	17.592	−2.208	.089
5500	9.466	72.840	64.401	46.413	17.573	−2.578	.102
5600	9.481	73.010	64.553	47.360	17.554	−2.942	.115
5700	9.496	73.178	64.703	48.309	17.534	−3.310	.127
5800	9.511	73.344	64.851	49.259	17.514	−3.674	.138
5900	9.526	73.506	64.996	50.211	17.494	−4.043	.150
6000	9.542	73.667	65.139	51.165	17.474	−4.403	.160

July 31, 1972

$D_0^\circ = 105.070 \pm 0.002$ kcal mol^{-1} $\Delta Hf_{298.15}^\circ = 0$

Ground State Configuration $^1\Sigma_g^+$ $S_{298.15}^\circ = 34.622 \pm 0.01$ cal deg^{-1}mol^{-1}

$\omega_e = 3118.46$ cm^{-1} $\omega_e x_e = 64.10$ cm^{-1} $D_e = 0.01159$ cm^{-1} $\sigma = 2$

$B_e = 30.429$ cm^{-1} $\alpha_e = 1.0492$ cm^{-1} $r_e = 0.7416$ Å

<u>Heat Capacity and Entropy</u>

The thermodynamic functions were generated from the table of the current series for H_2(q.v.) by adding those for "equilibrium" D_2 and subtracting those for "equilibrium" H_2, the added and subtracted tables being those from L. Haar, A. S. Friedman, and C. W. Beckett, Nat. Bur. Standards Monograph 20 (1961). (In using these tables of Monograph 20, C_p° was extrapolated smoothly from 5000 to 6000 K by comparing with the harmonic oscillator-rigid rotor values.) This procedure is believed to give a table approaching in accuracy the current table for H_2, which is based on the direct-summation method of H. W. Woolley, R. B. Scott, and F. G. Brickwedde, J. Research Nat. Bur. Standards <u>41</u>, . 379 (1948). The tables of Monograph 20, while involving summation at low temperatures, approximated by closed expressions the high-temperature first-order contributions due to anharmonicity, rotation-vibration coupling, and rotational stretching. At 2000 K the values of Woolley et al. for C_p° and S° of D_2 are 0.03% lower and 0.01% higher respectively, than the present table. (Woolley et al. gave no values for D_2 above 2000 K.) The value for D_0° is taken from G. Herzberg, J. Molec. Spectroscopy <u>33</u>, 147 (1970).

Deuterium, Diatomic (D₂)

(Ideal Gas, Reference State)   GFW = 4.0282

T, °K	Cp°	S°	−(G°−H°₂₉₈)/T	H°−H°₂₉₈	ΔHf°	ΔGf°	Log Kp
	gibbs/mol			kcal/mol			
0	.000	.000	INFINITE	−2.048	.000	.000	.000
100	7.246	26.932	40.839	−1.391	.000	.000	.000
200	6.980	31.836	35.260	−.685	.000	.000	.000
298	6.978	34.622	34.622	.000	.000	.000	.000
300	6.978	34.665	34.622	.013	.000	.000	.000
400	6.989	36.672	34.896	.710	.000	.000	.000
500	7.018	38.235	35.413	1.411	.000	.000	.000
600	7.079	39.519	35.992	2.116	.000	.000	.000
700	7.172	40.617	36.576	2.829	.000	.000	.000
800	7.297	41.582	37.143	3.551	.000	.000	.000
900	7.429	42.450	37.686	4.288	.000	.000	.000
1000	7.561	43.239	38.202	5.037	.000	.000	.000
1100	7.689	43.966	38.694	5.799	.000	.000	.000
1200	7.813	44.641	39.161	6.576	.000	.000	.000
1300	7.934	45.270	39.607	7.362	.000	.000	.000
1400	8.055	45.863	40.033	8.162	.000	.000	.000
1500	8.178	46.423	40.441	8.973	.000	.000	.000
1600	8.277	46.954	40.831	9.797	.000	.000	.000
1700	8.367	47.459	41.206	10.630	.000	.000	.000
1800	8.450	47.939	41.567	11.470	.000	.000	.000
1900	8.529	48.398	41.914	12.320	.000	.000	.000
2000	8.601	48.837	42.250	13.174	.000	.000	.000
2100	8.669	49.259	42.573	14.041	.000	.000	.000
2200	8.732	49.664	42.887	14.909	.000	.000	.000
2300	8.792	50.053	43.190	15.785	.000	.000	.000
2400	8.848	50.429	43.484	16.668	.000	.000	.000
2500	8.901	50.790	43.769	17.552	.000	.000	.000
2600	8.951	51.141	44.046	18.447	.000	.000	.000
2700	8.997	51.479	44.315	19.343	.000	.000	.000
2800	9.041	51.807	44.577	20.244	.000	.000	.000
2900	9.081	52.126	44.832	21.153	.000	.000	.000
3000	9.117	52.434	45.080	22.062	.000	.000	.000
3100	9.158	52.735	45.322	22.980	.000	.000	.000
3200	9.197	53.025	45.558	23.894	.000	.000	.000
3300	9.237	53.308	45.788	24.816	.000	.000	.000
3400	9.276	53.584	46.014	25.738	.000	.000	.000
3500	9.316	53.854	46.234	26.670	.000	.000	.000
3600	9.355	54.117	46.450	27.601	.000	.000	.000
3700	9.393	54.374	46.660	28.542	.000	.000	.000
3800	9.432	54.625	46.866	29.484	.000	.000	.000
3900	9.470	54.871	47.068	30.432	.000	.000	.000
4000	9.508	55.111	47.266	31.380	.000	.000	.000
4100	9.545	55.346	47.460	32.333	.000	.000	.000
4200	9.581	55.577	47.651	33.289	.000	.000	.000
4300	9.619	55.802	47.838	34.245	.000	.000	.000
4400	9.655	56.024	48.022	35.209	.000	.000	.000
4500	9.691	56.241	48.201	36.180	.000	.000	.000
4600	9.725	56.455	48.379	37.150	.000	.000	.000
4700	9.759	56.664	48.553	38.122	.000	.000	.000
4800	9.794	56.870	48.725	39.096	.000	.000	.000
4900	9.827	57.072	48.893	40.077	.000	.000	.000
5000	9.860	57.271	49.058	41.065	.000	.000	.000
5100	9.893	57.467	49.221	42.053	.000	.000	.000
5200	9.927	57.659	49.381	43.044	.000	.000	.000
5300	9.960	57.848	49.539	44.038	.000	.000	.000
5400	9.993	58.035	49.695	45.035	.000	.000	.000
5500	10.025	58.218	49.848	46.036	.000	.000	.000
5600	10.056	58.399	49.999	47.039	.000	.000	.000
5700	10.088	58.577	50.148	48.046	.000	.000	.000
5800	10.120	58.753	50.295	49.057	.000	.000	.000
5900	10.149	58.926	50.440	50.070	.000	.000	.000
6000	10.180	59.097	50.583	51.086	.000	.000	.000

July 31, 1972

Point Group　C$_{2v}$　　　　　　　　　　　　　　　$\Delta Hf^{\circ}_{298.15}$ = 44.3 ± 2 kcal mol^{-1}

S$^{\circ}_{298.15}$ = 48.801 gibbs mol^{-1}

Electronic Level (quantum weight) and Vibrational Frequencies (Degeneracies)

ε, cm^{-1}	(g)		ω, cm^{-1}	(g)	
0	(2)	[2305] (1)	1110 (1)		[2367] (1)
10393	(2)	[2305] (1)	[500] (1)		[2367] (1)

Bond Distance:　N–D = 1.024Å

Bond Angle:　　D–N–D = 103.4°

Products of Moments of Inertia:　$I_A I_B I_C$ = 58.53 x 10^{-120} g^3 cm^6　　　　　σ = 2

Heat of Formation

ΔHf°_{298} of ND$_2$(g) was calculated from the JANAF selection for ΔHf°_{298} of NH$_2$(g), the JANAF thermal functions and the zero point energies of H$_2$(g), D$_2$(g), NH$_2$(g), and ND$_2$(g). The zero point energies of H$_2$(g), D$_2$(g) were those given by G. Herzberg and A. Monfils, J. Mol. Spectroscopy 5, 482 (1960). The zero point energies of NH$_2$(g) and ND$_2$(g) were estimated from vibrational frequencies given by D. E. Milligan and M. E. Jacox, J. Chem. Phys. 43, 4487 (1965) who observed the infrared and visible spectrum of matrix isolated NH$_2$ and ND$_2$.

Heat Capacity and Entropy

The bond distances and angles are from the electronic absorption spectrum (c.f. NH$_2$). The vibrational frequencies are from D. E. Milligan and M. E. Jacox, J. Chem. Phys. 43, 4487 (1965).

(IDEAL GAS)   GFW = 18.0349

T, °K	gibbs/mol			kcal/mol			
	Cp°	S°	−(G°−H°₂₉₈)/T	H°−H°₂₉₈	ΔHf°	ΔGf°	Log Kp
0	.000	.000	INFINITE	-2.385	44.999	44.999	INFINITE
100	7.949	40.057	55.959	-1.590	44.790	45.386	-99.192
200	7.992	45.573	49.544	-.794	44.532	46.084	-50.358
298	8.227	48.801	48.801	.000	44.300	46.896	-34.376
300	8.233	48.852	48.801	.015	44.296	46.912	-34.175
400	8.619	51.271	49.128	.857	44.092	47.816	-26.126
500	9.070	53.241	49.759	1.741	43.924	48.767	-21.316
600	9.549	54.937	50.484	2.672	43.793	49.748	-18.121
700	10.025	56.445	51.230	3.651	43.695	50.748	-15.844
800	10.472	57.814	51.969	4.676	43.627	51.761	-14.140
900	10.877	59.071	52.689	5.744	43.578	52.781	-12.817
1000	11.235	60.236	53.386	6.850	43.548	53.805	-11.759
1100	11.546	61.321	54.059	7.989	43.532	54.833	-10.894
1200	11.817	62.338	54.707	9.158	43.523	55.859	-10.173
1300	12.051	63.293	55.331	10.351	43.525	56.887	-9.564
1400	12.256	64.194	55.932	11.567	43.530	57.915	-9.041
1500	12.437	65.046	56.511	12.802	43.539	58.943	-8.588
1600	12.599	65.854	57.070	14.054	43.549	59.969	-8.191
1700	12.746	66.622	57.610	15.321	43.562	60.994	-7.841
1800	12.882	67.355	58.131	16.603	43.579	62.019	-7.530
1900	13.009	68.055	58.635	17.897	43.597	63.043	-7.252
2000	13.130	68.725	59.123	19.204	43.621	64.067	-7.001
2100	13.247	69.368	59.596	20.523	43.642	65.086	-6.774
2200	13.361	69.987	60.054	21.854	43.672	66.110	-6.567
2300	13.473	70.584	60.499	23.195	43.703	67.128	-6.379
2400	13.582	71.159	60.931	24.548	43.737	68.146	-6.206
2500	13.690	71.716	61.351	25.912	43.779	69.163	-6.046
2600	13.796	72.255	61.760	27.286	43.820	70.177	-5.899
2700	13.900	72.778	62.159	28.671	43.869	71.190	-5.762
2800	14.003	73.285	62.547	30.066	43.923	72.201	-5.636
2900	14.103	73.778	62.926	31.471	43.978	73.211	-5.517
3000	14.201	74.258	63.296	32.886	44.042	74.218	-5.407
3100	14.296	74.725	63.657	34.311	44.106	75.221	-5.303
3200	14.387	75.181	64.010	35.745	44.182	76.224	-5.206
3300	14.476	75.625	64.355	37.189	44.258	77.222	-5.114
3400	14.560	76.058	64.693	38.640	44.343	78.222	-5.028
3500	14.641	76.481	65.024	40.101	44.425	79.216	-4.946
3600	14.718	76.895	65.348	41.569	44.515	80.212	-4.870
3700	14.790	77.299	65.666	43.044	44.602	81.199	-4.796
3800	14.858	77.694	65.977	44.526	44.695	82.186	-4.727
3900	14.922	78.081	66.282	46.015	44.788	83.171	-4.661
4000	14.982	78.460	66.582	47.511	44.886	84.153	-4.598
4100	15.037	78.830	66.876	49.012	44.985	85.133	-4.538
4200	15.088	79.193	67.165	50.518	45.085	86.114	-4.481
4300	15.134	79.549	67.449	52.029	45.190	87.090	-4.426
4400	15.177	79.897	67.728	53.545	45.291	88.064	-4.374
4500	15.215	80.239	68.002	55.064	45.388	89.030	-4.324
4600	15.250	80.574	68.272	56.587	45.489	90.003	-4.276
4700	15.280	80.902	68.537	58.114	45.592	90.969	-4.230
4800	15.306	81.224	68.798	59.643	45.694	91.938	-4.186
4900	15.331	81.540	69.055	61.175	45.792	92.897	-4.143
5000	15.352	81.850	69.308	62.709	45.885	93.857	-4.102
5100	15.369	82.154	69.557	64.246	45.979	94.815	-4.063
5200	15.384	82.452	69.802	65.783	46.072	95.771	-4.025
5300	15.395	82.746	70.043	67.322	46.162	96.723	-3.988
5400	15.405	83.033	70.281	68.862	46.250	97.680	-3.953
5500	15.411	83.316	70.516	70.403	46.334	98.629	-3.919
5600	15.416	83.594	70.747	71.944	46.416	99.580	-3.886
5700	15.418	83.867	70.974	73.486	46.494	100.529	-3.854
5800	15.418	84.135	71.199	75.028	46.568	101.477	-3.824
5900	15.417	84.398	71.421	76.570	46.639	102.421	-3.794
6000	15.414	84.658	71.639	78.111	46.707	103.367	-3.765

July 31, 1972

Point Group C_{2v}

$\Delta Hf^\circ_{298.15}$ = 49.5 ± 0.5 kcal mol^{-1}

$S^\circ_{298.15}$ = 53.616 gibbs mol^{-1}

Ground State Quantum Weight = 1

Vibrational Frequencies and Degeneracies

ω, cm^{-1}		ω, cm^{-1}	
[2300]	(1)	[2400]	(1)
[1490]	(1)	[1150]	(1)
[1058]	(1)	[750]	(1)

Bond Distance: N-N = [1.230]Å   N-H = [1.014]Å

Bond Angle: H-N-H = [100°] $\sigma = 2$

Product of Moments of Inertia: $I_A I_B I_G$ = 3.8165 x 10^{-117} g^3 cm^6

Heat of Formation

ΔHf°_{298} of N_2D_2(g) was estimated from ΔHf°_{298} of N_2H_2(g), 50.9 ± 5 kcal mol^{-1}, given in JANAF Thermochemical Tables, 2nd Edition, NSRDS-NBS-37, June (1971), the appropriate thermal functions (see tables for N_2D_2, H_2, D_2 and N_2H_2 (JANAF loc. cit.)) and the estimated zero point energies. The energies for H_2(g), D_2(g) are those given by G. Herzberg and A. Monfils, J. Molec. Spectroscopy $\underline{5}$, 482 (1960). The energies for N_2D_2(g) and N_2H_2(g) are taken to be one half the sum of the vibrational frequencies given above and for N_2H_2(g) (JANAF, loc. cit.).

Heat Capacity and Entropy

The bond distances and angle were obtained from a quantum mechanical calculation by G. W. Wheland and P. S. K. Chen, J. Chem. Phys. $\underline{24}$, 67 (1956). The three principal moments of inertia are I_A = 0.6122, I_B = 2.2094, I_c = 2.8216 x 10^{-39} g cm^2. The infrared spectrum of N_2D_2(g) has been observed using matrix isolation techniques by K. Rosengren and G. Pimentel, J. Chem. Phys. $\underline{43}$, 507 (1965). They have observed ω_1 or ω_4 = 2400 cm^{-1}, ω_2 = 1490 cm^{-1}, and ω_3 = 1058 cm^{-1}.

T, °K	Cp°	S°	−(G°−H°298)/T	H°−H°298	ΔHf°	ΔGf°	Log Kp
		gibbs/mol			kcal/mol		
0	.000	.000	INFINITE	−2.464	51.156	51.156	INFINITE
100	7.954	44.544	61.231	−1.669	50.601	52.657	−115.082
200	9.310	50.125	54.433	−.862	50.006	54.947	−60.043
298	9.327	53.616	53.616	.000	49.500	57.483	−42.136
300	9.350	53.674	53.617	.017	49.491	57.532	−41.912
400	10.632	56.538	53.998	1.016	49.096	60.277	−32.934
500	11.867	59.045	54.762	2.142	48.818	63.106	−27.583
600	12.972	61.309	55.667	3.385	48.644	65.981	−24.034
700	13.930	63.382	56.623	4.731	48.549	68.878	−21.505
800	14.747	65.297	57.589	6.166	48.519	71.785	−19.611
900	15.437	67.075	58.546	7.676	48.533	74.694	−18.138
1000	16.018	68.733	59.483	9.250	48.584	77.597	−16.959
1100	16.505	70.283	60.395	10.877	48.661	80.496	−15.993
1200	16.914	71.737	61.280	12.548	48.754	83.385	−15.187
1300	17.260	73.105	62.138	14.258	48.867	86.266	−14.503
1400	17.552	74.395	62.967	15.999	48.987	89.139	−13.915
1500	17.802	75.615	63.770	17.767	49.115	92.003	−13.405
1600	18.015	76.770	64.547	19.558	49.246	94.858	−12.957
1700	18.198	77.868	65.299	21.369	49.381	97.704	−12.561
1800	18.357	78.913	66.026	23.196	49.519	100.542	−12.207
1900	18.495	79.909	66.731	25.039	49.659	103.373	−11.891
2000	18.616	80.861	67.414	26.895	49.803	106.199	−11.605
2100	18.722	81.772	68.076	28.762	49.941	109.012	−11.345
2200	18.816	82.645	68.718	30.639	50.084	111.824	−11.109
2300	18.899	83.484	69.342	32.525	50.225	114.626	−10.892
2400	18.972	84.289	69.948	34.419	50.364	117.424	−10.693
2500	19.038	85.065	70.538	36.319	50.506	120.215	−10.509
2600	19.097	85.813	71.111	38.226	50.641	123.001	−10.339
2700	19.150	86.535	71.669	40.138	50.778	125.782	−10.181
2800	19.198	87.232	72.212	42.056	50.914	128.557	−10.034
2900	19.241	87.907	72.742	43.978	51.045	131.329	−9.897
3000	19.261	88.560	73.258	45.904	51.177	134.095	−9.769
3100	19.317	89.192	73.762	47.834	51.303	136.855	−9.648
3200	19.349	89.806	74.254	49.767	51.434	139.612	−9.535
3300	19.379	90.402	74.734	51.704	51.559	142.364	−9.428
3400	19.407	90.981	75.204	53.643	51.686	145.118	−9.328
3500	19.432	91.544	75.663	55.585	51.804	147.861	−9.233
3600	19.455	92.092	76.111	57.529	51.923	150.607	−9.143
3700	19.477	92.625	76.551	59.476	52.035	153.344	−9.058
3800	19.497	93.145	76.980	61.425	52.146	156.080	−8.977
3900	19.515	93.651	77.401	63.375	52.252	158.814	−8.900
4000	19.532	94.146	77.814	65.328	52.359	161.543	−8.826
4100	19.548	94.628	78.218	67.282	52.461	164.270	−8.756
4200	19.563	95.100	78.615	69.237	52.560	166.999	−8.690
4300	19.577	95.560	79.003	71.194	52.661	169.724	−8.626
4400	19.590	96.010	79.385	73.153	52.754	172.446	−8.565
4500	19.602	96.451	79.759	75.112	52.839	175.160	−8.507
4600	19.613	96.882	80.127	77.073	52.927	177.883	−8.451
4700	19.624	97.304	80.488	79.035	53.013	180.597	−8.398
4800	19.634	97.717	80.842	80.998	53.096	183.316	−8.347
4900	19.643	98.122	81.191	82.962	53.173	186.023	−8.297
5000	19.652	98.519	81.533	84.926	53.242	188.734	−8.250
5100	19.661	98.908	81.870	86.892	53.312	191.441	−8.204
5200	19.669	99.290	82.202	88.858	53.379	194.150	−8.160
5300	19.676	99.664	82.528	90.826	53.443	196.853	−8.117
5400	19.683	100.032	82.848	92.794	53.504	199.561	−8.077
5500	19.690	100.394	83.164	94.762	53.559	202.265	−8.037
5600	19.696	100.748	83.475	96.732	53.614	204.968	−7.999
5700	19.702	101.097	83.781	98.702	53.664	207.672	−7.963
5800	19.708	101.440	84.083	100.672	53.709	210.374	−7.927
5900	19.713	101.777	84.380	102.643	53.752	213.072	−7.893
6000	19.719	102.108	84.672	104.615	53.792	215.773	−7.860

July 31, 1972

DIDEUTERO-WATER (D_2O) (IDEAL GAS) GFW = 20.027

Point Group C_{2v} ΔHf_0° = -58.856 kcal mol^{-1}

$S_{298.15}^\circ$ = 47.378 cal deg^{-1}mol^{-1} $\Delta Hf_{298.15}^\circ$ = -59.561 ± 0.016 kcal mol^{-1}

Ground State Quantum Weight = 1

<u>Vibrational Levels and Multiplicities</u>

ω, cm^{-1}

2671.69 (1)
1178.33 (1)
2788.02 (1)

Bond Lengths and Angle: O–D Distance = 0.958Å σ = 2
D–O–D Angle = 104.45°
Product of Moments of Inertia: $I_A I_B I_C$ = 39.948 x 10^{-120} g^3 cm^6

Heat of Formation

Rossini, Knowlton, and Johnston (1) measured the ratio of the heats of formation of $D_2O(\ell)$. Recalculation of their results (using ΔHf_{298}° of $H_2O(\ell)$ = -68.315 ± 0.010 kcal mol^{-1}, see $H_2O(g)$ table) yields ΔHf_{298}° of $D_2O(\ell)$ - $H_2O(\ell)$ = -2.1098 ± 0.01492 x ΔHf_{298}°[HDO(ℓ)–$H_2O(\ell)$] ± .016 kcal mol^{-1}. Using a value of 32 ± 30 cal. for the reaction $H_2O(\ell)$ + $D_2O(\ell)$ = 2HDO(ℓ) (from (2); some justification that the uncertainty may be smaller is given by Van Hook (3), see also HDO tables) one obtains ΔHf_{298}°[$D_2O(\ell)$–$H_2O(\ell)$] = -2.094 ± 0.016 kcal mol^{-1}.

The difference between the heats of vaporization of $D_2O(\ell)$ and $H_2O(\ell)$ at 298K were evaluated as follows. By direct calorimetry, Rossini, Knowlton, and Johnston (1) determined the ratio of the heats of vaporization of $H_2O(\ell)$/$D_2O(\ell)$ at 298K and zero pressure to be 0.969503 ± 0.00070; (2) Bartholomé and Clusius (4) determined the heat of vaporization of $D_2O(\ell)$ by direct calorimetry at 0°C. Recalculation of their results using the energy equivalent of a Bunsen ice calorimeter given by (5) (compression correction assumed zero) and neglecting gas imperfection corrections yields 12.637 ± 0.026 kcal mol^{-1}. The heat of vaporization of $D_2O(\ell)$ at 25°C was calculated using the heat of fusion of $D_2O(\ell)$ selected by (6) and (7), the condensed phase heat capacity data of $D_2O(\ell)$ given by Long and Kemp (8) and the gas phase thermal functions of Friedman and Haar (see next section); (3) The difference in heats of vaporization of $D_2O(\ell)$ and $D_2O(g)$ was derived by differentiating the formula given by Jones (9) (see (10) for a comparison with other measurements) for the ratio of the vapor pressures of $H_2O(\ell)$/$D_2O(\ell)$ as a function of temperature and assuming negligible corrections for gas imperfection corrections (see (11), however).

Source	Method	$\Delta H_{v,298}^\circ$[$D_2O(\ell)$–$H_2O(\ell)$], kcal mol^{-1}
Knowlton, Johnston, Rossini	Calorimetry	0.331 ± 0.008*
Bartholomé amd Clusius	Calorimetry	0.340 ± 0.028*
Jones	Vapor Pressure	0.307 ± 0.020

*Calculated from $\Delta H_{v\ 298}^\circ$ of $H_2O(\ell)$ = 10.520 ± 0.002 kcal mol^{-1}(12).

Selecting 0.331 ± .008 kcal mol^{-1} for the difference in the heats of vaporization, one obtains -1.763 ± 0.018 kcal mol^{-1} for ΔHf_{298}° of $D_2O(g)$–$H_2O(g)$. The "spectroscopic" value for this difference was calculated to be -1.768 ± 0.015 kcal mol^{-1} based on the zero point energies given by Hulston (13) for $H_2O(g)$, $D_2O(g)$, Herzberg and Monfils (14) for $H_2(g)$, $D_2(g)$, and the appropriate thermal functions ($H_2O(g)$ (15), see tables for $H_2(g)$, $D_2(g)$, $D_2O(g)$). To close the consistency check, the "spectroscopic" value of ΔHf_{298}° of $D_2O(g)$ minus HDO(g) is -0.916 ± 0.0015 kcal mol^{-1} and the "nonspectroscopic" value for this difference is (see HDO tables, reaction A) is (-1.763±0.0018) + (0.846±0.006) = -0.917±0.019 kcal mol^{-1}. ΔHf_{298}° of $D_2O(g)$–$H_2O(g)$ and ΔHf_{298}° of $H_2O(g)$ = -57.795±0.010 kcal mol^{-1} (12).

Heat Capacity and Entropy

The thermodynamic functions of this table are analogous to those in the JANAF table for $H_2O(g)$ (dated March 31, 1961): both tables are taken from A. S. Friedman and L. Haar, J. Chem. Phys. 22, 2051 (1954). Friedman and Haar applied their non-rigid-rotor, anharmonic-oscillator treatment (with vibrational-rotational coupling terms and low-temperature rotational corrections) to the infrared-spectra analyses of W. S. Benedict, N. Gailar, and E. K. Plyler, J. Chem. Phys. 21, 1301 (1953) and of W. S. Benedict, H. H. Claasen, and J. H. Shaw, J. Research Nat. Bur. Standards 49, 91 (1952). In the present table for D_2O, the values of C_p° of Friedman and Haar between 4000 and 5000 K were extrapolated linearly (except with a term in T^{-2}) from 5000 to 6000 K.

References
1. F. D. Rossini, J. W. Knowlton, and H. L. Johnston, J. Res. Nat. Bur. Standards 24, 369 (1940).
2. W. C. Duer and G. L. Bertrand, J. Chem. Phys. 53, 3020 (1970).
3. W. A. Van Hook, J. Phys. Chem. 72, 1234 (1968).
4. E. Bartholomé and K. Clusius, Zeit, Physik. Chem. B28, 167 (1935).
5. D. A. Ditmars and T. B. Douglas, J. Res. Nat. Bur. Standards 75A, 401 (1971).
6. I. Kirshenbaum, Physical Properties and Analysis of Heavy Water (McGraw-Hill, New York, 1951).
7. V. A. Kirillin, Editor, Heavy Water Thermophysical Properties (U. S. Dept. of Commerce, National Technical Information Service, Springfield, Va., TT70-50094, 1971).
8. E. A. Long and J. D. Kemp, J. Chem. Soc. 58, 1829 (1936).
9. W. M. Jones, J. Chem. Phys. 48, 207 (1968).
10. C. Liu and W. T. Lindsay, Jr., J. Chem. Eng. Data 15, 510 (1970).
11. G. S. Kell, G. F. Laurin, and E. Whalley, J. Chem. Phys. 49, 2839 (1968).
12. CODATA Task Group on Key Values for Thermodynamics, Final Set of Key Values for Thermodynamics-Part I (Bulletin No. 5) November 1971.
13. J. R. Hulston, J. Chem. Phys. 50, 1483 (1969) see also M. Wolfsberg, J. Chem. Phys. 50, 1484 (1969).
14. G. Herzberg and A. Monfils, J. Molec. Spectroscopy 5, 482 (1960).

(Ideal Gas)   GFW = 20.027

T, °K	Cp°	S°	−(G°−H°₂₉₈)/T	H°−H°₂₉₈	ΔHf°	ΔGf°	Log Kp
		gibbs/mol			kcal/mol		
0	.000	.000	INFINITE	−2.380	−58.856	−58.856	INFINITE
100	7.958	38.634	54.529	−1.590	−59.069	−58.169	127.129
200	7.994	44.156	48.119	−.793	−59.326	−57.168	62.471
298	8.187	47.378	47.378	.000	−59.561	−56.059	41.092
300	8.192	47.429	47.378	.015	−59.565	−56.037	40.823
400	8.517	49.828	47.703	.850	−59.783	−54.827	29.956
500	8.887	51.768	48.328	1.720	−59.979	−53.565	23.413
600	9.282	53.423	49.042	2.628	−60.154	−52.267	19.038
700	9.690	54.884	49.775	3.577	−60.307	−50.940	15.904
800	10.098	56.205	50.497	4.566	−60.439	−49.593	13.548
900	10.490	57.417	51.200	5.596	−60.553	−48.230	11.712
1000	10.856	58.542	51.878	6.664	−60.648	−46.855	10.240
1100	11.191	59.592	52.532	7.766	−60.727	−45.471	9.034
1200	11.494	60.580	53.162	8.901	−60.793	−44.082	8.028
1300	11.765	61.510	53.769	10.064	−60.845	−42.687	7.176
1400	12.006	62.391	54.354	11.253	−60.888	−41.289	6.445
1500	12.222	63.227	54.917	12.464	−60.923	−39.887	5.811
1600	12.413	64.022	55.462	13.696	−60.953	−38.485	5.257
1700	12.584	64.780	55.988	14.946	−60.977	−37.079	4.767
1800	12.737	65.504	56.497	16.213	−60.995	−35.673	4.331
1900	12.874	66.196	56.989	17.493	−61.012	−34.267	3.942
2000	12.997	66.860	57.466	18.787	−61.023	−32.858	3.591
2100	13.109	67.496	57.929	20.092	−61.037	−31.451	3.273
2200	13.210	68.108	58.377	21.408	−61.045	−30.039	2.984
2300	13.301	68.698	58.814	22.734	−61.053	−28.631	2.721
2400	13.385	69.266	59.237	24.068	−61.063	−27.220	2.479
2500	13.462	69.814	59.650	25.410	−61.069	−25.810	2.256
2600	13.533	70.343	60.051	26.760	−61.080	−24.399	2.051
2700	13.598	70.855	60.441	28.117	−61.088	−22.989	1.861
2800	13.658	71.351	60.822	29.480	−61.098	−21.576	1.684
2900	13.714	71.831	61.194	30.849	−61.112	−20.164	1.520
3000	13.766	72.297	61.556	32.222	−61.124	−18.753	1.366
3100	13.815	72.749	61.910	33.602	−61.140	−17.339	1.222
3200	13.860	73.188	62.255	34.986	−61.152	−15.927	1.088
3300	13.904	73.615	62.593	36.375	−61.168	−14.515	.961
3400	13.944	74.031	62.923	37.766	−61.184	−13.099	.842
3500	13.982	74.436	63.246	39.163	−61.206	−11.685	.730
3600	14.018	74.830	63.563	40.562	−61.227	−10.268	.623
3700	14.052	75.235	63.893	41.967	−61.254	−8.929	.527
3800	14.085	75.590	64.176	43.373	−61.283	−7.438	.428
3900	14.116	75.956	64.473	44.783	−61.315	−6.023	.338
4000	14.145	76.314	64.765	46.196	−61.346	−4.606	.252
4100	14.173	76.664	65.051	47.611	−61.381	−3.188	.170
4200	14.200	77.005	65.332	49.030	−61.416	−1.766	.092
4300	14.226	77.340	65.607	50.452	−61.451	−.344	.017
4400	14.251	77.667	65.878	51.875	−61.493	1.078	−.054
4500	14.275	77.988	66.143	53.301	−61.540	2.496	−.121
4600	14.298	78.302	66.404	54.731	−61.584	3.925	−.186
4700	14.320	78.610	66.661	56.161	−61.631	5.348	−.249
4800	14.341	78.911	66.912	57.594	−61.677	6.779	−.309
4900	14.361	79.207	67.160	59.030	−61.729	8.202	−.366
5000	14.381	79.498	67.404	60.467	−61.788	9.627	−.421
5100	14.401	79.782	67.644	61.905	−61.846	11.059	−.474
5200	14.420	80.062	67.880	63.347	−61.904	12.485	−.525
5300	14.438	80.337	68.113	64.790	−61.965	13.916	−.574
5400	14.456	80.607	68.342	66.234	−62.028	15.351	−.621
5500	14.473	80.872	68.567	67.681	−62.093	16.783	−.667
5600	14.490	81.134	68.789	69.129	−62.159	18.217	−.711
5700	14.507	81.390	69.008	70.578	−62.229	19.651	−.753
5800	14.523	81.643	69.224	72.030	−62.301	21.090	−.795
5900	14.539	81.891	69.436	73.483	−62.374	22.528	−.834
6000	14.555	82.135	69.646	74.938	−62.448	23.970	−.873

DEUTERIUM SULFIDE (D_2S) (IDEAL GAS) GFW = 36.0882

Point Group C_{2v}

$S^{\circ}_{298.15}$ = 51.428 cal deg^{-1} mol^{-1}

Ground State Quantum Weight = 1

ΔHf°_0 = -5.02 ± 0.2 kcal mol^{-1}

$\Delta Hf^{\circ}_{298.15}$ = -5.71 ± 0.2 kcal mol^{-1}

Vibrational Frequencies and Degeneracies

ω, cm^{-1}

1896.38 (1)

855.45 (1)

1999 (1)

Bond Distance: S-D = 1.328 Å

Bond Angle: D-S-D = 92.2°

Product of the Moments of Inertia: $I_A I_B I_C$ = 6.016 x 10^{-119} g^3 cm^6

σ = 2

Heat of Formation

ΔHf°_{298} of D_2S(g) was determined by Kapustinskii and Kankovskii (1) to be -5.69$_2$ ± 0.06 kcal mol^{-1} (recalculated) from the reaction: D_2S(g) + 3/2O$_2$(g) = SO$_2$(g) + D$_2$O(ℓ) + S(rhombic). The difference of ΔHf°_{298} of D_2S(g) minus H_2S(g) for their work was calculated using their results for ΔHf°_{298} of NH$_3$(g), -4.92 ± 0.08 kcal mol^{-1} (recalculated) in the hope of eliminating possible systematic error due to uncertainty in the product formed.

The "spectroscopic" value of ΔHf°_{298} of D_2S(g) minus H_2S(g) was calculated from the appropriate thermal functions (see H_2, D_2, H_2S) and the zero point energies of H_2S(g), D_2S(g) (2), D_2(g) (3), and H_2(g) (3).

The equilibrium data of Grafe, Clusius, and Kruis (4) for the exchange reaction H_2(g) + D_2S(g) = D_2(g) + H_2S(g) was analyzed by third and second law methods.

A weighted average of -0.81 ± 0.02 kcal mol^{-1} was selected for ΔHf°_{298} of D_2S(g) minus H_2S(g) was added to the selected value of ΔHf°_{298} of H_2S(g) to determine ΔHf°_{298} of D_2S(g).

Source		ΔHf°_{298} of D_2S(g) - H_2S(g) (kcal mol^{-1})
Kapustinskii and Kankovskii (1) (1958)		-0.771 ± 0.10
Spectroscopic (2,3)		-0.810 ± 0.01
Grafe, Clusius, and Kruis (4)	Third Law	-0.826 ± 0.05; drift 0.0 e.u.
	Second Law	-0.887 ± 0.02; ΔSf°_{298} (obsv.-calc.) = +0.18 ± 0.02 e.u.

Heat Capacity and Entropy

The thermodynamic functions were estimated from those in the present table for H_2S(g) (q.v.) by adding those for D_2S(g) and subtracting those for H_2S(g), where both the added and subtracted functions were generated using the rigid-rotor harmonic oscillator approximation. In this calculation the molecular constants for D_2S were taken from reference (2a).

References

1. A. F. Kapustinskii and R. T. Kankovskii, Zhur. Fiz. Khim. **32**, 2810 (1958).

2a. R. E. Miller, G. E. Leroi, D. F. Meggers, J. Chem. Phys. **46**, 2292 (1967);

2b. H. C. Allen and E. K. Plyler, J. Chem. Phys. **25**, 1132 (1956).

3. G. Herzberg and A. Monfils, J. Mol. Spectroscopy **5**, 482 (1960).

4. D. Grafe, K. Clusius, and A. Kruis, Z. Physik. Chem. **B43**, 1 (1939).

DEUTERIUM SULFIDE (D₂S)

(IDEAL GAS)   GFW = 36.0882

T, °K	Cp°	S°	−(G°−H°₂₉₈)/T	H°−H°₂₉₈	ΔHf°	ΔGf°	Log Kp
		gibbs/mol			kcal/mol		
0	.000	.000	INFINITE	−2.411	−5.020	−5.020	INFINITE
100	7.950	42.510	58.667	−1.616	−5.046	−6.307	13.784
200	8.110	48.050	52.130	−.816	−5.345	−7.463	8.156
298	8.547	51.428	51.428	.000	−5.710	−8.445	6.191
300	8.555	51.481	51.429	.016	−5.717	−8.463	6.165
400	9.082	54.013	51.769	.898	−6.631	−9.298	5.080
500	9.642	56.100	52.433	1.834	−7.334	−9.883	4.320
600	10.199	57.908	53.197	2.826	−7.904	−10.337	3.765
700	10.716	59.519	53.988	3.872	−8.371	−10.682	3.335
800	11.173	60.981	54.772	4.967	−21.823	−12.251	3.347
900	11.569	62.321	55.537	6.105	−21.860	−11.052	2.684
1000	11.909	63.558	56.279	7.279	−21.876	−9.851	2.153
1100	12.196	64.706	56.993	8.485	−21.875	−8.648	1.718
1200	12.440	65.778	57.681	9.717	−21.864	−7.446	1.356
1300	12.649	66.783	58.343	10.972	−21.840	−6.245	1.050
1400	12.828	67.726	58.979	12.246	−21.813	−5.046	.788
1500	12.983	68.617	59.593	13.536	−21.782	−3.851	.561
1600	13.118	69.459	60.183	14.842	−21.748	−2.656	.363
1700	13.236	70.258	60.752	16.160	−21.712	−1.463	.188
1800	13.342	71.018	61.302	17.489	−21.673	−.275	.033
1900	13.434	71.741	61.833	18.827	−21.635	.913	−.105
2000	13.520	72.433	62.345	20.175	−21.592	2.101	−.230
2100	13.595	73.094	62.841	21.531	−21.555	3.281	−.342
2200	13.603	73.728	63.322	22.894	−21.512	4.467	−.444
2300	13.726	74.337	63.788	24.263	−21.472	5.645	−.536
2400	13.785	74.922	64.239	25.639	−21.432	6.826	−.622
2500	13.839	75.487	64.679	27.020	−21.388	8.001	−.699
2600	13.888	76.030	65.104	28.406	−21.351	9.176	−.771
2700	13.934	76.555	65.518	29.798	−21.309	10.350	−.833
2800	13.977	77.062	65.922	31.193	−21.270	11.520	−.899
2900	14.017	77.553	66.315	32.593	−21.234	12.691	−.956
3000	14.056	78.030	66.697	33.996	−21.196	13.861	−1.010
3100	14.093	78.491	67.070	35.404	−21.161	15.029	−1.060
3200	14.128	78.940	67.435	36.815	−21.121	16.192	−1.105
3300	14.160	79.375	67.790	38.229	−21.085	17.354	−1.149
3400	14.192	79.798	68.137	39.647	−21.046	18.525	−1.191
3500	14.223	80.210	68.476	41.068	−21.015	19.684	−1.229
3600	14.252	80.611	68.807	42.491	−20.980	20.850	−1.266
3700	14.280	81.001	69.131	43.919	−20.952	22.012	−1.300
3800	14.307	81.382	69.449	45.347	−20.924	23.171	−1.333
3900	14.334	81.755	69.760	46.780	−20.898	24.326	−1.363
4000	14.360	82.118	70.064	48.214	−20.871	25.491	−1.393
4100	14.385	82.473	70.363	49.651	−20.846	26.645	−1.420
4200	14.410	82.820	70.655	51.091	−20.822	27.806	−1.447
4300	14.434	83.159	70.942	52.533	−20.796	28.965	−1.472
4400	14.457	83.491	71.224	53.978	−20.776	30.121	−1.496
4500	14.481	83.816	71.499	55.425	−20.761	31.277	−1.519
4600	14.502	84.134	71.770	56.874	−20.743	32.436	−1.541
4700	14.524	84.447	72.037	58.325	−20.725	33.591	−1.562
4800	14.547	84.753	72.299	59.779	−20.707	34.749	−1.582
4900	14.568	85.053	72.556	61.235	−20.694	35.908	−1.602
5000	14.590	85.347	72.809	62.693	−20.687	37.056	−1.620
5100	14.609	85.636	73.057	64.153	−20.678	38.215	−1.638
5200	14.631	85.921	73.303	65.615	−20.670	39.365	−1.654
5300	14.651	86.199	73.543	67.079	−20.663	40.518	−1.671
5400	14.671	86.474	73.780	68.545	−20.658	41.675	−1.687
5500	14.691	86.743	74.014	70.013	−20.655	42.824	−1.702
5600	14.711	87.008	74.243	71.483	−20.653	43.985	−1.717
5700	14.731	87.268	74.469	72.955	−20.653	45.138	−1.731
5800	14.749	87.525	74.692	74.429	−20.655	46.288	−1.744
5900	14.770	87.777	74.912	75.906	−20.656	47.440	−1.757
6000	14.788	88.025	75.128	77.383	−20.661	48.602	−1.770

July 31, 1972

TRIDEUTERO-AMMONIA (ND$_3$)   (IDEAL GAS)   GFW = 20.0490

Point Group   C$_{3v}$ ΔHf_0° = -12.34 kcal mol^{-1}

$S_{298.15}^\circ$ = 48.715 cal deg^{-1} mol^{-1} $\Delta Hf_{298.15}^\circ$ = -14.00 ± 0.1 kcal mol^{-1}

Ground State Quantum Weight = 1

Vibrational Levels and Multiplicities

ω, cm^{-1}

2495 (1)

793 (1)

2652 (2)

1225 (2)

Bond Length: N-D = 1.0124 Å   Bond Angle: 106.67   σ = 3

Product of the Moments of Inertia: $I_A I_B I_C$ = 25.775 x 10^{-119} g^3 cm^6

Heat of Formation

A "spectroscopic" value for ΔHf_{298}° of ND$_3$(g) minus NH$_3$(g) of -3.029 ± 0.01 kcal mol^{-1} was calculated from the appropriate thermal functions (see H$_2$, D$_2$, NH$_3$) zero point energies of ND$_3$(g) and NH$_3$(g) [see J. L. Duncan, I. M. Mills, Spectrochim. Acta 20, 523 (1957) and W. S. Benedict, E. K. Plyler, Canad. J. Phys. 35, 1235 (1964)], and the zero point energies of H$_2$(g) and D$_2$(g) given by G. Herzberg and A. Monfils, J. Molec. Spectroscopy 5, 482 (1960).

Analysis of the equilibrium data of Schulz and Schaefer, Ber. Bunsenges. Physik. Chem. 70, 21 (1966) for K$_p^\circ$ (1 atm, 660-773K) for N$_2$(g) + 3/2D$_2$(g) = ND$_3$(g) gave the following:

	ΔHf_{298}°(kcal mol^{-1})	Drift (e.u.)	ΔS_{298}(obsv.-calc.)
Third Law	-13.80	-1.2	---
Second Law[1]	-13.0 ± 0.38	--	+4.3 ± 0.5 e.u.

[1] Assuming ΔC_p° = 1.237 - 0.00608 (T-700) cal. mol^{-1}

Using the results from the same authors data for NH$_3$(g) (see NH$_3$(g) evaluation) one obtains values of ΔHf_{298}° of ND$_3$(g) minus NH$_3$(g) of -2.93 ± 0.14 kcal mol^{-1} (third law) and -3.22 ± 0.20 kcal mol^{-1} (second law). Both values agree with the "spectroscopic" value within combined uncertainty intervals.

A value of -3.03 ± 0.010 kcal mol^{-1} was added to the JANAF selection for ΔHf_{298}° of NH$_3$(g), -10.97 ± 0.10 kcal mol^{-1}, to obtain ΔHf_{298}° of ND$_3$(g).

Heat Capacity and Entropy

The thermodynamic functions were estimated from those in the present table for NH$_3$(g) (q.v.) by adding those for ND$_3$(g) and subtracting those for NH$_3$(g), where both the added and subtracted functions were generated using the rigid-rotor harmonic-oscillator approximation. In this calculation the molecular constants for ND$_3$ were taken from J. L. Duncan, I. M. Mills, Spectrochim. Acta 20, 523 (1964) and W. S. Benedict, E. K. Plyler, Can. J. Phys. 35, 1235 (1957).

T, °K	Cp°	S°	—gibbs/mol— -(G°-H°₂₉₈)/T	H°-H°₂₉₈	—kcal/mol— ΔHf°	ΔGf°	Log Kp
0	.000	.000	INFINITE	-2.446	-12.338	-12.338	INFINITE
100	7.958	39.695	56.253	-1.656	-12.880	-10.901	23.824
200	8.258	45.267	49.519	-.850	-13.481	-8.685	9.490
298	9.136	48.715	48.715	.000	-14.000	-6.217	4.557
300	9.155	48.771	48.715	.017	-14.009	-6.169	4.494
400	10.259	51.555	49.087	.987	-14.433	-3.488	1.906
500	11.323	53.961	49.826	2.067	-14.756	-.713	.312
600	12.302	56.113	50.697	3.249	-14.987	2.118	-.771
700	13.195	58.077	51.613	4.525	-15.145	4.981	-1.555
800	14.003	59.893	52.536	5.885	-15.239	7.864	-2.148
900	14.723	61.585	53.449	7.322	-15.287	10.755	-2.612
1000	15.358	63.170	54.342	8.827	-15.293	13.650	-2.983
1100	15.912	64.660	55.213	10.391	-15.266	16.544	-3.287
1200	16.394	66.066	56.060	12.007	-15.216	19.432	-3.539
1300	16.813	67.395	56.881	13.668	-15.140	22.316	-3.752
1400	17.177	68.654	57.677	15.368	-15.050	25.194	-3.933
1500	17.495	69.851	58.449	17.102	-14.947	28.067	-4.089
1600	17.773	70.989	59.198	18.866	-14.837	30.929	-4.225
1700	18.016	72.074	59.924	20.655	-14.719	33.786	-4.344
1800	18.231	73.110	60.627	22.468	-14.591	36.635	-4.448
1900	18.420	74.100	61.311	24.301	-14.459	39.477	-4.541
2000	18.587	75.050	61.974	26.151	-14.319	42.315	-4.624
2100	18.735	75.960	62.619	28.017	-14.184	45.140	-4.698
2200	18.867	76.835	63.245	29.898	-14.039	47.965	-4.765
2300	18.984	77.676	63.854	31.790	-13.895	50.779	-4.825
2400	19.089	78.486	64.447	33.694	-13.751	53.589	-4.880
2500	19.182	79.267	65.024	35.608	-13.601	56.392	-4.930
2600	19.264	80.021	65.587	37.530	-13.460	59.188	-4.975
2700	19.337	80.750	66.135	39.460	-13.313	61.979	-5.017
2800	19.403	81.454	66.670	41.397	-13.168	64.767	-5.055
2900	19.459	82.136	67.191	43.340	-13.029	67.548	-5.091
3000	19.511	82.797	67.700	45.289	-12.886	70.324	-5.123
3100	19.555	83.437	68.198	47.242	-12.753	73.094	-5.153
3200	19.592	84.059	68.684	49.200	-12.611	75.860	-5.181
3300	19.626	84.662	69.159	51.161	-12.478	78.620	-5.207
3400	19.652	85.248	69.624	53.124	-12.342	81.382	-5.231
3500	19.676	85.818	70.078	55.091	-12.220	84.135	-5.254
3600	19.696	86.373	70.523	57.059	-12.095	86.891	-5.275
3700	19.709	86.913	70.959	59.030	-11.983	89.634	-5.294
3800	19.720	87.439	71.386	61.001	-11.873	92.378	-5.313
3900	19.726	87.951	71.804	62.974	-11.770	95.120	-5.330
4000	19.730	88.450	72.214	64.946	-11.668	97.858	-5.347
4100	19.730	88.938	72.616	66.919	-11.574	100.593	-5.362
4200	19.726	89.413	73.010	68.892	-11.485	103.332	-5.377
4300	19.721	89.877	73.397	70.864	-11.397	106.066	-5.391
4400	19.710	90.330	73.777	72.836	-11.323	108.797	-5.404
4500	19.699	90.773	74.150	74.806	-11.260	111.519	-5.416
4600	19.682	91.206	74.516	76.776	-11.197	114.254	-5.428
4700	19.664	91.629	74.875	78.743	-11.140	116.979	-5.440
4800	19.643	92.043	75.229	80.708	-11.089	119.712	-5.451
4900	19.618	92.448	75.576	82.671	-11.051	122.432	-5.461
5000	19.590	92.845	75.918	84.634	-11.023	125.151	-5.470
5100	19.555	93.232	76.254	86.590	-11.003	127.875	-5.480
5200	19.546	93.611	76.584	88.544	-10.989	130.597	-5.489
5300	19.538	93.984	76.909	90.499	-10.981	133.314	-5.497
5400	19.529	94.349	77.228	92.452	-10.978	136.043	-5.506
5500	19.522	94.707	77.543	94.405	-10.982	138.762	-5.514
5600	19.514	95.059	77.853	96.357	-10.991	141.485	-5.522
5700	19.507	95.404	78.157	98.307	-11.008	144.208	-5.529
5800	19.500	95.744	78.458	100.258	-11.030	146.932	-5.537
5900	19.494	96.077	78.753	102.208	-11.057	149.654	-5.544
6000	19.488	96.404	79.045	104.157	-11.090	152.381	-5.550

July 31, 1972

$S^\circ_{298.15}$ = 41.508 cal $K^{-1}mol^{-1}$ $\Delta Hf^\circ_{298.15}$ = -65.14 ± 0.2 kcal mol^{-1}

Electronic States and Molecular Constants

State	ϵ, cm^{-1}	g	ω_e, cm^{-1}	$\chi_e\omega_e$, cm^{-1}	B_e, cm^{-1}	α_e, cm^{-1}	r_e, Å
$X^1\Sigma^+$	0	1	4138.73	90.05	20.9555	0.7958	0.9168
$V^1\Sigma^+$	83275	1	1158.46	17.718	4.0263	0.0173	2.091

σ = 1

Heat of Formation

The heat of formation selected in JANAF Thermochemical Tables, 2nd Edition, June 1971 (U. S. Govt. Printing Office, Washington, D. C. 20402) was adopted.

Heat Capacity and Entropy

The vibrational and rotational constants of the respective electronic levels were taken from B. Rosen, Spectroscopic Data Relative to Diatomic Molecules, Pergamon Press, Oxford, 1970. These constants do not differ appreciably from those given in the JANAF (loc. cit.) tables. The values of ΔHf°, ΔG°, and log Kp are appreciably different because of the new thermal functions for $F_2(g)$ (see $F_2(g)$ tables).

HYDROGEN FLUORIDE (HF)

(IDEAL GAS)   GFW = 20.0064

T, °K	Cp°	S°	−(G°−H°₂₉₈)/T	H°−H°₂₉₈	ΔHf°	ΔGf°	Log Kp
	gibbs/mol				kcal/mol		
0	.000	.000	INFINITE	−2.055	−65.129	−65.129	INFINITE
100	6.962	33.902	47.698	−1.380	−65.159	−65.312	142.739
200	6.962	38.727	42.144	−.683	−65.135	−65.475	71.547
298	6.964	41.508	41.508	.000	−65.140	−65.642	48.117
300	6.964	41.551	41.508	.013	−65.141	−65.645	47.822
400	6.967	43.554	41.781	.709	−65.176	−65.808	35.956
500	6.972	45.110	42.297	1.406	−65.230	−65.960	28.831
600	6.986	46.382	42.875	2.104	−65.297	−66.101	24.077
700	7.015	47.461	43.455	2.804	−65.372	−66.228	20.677
800	7.063	48.400	44.015	3.508	−65.452	−66.345	18.125
900	7.129	49.236	44.550	4.217	−65.535	−66.452	16.137
1000	7.210	49.991	45.057	4.934	−65.617	−66.550	14.544
1100	7.303	50.682	45.537	5.660	−65.697	−66.638	13.240
1200	7.402	51.322	45.993	6.395	−65.775	−66.721	12.152
1300	7.504	51.919	46.426	7.140	−65.849	−66.797	11.230
1400	7.606	52.478	46.839	7.896	−65.920	−66.867	10.438
1500	7.705	53.007	47.232	8.661	−65.989	−66.932	9.752
1600	7.800	53.507	47.609	9.436	−66.056	−66.993	9.151
1700	7.891	53.983	47.970	10.221	−66.119	−67.049	8.620
1800	7.977	54.436	48.317	11.015	−66.179	−67.102	8.147
1900	8.058	54.869	48.650	11.816	−66.238	−67.152	7.724
2000	8.133	55.285	48.972	12.626	−66.294	−67.198	7.343
2100	8.204	55.683	49.282	13.443	−66.348	−67.242	6.998
2200	8.270	56.066	49.582	14.266	−66.401	−67.284	6.684
2300	8.331	56.435	49.872	15.097	−66.451	−67.322	6.397
2400	8.389	56.791	50.153	15.933	−66.501	−67.359	6.134
2500	8.442	57.135	50.425	16.774	−66.550	−67.396	5.892
2600	8.493	57.467	50.690	17.621	−66.597	−67.427	5.668
2700	8.540	57.788	50.947	18.473	−66.644	−67.459	5.460
2800	8.584	58.100	51.197	19.329	−66.690	−67.489	5.268
2900	8.625	58.402	51.440	20.189	−66.735	−67.514	5.088
3000	8.664	58.695	51.677	21.054	−66.780	−67.541	4.920
3100	8.701	58.979	51.908	21.922	−66.825	−67.567	4.763
3200	8.735	59.256	52.133	22.794	−66.869	−67.590	4.616
3300	8.768	59.525	52.353	23.669	−66.914	−67.611	4.478
3400	8.799	59.788	52.568	24.547	−66.958	−67.633	4.347
3500	8.829	60.043	52.778	25.429	−67.002	−67.650	4.224
3600	8.857	60.292	52.983	26.313	−67.047	−67.669	4.108
3700	8.884	60.535	53.184	27.200	−67.093	−67.684	3.998
3800	8.910	60.773	53.381	28.090	−67.139	−67.700	3.894
3900	8.934	61.004	53.573	28.982	−67.185	−67.715	3.795
4000	8.958	61.231	53.762	29.877	−67.232	−67.728	3.700
4100	8.980	61.452	53.947	30.774	−67.280	−67.739	3.611
4200	9.002	61.669	54.128	31.673	−67.329	−67.749	3.525
4300	9.023	61.881	54.306	32.574	−67.378	−67.759	3.444
4400	9.043	62.089	54.480	33.477	−67.429	−67.769	3.366
4500	9.063	62.292	54.652	34.383	−67.480	−67.775	3.292
4600	9.082	62.492	54.820	35.290	−67.532	−67.780	3.220
4700	9.100	62.687	54.985	36.199	−67.585	−67.785	3.152
4800	9.115	62.879	55.148	37.110	−67.639	−67.789	3.087
4900	9.135	63.067	55.307	38.022	−67.694	−67.792	3.024
5000	9.152	63.252	55.464	38.937	−67.749	−67.795	2.963
5100	9.168	63.433	55.619	39.853	−67.806	−67.794	2.905
5200	9.184	63.611	55.771	40.770	−67.864	−67.793	2.849
5300	9.199	63.786	55.920	41.690	−67.922	−67.789	2.795
5400	9.215	63.959	56.068	42.610	−67.983	−67.788	2.744
5500	9.230	64.128	56.213	43.532	−68.044	−67.784	2.693
5600	9.244	64.294	56.356	44.456	−68.105	−67.779	2.645
5700	9.258	64.458	56.496	45.381	−68.168	−67.772	2.598
5800	9.272	64.619	56.635	46.308	−68.233	−67.766	2.553
5900	9.286	64.778	56.772	47.236	−68.298	−67.756	2.510
6000	9.300	64.934	56.906	48.165	−68.363	−67.748	2.468

July 31, 1972

273

FLUORINE, DIATOMIC (F_2)　　　　　　　(IDEAL GAS, REFERENCE STATE)　　　　　　　GFW = 37.9968

Ground State Configuration $^1\Sigma^+$　　　　　　　　　　$\Delta Hf_0^\circ = 0$

$S_{298.15}^\circ = 48.44$ gibbs mol^{-1}　　　　　　　　　　$\Delta Hf_{298.15}^\circ = 0$

Electronic States and Molecular Constants

State	ε, cm^{-1}	g	ω_e, cm^{-1}	$\chi_e\omega_e$, cm^{-1}	B_e, cm^{-1}	α_e, cm^{-1}	r_e, Å
$^1\Sigma^+$	0	1	917.85	11.95	0.8892	0.0131	1.40

$\sigma = 2$

Heat Capacity and Entropy

Molecular and spectroscopic constants were taken from G. DiLonardo and A. E. Douglas, J. Chem. Phys. 56, 5185 (1972).

(IDEAL GAS, REFERENCE STATE)   GFW = 37.9968

T, °K	Cp°	S°	-(G°-H°$_{298}$)/T	H°-H°$_{298}$	ΔHf°	ΔGf°	Log Kp
	gibbs/mol			kcal/mol			
0	.000	.000	INFINITE	-2.109	.000	.000	.000
100	6.958	40.694	54.838	-1.414	.000	.000	.000
200	7.095	45.542	49.113	-.714	.000	.000	.000
298	7.481	48.442	48.442	.000	.000	.000	.000
300	7.489	48.489	48.442	.014	.000	.000	.000
400	7.833	50.699	48.741	.783	.000	.000	.000
500	8.183	52.492	49.318	1.597	.000	.000	.000
600	8.399	54.004	49.976	2.417	.000	.000	.000
700	8.554	55.311	50.647	3.265	.000	.000	.000
800	8.670	56.461	51.303	4.126	.000	.000	.000
900	8.759	57.488	51.934	4.998	.000	.000	.000
1000	8.829	58.414	52.537	5.878	.000	.000	.000
1100	8.887	59.259	53.110	6.763	.000	.000	.000
1200	8.935	60.034	53.655	7.655	.000	.000	.000
1300	8.976	60.751	54.174	8.550	.000	.000	.000
1400	9.012	61.417	54.668	9.450	.000	.000	.000
1500	9.044	62.040	55.139	10.352	.000	.000	.000
1600	9.074	62.625	55.588	11.258	.000	.000	.000
1700	9.101	63.176	56.019	12.167	.000	.000	.000
1800	9.126	63.697	56.431	13.078	.000	.000	.000
1900	9.149	64.191	56.826	13.992	.000	.000	.000
2000	9.172	64.661	57.207	14.908	.000	.000	.000
2100	9.193	65.109	57.572	15.827	.000	.000	.000
2200	9.214	65.537	57.925	16.747	.000	.000	.000
2300	9.234	65.947	58.265	17.669	.000	.000	.000
2400	9.253	66.340	58.593	18.594	.000	.000	.000
2500	9.272	66.718	58.910	19.520	.000	.000	.000
2600	9.290	67.082	59.218	20.448	.000	.000	.000
2700	9.308	67.433	59.516	21.378	.000	.000	.000
2800	9.326	67.772	59.804	22.310	.000	.000	.000
2900	9.343	68.100	60.085	23.243	.000	.000	.000
3000	9.360	68.417	60.357	24.178	.000	.000	.000
3100	9.377	68.724	60.622	25.115	.000	.000	.000
3200	9.394	69.022	60.880	26.054	.000	.000	.000
3300	9.411	69.311	61.131	26.994	.000	.000	.000
3400	9.427	69.592	61.376	27.936	.000	.000	.000
3500	9.444	69.866	61.615	28.879	.000	.000	.000
3600	9.460	70.132	61.848	29.825	.000	.000	.000
3700	9.476	70.392	62.075	30.771	.000	.000	.000
3800	9.492	70.645	62.297	31.720	.000	.000	.000
3900	9.508	70.891	62.514	32.670	.000	.000	.000
4000	9.524	71.132	62.727	33.621	.000	.000	.000
4100	9.540	71.368	62.935	34.575	.000	.000	.000
4200	9.556	71.598	63.138	35.529	.000	.000	.000
4300	9.571	71.823	63.338	36.486	.000	.000	.000
4400	9.587	72.043	63.533	37.444	.000	.000	.000
4500	9.603	72.259	63.725	38.403	.000	.000	.000
4600	9.618	72.470	63.912	39.364	.000	.000	.000
4700	9.634	72.677	64.097	40.327	.000	.000	.000
4800	9.649	72.880	64.278	41.291	.000	.000	.000
4900	9.665	73.079	64.455	42.257	.000	.000	.000
5000	9.680	73.274	64.630	43.224	.000	.000	.000
5100	9.695	73.466	64.801	44.193	.000	.000	.000
5200	9.711	73.655	64.969	45.163	.000	.000	.000
5300	9.727	73.840	65.135	46.135	.000	.000	.000
5400	9.742	74.022	65.298	47.109	.000	.000	.000
5500	9.757	74.201	65.458	48.084	.000	.000	.000
5600	9.773	74.377	65.616	49.060	.000	.000	.000
5700	9.788	74.550	65.771	50.038	.000	.000	.000
5800	9.803	74.720	65.924	51.018	.000	.000	.000
5900	9.819	74.888	66.074	51.999	.000	.000	.000
6000	9.834	75.053	66.223	52.981	.000	.000	.000

July 31, 1972

$S^{\circ}_{298.15}$ = 57.08 ± 1 cal $K^{-1}mol^{-1}$ ΔHf°_{0} = -135.4 ± 0.8 kcal mol^{-1}

Ground State Quantum Weight = 1 $\Delta Hf^{\circ}_{298.15}$ = -136.87 ± 0.8 kcal mol^{-1}

Vibrational Frequencies and Degeneracies

$$\omega, cm^{-1}$$

[4000] (1)

[3400] (1)

[1200] (2)

[720] (1)

[350] (1)

Bond Distance: F-F = 2.78 Å   Bond Angle: F $\cdots$ F-H = 108° σ = 2

Product of the Moments of Inertia: $I_A I_B I_C$ = 20.241 x 10^{-117} g^3 cm^6

Heat of Formation

The enthalpy of 2 HF(g) → H_2F_2(g) was taken as the mean of the third law values which were obtained from the following equilibrium data. G. Briegleb and W. Strohmeier, Z. Elektrochem. 57, 668 (1953) measured the vapor density of associated HF(g) between 26 to 56°C and between 30 and 700 torr. E. U. Franck and F. Meyer, Z. Elektrochem. 63, 571 (1959) measured heat capacity between -20 and 100°C and between 100 and 700 torr. Their second law values differed by 1.2 kcal; and using the molecular constants discussed below gave respectively mean third law values which differed by 0.34 kcal, a 0.14 kcal temperature trend for Briegleb and Strohmeier, and a 0.02 kcal temperature trend for Franck and Meyer. The $\Delta Hf^{\circ}_{298.15}$ of H_2F_2(g) was calculated by using $\Delta Hf^{\circ}_{298.15}$ = -65.14 kcal for HF(g).

Heat Capacity and Entropy

The product of the moments of inertia was calculated from I_A, 1/2 (I_B + I_C), F-F distance, and F $\cdots$ F-H angle which were given by T. R. Dyke, B. J. Howard, and W. Klemperer, J. Chem. Phys. 56, 2442 (1972). They also gave σ. Reliable experimental values of the vibrational frequencies of H_2F_2(g) are not available. The estimated frequencies are similar to those used for the higher polymers which were obtained from data on HF solid. The infrared absorption bands observed in the vapor (350 to 400 cm^{-1}, 700 to 800 cm^{-1}, and 1000-1200 cm^{-1} regions) are largely due to the higher polymers, such as the tetramer and hexamer. Calculated values (610, 443, and 144 cm^{-1}) were obtained from force constants given in a paper on theory of molecular interactions of the HF polymers by J. E. Del Bene and J. A. Pople, J. Chem. Phys. 55, 2296 (1971). The potential energy surface computed for the dimer suggests very anharmonic low frequency motions for the external hydrogen (estimated at 600 ± 200 cm^{-1}) and for the hydrogen bond stretching mode.

(IDEAL GAS) GFW = 40.013

T, °K	Cp°	S°	-(G°-H°₂₉₈)/T	H°-H°₂₉₈	ΔHf°	ΔGf°	Log Kp
		gibbs/mol			kcal/mol		
0	.000	.000	INFINITE	-2.683	-135.420	-135.420	INFINITE
100	8.287	46.942	65.762	-1.882	-136.031	-134.251	293.405
200	9.507	53.055	58.020	-.993	-136.486	-132.286	144.555
298	10.725	57.079	57.079	.000	-136.870	-130.140	95.395
300	10.747	57.145	57.079	.020	-136.877	-130.099	94.777
400	11.879	60.396	57.515	1.153	-137.207	-127.787	69.820
500	12.795	63.150	58.373	2.388	-137.475	-125.401	54.812
600	13.512	65.548	59.373	3.705	-137.688	-122.965	44.790
700	14.090	67.676	60.410	5.086	-137.857	-120.497	37.621
800	14.579	69.590	61.440	6.520	-137.990	-118.008	32.238
900	15.011	71.333	62.444	8.000	-138.094	-115.503	28.048
1000	15.404	72.935	63.414	9.521	-138.171	-112.990	24.694
1100	15.763	74.420	64.348	11.080	-138.223	-110.467	21.948
1200	16.093	75.806	65.246	12.673	-138.256	-107.943	19.659
1300	16.396	77.106	66.108	14.297	-138.271	-105.416	17.722
1400	16.673	78.332	66.938	15.951	-138.271	-102.890	16.062
1500	16.926	79.491	67.737	17.631	-138.259	-100.361	14.623
1600	17.155	80.591	68.506	19.335	-138.239	-97.837	13.364
1700	17.364	81.637	69.248	21.062	-138.208	-95.311	12.253
1800	17.553	82.635	69.964	22.807	-138.171	-92.789	11.266
1900	17.724	83.589	70.656	24.571	-138.127	-90.269	10.383
2000	17.880	84.502	71.326	26.352	-138.077	-87.751	9.589
2100	18.020	85.378	71.974	28.147	-138.025	-85.237	8.871
2200	18.148	86.219	72.603	29.955	-137.969	-82.724	8.218
2300	18.265	87.028	73.213	31.776	-137.909	-80.214	7.622
2400	18.371	87.808	73.805	33.608	-137.849	-77.707	7.076
2500	18.467	88.560	74.380	35.450	-137.788	-75.205	6.574
2600	18.556	89.286	74.939	37.301	-137.725	-72.701	5.111
2700	18.636	89.988	75.484	39.161	-137.662	-70.202	5.682
2800	18.710	90.667	76.014	41.028	-137.600	-67.706	5.285
2900	18.778	91.325	76.531	42.903	-137.536	-65.206	4.914
3000	18.840	91.962	77.034	44.784	-137.474	-62.715	4.569
3100	18.898	92.581	77.526	46.671	-137.412	-60.225	4.246
3200	18.951	93.182	78.006	48.563	-137.353	-57.736	3.943
3300	19.000	93.766	78.475	50.461	-137.294	-55.249	3.659
3400	19.045	94.334	78.933	52.363	-137.237	-52.766	3.392
3500	19.087	94.886	79.381	54.269	-137.183	-50.278	3.140
3600	19.126	95.425	79.819	56.180	-137.131	-47.799	2.902
3700	19.162	95.949	80.248	58.095	-137.081	-45.314	2.677
3800	19.196	96.461	80.668	60.012	-137.035	-42.835	2.464
3900	19.227	96.960	81.079	61.934	-136.991	-40.359	2.262
4000	19.257	97.447	81.482	63.858	-136.950	-37.881	2.070
4100	19.284	97.923	81.877	65.785	-136.913	-35.403	1.887
4200	19.310	98.388	82.265	67.715	-136.878	-32.927	1.713
4300	19.334	98.842	82.645	69.647	-136.848	-30.454	1.548
4400	19.356	99.287	83.018	71.581	-136.821	-27.982	1.390
4500	19.376	99.722	83.385	73.518	-136.797	-25.508	1.239
4600	19.396	100.148	83.745	75.457	-136.776	-23.033	1.094
4700	19.417	100.566	84.098	77.397	-136.761	-20.561	.956
4800	19.434	100.975	84.445	79.340	-136.747	-18.089	.824
4900	19.451	101.376	84.787	81.284	-136.738	-15.617	.697
5000	19.467	101.769	85.123	83.230	-136.732	-13.150	.575
5100	19.482	102.154	85.453	85.178	-136.730	-10.675	.457
5200	19.496	102.533	85.778	87.127	-136.731	-8.202	.345
5300	19.509	102.904	86.097	89.077	-136.737	-5.728	.236
5400	19.522	103.269	86.412	91.028	-136.748	-3.260	.132
5500	19.534	103.627	86.722	92.981	-136.761	-.786	.031
5600	19.546	103.979	87.027	94.935	-135.778	1.685	-.066
5700	19.556	104.325	87.327	96.890	-136.799	4.160	-.159
5800	19.567	104.666	87.623	98.846	-136.825	6.629	-.250
5900	19.577	105.000	87.915	100.804	-136.853	9.105	-.337
6000	19.585	105.329	88.202	102.762	-136.885	11.577	-.422

July 31, 1972

Point Group C_3

$S^\circ_{298.15}$ = 68.9 cal K^{-1} mol^{-1}

Ground State Quantum Weight = 1

ΔHf°_0 = -207.7 ± 3 kcal mol^{-1}

$\Delta Hf^\circ_{298.15}$ = 210.1 ± 3 kcal mol^{-1}

<u>Vibrational Frequencies and Degeneracies</u>

ω, cm^{-1}

[202](3)

[962](3)

[552](3)

[3060](3)

Bond Distance: [F-F = 2.5 Å]

σ = 3

Product of the Moments of Inertia: $I_A I_B I_C$ = 2.238 x 10^{-114} g^3 cm^6

Heat of Formation

The enthalpy of 3HF(g) → H_3F_3(g) was taken as the mean of third law values which were determined from the equilibrium data of two investigations. Briegleb and Stohmeier (1) measured the vapor density of HF between 20 and 60°C and between 50 and 650 torr. Franck and Meyer (2) measured C_p between -20 and 100°C and between 100 and 700 torr. Each investigation evaluated K_p at $\underline{n}$ = 2, 3, 4, ... for the reactions n(HF) → $(HF)_n$ and reported second law values of ΔH and ΔS. At $\underline{n}$ = 3 their second law values differed by 2.7 kcal, which was taken as an estimate of error, while the third law values differed by 0.20 kcal. Using ΔH°_{298} = -14.69 kcal mol^{-1} and Δf°_{298}(HF,g) = -65.14 ± 0.2 kcal mol^{-1} gives the heat of formation of H_3F_3(g).

Heat Capacity and Entropy

The molecular structure of H_3F_3 was assumed as planar with the F-atoms forming the vertices of a regular triangle and with the H atoms also lying on the circumscribed circle. That rings are more stable than open chains was confirmed by Del Bene and Pople's (3) theoretical molecular-orbital studies on HF polymers. The length of side (F-F axis) was taken from Atoji and Lipscomb's (4) x-ray studies of solid HF (F-F = 2.49 Å) and agrees with 2.52 Å which Janzen and Bartell (5) determined for HF gaseous polymers by electron diffraction. Vibrational frequencies were taken from Kittelberger and Hornig's (6) work on crystalline HF. Huong and Couzi (7) and Smith (8) have made spectral studies of the gas phase in the range from 350 to 4000 cm^{-1}.

References

1. G. Briegleb and W. Strohmeier, Z. Elektrochem. <u>56</u>, 668 (1953).

2. E. U. Franck and F. Meyer, Z. Elektrochem. <u>63</u>, 571 (1959).

3. J. E. Del Bene and J. A. Pople, J. Chem. Phys. <u>55</u>, 2296 (1971).

4. N. Atoji and W. N. Lipscomb, Acta Crysta. <u>7</u>, 173 (1954).

5. J. Janzen and L. S. Bartell, J. Chem. Phys. <u>50</u>, 3611 (1969).

6. J. S. Kittelberger and D. F. Hornig, J. Chem. Phys. <u>46</u>, 3099 (1967).

7. P. V. Huong and M. Couzi, J. Chim. Phys. <u>66</u>, 1309 (1969).

8. D. F. Smith, J. Chem. Phys. <u>28</u>, 1040 (1958); ibid <u>48</u>, 1429 (1968).

T, °K	Cp°	S°	−(G°−H°₂₉₈)/T	H°−H°₂₉₈	ΔHf°	ΔGf°	Log Kp
		gibbs/mol			kcal/mol		
0	.000	.000	INFINITE	−3.854	−207.765	−207.765	INFINITE
100	11.164	53.298	82.875	−2.958	−208.986	−204.605	447.163
200	15.087	62.298	70.482	−1.637	−209.681	−199.024	218.466
298	18.128	68.916	68.916	.000	−210.110	−195.036	142.965
300	18.177	69.028	68.916	.034	−210.117	−194.942	142.015
400	20.393	74.581	69.658	1.969	−210.376	−189.841	103.724
500	21.931	79.306	71.127	4.090	−210.510	−184.690	80.728
600	23.063	83.409	72.840	6.342	−210.553	−179.521	65.390
700	23.973	87.035	74.614	8.695	−210.525	−174.349	54.434
800	24.755	90.288	76.373	11.132	−210.438	−169.187	46.220
900	25.449	93.245	78.086	13.643	−210.303	−164.038	39.834
1000	26.071	95.959	79.739	16.219	−210.124	−158.908	34.729
1100	26.629	98.470	81.330	18.855	−209.905	−153.795	30.556
1200	27.127	100.809	82.856	21.543	−209.665	−148.706	27.083
1300	27.571	102.998	84.323	24.278	−209.379	−143.637	24.148
1400	27.965	105.056	85.731	27.056	−209.082	−138.593	21.635
1500	28.315	106.998	87.084	29.870	−208.770	−133.566	19.460
1600	28.625	108.835	88.387	32.717	−208.449	−128.564	17.561
1700	28.899	110.579	89.642	35.594	−208.116	−123.580	15.887
1800	29.143	112.238	90.851	38.496	−207.776	−118.617	14.402
1900	29.361	113.820	92.019	41.422	−207.430	−113.673	13.075
2000	29.554	115.331	93.147	44.367	−207.081	−108.747	11.883
2100	29.727	116.777	94.238	47.332	−206.731	−103.840	10.807
2200	29.882	118.163	95.294	50.312	−206.379	−98.049	9.830
2300	30.021	119.495	96.318	53.308	−206.025	−94.073	8.939
2400	30.147	120.775	97.310	56.316	−205.674	−89.214	8.124
2500	30.260	122.008	98.274	59.337	−205.325	−84.372	7.376
2600	30.362	123.197	99.209	62.368	−204.976	−79.538	6.686
2700	30.455	124.345	100.119	65.409	−204.631	−74.721	6.048
2800	30.539	125.454	101.004	68.458	−204.289	−69.917	5.457
2900	30.615	126.527	101.866	71.516	−203.947	−65.118	4.907
3000	30.687	127.566	102.705	74.581	−203.611	−60.339	4.396
3100	30.751	128.573	103.524	77.653	−203.276	−55.571	3.918
3200	30.810	129.550	104.322	80.732	−202.947	−50.811	3.470
3300	30.865	130.499	105.101	83.815	−202.622	−46.062	3.051
3400	30.915	131.422	105.861	86.904	−202.301	−41.326	2.656
3500	30.961	132.318	106.605	89.998	−201.985	−36.590	2.285
3600	31.004	133.191	107.331	93.096	−201.675	−31.873	1.935
3700	31.043	134.041	108.042	96.199	−201.370	−27.155	1.604
3800	31.080	134.870	108.737	99.305	−201.071	−22.450	1.291
3900	31.114	135.677	109.417	102.415	−200.778	−17.758	.995
4000	31.146	136.465	110.084	105.528	−200.489	−13.067	.714
4100	31.175	137.235	110.736	108.644	−200.208	−8.383	.447
4200	31.204	137.987	111.376	111.763	−199.932	−3.706	.193
4300	31.230	138.721	112.004	114.885	−199.663	.960	−.049
4400	31.254	139.439	112.619	118.009	−199.399	5.620	−.279
4500	31.277	140.142	113.223	121.135	−199.142	10.277	−.499
4600	31.298	140.830	113.816	124.264	−198.890	14.931	−.709
4700	31.318	141.503	114.398	127.395	−198.647	19.577	−.910
4800	31.337	142.162	114.969	130.528	−198.408	24.216	−1.103
4900	31.355	142.809	115.531	133.662	−198.176	28.852	−1.287
5000	31.372	143.442	116.083	136.799	−197.949	33.476	−1.463
5100	31.388	144.064	116.625	139.937	−197.730	38.107	−1.633
5200	31.403	144.673	117.159	143.076	−197.516	42.732	−1.796
5300	31.417	145.272	117.684	146.217	−197.309	47.353	−1.953
5400	31.430	145.859	118.200	149.360	−197.109	51.962	−2.103
5500	31.443	146.436	118.708	152.503	−196.915	56.575	−2.248
5600	31.455	147.003	119.208	155.648	−196.726	61.181	−2.388
5700	31.467	147.560	119.701	158.794	−196.544	65.787	−2.522
5800	31.478	148.107	120.186	161.941	−196.370	70.381	−2.652
5900	31.488	148.645	120.664	165.090	−196.201	74.984	−2.778
6000	31.498	149.174	121.135	168.239	−196.036	79.574	−2.898

Point Group C_{3v} $\Delta Hf_0^\circ = -30.20$ kcal mol^{-1}

$S_{298.15}^\circ = 62.29$ gibbs mol^{-1} $\Delta Hf_{298}^\circ = -31.57 \pm 0.27$ kcal mol^{-1}

Ground State Quantum Weight = 1

Vibrational Frequencies and Degeneracies

ω, cm^{-1}

1032 (1)

642 (1)

905 (2)

493 (2)

Bond Distance: N-F = 1.371Å   Bond Angle: F-N-F = 102°9' $\sigma = 3$

Product of the Moments of Inertia: $I_A I_B I_C = 8.8543 \times 10^{-115}$ g^3 cm^6

Heat of Formation

The adopted enthalpy of formation is the mean of values calculated from the reaction processes listed below, and weighted inversely as the squares of the standard deviations. Auxiliary enthalpies of formation were taken from NBS TN 270-3, or from simultaneous adjustment of several interconnecting pieces of data leading to values tabulated in JANAF tables, 1968 and later. Also given below are the references, individual and averaged measured values of enthalpies of reaction and their uncertainties (2S), the value of enthalpy of formation calculated from each process and its uncertainty, and the weighted mean.

	Reaction	ΔH_v(selected) kcal mol^{-1}	ΔHf°[NF$_3$] kcal mol^{-1}
A	NF$_3$(g) + 3/2 H$_2$(g) = 3HF (aq, 50H$_2$O) + 1/2 N$_2$(g)	-199.42 ± 0.22	-30.92 ± 1.72
	(1) -196.3 ± 64; (2) -199.49 ± 0.22; (3) we derive -196.23 ± 0.77		
B	S(c,rh) + 2 NF$_3$(g) = SF$_6$(g) + N$_2$(g)	-291.79 ± 0.24	-31.77 ± 0.33
	(4)		
C	NF$_3$(g) → 0 1/2 N$_2$(g) + 3/2 F$_2$(g)	31.44 ± 0.3	-31.44 ± 0.3
	(5)		
D	8 NF$_3$(g) + 3 C$_2$N$_2$(g) = 6 CF$_4$(g) + 7 N$_2$(g)	-1308.8 ± 1.3	-31.4 ± 4.4
	(6)		
E	B(c) + NF$_3$(g) = BF$_3$(g) + 1/2 N$_2$(g)	-239.7 ± 1.2	-31.7 ± 1.6
	(7)		
F	NF$_3$(g) + 4 NH$_3$(g) = 3 NH$_4$F(c) + N$_2$(g)	-259.5 ± 1.0	-29.0 ± 3.0
	Weighted mean		-31.57 ± 0.27

References

1. G. T. Armstrong, S. Marantz, and C. F. Coyle, J. Am. Chem. Soc. 81, 3798 (1959).

2. G. C. Sinke, J. Chem. Eng. Data 10, 295-296 (1965).

3. A. N. Zercheninov, V. I. Chesnokov, and A. V. Parkratov, Zh. Fiz. Khim. 43, 390-393 (1969).

4. L. C. Walker, J. Phys. Chem. 71, 361-363 (1967).

5. G. C. Sinke, J. Phys. Chem. 71, 359-360 (1967).

6. L. C. Walker, Unpublished data, See NF$_3$, JANAF tables, June 30, 1968.

7. J. R. Ludwig and W. J. Cooper, J. Chem. Eng. Data 8, 76 (1963).

Heat Capacity and Entropy

The vibrational and rotational constants are taken from JANAF Thermochemical Tables, 2nd Edition, June, 1971 (U. S. Govt. Printing Office, Washington, D. C. 20402).

T, °K	Cp°	S°	−(G°−H°298)/T	H°−H°298	ΔHf°	ΔGf°	Log Kp
		gibbs/mol			kcal/mol		
0	.000	.000	INFINITE	−2.830	−30.200	−30.200	INFINITE
100	8.132	51.550	71.875	−2.032	−30.792	−27.934	61.050
200	10.211	57.728	63.374	−1.129	−31.287	−24.870	27.177
298	12.744	62.288	62.288	.000	−31.570	−21.653	15.872
300	12.787	62.367	62.288	.024	−31.574	−21.592	15.730
400	14.776	66.334	62.815	1.408	−31.692	−18.243	9.967
500	16.143	69.788	63.872	2.958	−31.699	−14.878	6.503
600	17.068	72.818	65.116	4.621	−31.637	−11.518	4.196
700	17.704	75.500	66.412	6.362	−31.532	−8.174	2.552
800	18.155	77.895	67.700	8.156	−31.401	−4.845	1.324
900	18.482	80.054	68.955	9.989	−31.256	−1.534	.372
1000	18.727	82.014	70.164	11.850	−31.102	1.759	−.384
1100	18.913	83.808	71.324	13.732	−30.941	5.040	−1.001
1200	19.058	85.460	72.434	15.631	−30.780	8.302	−1.512
1300	19.173	86.990	73.496	17.543	−30.617	11.553	−1.942
1400	19.265	88.415	74.511	19.465	−30.455	14.788	−2.309
1500	19.341	89.746	75.483	21.395	−30.292	18.016	−2.625
1600	19.403	90.997	76.414	23.333	−30.132	21.232	−2.900
1700	19.455	92.175	77.307	25.276	−29.974	24.438	−3.142
1800	19.499	93.288	78.164	27.223	−29.817	27.634	−3.355
1900	19.536	94.343	78.988	29.175	−29.663	30.822	−3.545
2000	19.568	95.346	79.781	31.130	−29.511	34.002	−3.716
2100	19.596	96.302	80.545	33.089	−29.362	37.172	−3.869
2200	19.620	97.214	81.282	35.050	−29.214	40.337	−4.007
2300	19.641	98.086	81.994	37.013	−29.068	43.496	−4.133
2400	19.660	98.923	82.682	38.978	−28.926	46.646	−4.248
2500	19.676	99.726	83.348	40.945	−28.786	49.791	−4.353
2600	19.691	100.498	83.993	42.913	−28.648	52.932	−4.449
2700	19.704	101.241	84.618	44.883	−28.513	56.067	−4.538
2800	19.715	101.958	85.224	46.854	−28.380	59.197	−4.621
2900	19.726	102.650	85.813	48.826	−28.249	62.326	−4.697
3000	19.735	103.319	86.386	50.799	−28.121	65.447	−4.768
3100	19.744	103.966	86.943	52.773	−27.995	68.562	−4.834
3200	19.752	104.593	87.484	54.748	−27.873	71.674	−4.895
3300	19.759	105.201	88.012	56.723	−27.752	74.782	−4.953
3400	19.765	105.791	88.526	58.699	−27.634	77.887	−5.007
3500	19.771	106.364	89.028	60.676	−27.518	80.991	−5.057
3600	19.777	106.921	89.517	62.654	−27.406	84.087	−5.105
3700	19.782	107.463	89.995	64.632	−27.294	87.188	−5.150
3800	19.786	107.991	90.462	66.610	−27.187	90.280	−5.192
3900	19.791	108.505	90.918	68.589	−27.082	93.366	−5.232
4000	19.795	109.006	91.364	70.568	−26.978	96.453	−5.270
4100	19.798	109.494	91.800	72.548	−26.879	99.541	−5.306
4200	19.802	109.972	92.227	74.528	−26.780	102.624	−5.340
4300	19.805	110.438	92.645	76.508	−26.685	105.703	−5.372
4400	19.808	110.893	93.055	78.489	−26.592	108.778	−5.403
4500	19.811	111.338	93.456	80.470	−26.501	111.857	−5.433
4600	19.813	111.774	93.849	82.451	−26.413	114.931	−5.460
4700	19.816	112.200	94.235	84.432	−26.328	118.001	−5.487
4800	19.818	112.617	94.614	86.414	−26.245	121.072	−5.513
4900	19.820	113.026	94.986	88.396	−26.165	124.137	−5.537
5000	19.822	113.426	95.350	90.378	−26.087	127.203	−5.560
5100	19.824	113.819	95.709	92.361	−26.012	130.266	−5.582
5200	19.826	114.204	96.061	94.343	−25.939	133.337	−5.604
5300	19.828	114.581	96.407	96.326	−25.869	136.397	−5.624
5400	19.829	114.952	96.747	98.309	−25.802	139.457	−5.644
5500	19.831	115.316	97.081	100.292	−25.738	142.520	−5.663
5600	19.832	115.673	97.410	102.275	−25.675	145.579	−5.681
5700	19.834	116.024	97.733	104.258	−25.615	148.636	−5.699
5800	19.835	116.369	98.052	106.242	−25.558	151.689	−5.716
5900	19.836	116.708	98.365	108.225	−25.504	154.746	−5.732
6000	19.837	117.042	98.673	110.209	−25.451	157.801	−5.748

July 31, 1972

Point Group C_4

$S^\circ_{298.15}$ = 83.4 cal K^{-1} mol^{-1}

Ground State Quantum Weight = 1

ΔHf°_0 = -280.0 ± 5 kcal mol^{-1}

$\Delta Hf^\circ_{298.15}$ = -282.9 ± 5 kcal mol^{-1}

Vibrational Frequencies and Degeneracies

ω, cm^{-1}

[202](4)

[53](2)

[962](4)

[552](4)

[3060](4)

Bond Distance: [F-F = 2.5 Å] σ = 4

Product of the Moments of Inertia: $I_A I_B I_C$ = 1.7903 x 10^{-113} g^3 cm^6

Heat of Formation

The enthalpy of 4 HF(g) → H_4F_4(g) was taken as the mean of third law values which were determined from the equilibrium data of two investigations. Briegleb and Strohmeier (1) measured the vapor density of the associated HF between 20 and 60°C and between 50 and 650 torr. Franck and Meyer (2) measured C_p between -20 and 100°C and between 100 and 700 torr. Each investigation evaluated K_p at $\underline{n}$ = 2, 3, 4, ... for the reactions n(HF) → (HF)$_n$ and reported second law values of ΔH and ΔS. At $\underline{n}$ = 4 their second law values differed by 4.2 kcal, which was taken as an estimate of error, while the calculated third law values differed by 1.5 kcal. Using ΔH°_{298} = -22.38 kcal mol^{-1} and ΔHf°_{298} (HF,g) = -65.14 ± 0.2 kcal mol^{-1} gives the heat of formation of H_4F_4(g).

Heat Capacity and Entropy

The molecular structure of H_4F_4 was assumed as planar with the F atoms forming the vertices of a regular tetragon and with the H atoms also lying in the circumscribed circle. That rings are more stable than open chains was confirmed by Del Bene and Pople's (3) theoretical molecular-orbital studies on HF polymers. The length of side (F-F axis) was taken from Atoji and Lipscomb's (4) x-ray studies of solid HF (F-F = 2.49 Å) and agrees with the 2.52 Å which Janzen and Bartell (5) determined for the gaseous polymers by electron diffraction. The low F-bending frequency (53 cm^{-1}) was taken from Boutin, Safford, and Brajovic's (6) work. The other vibrational frequencies were taken from Kittelberger and Hornig's (7) work on crystalline HF. Huong and Couzi (8) and Smith (9) have made spectral studies of the gas phase in the range from 350 to 4000 cm^{-1}.

References

1. G. Briegleb and W. Strohmeier, Z. Elektrochem. 57, 668 (1953).

2. E. U. Franck and F. Meyer, Z. Elektrochem. 63, 571 (1959).

3. J. E. Del Bene and J. A. Pople, J. Chem. Phys. 55, 2296 (1971).

4. M. Atoji and W. N. Lipscomb, Acta Crysta. 7, 173 (1954).

5. J. Janzen and L. S. Bartell, J. Chem. Phys. 50, 3611 (1969).

6. H. Boutin, G. J. Safford, and V. Brajovic, J. Chem. Phys. 39, 3135 (1963).

7. J. S. Kittelberger and D. F. Hornig, J. Chem. Phys. 46, 3099 (1967).

8. P. V. Huong and M. Couzi, J. Chim. Phys. 66, 1309 (1969).

9. D. F. Smith, J. Chem. Phys. 28, 1040 (1958); ibid, 48, 1429 (1968).

T, °K	Cp°	S°	$-(G°-H°_{298})/T$	$H°-H°_{298}$	ΔHf°	ΔGf°	Log Kp
		gibbs/mol			kcal/mol		
0	.000	.000	INFINITE	-5.389	-280.063	-280.063	INFINITE
100	16.024	61.248	103.184	-4.194	-281.692	-274.868	600.723
200	21.395	74.096	85.642	-2.309	-282.495	-267.692	292.520
298	25.474	83.436	83.436	.000	-282.940	-260.321	190.820
300	25.540	83.594	83.436	.047	-282.947	-260.181	189.542
400	28.504	91.373	84.477	2.759	-283.161	-252.554	157.989
500	30.555	97.968	86.533	5.718	-283.208	-244.894	107.043
600	32.069	103.679	88.925	8.852	-283.134	-237.238	86.414
700	33.284	108.716	91.400	12.122	-282.964	-229.599	71.684
800	34.325	113.230	93.851	15.503	-282.717	-221.992	60.645
900	35.254	117.328	96.235	18.983	-282.405	-214.419	52.068
1000	36.064	121.086	98.535	22.551	-282.033	-206.887	45.215
1100	36.825	124.561	100.745	26.197	-281.609	-199.389	39.615
1200	37.493	127.794	102.866	29.914	-281.144	-191.937	34.956
1300	38.085	130.819	104.901	33.694	-280.642	-184.522	31.021
1400	38.611	133.661	106.855	37.529	-280.115	-177.150	27.654
1500	39.077	136.341	108.732	41.414	-279.566	-169.811	24.741
1600	39.490	138.877	110.538	45.342	-279.006	-162.514	22.198
1700	39.857	141.282	112.276	49.310	-278.430	-155.248	19.958
1800	40.182	143.570	113.952	53.312	-277.844	-148.020	17.972
1900	40.472	145.750	115.568	57.345	-277.251	-140.823	16.198
2000	40.730	147.833	117.130	61.406	-276.652	-133.658	14.605
2100	40.961	149.826	118.640	65.490	-276.054	-126.525	13.168
2200	41.167	151.736	120.101	69.597	-275.451	-119.418	11.863
2300	41.353	153.570	121.517	73.723	-274.847	-112.338	10.675
2400	41.520	155.334	122.889	77.867	-274.247	-105.286	9.588
2500	41.671	157.032	124.221	82.027	-273.649	-98.264	8.590
2600	41.807	158.669	125.515	86.201	-273.051	-91.256	7.671
2700	41.931	160.249	126.772	90.388	-272.458	-84.276	6.822
2800	42.044	161.776	127.995	94.586	-271.870	-77.320	6.035
2900	42.145	163.253	129.186	98.796	-271.282	-70.373	5.303
3000	42.240	164.684	130.345	103.015	-270.701	-63.459	4.623
3100	42.325	166.070	131.475	107.244	-270.122	-56.563	3.988
3200	42.405	167.415	132.578	111.480	-269.552	-49.683	3.393
3300	42.477	168.721	133.653	115.725	-268.985	-42.820	2.836
3400	42.544	169.990	134.703	119.976	-268.424	-35.081	2.313
3500	42.606	171.224	135.729	124.233	-267.871	-29.144	1.820
3600	42.663	172.425	136.732	128.497	-267.325	-22.336	1.356
3700	42.716	173.595	137.712	132.766	-266.786	-15.531	.917
3800	42.765	174.735	138.672	137.040	-266.254	-8.747	.503
3900	42.811	175.846	139.611	141.319	-265.731	-1.984	.111
4000	42.853	176.931	140.530	145.602	-265.214	4.775	-.261
4100	42.893	177.989	141.431	149.889	-264.707	11.521	-.614
4200	42.930	179.023	142.314	154.180	-264.206	18.255	-.950
4300	42.964	180.034	143.179	158.475	-263.715	24.970	-1.269
4400	42.997	181.022	144.028	162.773	-263.231	31.674	-1.573
4500	43.027	181.989	144.861	167.074	-262.756	38.372	-1.864
4600	43.055	182.935	145.679	171.378	-262.288	45.063	-2.141
4700	43.082	183.861	146.481	175.685	-261.831	51.739	-2.406
4800	43.108	184.768	147.269	179.995	-261.379	58.405	-2.659
4900	43.131	185.657	148.044	184.307	-260.937	65.063	-2.902
5000	43.154	186.529	148.805	188.621	-260.503	71.702	-3.134
5100	43.175	187.384	149.553	192.937	-260.079	78.349	-3.357
5200	43.195	188.222	150.288	197.256	-259.660	84.984	-3.572
5300	43.214	189.045	151.012	201.576	-259.252	91.612	-3.778
5400	43.232	189.853	151.724	205.899	-258.853	98.221	-3.975
5500	43.249	190.647	152.424	210.223	-258.461	104.832	-4.166
5600	43.265	191.426	153.114	214.549	-258.077	111.433	-4.349
5700	43.280	192.192	153.793	218.876	-257.702	118.030	-4.526
5800	43.295	192.945	154.461	223.205	-257.337	124.611	-4.695
5900	43.309	193.685	155.120	227.535	-256.979	131.199	-4.860
6000	43.322	194.413	155.769	231.866	-256.628	137.770	-5.018

July 31, 1972

HYDROGEN FLUORIDE CYCLIC PENTAMER (H_5F_5)　　　　(IDEAL GAS)　　　　GFW = 100.032

Point Group　C_5　　　　　　　　　　　　ΔHf_0° = -352.6 ± 6 kcal mol^{-1}

$S_{298.15}^\circ$ = 97.6 cal K^{-1} mol^{-1}　　　　　　$\Delta Hf_{298.15}^\circ$ = -356.0 ± 6 kcal mol^{-1}

Ground State Quantum Weight = 1

Vibrational Frequencies and Degeneracies

ω, cm^{-1}

[202] (5)

[53] (4)

[962] (5)

[552] (5)

[3060] (5)

Bond Distance: [F-F = 2.5 Å]　　　　　　　　　　　　　　σ = 5

Product of the Moments of Inertia: $I_A I_B I_C$ = 1.0598 x 10^{-112} g^3 cm^6

Heat of Formation

The enthalpy of 5 HF(g) → H_5F_5(g) was taken as the mean of third law values which were determined from the equilibrium data of two investigations. Briegleb and Strohmeier (1) measured the vapor density of the associated HF between 20 and 60°C and between 50 and 650 torr. Franck and Meyer (2) measured C_p between −20 and 100°C and between 100 and 700 torr. Each investigation evaluated K_p at $\underline{n}$ = 2, 3, 4, ... for the reactions n(HF) → (HF)$_n$ and reported second law values of ΔH and ΔS. At $\underline{n}$ = 5 their second law values differed by 5.2 kcal, which was taken as an estimate of error, while the calculated third law values differed by 3.1 kcal. Using ΔH_{298}° = -30.35 kcal mol^{-1} and ΔHf_{298}°(HF,g) = -65.14 ± 0.2 kcal mol^{-1} gives the heat of formation of H_5F_5(g).

Heat Capacity and Entropy

The molecular structure of H_5F_5 was assumed as planar with the F atoms forming the vertices of a regular pentagon and with the H atoms also lying on the circumscribed circle. That rings are more stable than open chains was confirmed by Del Bene and Pople's (3) theoretical molecular-orbital studies on HF polymers. The length of side (F-F axis) was taken from Atoji and Lipscomb's (4) x-ray studies of solid HF (F-F = 2.49 Å) and agrees with the 2.52 Å which Janzen and Bartell (5) determined for HF gaseous polymers by electron diffraction. The low F-bending frequency (53 cm^{-1}) was taken from Boutin, Safford, and Brajovic's (6) work. The other vibrational frequencies were taken from Kittelberger and Hornig's (7) work on crystalline HF. Huong and Couzi (8) and Smith (9) have made spectral studies of the gas phase in the range from 350 to 4000 cm^{-1}.

References

1. G. Briegleb and W. Strohmeier, Z. Elektrochem. 57, 668 (1953).

2. E. U. Franck and F. Meyer, Z. Elektrochem. 63, 571 (1959).

3. J. E. Del Bene and J. A. Pople, J. Chem. Phys. 55, 2296 (1971).

4. M. Atoji and W. N. Lipscomb, Acta Crysta. 7, 173 (1954).

5. J. Janzen and L. S. Bartell, J. Chem. Phys. 50, 3611 (1969).

6. H. Boutin, G. J. Safford, and V. Brajovic, J. Chem. Phys. 39, 3135 (1963).

7. J. S. Kittelberger and D. F. Hornig, J. Chem. Phys. 46, 3099 (1967).

8. P. V. Huong and M. Couzi, J. Chim. Phys. 66, 1309 (1969).

9. D. F. Smith, J. Chem. Phys. 28, 1040 (1958); ibid, 48, 1429 (1968).

T, °K	Cp°	S°	−(G°−H°298)/T	H°−H°298	ΔHf°	ΔGf°	Log Kp
		gibbs/mol			kcal/mol		
0	.000	.000	INFINITE	−6.924	−352.641	−352.641	INFINITE
100	20.853	68.836	123.129	−5.429	−354.677	−345.375	754.815
200	27.699	85.530	100.440	−2.982	−355.589	−335.667	366.800
298	32.820	97.592	97.592	.000	−356.050	−325.778	236.802
300	32.902	97.796	97.593	.061	−356.057	−325.590	237.192
400	36.614	107.803	98.932	3.548	−356.227	−315.402	172.327
500	39.185	116.266	101.575	7.346	−356.187	−305.197	133.402
600	41.076	123.585	104.647	11.363	−355.995	−295.017	107.460
700	42.596	130.034	107.822	15.549	−355.684	−284.875	88.942
800	43.901	135.809	110.966	19.875	−355.275	−274.786	75.068
900	45.059	141.048	114.021	24.324	−354.786	−264.753	64.291
1000	46.097	145.850	116.968	28.883	−354.222	−254.783	55.683
1100	47.027	150.288	119.798	33.540	−353.593	−244.864	48.650
1200	47.859	154.417	122.512	38.285	−352.913	−235.011	42.801
1300	48.599	158.277	125.117	43.109	−352.186	−225.215	37.862
1400	49.256	161.903	127.616	48.002	−351.428	−215.479	33.638
1500	49.839	165.322	130.017	52.957	−350.643	−205.790	29.984
1600	50.356	168.555	132.325	57.968	−349.842	−196.163	26.795
1700	50.814	171.622	134.548	63.027	−349.023	−186.579	23.986
1800	51.221	174.538	136.689	68.129	−348.191	−177.049	21.497
1900	51.583	177.317	138.755	73.269	−347.351	−167.563	19.274
2000	51.906	179.972	140.750	78.444	−346.504	−158.122	17.279
2100	52.194	182.511	142.678	83.649	−345.656	−148.726	15.478
2200	52.452	184.945	144.545	88.882	−344.803	−139.368	13.845
2300	52.684	187.282	146.352	94.139	−343.949	−130.048	12.357
2400	52.893	189.529	148.105	99.418	−343.100	−120.767	10.997
2500	53.082	191.692	149.805	104.717	−342.253	−111.527	9.750
2600	53.252	193.777	151.457	110.034	−341.406	−102.310	8.600
2700	53.407	195.790	153.062	115.367	−340.566	−93.131	7.538
2800	53.548	197.735	154.623	120.715	−339.730	−83.985	6.555
2900	53.676	199.616	156.142	126.076	−338.897	−74.855	5.641
3000	53.794	201.438	157.621	131.449	−338.070	−65.769	4.791
3100	53.901	203.204	159.064	136.834	−337.248	−56.709	3.998
3200	54.000	204.917	160.470	142.229	−336.436	−47.672	3.256
3300	54.090	206.580	161.842	147.634	−335.629	−38.660	2.560
3400	54.174	208.196	163.182	153.047	−334.828	−29.680	1.908
3500	54.251	209.767	164.490	158.469	−334.036	−20.706	1.293
3600	54.322	211.296	165.769	163.897	−333.255	−11.771	.715
3700	54.388	212.786	167.020	169.333	−332.482	−2.842	.168
3800	54.450	214.237	168.244	174.775	−331.718	6.057	−.348
3900	54.507	215.652	169.441	180.223	−330.965	14.928	−.837
4000	54.560	217.033	170.614	185.676	−330.219	23.790	−1.300
4100	54.609	218.381	171.762	191.134	−329.486	32.634	−1.740
4200	54.655	219.697	172.888	196.598	−328.760	41.462	−2.157
4300	54.699	220.984	173.992	202.065	−328.047	50.262	−2.555
4400	54.739	222.242	175.074	207.537	−327.343	59.047	−2.933
4500	54.777	223.472	176.136	213.013	−326.649	67.822	−3.294
4600	54.813	224.677	177.178	218.493	−325.965	76.586	−3.639
4700	54.845	225.856	178.201	223.976	−325.294	85.330	−3.968
4800	54.878	227.011	179.206	229.462	−324.631	94.056	−4.283
4900	54.906	228.143	180.193	234.951	−323.979	102.774	−4.584
5000	54.935	229.252	181.163	240.443	−323.337	111.465	−4.872
5100	54.962	230.340	182.117	245.938	−322.707	120.163	−5.149
5200	54.987	231.408	183.055	251.436	−322.084	128.845	−5.415
5300	55.011	232.455	183.977	256.935	−321.474	137.517	−5.671
5400	55.033	233.484	184.884	262.438	−320.877	146.161	−5.915
5500	55.055	234.494	185.777	267.942	−320.288	154.808	−6.152
5600	55.075	235.486	186.655	273.449	−319.709	163.439	−6.378
5700	55.094	236.461	187.521	278.957	−319.140	172.065	−6.597
5800	55.112	237.419	188.373	284.468	−318.585	180.668	−6.808
5900	55.130	238.362	189.213	289.980	−318.038	189.279	−7.011
6000	55.146	239.288	190.039	295.493	−317.499	197.866	−7.207

Point Group C_6 ΔHf_0° = -428.1 ± 2 kcal mol^{-1}

$S_{298.15}^\circ$ = 111.4 cal K^{-1}mol^{-1} $\Delta Hf_{298.15}^\circ$ = -432.0 ± 2 kcal mol^{-1}

Ground State Quantum Weight = 1

Vibrational Frequencies and Degeneracies

ω, cm^{-1}

[202](6)

[53](6)

[962](6)

[552](6)

[3060](6)

Bond Distance: [F-F = 2.5 Å]   σ = 6

Product of the Moments of Inertia: $I_A I_B I_C$ = 4.834 x 10^{-112} g^3 cm^6

Heat of Formation

The enthalpy of 6 HF(g) → H_6F_6(g) was taken as the mean of third law values which were determined from the equilibrium data of two investigations. Briegleb and Strohmeier (1) measured the vapor density of the associated HF between 20 and 60°C and between 50 and 650 torr. Franck and Meyer (2) measured C_p between -20 and 100°C and between 100 and 700 torr. Each investigation evaluated K_p at n = 2, 3, 4, ... for the reactions n(HF) → (HF)$_n$ and reported second law values of ΔH and ΔS. At n = 6 their second law values differed by 0.8 kcal, which was taken as an estimate of error, while the calculated third law values differed by 0.6 kcal. Using ΔH_{298}° = -41.20 kcal mol^{-1} and ΔHf_{298}° (HF,g) = -65.14 ± 0.2 kcal mol^{-1} gives the heat of formation of H_6F_6(g).

Heat Capacity and Entropy

The molecular structure of H_6F_6 was assumed as planar with the F atoms forming the vertices of a regular hexagon and with the H atoms also lying on the circumscribed circle. That rings are more stable than open chains was confirmed by Del Bene and Pople's (3) theoretical molecular-orbital studies on HF polymers. The length of side (F-F axis) was taken from Atoji and Lipscomb's (4) x-ray studies of solid HF (F-F = 2.49 Å) and agrees with the 2.52 Å which Janzen and Bartell (5) determined for HF gaseous polymers by electron diffraction. The low F-bending frequency (53 cm^{-1}) was taken from Boutin, Safford, and Brajovic's (6) work. The other vibrational frequencies were taken from Kittelberger and Hornig's (7) work on crystalline HF. Huong and Couzi (8) and Smith (9) have made spectral studies of the gas phase in the range from 350 to 4000 cm^{-1}.

References

1. G. Briegleb and W. Strohmeier, Z. Elektrochem. 57, 668 (1953).

2. E. U. Franck and F. Meyer, Z. Elektrochem. 63, 571 (1959).

3. J. E. Del Bene and J. A. Pople, J. Chem. Phys. 55, 2296 (1971).

4. M. Atoji and W. N. Lipscomb, Acta Crysta. 7, 173 (1954).

5. J. Janzen and L. S. Bartell, J. Chem. Phys. 50, 3611 (1969).

6. H. Boutin, G. J. Safford, and V. Brajovic, J. Chem. Phys. 39, 3135 (1963).

7. J. S. Kittelberger and D. F. Hornig, J. Chem. Phys. 46, 3099 (1967).

8. P. V. Huong and M. Couzi, J. Chim. Phys. 66, 1309 (1969).

9. D. F. Smith, J. Chem. Phys. 28, 1040 (1958); ibid, 48, 1429 (1968).

Hydrogen Fluoride Cyclic Hexamer (H₆F₆)

F_6H_6

(Ideal Gas)   GFW = 120.038

T, °K	Cp°	S°	-(G°-H°₂₉₈)/T	H°-H°₂₉₈	ΔHf°	ΔGf°	Log Kp
		gibbs/mol			kcal/mol		
0	.000	.000	INFINITE	-8.459	-428.100	-428.100	INFINITE
100	25.742	76.123	142.774	-6.665	-430.542	-418.732	915.137
200	34.005	96.665	114.937	-3.654	-431.563	-406.462	444.161
298	40.160	111.449	111.449	.000	-432.040	-394.026	288.828
300	40.265	111.698	111.450	.074	-432.047	-393.790	286.876
400	44.725	123.932	113.088	4.338	-432.172	-381.010	208.174
500	47.813	134.264	116.317	8.974	-432.045	-368.230	160.953
600	50.083	143.191	120.069	13.873	-431.736	-355.495	129.489
700	51.908	151.053	123.945	18.976	-431.283	-342.821	107.033
800	53.474	158.088	127.780	24.246	-430.714	-330.221	90.212
900	54.864	164.469	131.508	29.665	-430.047	-317.697	77.147
1000	56.110	170.315	135.100	35.214	-429.292	-305.258	66.714
1100	57.227	175.716	138.550	40.882	-428.457	-292.889	58.192
1200	58.225	180.739	141.859	46.656	-427.561	-280.607	51.105
1300	59.113	185.435	145.032	52.524	-426.610	-268.398	45.122
1400	59.845	189.845	148.077	58.475	-425.621	-256.268	40.005
1500	60.601	194.003	151.002	64.501	-424.599	-244.201	35.580
1600	61.221	197.934	153.813	70.593	-423.559	-232.212	31.719
1700	61.771	201.662	156.519	76.743	-422.497	-220.281	28.319
1800	62.260	205.207	159.127	82.945	-421.419	-208.418	25.305
1900	62.694	208.585	161.641	89.193	-420.331	-196.614	22.616
2000	63.081	211.811	164.070	95.482	-419.235	-184.867	20.201
2100	63.427	214.897	166.417	101.808	-418.138	-173.178	18.023
2200	63.737	217.855	168.689	108.166	-417.036	-161.539	16.047
2300	64.018	220.695	170.888	114.554	-415.931	-149.949	14.248
2400	64.267	223.425	173.021	120.969	-414.832	-138.409	12.604
2500	64.493	226.053	175.090	127.407	-413.737	-126.921	11.095
2600	64.698	228.586	177.099	133.867	-412.641	-115.465	9.706
2700	64.883	231.031	179.052	140.346	-411.553	-104.057	8.423
2800	65.052	233.394	180.950	146.843	-410.471	-92.691	7.235
2900	65.206	235.680	182.798	153.356	-409.391	-81.348	6.131
3000	65.347	237.893	184.598	159.884	-408.320	-70.061	5.104
3100	65.476	240.038	186.352	166.425	-407.254	-58.807	4.146
3200	65.594	242.118	188.062	172.978	-406.200	-47.583	3.250
3300	65.703	244.138	189.731	179.543	-405.152	-36.391	2.410
3400	65.803	246.101	191.361	186.119	-404.111	-25.240	1.622
3500	65.896	248.010	192.952	192.704	-403.082	-14.100	.880
3600	65.981	249.868	194.507	199.298	-402.065	-3.008	.183
3700	66.061	251.677	196.028	205.900	-401.058	8.074	-.477
3800	66.134	253.439	197.516	212.510	-400.061	19.119	-1.100
3900	66.203	255.158	198.972	219.127	-399.078	30.128	-1.688
4000	66.266	256.835	200.398	225.750	-398.104	41.124	-2.247
4100	66.326	258.472	201.794	232.380	-397.144	52.097	-2.777
4200	66.381	260.071	203.163	239.015	-396.194	63.047	-3.281
4300	66.433	261.634	204.504	245.656	-395.259	73.963	-3.759
4400	66.482	263.161	205.820	252.302	-394.334	84.859	-4.215
4500	66.527	264.656	207.111	258.952	-393.423	95.741	-4.650
4600	66.570	266.119	208.378	265.607	-392.522	106.607	-5.065
4700	66.611	267.551	209.622	272.266	-391.638	117.448	-5.461
4800	66.648	268.954	210.843	278.929	-390.762	128.269	-5.840
4900	66.684	270.328	212.043	285.596	-389.900	139.073	-6.203
5000	66.718	271.675	213.223	292.266	-389.050	149.846	-6.550
5100	66.749	272.997	214.382	298.939	-388.215	160.626	-6.883
5200	66.780	274.294	215.521	305.616	-387.388	171.385	-7.203
5300	66.809	275.566	216.642	312.295	-386.577	182.129	-7.510
5400	66.835	276.815	217.745	318.977	-385.781	192.840	-7.805
5500	66.860	278.042	218.830	325.662	-384.994	203.552	-8.088
5600	66.885	279.247	219.898	332.349	-384.220	214.244	-8.361
5700	66.908	280.431	220.950	339.039	-383.458	224.928	-8.624
5800	66.929	281.594	221.986	345.731	-382.712	235.583	-8.877
5900	66.950	282.739	223.006	352.425	-381.976	246.246	-9.122
6000	66.970	283.864	224.011	359.121	-381.250	256.879	-9.357

July 31, 1972

Point Group C_7

$S^\circ_{298.15} = 125.1$ cal $K^{-1} mol^{-1}$

Ground State Quantum Weight = 1

$\Delta Hf^\circ_0 = -498.0 \pm 9$ kcal mol^{-1}

$\Delta Hf^\circ_{298.15} = -502.5 \pm 9$ kcal mol^{-1}

Vibrational Frequencies and Degeneracies

ω, cm^{-1}

[202](7)

[53](8)

[962](7)

[552](7)

[3060](7)

Bond Distance: [F-F = 2.5 Å] $\sigma = 7$

Product of the Moments of Inertia: $I_A I_B I_C = 1.7977 \times 10^{-111}$ g^3 cm^6

Heat of Formation

The enthalpy of 7 HF(g) → H_7F_7(g) was taken as the mean of third law values which were determined from the equilibrium data of two investigations. Briegleb and Strohmeier (1) measured the vapor density of the associated HF between 20 and 60°C and between 50 and 650 torr. Franck and Meyer (2) measured C_p between -20 and 100°C and between 100 and 700 torr. Each investigation evaluated K_p at $\underline{n}$ = 2, 3, 4, ... for the reactions n(HF) → $(HF)_n$ and reported second law values of ΔH and ΔS. At $\underline{n}$ = 7 their second law values differed by 7.3 kcal, which was taken as an estimate of error, while the calculated third law values differed by 6.4 kcal. Using ΔH°_{298} = -46.54 kcal mol^{-1} and ΔHf°_{298}(HF,g) = -65.14 ± 0.2 kcal mol^{-1} gives the heat of formation of H_7F_7(g).

Heat Capacity and Entropy

The molecular structure of H_7F_7 was assumed as planar with the F atoms forming the vertices of a regular septemgon and the H atoms also lying on the circumscribed circle. That rings are more stable than open chains was confirmed by Del Bene and Pople's (3) theoretical molecular-orbital studies on HF polymers. The length of side (F-F axis) was taken from Atoji and Lipscomb's (4) x-ray studies of solid HF (F-F = 2.49 Å) and agrees with the 2.52 Å which Janzen and Bartell (5) determined for HF gaseous polymers by electron diffraction. The low F-bending frequency (53 cm^{-1}) was taken from Boutin, Safford, and Brajovic's (6) work. The other vibrational frequencies were taken from Kittelberger and Hornig's (7) work on crystalline HF. Huong and Couzi (8) and Smith (9) have made spectral studies of the gas phase in the range from 350 to 4000 cm^{-1}.

References

1. G. Briegleb and W. Strohmeier, Z. Elektrochem. 57, 668 (1953).

2. E. U. Franck and F. Meyer, Z. Elektrochem. 63, 571 (1959).

3. J. E. Del Bene and J. A. Pople, J. Chem. Phys. 55, 2296 (1971).

4. M. Atoji and W. N. Lipscomb, Acta Crysta. 7, 173 (1954).

5. J. Janzen and L. S. Bartell, J. Chem. Phys. 50, 3611 (1969).

6. H. Boutin, G. J. Safford, and V. Brajovic, J. Chem. Phys. 39, 3135 (1963).

7. J. S. Kittelberger and D. F. Hornig, J. Chem. Phys. 46, 3099 (1967).

8. P. V. Huong and M. Couzi, J. Chim. Phys. 66, 1309 (1969).

9. D. F. Smith, J. Chem. Phys. 28, 1040 (1958); ibid, 48, 1429 (1968).

(IDEAL GAS)   GFW = 140.045

T, °K	Cp°	S°	--(G°—H°298)/T	H°—H°298	ΔHf°	ΔGf°	Log Kp
		gibbs/mol			kcal/mol		
0	.000	.000	INFINITE	-9.993	-498.048	-498.046	INFINITE
100	30.601	83.180	162.189	-7.901	-500.897	-486.555	1063.365
200	40.310	107.570	129.204	-4.327	-502.027	-471.701	515.451
296	47.512	125.075	125.075	.000	-502.520	-456.694	334.706
300	47.627	125.370	125.076	.088	-502.526	-456.410	332.495
400	52.836	139.831	127.013	5.127	-502.608	-441.016	240.960
500	56.440	152.032	130.828	10.602	-502.394	-425.638	186.046
600	59.090	162.567	135.260	16.384	-501.967	-410.326	149.461
700	61.220	171.840	139.837	22.403	-501.373	-395.095	123.354
800	63.048	180.137	144.365	28.618	-500.642	-379.961	103.801
900	64.670	187.658	148.764	35.005	-499.799	-364.924	88.616
1000	66.125	194.549	153.002	41.546	-498.851	-349.993	76.491
1100	67.426	200.913	157.072	48.225	-497.811	-335.151	66.588
1200	68.590	206.831	160.975	55.027	-496.700	-320.415	58.356
1300	69.627	212.363	164.717	61.939	-495.524	-305.771	51.405
1400	70.547	217.557	168.308	68.948	-494.304	-291.224	45.462
1500	71.363	222.453	171.756	76.045	-493.045	-276.755	40.323
1600	72.057	227.082	175.071	83.218	-491.766	-262.382	35.840
1700	72.728	231.472	178.260	90.459	-490.461	-248.080	31.893
1800	73.298	235.645	181.333	97.761	-489.137	-233.862	28.395
1900	73.805	239.622	184.297	105.117	-487.801	-219.716	25.273
2000	74.257	243.419	187.159	112.520	-486.456	-205.640	22.471
2100	74.661	247.052	189.925	119.967	-485.110	-191.635	19.944
2200	75.023	250.534	192.602	127.451	-483.758	-177.692	17.652
2300	75.347	253.876	195.194	134.970	-482.403	-163.808	15.565
2400	75.640	257.089	197.706	142.520	-481.055	-149.987	13.658
2500	75.904	260.183	200.144	150.097	-479.711	-136.229	11.909
2600	76.143	263.164	202.511	157.699	-478.367	-122.509	10.298
2700	76.360	266.042	204.811	165.325	-477.031	-108.849	8.811
2800	76.557	268.823	207.047	172.971	-475.702	-95.242	7.434
2900	76.735	271.512	209.224	180.636	-474.376	-81.662	6.154
3000	76.901	274.117	211.344	188.318	-473.060	-68.149	4.965
3100	77.051	276.641	213.410	196.015	-471.750	-54.678	3.855
3200	77.189	279.089	215.424	203.727	-470.454	-41.245	2.817
3300	77.316	281.466	217.390	211.453	-469.165	-27.851	1.844
3400	77.433	283.776	219.309	219.190	-467.885	-14.506	.932
3500	77.541	286.022	221.183	226.939	-465.618	-1.176	.073
3600	77.641	288.208	223.014	234.698	-465.365	12.096	-.734
3700	77.733	290.337	224.805	242.467	-464.124	25.355	-1.496
3800	77.819	292.411	226.557	250.244	-462.895	38.568	-2.218
3900	77.899	294.433	228.272	258.030	-461.682	51.738	-2.899
4000	77.973	296.407	229.951	265.824	-460.479	64.891	-3.545
4100	78.045	298.333	231.595	273.625	-459.293	78.015	-4.159
4200	78.107	300.214	233.206	281.432	-458.118	91.111	-4.741
4300	78.168	302.053	234.786	289.245	-456.961	104.166	-5.294
4400	78.225	303.851	236.336	297.066	-455.816	117.196	-5.821
4500	78.278	305.609	237.856	304.891	-454.686	130.207	-6.324
4600	78.328	307.330	239.347	312.721	-453.569	143.200	-6.804
4700	78.375	309.015	240.812	320.556	-452.472	156.161	-7.261
4800	78.419	310.666	242.250	328.396	-451.383	169.098	-7.699
4900	78.460	312.283	243.663	336.240	-450.312	182.014	-8.118
5000	78.500	313.869	245.051	344.088	-449.254	194.891	-8.519
5100	78.537	315.423	246.416	351.940	-448.213	207.775	-8.904
5200	78.572	316.949	247.757	359.795	-447.183	220.634	-9.273
5300	78.605	318.446	249.077	367.654	-446.170	233.475	-9.628
5400	78.635	319.915	250.375	375.515	-445.175	246.275	-9.967
5500	78.666	321.358	251.653	383.381	-444.191	259.075	-10.295
5600	78.694	322.775	252.910	391.250	-443.221	271.850	-10.609
5700	78.721	324.169	254.148	399.120	-442.266	284.616	-10.913
5800	78.747	325.539	255.367	406.994	-441.330	297.346	-11.204
5900	78.771	326.885	256.558	414.870	-440.405	310.084	-11.486
6000	78.794	328.209	257.751	422.748	-439.492	322.787	-11.758

$S^{\circ}_{298.15} = 43.3$ gibbs mol^{-1} $\Delta Hf^{\circ}_{0} = 90 \pm 4$ kcal mol^{-1}

$\Delta Hf^{\circ}_{298} = 90 \pm 4$ kcal mol^{-1}

Electronic States and Molecular Constants

State	ϵ, cm^{-1}	g	ω_e, cm^{-1}	$\chi_e\omega_e$, cm^{-1}	B_e, cm^{-1}	α_e, cm^{-1}	r_e, Å
$^3\Sigma^+$	0	3	3315	94.7	16.6684	0.646	1.038

$\sigma = 1$

Heat of Formation

The electron impact appearance potential of N_2^+ from HN_3, determined by J. L. Franklin, V. H. Dibeler, R. M. Reese, and M. Krauss, J. Am. Chem. Soc. <u>80</u>, 298 (1958) leads to a value $\Delta Hf^{\circ}_{0}(NH,g) = 81.7 \pm .5$ kcal mol^{-1}. R. I. Reed and W. Snedden, J. Chem. Soc. 4132 (1959) determined the electron impact appearance potential of NH^+ from NH_3. This combined with the directly measured electron impact ionization potential of NH, 13.1 eV gives $\Delta Hf^{\circ}_{0} = 82.9$ kcal mol^{-1}. This value of the ionization potential of NH has also been obtained by S. N. Foner and R. L. Hudson, J. Chem. Phys. <u>45</u>, 40 (1966). However, all of these electron impact experiments are subject to errors of several tenths of an electron volt or more.

More recently, K. E. Seal and A. G. Gaydon, Proc. Phys. Soc. <u>89</u>, 459 (1966) measured the concentration of NH in reflected shock waves in nitrogen-hydrogen-krypton and ammonia-krypton mixtures. These led to D(NH) = 3.21 ± 0.16 eV, corresponding to $\Delta Hf^{\circ}_{0}(NH,g) = 90.13 \pm 3.7$ kcal mol^{-1}. W. E. Kaskan and M. P. Nadler, J. Chem. Phys. <u>56</u>, 2220 (1972) determined NH, NH_3, and OH concentrations in a flat NH_3-D_2-N_2 flame and concluded $\Delta Hf^{\circ}_{0}(NH) = 90 \pm 4$ kcal mol^{-1}. D. H. Stedman, J. Chem. Phys. <u>52</u>, 3966 (1970) studied the NH emission spectrum obtained by collision of metastable rare gas atoms with HN_3. Taking the highest level of NH as observed in emission as a bound, he concluded that $\Delta Hf^{\circ}_{0}(NH,g) > 80$ kcal mol^{-1}. From analogous considerations on N_2 emission observed by collision of metastable argon atoms with HN_3 he concluded that $\Delta Hf^{\circ}_{0}(NH,g) \leq 94$ kcal mol^{-1}.

Quantum chemical calculation of the dissociation energy of small molecules is possible with estimated accuracies of 0.1 to 0.2 eV. A theoretical calculation of the dissociation energy, D_3, of $NH(X^3\Sigma^-)$, applying the techniques of A. C. Wahl and G. Das, Advan. Quantum Chem. <u>5</u>, 261 (1970), has been determined by W. Stevens (unpublished) to yield $D_e = 3.4$ eV. This result corroborates the results of Seal and Gaydon and would support $\Delta Hf^{\circ}_{0}(NH) = 90 \pm 4$ kcal mol^{-1}. Theoretical calculations of this type can be used to distinguish between disparate experimental results that differ by more than 0.2 eV.

Heat Capacity and Entropy

The vibrational and rotational constants are taken from the JANAF Thermochemical Tables, 2nd Edition, June 1971 (U. S. Govt. Printing Office, Washington, D. C. 20402).

(IDEAL GAS)   GFW = 15.0147

T, °K	Cp°	S°	$-(G°-H°_{298})/T$	$H°-H°_{298}$	$\Delta Hf°$	$\Delta Gf°$	Log Kp
		gibbs/mol			kcal/mol		
0	.000	.000	INFINITE	-2.060	90.000	90.000	INFINITE
100	6.961	35.687	49.484	-1.380	89.975	89.518	-195.640
200	6.963	40.512	43.930	-.684	90.001	89.050	-97.309
298	6.966	43.293	43.293	.000	90.012	88.580	-64.931
300	6.966	43.336	43.293	.013	90.012	88.571	-64.524
400	6.973	45.341	43.566	.710	90.013	88.090	-48.130
500	6.994	46.899	44.083	1.408	90.010	87.609	-38.294
600	7.041	48.177	44.662	2.109	90.006	87.130	-31.737
700	7.119	49.268	45.244	2.817	89.999	86.651	-27.054
800	7.222	50.225	45.808	3.534	89.991	86.173	-23.541
900	7.343	51.083	46.347	4.262	89.984	85.696	-20.810
1000	7.471	51.863	46.860	5.003	89.978	85.220	-18.625
1100	7.601	52.581	47.348	5.756	89.975	84.744	-16.837
1200	7.727	53.248	47.812	6.523	89.974	84.269	-15.347
1300	7.847	53.871	48.255	7.302	89.975	83.793	-14.087
1400	7.960	54.457	48.677	8.092	89.978	83.317	-13.006
1500	8.064	55.010	49.081	8.893	89.982	82.842	-12.070
1600	8.161	55.533	49.468	9.705	89.986	82.365	-11.251
1700	8.249	56.031	49.840	10.525	89.992	81.890	-10.528
1800	8.331	56.505	50.197	11.354	89.998	81.412	-9.885
1900	8.405	56.957	50.541	12.191	90.005	80.936	-9.310
2000	8.474	57.390	50.873	13.035	90.013	80.458	-8.792
2100	8.537	57.805	51.193	13.886	90.020	79.980	-8.324
2200	8.596	58.204	51.503	14.742	90.028	79.502	-7.898
2300	8.650	58.587	51.802	15.605	90.036	79.023	-7.509
2400	8.700	58.956	52.093	16.472	90.045	78.545	-7.152
2500	8.747	59.312	52.374	17.345	90.052	78.064	-6.824
2600	8.791	59.656	52.648	18.222	90.061	77.585	-6.522
2700	8.832	59.989	52.914	19.103	90.069	77.105	-6.241
2800	8.870	60.311	53.172	19.988	90.077	76.624	-5.981
2900	8.906	60.622	53.424	20.877	90.086	76.145	-5.738
3000	8.941	60.925	53.669	21.769	90.093	75.663	-5.512
3100	8.973	61.219	53.908	22.665	90.102	75.181	-5.300
3200	9.004	61.504	54.140	23.564	90.110	74.700	-5.102
3300	9.033	61.782	54.368	24.465	90.117	74.219	-4.915
3400	9.061	62.052	54.590	25.370	90.126	73.737	-4.740
3500	9.088	62.315	54.807	26.278	90.133	73.255	-4.574
3600	9.114	62.571	55.019	27.188	90.139	72.772	-4.418
3700	9.139	62.821	55.226	28.100	90.145	72.290	-4.270
3800	9.163	63.065	55.430	29.015	90.151	71.808	-4.130
3900	9.185	63.304	55.628	29.933	90.157	71.326	-3.997
4000	9.206	63.536	55.823	30.853	90.162	70.842	-3.871
4100	9.230	63.764	56.014	31.774	90.166	70.359	-3.750
4200	9.251	63.987	56.201	32.699	90.170	69.877	-3.636
4300	9.271	64.205	56.385	33.625	90.173	69.393	-3.527
4400	9.291	64.418	56.565	34.553	90.176	68.909	-3.423
4500	9.311	64.627	56.742	35.483	90.177	68.424	-3.323
4600	9.330	64.832	56.916	36.415	90.179	67.944	-3.228
4700	9.349	65.033	57.086	37.349	90.180	67.460	-3.137
4800	9.367	65.230	57.254	38.285	90.181	66.977	-3.050
4900	9.385	65.423	57.418	39.222	90.181	66.492	-2.966
5000	9.402	65.613	57.580	40.162	90.180	66.009	-2.885
5100	9.420	65.799	57.740	41.103	90.179	65.524	-2.808
5200	9.437	65.982	57.897	42.046	90.178	65.042	-2.734
5300	9.453	66.162	58.051	42.990	90.175	64.559	-2.662
5400	9.470	66.339	58.203	43.936	90.172	64.074	-2.593
5500	9.486	66.513	58.352	44.884	90.168	63.593	-2.527
5600	9.502	66.684	58.499	45.833	90.164	63.108	-2.463
5700	9.516	66.852	58.645	46.784	90.160	62.627	-2.401
5800	9.534	67.018	58.787	47.737	90.154	62.144	-2.342
5900	9.549	67.181	58.928	48.691	90.149	61.660	-2.284
6000	9.564	67.342	59.067	49.647	90.142	61.176	-2.228

July 31, 1972

$S^{\circ}_{298.15} = 43.890$ cal K^{-1} mol $^{-1*}$

$\Delta Hf^{\circ}_{0} = 9.26_{1}$ kcal mol $^{-1*}$

$\Delta Hf^{\circ}_{298.15} = 9.31_{8} \pm 0.29$ kcal mole^{-1}

Electronic States and Molecular Constants

State	ϵ, cm^{-1}	g	ω_e, cm^{-1}	$\chi_e\omega_e$, cm^{-1}	B_e, cm^{-1}	α_e, cm^{-1}	r_e, Å
$X^2\Pi_i$	$\left\{\begin{array}{l} 0 \\ 139.7 \end{array}\right.$	2 / 2 $\}$	3735.21	82.81	18.871	0.714	0.9706
$A^2\Sigma^+$	32403	2	3184.28	97.84	17.355	0.807	1.0121
$B^2\Sigma^+$	68372	2	940	105	5.54	0.65	1.80
$C^2\Sigma^+$	89420	2	2339	32	4.20	0.16	2.16

$\sigma = 1$

Heat of Formation

$\Delta Hf^{\circ}_{0}(OH)$ was calculated from the relation $\Delta Hf^{\circ}_{0}(OH) = 1/2 \ D^{\circ}_{0}(O_2) + 1/2 \ D^{\circ}_{0}(H_2) - D^{\circ}_{0}(OH)$. The values employed were as follows: $D^{\circ}_{0}(O_2) = 117.967 \pm 0.042$ kcal mol^{-1}; and $D^{\circ}_{0}(H_2) = 103.267 \pm 0.003$ kcal mol^{-1} were taken from the CODATA (1) selection. $D^{\circ}_{0}(OH)$: Barrow (2) in a refinement of the work of Barrow and Downie (3) obtains a value of D°_{0} for $OH(X^2\Pi_{3/2}) = O(^3P_2) + H(^2S_{1/2})$ of 35427 cm^{-1} from an extrapolation of ΔG_v versus v; it was increased to 35450 $\pm$ 100 cm^{-1} to account for the fact that ΔG_v yields slightly low values at high v. Fehlenbok (4) obtains a value of D°_{e} for $OH(B^2\Sigma^+)$ of 1315 cm^{-1} and G(0) for this state of 441 cm^{-1}. Using $T_e(B^2\Sigma^+)$ given by Rosen (5) and the zero point energy of HO(including the Dunham correction, see Herzberg (6) of 847.0 cm^{-1}, this yields $D^{\circ}_{0}(OH) = 35451$ cm^{-1} with an estimated uncertainty of ± 100 cm^{-1}. A value of $D^{\circ}_{0}(OH) = 35450 \pm 100$ cm$^{-1} = 101.35_{6} \pm 0.29$ kcal mol^{-1} was adopted. Combining the above values, one obtains $\Delta Hf^{\circ}_{0}(OH) = 9.261 \pm 0.29$ kcal mol^{-1} which is in good agreement with the last JANAF (7) selection.

A review of earlier work is given in references (7-9).

*Heat Capacity and Entropy

The vibrational and rotational constants of the respective electronic levels were taken from B. Rosen, Spectroscopic Data Relative to Diatomic Molecules, Pergamon Press, Oxford, 1970. Comparison of the results of these calculations with those of the more exact treatment given by L. Haar, A. S. Friedman and C. W. Beckett, NBS Monograph 20, May 29, 1961, (U. S. Govt. Printing Office, Washington, D. C. 20402) suggests the errors in the tables due to approximations in our calculations may be neglected above 400 K. Below this, they may be appreciable. It is recommended that $H^{\circ}_{0} - H^{\circ}_{298}$, S°_{298}, and $C^{\circ}_{p \ 298}$ be taken as -2.107 kcal mol^{-1}, 43.890 gibbs mol^{-1}, and 7.144 cal deg^{-1} mol^{-1}, respectively. For causes of errors, see the text (page 256) of the table for Deutero-hydroxyl (O D).

References

1. CODATA Task Group on Key Values for Thermodynamics, Final Set of Key Values for Thermodynamics – Part I, November 1971 (Bulletin No. 5).

2. R. F. Barrow, Arkiv Fysik 11, 281 (1956).

3. R. F. Barrow and A. R. Downie, Proc. Phys. Soc. (London) A69, 178 (1956).

4. P. Felenbok, Ann. d'Astr. 26, 393 (1963).

5. B. Rosen, Spectroscopic Data Relative to Diatomic Molecules, (Pergamon Press, Oxford, 1970).

6. G. Herzberg and A. Monfils, J. Molec. Spectroscopy 5, 482 (1960).

7. JANAF Thermochemical Tables, 2nd Edition, NSRDS–NBS 37, June 1971 (U. S. Govt. Printing Office, Washington, D. C., 20402).

8. P. Gray, Trans. Farad. Soc. 55, 408 (1959).

9. R. Edse, Third Combustion Symposium (Williams and Wilkins Co., Baltimore, 1949) p. 611.

(IDEAL GAS)   GFW = 17.0074

T, °K	Cp°	S°	−(G°−H°298)/T	H°−H°298	ΔHf°	ΔGf°	Log Kp
		gibbs/mol			kcal/mol		
0	.000	.000	INFINITE	−2.192	9.175	9.175	INFINITE
100	7.798	35.726	50.398	−1.467	9.195	8.894	−19.439
200	7.356	40.985	44.541	−.711	9.281	8.557	−9.351
298	7.167	43.880	43.880	.000	9.318	8.193	−6.005
300	7.165	43.925	43.881	.013	9.318	8.186	−5.963
400	7.087	45.974	44.160	.725	9.328	7.806	−4.265
500	7.055	47.551	44.687	1.432	9.320	7.426	−3.246
600	7.057	48.837	45.275	2.137	9.297	7.049	−2.568
700	7.090	49.927	45.863	2.845	9.265	6.677	−2.085
800	7.150	50.877	46.432	3.556	9.224	6.310	−1.724
900	7.233	51.724	46.974	4.275	9.180	5.948	−1.444
1000	7.332	52.491	47.488	5.003	9.136	5.592	−1.222
1100	7.439	53.195	47.975	5.742	9.092	5.239	−1.041
1200	7.549	53.847	48.437	6.491	9.050	4.891	−.891
1300	7.659	54.455	48.877	7.252	9.010	4.546	−.764
1400	7.766	55.027	49.296	8.023	8.972	4.204	−.656
1500	7.867	55.566	49.696	8.805	8.936	3.865	−.563
1600	7.963	56.077	50.079	9.596	8.900	3.528	−.482
1700	8.053	56.563	50.447	10.397	8.866	3.194	−.411
1800	8.137	57.025	50.799	11.207	8.833	2.861	−.347
1900	8.214	57.467	51.139	12.024	8.800	2.530	−.291
2000	8.286	57.891	51.466	12.849	8.767	2.200	−.240
2100	8.353	58.296	51.782	13.681	8.735	1.873	−.195
2200	8.415	58.686	52.087	14.520	8.701	1.547	−.154
2300	8.472	59.062	52.382	15.364	8.668	1.222	−.116
2400	8.526	59.424	52.668	16.214	8.634	.901	−.082
2500	8.576	59.773	52.945	17.069	8.597	.577	−.050
2600	8.622	60.110	53.214	17.929	8.561	.258	−.022
2700	8.665	60.436	53.476	18.794	8.523	−.060	.005
2800	8.705	60.752	53.730	19.662	8.484	−.378	.030
2900	8.744	61.058	53.977	20.535	8.443	−.692	.052
3000	8.780	61.355	54.218	21.411	8.401	−1.008	.073
3100	8.814	61.644	54.453	22.291	8.358	−1.321	.093
3200	8.846	61.924	54.682	23.174	8.313	−1.632	.111
3300	8.877	62.197	54.906	24.060	8.267	−1.942	.129
3400	8.905	62.462	55.124	24.949	8.219	−2.252	.145
3500	8.933	62.721	55.338	25.841	8.169	−2.559	.160
3600	8.959	62.973	55.546	26.735	8.118	−2.864	.174
3700	8.985	63.218	55.750	27.633	8.065	−3.168	.187
3800	9.009	63.458	55.950	28.532	8.011	−3.470	.200
3900	9.032	63.693	56.145	29.434	7.955	−3.773	.211
4000	9.055	63.922	56.337	30.339	7.898	−4.073	.223
4100	9.076	64.146	56.525	31.245	7.839	−4.371	.233
4200	9.097	64.365	56.709	32.154	7.779	−4.668	.243
4300	9.118	64.579	56.889	33.065	7.717	−4.963	.252
4400	9.138	64.789	57.066	33.978	7.654	−5.259	.261
4500	9.157	64.994	57.240	34.892	7.589	−5.552	.270
4600	9.175	65.195	57.411	35.809	7.524	−5.840	.277
4700	9.195	65.393	57.579	36.728	7.456	−6.130	.285
4800	9.213	65.587	57.744	37.648	7.389	−6.419	.292
4900	9.231	65.777	57.906	38.570	7.320	−6.707	.299
5000	9.249	65.964	58.065	39.494	7.250	−6.995	.306
5100	9.267	66.147	58.222	40.420	7.179	−7.276	.312
5200	9.284	66.327	58.376	41.348	7.107	−7.561	.318
5300	9.301	66.504	58.528	42.277	7.035	−7.839	.323
5400	9.319	66.678	58.677	43.208	6.961	−8.123	.329
5500	9.335	66.850	58.824	44.141	6.888	−8.399	.334
5600	9.352	67.018	58.969	45.075	6.813	−8.679	.339
5700	9.369	67.184	59.111	46.011	6.738	−8.954	.343
5800	9.386	67.347	59.252	46.949	6.662	−9.228	.348
5900	9.403	67.507	59.391	47.888	6.586	−9.501	.352
6000	9.420	67.665	59.527	48.829	6.510	−9.774	.356

July 31, 1972

$S^\circ_{298.15}$ = 46.74 cal K^{-1} mol^{-1} ± $\Delta Hf^\circ_{298.15}$ = 33.3 ± 1.2 kcal mol^{-1}

Electronic States and Molecular Constants

State	ε, cm^{-1}	g	ω_e, cm^{-1}	$\chi_e\omega_e$, cm^{-1}	B_e, cm^{-1}	α_e, cm^{-1}	r_e, Å
$X^2\Pi_i$	$\begin{cases} 0 \\ 377.01 \end{cases}$	2 / 2	2689.6	45.5	9.601	0.285	1.345
$A^2\Sigma^+$	30663	2	1979.8	97.65	8.521	0.464	1.423
$B^2\Sigma$	59622	2	2670.6	56.8	8.785	0.259	1.428
$C^2\Delta$	[63900]	4					
$D^2\Delta$	71195	4					
$E^2\Sigma$	71318	2					
$F^2\Delta$	76708	4	[2689.6]	[45.5]	[9.601]	[0.285]	
$G^2\Delta$	79343	4					
$H^2\Delta$	80848	4					

$\sigma = 1$

Heat of Formation

The previous JANAF (1) selection for ΔHf°_{298} of HS(g) was Mackle's (2) estimate of 34.6 ± 4 kcal which he derived from the average of three independent determinations. Of these, the uncertainty in the determination involving the calculation of ΔHf°_{298} of HS(g) from ΔHf°_{298} of H_2S(g), the ionization potential of HS(g), and the appearance potential of HS$^+$(g) from H_2S(g) can be reduced. A summary of previous work on the ionization potential is given below. From the spectroscopic and photoionization work we arrive at a value of ΔHf°_0 for the reaction H_2S = HS + H of 89.02 ± 1.15 kcal mol^{-1}. Using the appropriate thermal functions for each of the species (see tables for H_2S, HS, and H (1)) and the selected heats of formation of H_2S(g), H(g) of -4.90 ± 0.2 kcal mol^{-1} (see H_2S(g) table) and 52.103 ± 0.001 kcal mol^{-1} (8), one obtains 33.3 ± 1.2 kcal mol^{-1} for ΔHf°_{298} of HS(g) versus Mackle's (2) value of 33.7 ± 3 kcal mol^{-1} for this determination. The new value is preferred because it is based on photoionization rather than electron impact studies.

Source	Method	Potential (EV)
HS → HS$^+$ e$^-$:		
Morrow (3) (1966)	Rydberg Extrapolation	10.40 ± 0.03
Palmer and Lossing (4) (1962)	Electron Impact	10.5 ± 0.1
H_2S → HS$^+$ + H + e$^-$:		
Dibeler and Liston (5) (1968)	Photoionization	14.27 ± 0.04*
Dibeler and Rosenstock (6) (1963)	Electron Impact	14.43 ± 0.1
Palmer and Lossing (4) (1962)	Electron Impact	14.43 ± 0.1
Neuert and Clasen (7) (1952)	Electron Impact	15.2 ± 0.5

*The uncertainty given by the authors was doubled because the threshold value was not corrected to absolute zero.

References

1. D. R. Stull and H. Prophet, "JANAF Thermochemical Tables", 2nd Edition, NSRDS-NBS-37, CODEN-NSRDA (U. S. Supt. of Documents, U. S. Govt. Printing Office, Washington, D. C., 1971).

2. H. Mackle, Tetrahedron. 19, 1159 (1963).

3. B. A. Morrow, Canad. J. Phys. 44, 2447 (1966).

4. T. F. Palmer and F. P. Lossing, J. Am. Chem. Soc. 84, 4661 (1962).

5. V. H. Dibeler and S. K. Liston, J. Chem. Phys. 49, 482 (1968).

6. V. H. Dibeler and H. M. Rosenstock, J. Chem. Phys. 39, 3106 (1963).

7. H. Neuert and H. Clasen, Z. Naturforschung 79, 410 (1952).

8. CODATA Task Group on Key Values for Thermodynamics, Final Set of Key Values for Thermodynamics - Part I, November, 1971.

± Heat Capacity and Entropy

Calculations were made as described in JANAF Thermochemical Tables, 2nd Edition, NSRDS-NBS 37, June, 1971 (U. S. Govt. Printing Office, Washington, D. C., 20402) but using the vibrational and rotational constants at the respective electronic levels taken from B. Rosen, Spectroscopic Data Relative to Diatomic Molecules, Pergamon Press, Oxford, 1970. Comparison of the results of the more exact treatment of L. Haar, A. S. Friedman, and C. W. Beckett, NBS Monograph 20, May 29, 1961 (U. S. Govt. Printing Office, Washington, D. C., 20402) with those given in the previous JANAF (loc. cit.) calculations (both used the same molecular constants for the ground state) suggests errors in our calculations are negligible above 400 K. Below this, they can be appreciable. In particular, it is recommended that 0.045 kcal mol^{-1}, 0.012 gibbs/mol, and -0.028 cal mol^{-1} deg^{-1} be added to our values of $H^\circ_0 - H^\circ_{298}$, S°_{298}, and $C^\circ_{p\ 298}$. For the cause of these errors, see the text (page 256) of the table for Deutero-hydroxyl (0 D).

(IDEAL GAS)   GFW = 33.072

T, °K	Cp°	S°	-(G°-H°₂₉₈)/T	H°-H°₂₉₈	ΔHf°	ΔGf°	Log Kp
		gibbs/mol			kcal/mol		
0	.000	.000	INFINITE	-2.216	33.149	33.149	INFINITE
100	7.214	38.378	53.629	-1.525	33.317	30.079	-67.703
200	7.815	43.610	47.443	-.767	33.361	28.615	-31.269
298	7.755	46.730	46.730	.000	33.300	26.295	-19.275
300	7.752	46.778	46.730	.014	33.298	26.252	-19.124
400	7.575	48.983	47.032	.781	32.618	23.944	-13.082
500	7.477	50.662	47.596	1.533	32.083	21.837	-9.545
600	7.464	52.022	48.224	2.279	31.622	19.833	-7.224
700	7.517	53.176	48.851	3.027	31.219	17.925	-5.596
800	7.611	54.186	49.456	3.784	17.798	14.782	-4.038
900	7.724	55.089	50.033	4.550	17.770	14.407	-3.499
1000	7.843	55.909	50.580	5.329	17.749	14.035	-3.067
1100	7.959	56.662	51.099	6.119	17.733	13.663	-2.715
1200	8.069	57.359	51.592	6.920	17.723	13.295	-2.421
1300	8.170	58.009	52.061	7.732	17.718	12.927	-2.173
1400	8.265	58.619	52.508	8.554	17.716	12.558	-1.960
1500	8.346	59.191	52.934	9.384	17.715	12.189	-1.776
1600	8.422	59.732	53.342	10.223	17.717	11.821	-1.615
1700	8.491	60.244	53.733	11.069	17.720	11.452	-1.472
1800	8.553	60.732	54.109	11.921	17.724	11.083	-1.346
1900	8.609	61.196	54.470	12.779	17.729	10.715	-1.233
2000	8.660	61.638	54.817	13.643	17.734	10.345	-1.130
2100	8.707	62.062	55.152	14.511	17.739	9.975	-1.038
2200	8.750	62.468	55.475	15.384	17.743	9.606	-.954
2300	8.790	62.858	55.788	16.261	17.748	9.236	-.878
2400	8.826	63.233	56.090	17.142	17.752	8.867	-.807
2500	8.860	63.594	56.383	18.026	17.756	8.495	-.743
2600	8.892	63.942	56.668	18.914	17.760	8.125	-.683
2700	8.922	64.278	56.943	19.804	17.763	7.754	-.628
2800	8.950	64.603	57.211	20.698	17.765	7.381	-.576
2900	8.976	64.918	57.471	21.594	17.767	7.012	-.528
3000	9.001	65.222	57.725	22.493	17.768	6.641	-.484
3100	9.024	65.518	57.971	23.394	17.770	6.270	-.442
3200	9.047	65.805	58.212	24.298	17.770	5.899	-.403
3300	9.068	66.083	58.446	25.204	17.770	5.527	-.366
3400	9.089	66.355	58.675	26.112	17.770	5.157	-.332
3500	9.109	66.618	58.898	27.021	17.767	4.785	-.299
3600	9.128	66.875	59.116	27.933	17.765	4.414	-.268
3700	9.147	67.125	59.329	28.847	17.761	4.045	-.239
3800	9.165	67.370	59.537	29.763	17.757	3.674	-.211
3900	9.182	67.608	59.741	30.680	17.751	3.302	-.185
4000	9.200	67.841	59.941	31.599	17.746	2.935	-.160
4100	9.217	68.068	60.136	32.520	17.739	2.563	-.137
4200	9.233	68.290	60.328	33.442	17.731	2.194	-.114
4300	9.250	68.508	60.516	34.366	17.723	1.823	-.093
4400	9.266	68.721	60.700	35.292	17.713	1.453	-.072
4500	9.282	68.929	60.880	36.220	17.703	1.084	-.053
4600	9.295	69.133	61.057	37.149	17.692	.715	-.034
4700	9.314	69.333	61.231	38.079	17.681	.346	-.016
4800	9.330	69.530	61.402	39.011	17.668	-.025	.001
4900	9.346	69.722	61.570	39.945	17.656	-.389	.017
5000	9.362	69.911	61.735	40.881	17.642	-.761	.033
5100	9.378	70.097	61.897	41.818	17.627	-1.126	.048
5200	9.394	70.279	62.057	42.756	17.613	-1.494	.063
5300	9.410	70.458	62.213	43.696	17.598	-1.861	.077
5400	9.425	70.634	62.368	44.638	17.582	-2.228	.090
5500	9.442	70.807	62.520	45.581	17.565	-2.595	.103
5600	9.459	70.977	62.669	46.527	17.548	-2.961	.116
5700	9.475	71.145	62.816	47.473	17.531	-3.328	.128
5800	9.492	71.310	62.961	48.422	17.513	-3.694	.139
5900	9.509	71.472	63.104	49.372	17.496	-4.062	.150
6000	9.526	71.632	63.245	50.323	17.477	-4.424	.161

July 31, 1972

$D_0^\circ = 103.266 \pm 0.003$ kcal mol^{-1}

Ground State Configuration $^1\Sigma_g^+$

$\Delta Hf_{298.15}^\circ = 0$

$S_{298.15}^\circ = 31.208 \pm 0.01$ cal deg^{-1} mol^{-1}

$\omega_e = 4405.3$ cm^{-1}	$\omega_e x_e = 125.325$ cm^{-1}	$D_e = 0.04644$ cm^{-1}	$\sigma = 2$
$B_e = 60.848$ cm^{-1}	$\alpha_e = 3.0664$ cm^{-1}	$r_e = 0.7417$ Å	

Heat Capacity and Entropy

Except for the changes at 100° and 200°K noted below, the table was taken from the JANAF table for H_2 (dated March 31, 1961), whose thermodynamic functions follow very closely those calculated up to 5000 K by H. W. Woolley, R. B. Scott, and F. G. Brickwedde, J. Research Nat. Bur. Standards 41, 379 (1948), who used spectroscopic constants derived from an analysis of U.V. band spectra. (As in the JANAF table, a nuclear-spin entropy of Rln 4 was omitted at all temperatures, but the entropy due to the mixing of ortho and para hydrogen, which is a consequence of nuclear spin, is included.)

The JANAF table for H_2 is for "normal" H_2 (75% ortho and 25% para) except at 0°K, where the values are for "equilibrium" H_2 (100% para at that temperature). The present table eliminates that inconsistency since it applies to "equilibrium" H_2 at all temperatures; the values at 100° and 200°K, which differ substantially from those for normal H_2 but are not suitable for interpolation anyhow, were taken from L. Haar, A. S. Friedman, and C. W. Beckett, Nat. Bur. Standards Monograph 20 (1961), but the thermodynamic functions of the two forms differ negligibly (by less than 0.01%) at 298.15 K and all higher temperatures.

A more practical consistent table for H_2 might seem to be one for normal H_2 at all temperatures, since this form of the gas is essentially the one always encountered except in its generation or catalytic ortho-para equilibration at low temperatures. However, $H_{298}^\circ - H_0^\circ$ is 0.156 kcal mol^{-1} less for the "normal" than for the "equilibrium" form, and it was considered undesirable to offer a reference table for H_2 whose use would change the difference between ΔHf_0° and $\Delta Hf_{298.15}^\circ$ for all compounds containing hydrogen by corresponding amounts. "Equilibrium" H_2 is the form which parallels the great majority of substances (those maintaining equilibrium among all rotational states).

The present reference-state table for H_2 was used in generating all tables of the present series for compounds containing the isotope ^1H.

The value of D_0° is taken from G. Herzberg, J. Molec. Spectroscopy 33, 147 (1970).

(IDEAL GAS, REFERENCE STATE) GFW = 2.016

T, °K	Cp°	S°	−(G°−H°₂₉₈)/T	H°−H°₂₉₈	ΔHf°	ΔGf°	Log Kp
		gibbs/mol			kcal/mol		
0	.000	.000	INFINITE	−2.024	.000	.000	.000
100	6.728	24.049	37.118	−1.307	.000	.000	.000
200	6.560	28.515	31.830	−.663	.000	.000	.000
298	6.893	31.208	31.208	.000	.000	.000	.000
300	6.894	31.251	31.208	.013	.000	.000	.000
400	6.975	33.247	31.480	.707	.000	.000	.000
500	6.993	34.806	31.995	1.405	.000	.000	.000
600	7.009	36.082	32.572	2.106	.000	.000	.000
700	7.036	37.165	33.154	2.808	.000	.000	.000
800	7.087	38.107	33.714	3.514	.000	.000	.000
900	7.148	38.946	34.250	4.226	.000	.000	.000
1000	7.219	39.702	34.758	4.944	.000	.000	.000
1100	7.300	40.394	35.239	5.670	.000	.000	.000
1200	7.390	41.033	35.696	6.404	.000	.000	.000
1300	7.490	41.628	36.130	7.148	.000	.000	.000
1400	7.600	42.187	36.543	7.902	.000	.000	.000
1500	7.720	42.716	36.937	8.668	.000	.000	.000
1600	7.823	43.217	37.313	9.446	.000	.000	.000
1700	7.921	43.695	37.676	10.233	.000	.000	.000
1800	8.016	44.150	38.022	11.030	.000	.000	.000
1900	8.108	44.586	38.357	11.836	.000	.000	.000
2000	8.195	45.004	38.679	12.651	.000	.000	.000
2100	8.279	45.406	38.989	13.475	.000	.000	.000
2200	8.358	45.793	39.290	14.307	.000	.000	.000
2300	8.434	46.166	39.581	15.146	.000	.000	.000
2400	8.506	46.527	39.863	15.993	.000	.000	.000
2500	8.575	46.875	40.136	16.848	.000	.000	.000
2600	8.639	47.213	40.402	17.708	.000	.000	.000
2700	8.700	47.540	40.660	18.575	.000	.000	.000
2800	8.757	47.857	40.911	19.448	.000	.000	.000
2900	8.810	48.166	41.157	20.326	.000	.000	.000
3000	8.859	48.465	41.395	21.210	.000	.000	.000
3100	8.911	48.756	41.628	22.098	.000	.000	.000
3200	8.962	49.040	41.855	22.992	.000	.000	.000
3300	9.012	49.317	42.077	23.891	.000	.000	.000
3400	9.061	49.586	42.294	24.794	.000	.000	.000
3500	9.110	49.850	42.506	25.703	.000	.000	.000
3600	9.158	50.107	42.714	26.616	.000	.000	.000
3700	9.205	50.359	42.917	27.535	.000	.000	.000
3800	9.252	50.605	43.116	28.457	.000	.000	.000
3900	9.297	50.846	43.311	29.385	.000	.000	.000
4000	9.342	51.082	43.503	30.317	.000	.000	.000
4100	9.386	51.313	43.690	31.253	.000	.000	.000
4200	9.429	51.540	43.875	32.194	.000	.000	.000
4300	9.472	51.762	44.055	33.139	.000	.000	.000
4400	9.514	51.980	44.233	34.088	.000	.000	.000
4500	9.555	52.194	44.407	35.042	.000	.000	.000
4600	9.595	52.405	44.579	35.999	.000	.000	.000
4700	9.634	52.612	44.748	36.961	.000	.000	.000
4800	9.673	52.815	44.914	37.926	.000	.000	.000
4900	9.711	53.015	45.077	38.895	.000	.000	.000
5000	9.748	53.211	45.237	39.868	.000	.000	.000
5100	9.785	53.405	45.396	40.845	.000	.000	.000
5200	9.822	53.595	45.552	41.825	.000	.000	.000
5300	9.859	53.783	45.706	42.809	.000	.000	.000
5400	9.895	53.967	45.856	43.797	.000	.000	.000
5500	9.930	54.149	46.006	44.788	.000	.000	.000
5600	9.965	54.328	46.152	45.783	.000	.000	.000
5700	10.000	54.505	46.298	46.781	.000	.000	.000
5800	10.034	54.679	46.441	47.783	.000	.000	.000
5900	10.067	54.851	46.582	48.788	.000	.000	.000
6000	10.100	55.020	46.721	49.796	.000	.000	.000

July 31, 1972

Point Group C$_{2v}$ $\Delta Hf^\circ_{298.15}$ = 45.5 ± 1.5 kcal mol^{-1}

S$^\circ_{298.15}$ = 46.51 gibbs mol^{-1}

Electronic Levels (Quantum Weight) and Vibrational Frequencies (Degeneracies)

ϵ, cm^{-1}	(g)	ω, cm^{-1}	(g)		
0	(2)	3173 (1)	1497.2	(1)	3220 (1)
10249	(2)	3325 (1)	633	(1)	[3220](1)

Bond Distance: N–N = 1.024Å   Bond Angle: H–N–H = 103°   o = 2

Product of the Moments of Inertia: I$_A$I$_B$I$_C$ = 8.742 x 10^{-120} g^3 cm^6

Heat of Formation

Direct kinetic studies [1–5] on the decomposition of hydrazine, $N_2H_4(g) \underset{k_r}{\overset{k_d}{\rightleftarrows}} 2NH_2(g)$, give activation energies which suggest ΔHf°_{298} of NH$_2$ $\leq$ 40 kcal. The pre-exponential factor suggests $k_r \sim$ 10^7–10^8 liters/mol sec. This is exceptionally slow for a radical combination reaction [6] and is at variance with the most recent direct measurements of k_r = 10$^{10.8}$ liters/mol sec (300K, 1500 mm Hg) [7] and k_r = 10$^{9.4}$ liters/mol sec (300K, 10 mm Hg) [8]. A possible explanation for this discrepancy is that the hydrazine decomposition studies have been carried out in the energy dependent region [9,10]. This has been confirmed on the basis of RRKM calculations. With a ΔHf°_{298} equal to 40 kcal, it is not possible to simultaneously reproduce the measured forward (k_d) and backward (k_r) rates by orders of magnitude. With a value of ΔHf°_{298} of 45.5 kcal, all of the rate data can be fitted to a factor of three. For higher values of ΔHf°_{298}, the discrepancy increases.

Data on the thermal decomposition of benzylamine from toluene carrier studies [2,11] yield ΔHf°_{298} = 36 kcal. This technique, however, has consistently yielded erroneous rate parameters [12]. Using their very low pressure pyrolysis technique, Golden and coworkers [13] find ΔHf°_{298} of NH$_2$ equals 47.2 kcal. This is in reasonable agreement with the recommended value.

Heat Capacity and Entropy

The bond distance and angle from the electronic absorption spectrum (c.f. G. Herzberg, Electronic Spectra of Polyatomic Molecules, D. Van Nostrand Co., Inc., Princeton, N. J., 1966 for references and discussion). The vibrational frequencies for the ground electronic state were obtained from the matrix isolation studies by D. E. Milligan and M. E. Jacox, J. Chem. Phys. 43, 4487 (1956). The vibrational frequencies of the upper electronic level have been obtained from both the gas phase and matrix isolated electronic absorption spectra.

References

1. M. Szwarc, Proc. Roy. Soc. A198, 267 (1949).

2. J. A. Kerr, R. C. Sekhar, and A. F. Trotman-Dickenson, J. Chem. Soc. 3217 (1963).

3. E. T. McHale, B. E. Knox, and H. B. Palmer, Tenth Symposium on Combustion (International), p. 341 (The Combustion Institute, Pittsburgh, Pa., 1965).

4. K. W. Michel and H. Gg. Wagner, Tenth Symposium on Combustion (International) p. 353 (The Combustion Institute, Pittsburgh, Pa., 1965).

5. E. Meyer, H. A. Olscheusek, J. Troe, and H. Gg. Wagner Eleventh Symposium on Combustion (International) p. 345 (The Combustion Institute, Pittsburgh, Pa., 1967).

6. S. W. Benson and H. E. O'Neal, Kinetic Data on Gas Phase Unimolecular Reactions, p. 34, NSRDS–NBS 21, (U. S. Govt. Printing Office, Washington, D. C., 20402, 1970).

7. S. Gordon, W. Mulac, and P. Nangia, J. Phys. Chem. 75, 2087 (1971).

8. J. D. Saltzman and E. J. Bair, J. Chem. Phys. 41, 3564 (1964).

9. M. Gilbert, Combustion and Flame 2, 137, 149 (1958).

10. D. W. Setzer and W. C. Richardson, Canad. J. Chem. 47, 2593 (1969).

11. M. Szwarc, Proc. Roy. Soc. A198, 285 (1949).

12. S. W. Benson, J. Chem. Education 42, 505 (1965).

13. D. M. Golden, R. K. Solly, N. A. Gac, and S. W. Benson, J. Am. Chem. Soc. 94, 363 (1972).

(IDEAL GAS)   GFW = 16.0226

T, °K	Cp°	S°	$-(G°-H°_{298})/T$	$H°-H°_{298}$	$\Delta Hf°$	$\Delta Gf°$	Log Kp
		gibbs/mol			kcal/mol		
0	.000	.000	INFINITE	-2.373	46.187	46.187	INFINITE
100	7.949	37.815	53.597	-1.578	45.918	46.450	-101.517
200	7.954	43.325	47.241	-.783	45.721	47.058	-51.423
298	8.024	46.510	46.510	.000	45.500	47.761	-35.010
300	8.027	46.560	46.510	.015	45.495	47.775	-34.804
400	8.221	48.893	46.827	.826	45.264	48.569	-26.537
500	8.493	50.756	47.433	1.662	45.049	49.421	-21.602
600	8.805	52.331	48.121	2.526	44.858	50.314	-18.327
700	9.143	53.714	48.823	3.424	44.689	51.237	-15.997
800	9.492	54.957	49.513	4.355	44.543	52.182	-14.255
900	9.842	56.096	50.182	5.322	44.418	53.145	-12.905
1000	10.181	57.150	50.827	6.323	44.315	54.120	-11.828
1100	10.503	58.136	51.447	7.358	44.229	55.105	-10.948
1200	10.802	59.063	52.044	8.423	44.160	56.097	-10.217
1300	11.079	59.939	52.618	9.517	44.105	57.094	-9.598
1400	11.333	60.769	53.170	10.638	44.061	58.095	-9.069
1500	11.566	61.559	53.704	11.783	44.026	59.099	-8.611
1600	11.781	62.312	54.218	12.951	43.997	60.104	-8.210
1700	11.981	63.033	54.716	14.139	43.977	61.113	-7.857
1800	12.167	63.723	55.197	15.346	43.963	62.120	-7.542
1900	12.344	64.385	55.663	16.572	43.956	63.130	-7.262
2000	12.511	65.023	56.115	17.815	43.955	64.139	-7.009
2100	12.672	65.637	56.554	19.074	43.959	65.148	-6.780
2200	12.826	66.230	56.981	20.349	43.969	66.157	-6.572
2300	12.975	66.804	57.395	21.639	43.985	67.165	-6.382
2400	13.120	67.359	57.799	22.944	44.008	68.174	-6.208
2500	13.261	67.897	58.192	24.263	44.034	69.177	-6.047
2600	13.397	68.420	58.576	25.596	44.069	70.184	-5.900
2700	13.529	68.928	58.950	26.942	44.109	71.188	-5.762
2800	13.656	69.423	59.315	28.301	44.154	72.188	-5.635
2900	13.782	69.904	59.672	29.673	44.207	73.191	-5.516
3000	13.901	70.373	60.021	31.058	44.265	74.188	-5.405
3100	14.016	70.831	60.362	32.454	44.330	75.183	-5.300
3200	14.126	71.279	60.696	33.861	44.399	76.178	-5.203
3300	14.231	71.714	61.024	35.279	44.473	77.171	-5.111
3400	14.331	72.140	61.344	36.707	44.553	78.159	-5.024
3500	14.426	72.557	61.659	38.145	44.636	79.147	-4.942
3600	14.516	72.965	61.967	39.592	44.723	80.132	-4.865
3700	14.600	73.364	62.270	41.048	44.813	81.115	-4.791
3800	14.679	73.754	62.567	42.512	44.907	82.095	-4.722
3900	14.752	74.136	62.859	43.983	45.003	83.073	-4.655
4000	14.821	74.511	63.145	45.462	45.100	84.047	-4.592
4100	14.864	74.878	63.427	46.947	45.200	85.019	-4.532
4200	14.942	75.237	63.704	48.439	45.301	85.991	-4.475
4300	14.995	75.589	63.976	49.935	45.402	86.957	-4.420
4400	15.044	75.934	64.244	51.437	45.504	87.921	-4.367
4500	15.088	76.273	64.508	52.944	45.606	88.882	-4.317
4600	15.127	76.605	64.767	54.455	45.708	89.847	-4.269
4700	15.162	76.931	65.022	55.969	45.808	90.805	-4.222
4800	15.194	77.250	65.274	57.487	45.908	91.761	-4.178
4900	15.221	77.564	65.521	59.008	46.007	92.714	-4.135
5000	15.245	77.872	65.765	60.531	46.104	93.666	-4.094
5100	15.266	78.174	66.006	62.057	46.198	94.617	-4.055
5200	15.283	78.470	66.243	63.584	46.292	95.565	-4.016
5300	15.297	78.762	66.476	65.113	46.382	96.514	-3.980
5400	15.309	79.048	66.706	66.644	46.469	97.455	-3.944
5500	15.318	79.329	66.933	68.175	46.554	98.401	-3.910
5600	15.324	79.605	67.157	69.707	46.635	99.341	-3.877
5700	15.328	79.876	67.378	71.240	46.713	100.284	-3.845
5800	15.331	80.143	67.596	72.773	46.787	101.222	-3.814
5900	15.331	80.405	67.810	74.306	46.857	102.160	-3.784
6000	15.329	80.662	68.022	75.839	46.924	103.095	-3.755

July 31, 1972

Point Group C_{2v}

$S^\circ_{298.15}$ = 49.15 cal deg^{-1} mol^{-1}

Ground State Quantum Weight = 1

ΔHf°_0 = -4.20 ± 0.2 kcal mol^{-1}

$\Delta Hf^\circ_{298.15}$ = -4.90 ± 0.2 kcal mol^{-1}

Vibrational Frequencies and Degeneracies

ω, cm^{-1}

2614.6 (1)

1182.7 (1)

2627.5 (1)

Bond Distance: S-H = 1.328Å

Bond Angle: H-S-H = 92.2°

Product of the Moments of Inertia: $I_A I_B I_C$ = 4.69 x 10^{-119} g^3 cm^6

σ = 2

Heat of Formation

The heats of formation of H_2S(g) determined by various workers including those reviewed in the previous JANAF analysis (1) were recalculated with the results shown below. No weight was given to the work performed prior to 1934 and less weight was given to the work of Kapustinskii and Kankovskii (7) because of the difficulty of establishing the state of the products.

Source	Reaction*	ΔHf°_{298} [from (1)]	(kcal mol^{-1}) Recalculated
Thomsen (2) (1882)	H_2S(g) + HI_3(aq) = 3HI(aq) + S(amph)	----	-4.4, -5.1 if S(rhombic)
Thomsen (3) (1882)	H_2S(g) + O_2(g) = SO_2(g) + $H_2SO_4 \cdot H_2O$	----	-2.0
Pollitzer (4) (1909)	H_2S(g) + I_2(C) = 2HI(g) + S(rh)	----	-4.7, -4.0 if S(amph)
Lewis and Randall (5) (1918)	3S(liq) + $2H_2O$(g) = SO_2(g) + $2H_2S$(g)	----	-3.6 ± 0.2
Zeumer and Roth (6) (1934)	H_2S(g) + O_2(g) = SO_2(g) + $H_2SO_4 \cdot H_2O$	-4.80±0.15	-4.89 ± 0.24
Kapustinskii and Kankovskii (7) (1958)	H_2S(g) + $\frac{3}{2}O_2$(g) = SO_2(g) + H_2O(ℓ) + S(rhombic)	-4.94±0.08	-4.92 ± 0.08

*Equations may not be balanced.

Heat Capacity and Entropy

The thermodynamic functions were taken from the JANAF table for H_2S(g) dated Dec. 31, 1965, which in turn were calculated by the rigid-rotor, harmonic-oscillator approximation below 298°K. Gordon had calculated C°_p from 298° to 6000 K by a method which takes into account second-order corrections for vibrational anharmonicity, vibration-rotation interaction, and centrifugal stretching. The spectroscopic constants used were taken from H. C. Allen, E. K. Plyler, J. Chem. Phys. 24, 35 (1956), and H. C. Allen, E. K. Plyler, J. Chem. Phys. 25, 1132 (1956).

References

1. JANAF Thermochemical Tables, 2nd Edition, NSRDS-NBS 37, U. S. Supt. Documents, U. S. Govt. Printing Office, Washington, D. C. 20402 (June, 1971).

2. J. Thomsen, Thermochemical Investigations Vol II, p. 60 (J. A. Barth, Leipzig, 1882).

3. J. Thomsen, Thermochemical Investigations Vol IV, p. 188 (J. A. Barth, Leipzig, 1882).

4. F. Pollitzer, Z. anorg. Chem. 64, 121 (1909).

5. G. N. Lewis and M. Randall, J. Am. Chem. Soc. 40, 362 (1918).

6. H. Zeumer and W. A. Roth, Z. Elektrochem. 40 [11], 777 (1934).

7. A. F. Kapustinskii and R. T. Kankovskii, Zhur. Fiz, Khim. 32, 2810 (1958).

HYDROGEN SULFIDE (H$_2$S)

H$_2$S

(IDEAL GAS) GFW = 34.076

T, °K	Cp°	S°	-(G°-H°₂₉₈)/T	H°-H°₂₉₈	ΔHf°	ΔGf°	Log Kp
		gibbs/mol			kcal/mol		
0	.000	.000	INFINITE	-2.381	-4.204	-4.204	INFINITE
100	7.949	40.359	56.219	-1.586	-4.290	-5.624	12.292
200	7.978	45.872	49.827	-.791	-4.532	-6.879	7.517
298	8.172	49.151	49.151	.000	-4.900	-7.975	5.845
300	8.176	49.202	49.152	.015	-4.908	-7.994	5.823
400	8.504	51.597	49.474	.849	-5.867	-8.937	4.883
500	8.889	53.536	50.100	1.718	-6.635	-9.616	4.203
600	9.306	55.193	50.813	2.628	-7.282	-10.149	3.697
700	9.737	56.660	51.546	3.580	-7.832	-10.558	3.296
800	10.162	57.988	52.269	4.575	-21.368	-12.182	3.328
900	10.567	59.209	52.973	5.612	-21.481	-11.027	2.678
1000	10.943	60.342	53.655	6.687	-21.565	-9.861	2.155
1100	11.261	61.401	54.311	7.799	-21.622	-8.688	1.726
1200	11.584	62.396	54.943	8.943	-21.656	-7.509	1.368
1300	11.853	63.334	55.553	10.115	-21.673	-6.329	1.064
1400	12.092	64.221	56.141	11.312	-21.677	-5.149	.804
1500	12.303	65.063	56.708	12.532	-21.671	-3.969	.578
1600	12.491	65.863	57.255	13.772	-21.657	-2.790	.381
1700	12.658	66.625	57.784	15.030	-21.635	-1.609	.207
1800	12.808	67.353	58.296	16.303	-21.609	-.434	.053
1900	12.941	68.049	58.791	17.590	-21.578	.743	-.085
2000	13.063	68.716	59.270	18.891	-21.543	1.917	-.209
2100	13.171	69.356	59.736	20.203	-21.507	3.088	-.321
2200	13.270	69.971	60.187	21.525	-21.469	4.260	-.423
2300	13.360	70.563	60.626	22.856	-21.430	5.427	-.516
2400	13.444	71.133	61.051	24.197	-21.389	6.597	-.601
2500	13.520	71.684	61.466	25.545	-21.349	7.759	-.678
2600	13.590	72.215	61.869	26.900	-21.308	8.925	-.750
2700	13.655	72.729	62.261	28.263	-21.266	10.086	-.816
2800	13.715	73.227	62.644	29.631	-21.226	11.243	-.878
2900	13.771	73.709	63.018	31.005	-21.185	12.406	-.935
3000	13.824	74.177	63.382	32.385	-21.145	13.562	-.988
3100	13.874	74.631	63.737	33.770	-21.103	14.718	-1.038
3200	13.921	75.073	64.085	35.160	-21.064	15.870	-1.084
3300	13.965	75.502	64.425	36.554	-21.025	17.024	-1.127
3400	14.007	75.919	64.756	37.953	-20.986	18.179	-1.169
3500	14.047	76.326	65.081	39.356	-20.950	19.328	-1.207
3600	14.085	76.722	65.399	40.762	-20.914	20.479	-1.243
3700	14.122	77.108	65.710	42.173	-20.881	21.632	-1.278
3800	14.156	77.485	66.015	43.586	-20.848	22.780	-1.310
3900	14.190	77.854	66.315	45.004	-20.817	23.924	-1.341
4000	14.223	78.213	66.607	46.424	-20.788	25.076	-1.370
4100	14.254	78.565	66.895	47.848	-20.759	26.219	-1.398
4200	14.285	78.909	67.177	49.275	-20.733	27.365	-1.424
4300	14.314	79.245	67.453	50.705	-20.708	28.510	-1.449
4400	14.343	79.575	67.725	52.138	-20.685	29.651	-1.473
4500	14.371	79.897	67.992	53.574	-20.664	30.798	-1.496
4600	14.397	80.213	68.254	55.012	-20.644	31.943	-1.518
4700	14.423	80.523	68.512	56.453	-20.626	33.086	-1.538
4800	14.450	80.827	68.765	57.897	-20.609	34.226	-1.558
4900	14.475	81.125	69.014	59.343	-20.594	35.374	-1.578
5000	14.500	81.418	69.260	60.792	-20.581	36.509	-1.596
5100	14.523	81.705	69.500	62.243	-20.570	37.657	-1.614
5200	14.548	81.988	69.739	63.697	-20.559	38.794	-1.630
5300	14.571	82.265	69.972	65.153	-20.550	39.939	-1.647
5400	14.594	82.538	70.203	66.611	-20.544	41.075	-1.662
5500	14.616	82.806	70.429	68.071	-20.539	42.216	-1.678
5600	14.639	83.069	70.652	69.534	-20.536	43.360	-1.692
5700	14.661	83.328	70.872	70.999	-20.534	44.503	-1.706
5800	14.682	83.584	71.090	72.466	-20.534	45.638	-1.720
5900	14.705	83.835	71.303	73.936	-20.534	46.779	-1.733
6000	14.725	84.082	71.514	75.407	-20.537	47.923	-1.746

July 31, 1972

Point Group   C$_{3v}$

$S^\circ_{298.15}$ = 46.047 ± 0.006 cal deg^{-1}mol^{-1}

Ground State Quantum Weight = 1

ΔHf°_0 = -9.30 kcal mol^{-1}

$\Delta Hf^\circ_{298.15}$ = -10.97 ± 0.1 kcal mol^{-1}

Vibrational Levels and Multiplicities

ω, cm^{-1}
3506 (1)
1022 (1)
3577 (2)
1691 (2)

Bond Length: N-H = 1.0124 Å   Bond Angle: 106.67° σ = 3

Product of the Moments of Inertia: $I_A I_B I_C$ = 3.4824 x 10^{-119} g^3 cm^6

Heat of Formation

Second and third law analyses of the equilibrium constant data for the reaction N$_2$(g)+3/2H$_2$(g) = NH$_3$(g) cited in the previous JANAF evaluation (1) plus the more recent work of Schulz and Schaefer (6) was made using the revised thermal functions for NH$_3$(g) (see below). All of the previously cited work in reaction calorimetry plus the early work of Berthelot (7,8) and Thomsen (9) were reevaluated. No significant differences in the third law calculations of the equilibrium data or in the corrections to the flow calorimetry data of Haber and Tamaru (12) and Wittig and Schmatz (13) were found. Thus, the 0.1 kcal discrepancy between the results of the equilibrium and reaction calorimetry measurements remains unresolved. The previous JANAF selection (1) for $\Delta Hf^\circ_{298.15}$ of NH$_3$(g) was adopted. A recent evaluation (14) which includes new indirect calorimetry measurements (unpublished) further confirms this selection.

Source	Method	ΔHf°_{298} (kcal mol^{-1})	Drift (e.u.)	ΔHf°_{298} (kcal mol^{-1})	ΔS°_{298}(obsv.-calc.) (e.u.)
Larson, Dodge [2] (1923)	K°_p[4] from K_p (10-1,000 atm,600-800K)	-10.88	-.07±.05	-10.70±0.11	+0.24±0.15[1]
Haber, Tamaru, Ponnaz [3] (1915)	K°_p[4] from K_p (30 atm, 800-1200K)	-10.86	.0± .05	-10.88±0.15	-0.02±0.15[2]
Haber, Mashke[5](1915)	K_p (1 atm, 900-1400K)	-10.85	-.26±.08	-10.62 ±.22	0.20±0.19[3]
Schulz, Schaefer [6] (1966)	K_p (1 atm, 567-673K)	-10.87	(.0 to -.3)	-10.78 ±.20	4.4± 0.3[4]
Berthelot [7] (1880)	Indirect; Reaction of Br (aq) and NH (aq)	-11.4			
Berthelot [8] (1880)	Indirect; Reaction of 0 (g) with NH (g)	-12.1			
Thomsen [9] (1882)	Indirect; Reaction of 0 (g) with NH (g)	-11.9			
Becker and Roth [10] (1934)	Indirect; Heat of combustion oxalates, etc.	-11.00$_2$±0.15			
Haber, Tamaru, Oeholm [11] (1915)	Flow calorimetry at 298K	-11.10 ± 0.05			
Haber, Tamaru [12] (1915)	Flow calorimetry (739-932K)	-10.97 ± 0.008			
Wittig, Schmatz [13] (1959)	Flow calorimetry at 823K	-10.99 ± 0.05			

*Second law analysis, calculations made assuming ΔC_p cal mol^{-1}, is given by (1) -2.672+0.00591 (T-700), (2) -1.236+0.00404 (T-1000), (3) -0.855+0.00305 (T-1100), (4) -3.287+0.00651 (T-600).

Heat Capacity and Entropy

The thermodynamic functions differ from those of the JANAF table of Sept. 30, 1965, in being taken directly from the later and more complete work of L. Haar, J. Research Nat. Bur. Standards 72A, 207 (1968). Haar treated in detail the contribution of the highly anharmonic out-of-plane vibrational mode, including its large coupling with rotation and its coupling with the other vibrational modes. Haar's values of C$^\circ_p$ pass through a shallow maximum between 4000 and 500 K, and were extrapolated from 5000 to 6000 K by assuming a constant value (19.300 cal deg^{-1}mol^{-1}). A summary of Haar's estimated uncertainties and of the differences of the JANAF table from the present table (in cal deg^{-1}mol^{-1}) is as follows:

T, °K	Uncertainties (Haar, loc.cit.)		JANAF table - this table	
	C$^\circ_p$	S$^\circ$	C$^\circ_p$	S$^\circ$
1000	0.006	0.006	-0.034	-0.033
3000	0.10	0.06	+ .142	- .122
5000	0.6	0.4	+1.775	+ .265

It may be noted that these tables for NH$_3$ assume equilibrium among all rotational states. Separation of NH$_3$ into ortho and para forms has not so far been observed.

References

1. JANAF Thermochemical Tables, 2nd Edition (July 1970).
2. A. T. Larson and R. L. Dodge, J. Am. Chem. Soc. 45, 2918 (1923).
3. F. Haber, S. Tamaru, and Ch. Ponnaz, A. Elektrochem. 21, 89 (1915).
4. C. C. Stephenson and H. O. McMahan, J. Am. Chem. Soc. 61, 437 (1939).
5. F. Haber and A. Maschke, Z. Elektrochem. 21, 128 (1915).
6. G. Schulz and H. Schaefer, Ber. Bunsenges. Physik. Chem. 70, 21 (1966).
7. M. Berthelot, Compt. Rend. 89, 877 (1879); Ann. Chim. Phys. [8] 20, 247 (1880).

8. M. Berthelot, Ann. Chim. Phys. [5] 20, 244 (1880).
9. J. Thomsen, Thermochemical Investigations Vol. II, p. 68 (Johann A. Barth, Leipzig, 1882).
10. G. Becker and W. A. Roth, Z. Elektrochem. 40, 836 (1934).
11. F. Haber and S. Tamaru, Oeholm. Z. Elektrochem. 21, 206 (1915).
12. F. Haber and S. Tamaru, Z. Elektrochem. 21, 191 (1915).
13. F. E. Wittig and W. Schmatz, Z. Elektrochem. 63, 475 (1959).
14. Private communication, W. H. Evans, U. S. Nat. Bur. Standards, July (1972); evaluation of ICSU-CODATA Task Group on Key Values for Thermodynamics, June(1972).

AMMONIA (NH$_3$)   H$_3$N

(IDEAL GAS)   GFW = 17.0307

T, °K	Cp°	S°	—(G°—H°₂₉₈)/T	H°—H°₂₉₈	ΔHf°	ΔGf°	Log Kp
		gibbs/mol			kcal/mol		
0	.000	.000	INFINITE	−2.401	−9.299	−9.299	INFINITE
100	7.955	37.220	53.321	−1.610	−9.930	−8.136	17.782
200	8.068	42.753	46.809	−.811	−10.445	−6.142	6.712
298	8.521	46.047	46.047	.000	−10.970	−3.919	2.873
300	8.533	46.100	46.048	.016	−10.980	−3.875	2.823
400	9.253	48.650	46.390	.904	−11.482	−1.430	.781
500	10.049	50.800	47.062	1.869	−11.917	1.134	−.496
600	10.825	52.701	47.846	2.913	−12.279	3.780	−1.377
700	11.557	54.425	48.665	4.032	−12.576	6.481	−2.024
800	12.245	56.014	49.486	5.223	−12.816	9.220	−2.519
900	12.894	57.494	50.294	6.480	−13.006	11.987	−2.911
1000	13.501	58.884	51.084	7.800	−13.150	14.772	−3.228
1100	14.068	60.198	51.854	9.179	−13.254	17.570	−3.491
1200	14.591	61.445	52.601	10.612	−13.323	20.376	−3.711
1300	15.071	62.632	53.328	12.096	−13.361	23.185	−3.898
1400	15.510	63.765	54.033	13.625	−13.373	25.997	−4.058
1500	15.909	64.849	54.718	15.196	−13.365	28.810	−4.198
1600	16.271	65.888	55.384	16.805	−13.341	31.619	−4.319
1700	16.599	66.884	56.032	18.449	−13.299	34.430	−4.426
1800	16.896	67.841	56.661	20.124	−13.244	37.234	−4.521
1900	17.165	68.762	57.274	21.828	−13.176	40.038	−4.605
2000	17.407	69.649	57.871	23.556	−13.099	42.837	−4.681
2100	17.627	70.504	58.452	25.308	−13.014	45.631	−4.749
2200	17.825	71.328	59.019	27.081	−12.922	48.422	−4.810
2300	18.004	72.125	59.571	28.873	−12.824	51.208	−4.866
2400	18.166	72.894	60.111	30.681	−12.721	53.992	−4.917
2500	18.314	73.639	60.637	32.505	−12.617	56.765	−4.962
2600	18.445	74.360	61.151	34.343	−12.508	59.541	−5.005
2700	18.564	75.058	61.653	36.194	−12.397	62.309	−5.044
2800	18.673	75.735	62.144	38.056	−12.285	65.072	−5.079
2900	18.769	76.392	62.624	39.928	−12.171	67.837	−5.112
3000	18.858	77.030	63.094	41.810	−12.058	70.591	−5.143
3100	18.936	77.650	63.553	43.699	−11.943	73.343	−5.171
3200	19.005	78.252	64.003	45.596	−11.831	76.093	−5.197
3300	19.069	78.838	64.444	47.500	−11.721	78.841	−5.221
3400	19.122	79.408	64.876	49.410	−11.611	81.581	−5.244
3500	19.172	79.963	65.299	51.324	−11.506	84.322	−5.265
3600	19.216	80.504	65.714	53.244	−11.403	87.058	−5.285
3700	19.252	81.031	66.121	55.167	−11.305	89.793	−5.304
3800	19.283	81.545	66.520	57.094	−11.209	92.524	−5.321
3900	19.309	82.046	66.912	59.024	−11.119	95.254	−5.338
4000	19.331	82.535	67.296	60.956	−11.034	97.979	−5.353
4100	19.349	83.013	67.674	62.890	−10.954	100.703	−5.368
4200	19.361	83.479	68.044	64.825	−10.880	103.428	−5.382
4300	19.371	83.935	68.409	66.762	−10.811	106.146	−5.395
4400	19.375	84.380	68.767	68.699	−10.748	108.863	−5.407
4500	19.377	84.816	69.119	70.637	−10.693	111.579	−5.419
4600	19.373	85.241	69.464	72.574	−10.642	114.301	−5.431
4700	19.367	85.658	69.804	74.512	−10.600	117.017	−5.441
4800	19.357	86.066	70.139	76.447	−10.565	119.731	−5.452
4900	19.343	86.465	70.468	78.382	−10.536	122.445	−5.461
5000	19.325	86.856	70.793	80.318	−10.513	125.153	−5.470
5100	19.300	87.238	71.111	82.248	−10.503	127.869	−5.480
5200	19.300	87.613	71.425	84.178	−10.497	130.582	−5.488
5300	19.300	87.981	71.734	86.108	−10.498	133.297	−5.497
5400	19.300	88.341	72.038	88.038	−10.505	136.005	−5.504
5500	19.300	88.696	72.338	89.968	−10.517	138.722	−5.512
5600	19.300	89.043	72.633	91.898	−10.536	141.431	−5.520
5700	19.300	89.385	72.924	93.828	−10.560	144.150	−5.527
5800	19.300	89.721	73.211	95.758	−10.590	146.862	−5.534
5900	19.300	90.051	73.493	97.688	−10.624	149.578	−5.541
6000	19.300	90.375	73.772	99.618	−10.664	152.291	−5.547

July 31, 1972

$S^\circ_{298.15}$ = 53.019 cal K^{-1}mol^{-1} $\Delta Hf^\circ_{298.15}$ = 1.2 ± 0.3 kcal mol^{-1}

Electronic States and Molecular Constants

State	ε, cm^{-1}	g	ω_e, cm^{-1}	$\chi_e\omega_e$, cm^{-1}	B_e, cm^{-1}	α_e, cm^{-1}	r_e, Å
$X^3\Sigma^-$	0	3	1148.19	6.12	0.72082	0.00574	1.4811
$a^1\Delta$	6350	2	[1148.19]	[6.12]	0.7119	[0.00574]	1.494
$b^1\Sigma^+$	10510	1	1067.66	7.8	0.70261	0.00635	1.5005
$A^3\Pi_0$	38292	6	415.2	1.6	0.6067	0.0194	
$A^3\Pi_1$	38455	6	413.3	1.6	0.6107	0.0194	1.6094
$A^3\Pi_2$	38616	6	412.7	1.7	0.6164	0.0204	
$B^3\Sigma^-$	41629	3	630.4	4.8	0.502	0.0062	1.775
$c^3\Pi$	42200	6	170	[0]	[0.5]	[0]	2.2

Heat of Formation

The selection for ΔHf°_0 of SO(g) 1.2 ± 0.3 kcal mol^{-1}, was derived from one of the two independent means, pointed out by Okabe, J. Chem. Phys. **56**, 3378 (1972), that employs principally spectroscopic data: $\Delta Hf^\circ_0(SO)$ = 1/2 $D^\circ_0(S_2)$ + 1/2 $D^\circ_0(O_2)$ − $D^\circ_0(SO)$ + 1/2 $\Delta Hf^\circ_0(S_2)$. The data employed are as follows. Ricks and Barrow, Can. J. Phys. **47**, 2423 (1969) give $D^\circ_0(S_2)$ = 100.69 ± 0.01 kcal mol^{-1}. Brix and Herzberg, Can. J. Phys. **32**, 110 (1954), give $D^\circ_0(O_2)$ = 117.97 ± 0.046 kcal mol^{-1}. On the basis of analysis of spectroscopic data to 1964, JANAF (Thermochemical Tables, 2nd Edition, NSRDS–NBS 37) gives $D^\circ_0(SO)$ = 123.5 ± 0.3 (?) kcal mol^{-1}. NBS Tech. Note 270-3 gives $\Delta Hf^\circ_0(S_2)$ = 30.65 ± 0.2 kcal mol^{-1}. Assuming the dissociation products of SO are S($^1D_2$) and O(^{3}P), R. Colin, Can. J. Phys. **47**, 979 (1969) concludes $D^\circ_0(SO)$ = 123.56 ± 0.23 kcal mole^{-1}. A systematic error of 0.65 kcal is incurred if the assumption is wrong. Support for this assumption is as follows: 1) Okabe, J. Am. Chem. Soc. **93**, 7095 (1971) concludes that $D^\circ_0(OS-O)$ = 130.06 ± 0.5 kcal mol^{-1} assuming the predissociation of SO$_2$ is to ground state products. Using $\Delta Hf^\circ_0(SO_2)$ = −70.336 kcal mol^{-1} from NBS-NSRDS TN 270-3 and the relation: $\Delta Hf^\circ_0(SO)$ = $D^\circ_0(OS-O)$ − 1/2 $D^\circ_0(O_2)$ + $\Delta Hf^\circ_0(SO_2)$, one obtains $\Delta Hf^\circ_0(SO)$ = 0.7 ± 0.7 kcal mol^{-1}; 2) Assuming the threshold energy for fluorescence of SO, 217.00 ± 0.7 kcal mol^{-1}, (see Okabe, J. Chem. Phys. 56, 3378 (1972)) corresponds to the minimum energy for the reaction: OSCl$_2$ = SO($A^3\Pi_0$) + 2Cl($^3P_{3/2}$) and using 108.43 kcal mol^{-1} for the difference in energy between the lowest vibrational levels of SO($A^3\Pi_0$) and SO($X^3\Sigma^-$) (Colin, loc. cit.) one obtains $\Delta Hf^\circ_0(SO)$ = 1.3 ± 0.7 kcal mol^{-1}. This is based on $\Delta Hf^\circ_0(OSCl_2)$ = −50.07 kcal mol^{-1} (NSRDS-NBS TN 270-3) and $D^\circ_0(Cl_2)$ = 57.177 ± 0.005 kcal mol^{-1} given by Douglas, Moller, and Stoicheff, Can. J. Phys. **41**, 1174 (1963); 3) Re-examination of the photoionization-yield curves of SO$_2^+$ and SO$^+$ obtained by Dibeler and Liston, J. Chem. Phys. **49**, 482 (1968), suggests that their reported threshold for SO → SO$^+$ + O + e$^-$ should be increased from 15.81 ± 0.02 eV to 16.00 eV. Using the latter and the ionization energy of SO given by Jonathan et al, Chem. Phys. Letters **9**, 217 (1971) of 10.34 ± 0.02 eV and the relation: $\Delta Hf^\circ_0(SO)$ = $D^\circ_0(OS-O)$ − 1/2 $D^\circ_0(O_2)$ + $\Delta Hf^\circ_0(SO_2)$, one obtains $\Delta Hf^\circ_0(SO)$ = 1.20 ± 0.5 kcal mol^{-1}.

Heat Capacity and Entropy

The vibrational and rotational constants of the respective electronic levels were taken from B. Rosen, Spectroscopic Data Relative to Diatomic Molecules, Pergamon Press, Oxford, 1970.

(IDEAL GAS)   GFW = 48.0634

T, °K		gibbs/mol				kcal/mol		
T, °K	Cp°	S°	−(G°−H°298)/T	H°−H°298	ΔHf°	ΔGf°	Log Kp
0	.000	.000	INFINITE	−2.087	1.203	1.203	INFINITE
100	6.956	45.364	59.288	−1.392	1.387	−.783	1.711
200	6.995	50.192	53.670	−.696	1.343	−2.949	3.223
298	7.212	53.019	53.019	.000	1.200	−5.027	3.685
300	7.217	53.064	53.019	.013	1.197	−5.066	3.690
400	7.543	55.184	53.306	.751	.480	−7.106	3.882
500	7.845	56.901	53.859	1.521	−.053	−8.939	3.907
600	8.087	58.353	54.490	2.318	−.491	−10.674	3.888
700	8.272	59.615	55.134	3.137	−.861	−12.317	3.846
800	8.414	60.729	55.765	3.971	−14.251	−15.199	4.152
900	8.526	61.727	56.373	4.818	−14.249	−15.317	3.720
1000	8.617	62.630	56.954	5.676	−14.246	−15.435	3.373
1100	8.695	63.455	57.508	6.541	−14.243	−15.556	3.091
1200	8.765	64.214	58.036	7.414	−14.238	−15.675	2.855
1300	8.830	64.918	58.538	8.294	−14.231	−15.794	2.655
1400	8.894	65.575	59.018	9.180	−14.224	−15.915	2.484
1500	8.956	66.191	59.476	10.073	−14.215	−16.037	2.337
1600	9.017	66.771	59.914	10.972	−14.203	−16.158	2.207
1700	9.078	67.319	60.333	11.876	−14.188	−16.281	2.093
1800	9.139	67.840	60.736	12.787	−14.172	−16.405	1.992
1900	9.199	68.336	61.123	13.704	−14.152	−16.528	1.901
2000	9.258	68.809	61.496	14.627	−14.131	−16.655	1.820
2100	9.315	69.262	61.855	15.556	−14.106	−16.782	1.747
2200	9.371	69.697	62.201	16.490	−14.080	−16.909	1.680
2300	9.425	70.115	62.536	17.430	−14.051	−17.039	1.619
2400	9.477	70.517	62.861	18.375	−14.020	−17.168	1.563
2500	9.528	70.905	63.175	19.325	−13.987	−17.301	1.512
2600	9.573	71.279	63.479	20.280	−13.952	−17.434	1.465
2700	9.618	71.641	63.775	21.240	−13.915	−17.569	1.422
2800	9.659	71.992	64.062	22.203	−13.878	−17.707	1.382
2900	9.699	72.332	64.341	23.171	−13.839	−17.843	1.345
3000	9.735	72.661	64.613	24.143	−13.800	−17.980	1.310
3100	9.769	72.981	64.878	25.118	−13.758	−18.121	1.277
3200	9.801	73.291	65.136	26.097	−13.718	−18.263	1.247
3300	9.830	73.593	65.388	27.078	−13.675	−18.407	1.219
3400	9.857	73.887	65.634	28.063	−13.633	−18.549	1.192
3500	9.882	74.173	65.873	29.050	−13.591	−18.697	1.168
3600	9.905	74.452	66.108	30.039	−13.548	−18.842	1.144
3700	9.926	74.724	66.337	31.031	−13.506	−18.989	1.122
3800	9.945	74.989	66.561	32.024	−13.463	−19.138	1.101
3900	9.963	75.247	66.781	33.020	−13.421	−19.290	1.081
4000	9.981	75.500	66.996	34.017	−13.379	−19.438	1.062
4100	9.997	75.746	67.206	35.016	−13.336	−19.590	1.044
4200	10.012	75.987	67.412	36.016	−13.294	−19.743	1.027
4300	10.028	76.223	67.614	37.018	−13.252	−19.897	1.011
4400	10.043	76.454	67.813	38.022	−13.211	−20.053	.996
4500	10.058	76.680	68.007	39.027	−13.170	−20.207	.981
4600	10.074	76.901	68.198	40.033	−13.128	−20.364	.967
4700	10.090	77.118	68.386	41.041	−13.086	−20.523	.954
4800	10.107	77.330	68.570	42.051	−13.043	−20.682	.942
4900	10.125	77.539	68.751	43.063	−13.000	−20.840	.930
5000	10.146	77.744	68.929	44.076	−12.957	−21.004	.918
5100	10.168	77.945	69.103	45.092	−12.913	−21.162	.907
5200	10.192	78.143	69.275	46.110	−12.867	−21.325	.896
5300	10.218	78.337	69.444	47.131	−12.819	−21.487	.886
5400	10.245	78.528	69.611	48.154	−12.770	−21.652	.876
5500	10.273	78.717	69.775	49.180	−12.719	−21.816	.867
5600	10.312	78.902	69.936	50.209	−12.666	−21.982	.858
5700	10.350	79.085	70.095	51.242	−12.610	−22.151	.849
5800	10.390	79.265	70.252	52.279	−12.551	−22.316	.841
5900	10.435	79.443	70.406	53.321	−12.487	−22.489	.833
6000	10.483	79.619	70.558	54.366	−12.421	−22.654	.825

July 31, 1972

Ground State Configuration $^2P_{3/2}$ ΔHf°_0 = 18.34 ± 0.12 kcal mol^{-1}

$S^\circ_{298.15}$ = 37.917 gibbs mol^{-1} $\Delta Hf^\circ_{298.15}$ = 18.84 ± 0.12 kcal mol^{-1}

<u>Electronic Levels and Quantum Weight</u>
Same as ref. (1)

Heat of Formation

A review of earlier work is given in ref. (1); a value of 37.72 ± 0.80 kcal mol^{-1} for the F_2 dissociation energy, D°_0, was selected. A review of later work, which follows, suggests the uncertainty in D°_0 of F_2 can be significantly reduced.

From a third law analysis of the equilibrium data of Doesher (2) and Wise (3) for the reaction $F_2(g) \rightarrow 2F(g)$, Stamper and Barrow (4) obtained $D^\circ_0(F_2)$ = <u>36.71</u> ± 0.13 kcal mol^{-1}. A more realistic uncertainty based on the analysis of ref. (1) is ±<u>0.80</u> kcal mol^{-1}.

The dissociation energy of F_2 may be derived from the relation: $D^\circ_0(F_2) = 2D^\circ_0(HF) + 2\Delta Hf^\circ_0(HF) - D^\circ_0(H_2)$. The following values were employed. $D^\circ_0(HF)$: DiLonardo and Douglas (5) report $D^\circ_0(HF)$ = 135.33 ± 0.17 kcal mol^{-1} from new measurements on the emission spectrum of HF. This confirms and refines the value of 135.13 ± 0.23 kcal mol^{-1} given by Johns and Barrow (6). Berkowitz et al (7) obtained $D^\circ_0(HF)$ = 134.79 ± 0.23 kcal mol^{-1} from dissociative photoionization, DI, of HF and explain the low results, 132.37 ± 0.69 kcal mol^{-1}, of Dibeler et al (8), who performed similar DI experiments, as due to the latter's failure to take into account the rotational excitation of the molecules undergoing ionization. $\Delta Hf^\circ_0(HF)$: The value selected in ref. (1), -65.13 ±0.2 kcal mol^{-1}, was adopted. This avoids possible circularity if the value in ref. (9) were used. (The latter is partly based on $D^\circ_0(HF)$ and $D^\circ_0(F_2)$.) $D^\circ_0(H_2)$: 103.263 ± 0.003 kcal mol^{-1} was taken from Herzberg (10). Combining these values one obtains $D^\circ_0(F_2)$ = <u>37.14</u> ± 0.6 kcal mol^{-1}.

Berkowitz et al (7) obtained 19.01 ± 0.01 eV for the DI threshold of F_2 ($F_2 \rightarrow F^+ + F + e^-$). Contribution to the F^+ yield due to ion-pair formation and the effects of rotationally excited molecules were taken into account. Dibeler et al (8), who did not make such corrections, reported the low value 18.76 ± 0.03 eV. Subtracting the ionization potential for F, 17.422 eV, given by Moore (11) from the former threshold, Berkowitz et al obtain $D^\circ_0(F_2)$ = <u>36.67 ± 0.23</u> kcal mol^{-1}.

Chupka and Berkowitz (12) have shown by kinetic energy measurements on positive ions formed by photoproduction of ion pairs ($H^+ + F^-$ from HF and $F^+ + F^-$ from F_2) that the results are consistent with the DI thresholds of Berkowitz et al (7) if EA(F) = 3.400 ± 0.002 eV. This is the electron affinity reported by Popp (13) and agrees with the value, 3.398 ± 0.002 eV, determined by Milstein and Berry (14). The ion pair threshold, 15.49 eV, reported by Dibeler et al (8), for F_2 agrees with that of Berkowitz et al (7) if it is reassigned to ion-pair formation from vibrationally excited molecules (F_2, v"=1) and yields $D^\circ_0(F)$ = <u>36.43 ± 0.69</u> kcal mol^{-1}.

The value of $D^\circ_0(F_2)$ = 36.67 ± 0.23 kcal mol^{-1} from the measurements of Berkowitz et al (7) on the DI of F_2 was adopted. The remaining values of $D^\circ_0(F_2)$ agree with this value within their stated uncertainties.

Heat Capacity and Entropy

Same as ref. (1).

References

1. JANAF Thermochemical Tables, 2nd Edition, NSRDS-NBS 37, June 1971 (U. S. Govt. Printing Office, Washington, D. C. 20402).

2. R. N. Doesher, J. Chem. Phys. <u>20</u>, 330 (1952).

3. H. Wise, J. Phys. Chem. <u>58</u>, 389 (1954).

4. J. G. Stamper and R. F. Barrow, Trans. Faraday Soc. <u>54</u>, 1592 (1958).

5. G. DiLonardo and A. E. Douglas, J. Chem. Phys. <u>56</u>, 5185 (1972).

6. J. W. C. Johns and R. F. Barrow, Proc. Roy. Soc. (London) <u>A251</u>, 504 (1959).

7. J. Berkowitz, W. A. Chupka, P. M. Guyon, J. H. Holloway, and R. Spohr, J. Chem. Phys. <u>54</u>, 5165 (1971).

8. V. H. Dibeler, J. A. Walker and K. E. McCulloh, J. Chem. Phys. <u>51</u>, 4230 (1969).

9. D. D. Wagman, W. H. Evans, V. B. Parker, I. Halow, S. M. Bailey, and R. H. Schumm, NBS Technical Note 270-3, January 1968 (U. S. Govt. Printing Office, Washington, D. C. 20402).

10. G. Herzberg, Phys. Rev. Lett. <u>23</u>, 1081 (1969).

11. C. E. Moore, NSRDS-NBS 34 (1970) (U. S. Govt. Printing Office, Washington, D. C. 20402).

12. W. A. Chupka and J. Berkowitz, J. Chem. Phys. <u>54</u>, 5126 (1971).

13. H. P. Popp, Z. Naturforsch. <u>22a</u>, 254 (1967).

14. R. Milstein and R. S. Berry, J. Chem. Phys. <u>55</u>, 4146 (1971).

WATER (H$_2$O) (IDEAL GAS) GFW = 18.0154

Point Group C$_{2v}$ $\Delta Hf^\circ_0 = -57.100$ kcal mol^{-1}

S$^\circ_{298.15}$ = 45.106 gibbs mol^{-1} $\Delta Hf^\circ_{298.15} = -57.795 \pm 0.010$ kcal mol^{-1}

Vibrational Levels and Multiplicities

same as ref. (1)

Heat of Formation

The CODATA selection (2) was adopted. Rossini (3,4) determined the heat of formation of H$_2$O(ℓ) by direct calorimetry to be $-285,781 \pm 41$ int. J mol^{-1} (1 int. J = 1.00017J, GFW (H$_2$O) = 18.0156) correcting to GFW (H$_2$O) = 18.0154 and adding a correction for imperfect gases (see (5), -3.6 int. J mol^{-1}) yields ΔHf°_{298} for H$_2$O(ℓ) = -68.315 ± 0.010 kcal mol^{-1}. The later and less precise work of King and Armstrong (6) (an auxiliary measurement) which gave ΔHf°_{298} of H$_2$O(ℓ) = -68.32 ± 0.08 kcal mol^{-1} is in good agreement. Work before 1931 is critically reviewed by Rossini (3). The heat of vaporization of H$_2$O(ℓ) at 298K corrected to zero pressure was taken from Keenan et al (7); ΔH°_{v298} of H$_2$O(ℓ) = 10.520 ± 0.001 kcal mol^{-1}. This value is in good agreement with the (recalculated) value determined by Rossini (5) from the work of Osborne, Stimson, and Ginnings (8) of 10.519 ± 0.003 kcal mol^{-1}.

Heat Capacity and Entropy

Same as ref. (1).

References

1. JANAF Thermochemical Tables, 2nd Edition, NSRDS–NBS 37, June, 1971 (U. S. Govt. Printing Office, Washington, D. D., 20402).

2. CODATA Task Group on Key Values for Thermodynamics, Final Set of Key Values for Thermodynamics – Part I, November 1971 (CODATA Bulletin No. 5).

3. F. D. Rossini, J. Res. Natl. Bur. Standards 6, 1 (1931).

4. F. D. Rossini, J. Res. Natl. Bur. of Standards 7, 329 (1931).

5. F. D. Rossini, J. Res. Natl. Bur. of Standards 22, 407 (1939).

6. R. C. King and G. T. Armstrong, J. Res. Natl. Bur. of Standards 72A, 113 (1968).

7. J. H. Keenan, F. G. Keyes, P. G. Hill, J. G. Moore, Steam Tables, Thermodynamic Properties of Water Including Vapor, Liquid, and Solid Phases – English Units (John Wiley and Sons, New York, 1969).

8. N. S. Osborne, H. F. Stimson, and D. C. Ginnings, J. Res. Natl. Bur. of Standards 23, 197 (1939).

DOCUMENT CONTROL DATA - R & D

(Security classification of title, body of abstract and indexing annotation must be entered when the overall report is classified)

1. ORIGINATING ACTIVITY (Corporate author)	2a. REPORT SECURITY CLASSIFICATION
NATIONAL BUREAU OF STANDARDS DEPARTMENT OF COMMERCE WASHINGTON, D.C. 20234	UNCLASSIFIED
	2b. GROUP

3. REPORT TITLE

INTERIM REPORT ON THE THERMODYNAMICS OF CHEMICAL SPECIES IMPORTANT IN AEROSPACE TECHNOLOGY (INCLUDING SPECIAL TOPICS IN CHEMICAL KINETICS)

4. DESCRIPTIVE NOTES (Type of report and inclusive dates)
Scientific   Interim

5. AUTHOR(S) (First name, middle initial, last name)

THOMAS B DOUGLAS   CHARLES W BECKETT

6. REPORT DATE	7a. TOTAL NO. OF PAGES	7b. NO. OF REFS
1 July 1972	321	418

8a. CONTRACT OR GRANT NO.	9a. ORIGINATOR'S REPORT NUMBER(S)
ISSA-71-0003	NBS REPORT 10 904
b. PROJECT NO. 9750-01	
c. 61102F	9b. OTHER REPORT NO(S) (Any other numbers that may be assigned this report)
d 681308	AFOSR-TR-72-2004

10. DISTRIBUTION STATEMENT

Distribution of this document is unlimited

11. SUPPLEMENTARY NOTES	12. SPONSORING MILITARY ACTIVITY
TECH, OTHER	AF Office of Scientific Research (AFSC) 1400 Wilson Boulevard Arlington, Virginia 22209

13. ABSTRACT The standard heat of formation of $MoF_6(\ell)$ was determined accurately by solution calorimetry. Transpiration measurements on $MoF_5(\ell)$ covered 70°, 90°, and 110°C. A direct vapor-pressure method was developed and accurately tested. Infrared and Raman spectroscopy led to a complete vibrational assignment for the MoF_5 molecule. Two drop-type apparati measured the heat capacity of Mo_2C, 273°-1475°K. The subsecond-duration pulse-heating technique measured the specific heat, electrical resistivity, and hemispherical total emittance of 90 Ta-10 W (1500°-3200°K) and 99Nb-1 Zr (1500°-2700°K); deviations from additivity were investigated. Pulse techniques measured the melting points of W and Nb (with 15 and 10 K uncertainties, respectively) and their electrical resistivities above their melting points. The feasibility of pulse-heating techniques was demonstrated for measuring heats of fusion (using Nb) and solid-solid transformations (using Fe). After critical data examination, suggested thermal rate constants were tabulated for the dissociation and recombination of molecular NH_3, N_2H_4, and N_2F_4 (10^{-5} to 100 atm, and 200°K, up to 4000°, 3000°, and 1800°K respectively); these results revised the heat of formation of $NH_2(g)$ and the N-N bond energy by 5 and 3 kcal/mol respectively. A bibliography on the chemical kinetics of 60 gas-phase reactions of fluorides of $C\ell$, N, and O covers 1934-1972. After a critical review and correlation, new ideal-gas thermochemical tables and texts (in the JANAF-Tables format) were given for 31 simple gas species (many containing deuterium or fluorine) of current interest in chemical laser research. (U)

DD FORM 1 NOV 65 1473

14. KEY WORDS	LINK A		LINK B		LINK C	
	ROLE	WT	ROLE	WT	ROLE	WT
THERMODYNAMIC PROPERTIES						
HIGH-SPEED MEASUREMENTS						
CRITICAL LITERATURE REVIEWS						
JANAF-LIKE THERMOCHEMICAL TABLES						
THERMOCHEMICAL CALORIMETRY						
SPECIFIC-HEAT CALORIMETRY						
INFRARED AND RAMAN SPECTROSCOPY						
EXPERIMENTAL VAPORIZATION THERMODYNAMICS						
MOLYBDENUM FLUORIDES						
CHEMICAL-KINETIC RATE CONSTANTS						
REFRACTORY-METAL ALLOYS						
ELECTRICAL RESISTIVITIES						
MOLYBDENUM CARBIDE						
THERMAL RADIATION PROPERTIES						
VAPOR DENSITY						
HEATS OF FUSION OF REFRACTORY METALS						
SOLID-SOLID TRANSFORMATIONS						
TABLES FOR CHEMICAL LASER RESEARCH						
MELTING POINTS OF REFRACTORY METALS						